Thesis for the degree of Doctor of Philosophy

UNIVERSITÀ DEGLI STUDI DI TORINO

PhD program in Pharmaceutical and Biomolecular Sciences (XXXV cycle)

Department of Neurosciences "Rita Levi Montalcini"

UNIVERSIDADE FEDERAL DE SANTA CATARINA

PhD program in Pharmacology

Department of Pharmacology

New pharmacological strategies to counteract the major inflammatory triggers of organ injury in cardiovascular diseases

Supervisors

Prof. Massimo Collino

Prof. Daniel Fernandes

PhD candidate

Gustavo Ferreira Alves

Torino (Italy), Florianópolis (Brazil)

2023

To my mother, Leoni Ferreira Alves, who is always present even overseas, and to my father, Osvaldo Donizetti Alves *in memoriam.*

New pharmacological strategies to counteract the major inflammatory triggers of organ injury in cardiovascular diseases

GUSTAVO FERREIRA ALVES

Department of Neurosciences "Rita Levi Montalcini"/Department of Pharmacology

University of Turin (Turin, Italy)/Federal University of Santa Catarina (Florianópolis, Brazil)

ABSTRACT

Cardiovascular diseases are the leading cause of death worldwide and two of the major public health concerns that manifest cardiovascular dysfunction include sepsis and haemorrhagic shock (HS). Sepsis and HS are life-threatening clinical conditions that are accompanied by systemic inflammatory imbalance that ultimately leads to multiple organ failure (MOF) and currently there are no specific pharmacological interventions that prevent the onset of MOF associated with these clinical conditions. Few kinases, such as the focal adhesion kinase (FAK), the proline-rich tyrosine kinase 2 (PyK2), the Bruton's tyrosine kinase (BTK) and the Janus kinase (JAK) as well as immunomodulatory mediators such as macrophage migration inhibitory factor (MIF) and Inducible T cell co-stimulator ligand (ICOSL) are among the most recently discovered molecular mechanisms involved in the development of an excessive inflammatory response in several clinical settings. However, so far, their role in the context of sepsis and HS has been poorly investigated. Therefore, the present thesis aimed to investigate the role of these key targets in the pathogenesis of sepsis/HS and to test in *in vivo* models of sepsis and HS the potential beneficial effects of their modulation by administering selective pharmacological tools. Interestingly some of the drugs here tested have been already approved to treat other inflammatory-related disorders. Adult rats or mice underwent caecal ligation and puncture (CLP) surgery to induce polymicrobial sepsis or blood withdrawn/reperfusion to mimic the HS injury. After the surgical procedure, the animals were randomly assigned to receive either vehicle or the compounds targeting the above-mentioned cascades (PF562271, Ibrutinib, Acalabrutinib, Fenebrutinib, Baricibinib, ISO-1 and ICOS-Fc for targeting FAK-PyK2, BTK, JAK1/2, MIF and ICOS-ICOSL, respectively). Organs and plasma were collected 4 and/or 24 h after surgery for analyses. The results here reported showed that the tested kinases (FAK, PyK2, BTK and JAK) and immune components (ICOSL and MIF) do indeed play a central role in the pathogenesis of sepsis and HS, demonstrating a key role of the distinct mediators in the activation of the NFκB-MAPK-NLRP3 axis, which results in systemic (cytokine storm) and local (hepatic, renal, cardiac) inflammation, leading ultimately to multiorgan injury. Most notably, we convincingly showed that the pharmacological targeting of these key proteins effectively protected against sepsis/HS by reducing systemic/local inflammation and hence related-organ dysfunction. Overall, the present PhD project leads to the identification of innovative pharmacological targets for the treatment of sepsis and HS, highlighting the potential for EMA- and FDA-approved drugs to be repurposed in these specific clinical settings.

Keywords: Sepsis, haemorrhagic shock, cardiovascular derangements, inflammation, kinases, immunomodulation, drug repurposing.

LIST OF PUBLICATIONS

This thesis is based on the work contained in the following published articles:

I. **Alves, Gustavo Ferreira**, Aimaretti E, Einaudi G, Mastrocola R, de Oliveira JG, Collotta D, Porchietto E, Aragno M, Cifani C, Sordi R, Thiemermann C, Fernandes D, Collino M. Pharmacological Inhibition of FAK-Pyk2 Pathway Protects Against Organ Damage and Prolongs the Survival of Septic Mice. Front Immunol. 2022 Feb 1;13:837180. DOI: 10.3389/fimmu.2022.837180.

II. O'Riordan CE, Purvis GSD, Collotta D, Krieg N, Wissuwa B, Sheikh MH, **Alves, Gustavo Ferreira,** Mohammad S, Callender LA, Coldewey SM, Collino M, Greaves DR, Thiemermann C. X-Linked Immunodeficient Mice With No Functional Bruton's Tyrosine Kinase Are Protected From Sepsis-Induced Multiple Organ Failure. Front Immunol. 2020 Oct 7;11:581758. DOI: 10.3389/fimmu.2020.581758.

III. Patel NM, Oliveira FRMB, Ramos HP, Aimaretti E, **Alves, Gustavo Ferreira**, Coldewey SM, Collino M, Sordi R, Thiemermann C. Inhibition of Bruton's Tyrosine Kinase Activity Attenuates Hemorrhagic Shock-Induced Multiple Organ Dysfunction in Rats. Ann Surg. 2021 Dec 27. DOI: 10.1097/SLA.0000000000005357.

IV. Patel NM, Collotta D, Aimaretti E, **Alves, Gustavo Ferreira**, Kröller S, Coldewey SM, Collino M, Thiemermann C. Inhibition of the JAK/STAT Pathway with Baricitinib Reduces the Multiple Organ Dysfunction Caused by Hemorrhagic Shock in Rats. Ann Surg. 2022 Jul 15. DOI: 10.1097/SLA.0000000000005571.

V. Patel NM, Yamada N, Oliveira FRMB, Stiehler L, Zechendorf E, Hinkelmann D, Kraemer S, Stoppe C, Collino M, Collotta D, **Alves, Gustavo Ferreira**, Ramos HP, Sordi R, Marzi I, Relja B, Marx G, Martin L, Thiemermann C. Inhibition of Macrophage Migration Inhibitory Factor Activity Attenuates Haemorrhagic Shock-Induced Multiple Organ Dysfunction in Rats. Front Immunol. 2022 Apr 6;13:886421. DOI: 10.3389/fimmu.2022.886421.

VI. **Alves, Gustavo Ferreira**, Stoppa I, Aimaretti E, Monge C, Mastrocola R, Porchietto E, Einaudi G, Collotta D, Bertocchi I, Boggio E, Gigliotti CL, Clemente N, Aragno M, Fernandes D, Cifani C, Thiemermann C, Dianzani C, Dianzani U, Collino M. ICOS-Fc as innovative immunomodulatory approach to counteract inflammation and organ injury in sepsis. Front Immunol. 2022 Sep 2;13:992614. DOI: 10.3389/fimmu.2022.992614.

Published articles not included in the thesis:

- Mastrocola R, Collotta D, Gaudioso G, Le Berre M, Cento AS, **Alves, Gustavo Ferreira**, Chiazza F, Verta R, Bertocchi I, Manig F, Hellwig M, Fava F, Cifani C, Aragno M, Henle T, Joshi L, Tuohy K, Collino M. Effects of Exogenous Dietary Advanced Glycation End

Products on the Cross-Talk Mechanisms Linking Microbiota to Metabolic Inflammation. Nutrients. 2020 Aug 19;12(9):2497. DOI: 10.3390/nu12092497.

- Penna C, Aragno M, Cento AS, Femminò S, Russo I, Bello FD, Chiazza F, Collotta D, **Alves, Gustavo Ferreira**, Bertinaria M, Zicola E, Mercurio V, Medana C, Collino M, Pagliaro P. Ticagrelor Conditioning Effects Are Not Additive to Cardioprotection Induced by Direct NLRP3 Inflammasome Inhibition: Role of RISK, NLRP3, and Redox Cascades. Oxid Med Cell Longev. 2020 Aug 3;2020:9219825. DOI: 10.1155/2020/9219825.

- Pinto JMO, Leão AF, **Alves, Gustavo Ferreira**, Mendes C, França MT, Fernandes D, Stulzer HK. New supersaturating drug delivery system as strategy to improve apparent solubility of candesartan cilexetil in biorelevant medium. Pharm Dev Technol. 2020 Jan;25(1):89-99. doi: 10.1080/10837450.2019.

- Collotta D, Hull W, Mastrocola R, Chiazza F, Cento AS, Murphy C, Verta R, **Alves, Gustavo Ferreira**, Gaudioso G, Fava F, Yaqoob M, Aragno M, Tuohy K, Thiemermann C, Collino M. Baricitinib counteracts metaflammation, thus protecting against diet-induced metabolic abnormalities in mice. Mol Metab. 2020 Sep;39:101009. DOI: 10.1016/j.molmet.2020.101009.

- Mohammad S, Al Zoubi S, Collotta D, Krieg N, Wissuwa B, **Alves, Gustavo Ferreira**, Purvis GSD, Norata GD, Baragetti A, Catapano AL, Solito E, Zechendorf E, Schürholz T, Correa-Vargas W, Brandenburg K, Coldewey SM, Collino M, Yaqoob MM, Martin L, Thiemermann C. A Synthetic Peptide Designed to Neutralize Lipopolysaccharides Attenuates Metaflammation and Diet-Induced Metabolic Derangements in Mice. Front Immunol. 2021 Jul 19;12:701275. DOI: 10.3389/fimmu.2021.701275.

- Mastrocola R, Aimaretti E, **Alves, Gustavo Ferreira**, Cento AS, Fornelli C, Dal Bello F, Ferraris C, Goitre L, Perrelli A, Retta SF. Heterozygous Loss of KRIT1 in Mice Affects Metabolic Functions of the Liver, Promoting Hepatic Oxidative and Glycative Stress. Int J Mol Sci. 2022 Sep 22;23(19):11151. DOI: 10.3390/ijms231911151.

- Mohammad S, O'Riordan CE, Verra C, Aimaretti E, **Alves, Gustavo Ferreira**, Dreisch K, Evenäs J, Gena P, Tesse A, Rützler M, Collino M, Calamita G, Thiemermann C. RG100204, A Novel Aquaporin-9 Inhibitor, Reduces Septic Cardiomyopathy and Multiple Organ Failure in Murine Sepsis. Front Immunol. 2022 Jun 14;13:900906. DOI: 10.3389/fimmu.2022.900906.

CONTRIBUTION REPORT

Articles I and VI: Gustavo Ferreira Alves (GFA) conceived, designed and performed the experiments, coordinated the samples analysis, analysed, and interpreted the data, and was responsible for writing the manuscripts.

Articles II, III, IV, and V: GFA participated in conducting *ex-vivo* experiments on sample tissues, such as western blot, immunohistochemistry, myeloperoxidase assay (when applicable), analysed and interpreted the data.

ABBREVIATIONS

AAA	Abdominal aortic aneurysm
ACA	Acalabrutinib
ALT	Alanine aminotransferase
ANOVA	Analysis of variance
APCs	Antigen-presenting cells
AQP9	Aquaporin-9
ASC	Apoptosis-associated speck like protein containing a caspase recruitment domain
AST	Aspartate aminotransferase
BCR	B-cell receptor
BMX	Bone marrow kinase on chromosome x
BSA	Bovine serum albumin
BTK	Bruton's tyrosine kinase
CCL1	Chemokine (c-c motif) ligand 1
CD	Cluster of differentiation
CK	Creatine kinase
CK2	Casein kinase 2
CLP	Caecal ligation and puncture
CVDs	Cardiovascular diseases
CXCL1	Chemokine (c-x-c motif) ligand 1
CXCR	Chemokine (cxc motif) receptor
CX3CL1	C-x3-c motif chemokine ligand 1
DAMPs	Damage-associated molecular patterns
DAB	3,3'-diaminobenzidine
DMSO	Dimethyl sulfoxide
ECL	Enhanced chemiluminescence
EDTA	Ethylenediaminetetraacetic acid
ELISA	Enzyme-linked immunosorbent assay
EF	Ejection fraction
EMA	European medicines agency
EPO	Erythropoietin
ErbB4	Erb-b2 receptor tyrosine kinase 4
FAK	Focal adhesin kinase
FAT	Focal adhesion targeting
FDA	Food and drug administration
FEN	Fenebrutinib
FS	Fractional shortening
G-CSF	Granulocyte colony-stimulating factor
GEO	Gene expression omnibus
GM-CSF	Granulocyte-macrophage colony-stimulating factor
HMGB1	High mobility group protein b1
HRP	Horseradish peroxidase
HS	Haemorrhagic shock
HTAB	Hexadecyltrimethylammonium bromide buffer
IC50	Half-maximal inhibitory concentration
ICOS	Inducible t cell co-stimulator
ICOSL	Icos ligand

ICU	Intensive care unit
IFN	Interferon-γ
IL	Interleukin
iNOS	Inducible nitric oxide synthase
ISO-1	[(S,r)-3-(4- hydroxyphenyl)-4,5-dihydro-5-isoxazole acetic acid methyl ester]
JAK	Janus kinase
LPS	Lipopolysaccharide
MAL	Myd88-adaptor-like
MAP	Mean arterial pressure
MAPK	Mitogen-activated protein kinases
MCL	Mantle cell lymphoma
MCP-1	Monocyte chemotactic protein-1
MIF	Macrophage migration inhibitory factor
MSU	Monosodium urate
MOF	Multiple organ failure
MyD88	Myeloid differentiation primary response 88
NETs	Neutrophil extracellular traps
NFκB	Nuclear factor kappa b
NLRP3	Nucleotide-binding oligomerization domain-like receptor pyrin domain-containing-3 (nlrp3)
NO	Nitric oxide
OPN	Osteopontin
PAMPs	Pathogen-associated molecular patterns
PF271	PF562271
PRRs	Pattern recognition receptors
Pyk2	Proline-rich tyrosine kinase-2
PVDF	Polyvinylidene fluoride
RAGEs	Receptors of advanced glycation end products
RIPK2	Receptor interacting serine/threonine kinase 2
ROS	Reactive oxygen species
SA-PE	Streptavidin-phycoerythrin
SD	Standard deviation
SDS-PAGE	Dodecyl sulphate polyacrylamide gel electrophoresis
SEM	Standard error of mean
SMKIs	Small molecule kinase inhibitors
SOFA	Sequential organ failure assessment
STAT	Signal transducer and activator of transcription
TMB	3,3′,5,5′-tetramethylbenzidine
TNF-α	Tumor necrosis factor-α
TPO	Thrombopoietin
TREG	T regulatory cells
TYK2	Tyrosin kinase 2
WHO	World health organization
WT	Wild-type
Xid	X-linked immunodeficient
XLA	X-linked agammaglobulinemia

INDEX

1 INTRODUCTION

Globally, cardiovascular diseases (CVDs) are the leading cause of death. According to the World Health Organization (WHO), nearly 18 million people die every year from CVDs, accounting for 31% of all deaths worldwide [1]. In view of this, two major public health concerns that manifest cardiovascular dysfunction include sepsis and haemorrhagic shock (HS), which in turn, survivors have shown a high risk of developing long-term cardiovascular disorders, along with other sequelae [2][3]. The most current data on the global sepsis burden reported 48.9 million incident cases and 11.0 million sepsis-related deaths, corresponding to nearly 20% of all deaths worldwide [4]. On the other hand, each year, there are approximately 6 million trauma-associated mortalities, of which almost 40% are due to trauma-associated haemorrhage [5][6].

Sepsis and HS are life-threatening clinical conditions that are ultimately accompanied by multiple organ failure (MOF) [7] and there are currently no specific pharmacological interventions that prevent the onset of MOF associated with sepsis or HS. According to the latest *Surviving Sepsis Campaign* guidelines, the management of septic patients consists primarily of antibiotic therapy, fluid supplementation, oxygen support and vasopressor agents [8]. Likewise, the management of traumatic haemorrhagic shock in the acute phase consists of stopping the bleeding, followed by the administration of resuscitation fluid, vasoactive drugs, and blood transfusion [9]. Whilst the number of early post-injury/sepsis deaths has declined in recent years secondary to improved care in the hospital settings, the prognosis in septic and/or trauma patients remains remarkably poor, reinforcing the urgent need for new target-specific therapies for critically ill patients.

In order to find an intertwined path between the two clinical conditions, the present research has been deepened into their common pathophysiological aspects. Despite sepsis and HS have distinct aetiologies, the early stages of both medical conditions share some similarities regarding their pathogenesis, for instance the inflammatory imbalance after the onset of these complications. Numerous triggering factors contribute to this dysregulation, including pro- and anti-inflammatory cytokines, chemokines, pathogen-associated molecular patterns (PAMPs) such as bacterial exotoxins and endotoxins, mycotoxins, and damage-associated molecular patterns (DAMPs) released by injured cells. Thus, while in sepsis there is a synergistic effect of PAMPs and DAMPs [10], in HS there is a predominant effect of DAMPs from the extensive tissue damage and ischaemia-reperfusion (I/R) injury [11][12]. This complex interplay involving such substances can lead to an aberrant immune system activation, leading to the so-called “cytokine storm” due to massive cytokine release, which ultimately can cause organ injury and dysfunction [13][14].

Solid evidence reports the involvement of selective inflammatory pathways, such as NFκB and NLRP3 inflammasome in the development of cytokine storm and hence, MOF associated with sepsis/HS [15][16][17].

Thus, since inflammation plays a central role in the pathogenesis of sepsis and HS, it is suggestive that pharmacological targeting of key components in the inflammatory cascade may be a promising therapeutic approach in the outcome of sepsis/HS. In light of this, this thesis aimed to test the effects of two different pharmacological approaches: targeting (a) kinases and (b) immunocomponents which are tightly liked to such inflammatory pathways, in order to prevent sepsis/HS-induced inflammatory derangement and MOF.

2 OBJECTIVES

The overall aim of the thesis was to pharmacologically target selective inflammatory pathways that drive multiorgan dysfunction in cardiovascular diseases by using rodent models of sepsis and haemorrhagic shock.

The specific objectives were:

a) Targeting kinases as pharmacological strategy to counteract multiorgan dysfunction in sepsis and haemorrhagic shock (**articles I, II, III and IV**).

b) Targeting immune system components as innovative pharmacological approach to counteract multiorgan failure in sepsis and haemorrhagic shock (**articles V and VI**)

The experiments here reported were conducted in the laboratory of cardiometabolic pharmacology in the Department of Neurosciences "Rita Levi Montalcini" (University of Turin, Italy), under the supervision of Professor Massimo Collino and at LabCARE in the Department of Pharmacology (Federal University of Santa Catarina, Brazil) under the supervision of Professor Daniel Fernandes.

3 BACKGROUND

3.1 Organ failure and inflammation

In the intensive care unit (ICU), critically ill patients undergo the Sequential Organ Failure Assessment (SOFA) score, either to measure the severity of organ dysfunction [18], or as a diagnostic criterion [7]. Multiple organ failure is the common outcome of septic and trauma patients with a poor prognosis that ends up leading to death, which in parallel, it has been shown that the greater the number of affected organs, the greater the mortality [19]. In brief, many of the mechanisms underlying organ dysfunction are similar for all organs in sepsis and trauma-associated haemorrhage and include a combination of hemodynamic and cellular changes that develop as a result of the effects of various inflammatory mediators which are involved in the host response to infection (sepsis) or cell injury (sterile inflammation – haemorrhagic shock).

In sepsis, upon infection, the invading pathogen is recognized by host innate immune system cells through pattern recognition receptors (PRRs). Such receptors recognize conserved structures of the microorganism, named pathogen-associated molecular patterns (PAMPs). In addition, PRRs can also recognize multiple cell-derived mediators, termed damage-associated molecular patterns (DAMPs) that are released from tissue/cell injury during inflammation, as occurs primarily in haemorrhagic shock in response to a significant loss of intravascular volume, which leads to reduced tissue perfusion and hence hypoxia [20]. Although many PAMPs have been described, the main pathogens' structures that trigger selective intracellular pathways are: lipoteichoic acid and peptidoglycans, from gram-positive bacteria (exotoxins); lipopolysaccharide (LPS), from gram-negative bacteria as the most widely studied endotoxin; and O-linked mannosides, which are polysaccharides found in yeast (*Candida spp*) membranes [21]. On the other hand, the main DAMPs released during sepsis/HS injury include high mobility group protein B1 (HMGB1), heat shock proteins, S100 proteins, mitochondrial DNA and metabolic molecules, such as ATP. In these circumstances, DAMPs can activate the same sequence of events as PAMPs, thus amplifying the initial host response [22]. In addition to PAMPs and DAMPs, other elements are continuously produced/released during the inflammatory imbalance seen in sepsis/HS injury which in turn can potentiate cell damage. These components include proteolytic enzymes, reactive oxygen species (ROS) and neutrophil extracellular traps (NETs; which are web-like structures released by activated neutrophils consisting of nuclear DNA decorated with histones, antimicrobial peptides and proteases) [23][24].

Successively, upon activation of PRRs, various downstream inflammatory pathways are triggered. To date, several categories of PRRs have been identified, however notably Toll-like receptors (TLRs) and nucleotide oligomerization domain (NOD)-like receptors (NLRs) are widely investigated in sepsis/HS. For instance, once TLRs recognize PAMPs and DAMPs, several intracellular mediators are recruited, resulting in an overactivation of key inflammatory pathways such as NFκB (Nuclear Factor kappa B), thus leading to the transcription of target genes, which ultimately induces the production of an arsenal of pro-inflammatory mediators/cytokines, including tumor necrosis factor-α (TNF-α), Interleukin-1β (IL-1β), IL-6, among others [25]. Alongside, PAMPs and DAMPs can lead to the activation of a class of NLRs, specifically the pyrin domain-containing 3 (NLRP3) inflammasome, which is a protein macromolecular complex

that regulates the activation of caspase-1 and the production/secretion of potent pro-inflammatory cytokines such as IL-1β and IL-18 [26]. Therefore, the overactivation of these inflammatory pathways during sepsis and HS results in the excessive cytokine release, characterizing the so-called "cytokine storm", which sequentially contributes to increased leukocyte infiltration, activation of the complement system, thus ultimately leading to cell death and tissue damage. Overall, all this complex inflammatory interplay designates the main molecular mechanisms behind multiorgan failure associated with sepsis/HS.

3.2 Potential pharmacological targets

In the overview of molecular mechanisms in organ failure, a complex crosstalk involving a multitude of inflammatory and immunological components takes place, which prompt us to consider two main pharmacological strategies to counteract the major inflammatory disorders observed in sepsis and HS: targeting pivotal kinases and immune system components which are potentially key-players in the development of MOF associated with these two clinical conditions.

3.2.1 Targeting key-kinases

Given the urgent need for new pharmacological strategies to prevent sepsis/HS-related multiorgan dysfunction, the concept of drug repurposing [27] stands out within the class of kinase inhibitors, considering that upstream the aforementioned inflammatory pathways are mainly activated/regulated by posttranslational modifications, such as kinase-mediated covalent phosphorilation [28][29].

In this scenario, approximately 700 kinases are encoded in the human genome [30], and although they were once perceived as undruggable targets, nowadays, kinases are among the most successful drug targets worldwide, accounting for over 100 kinase-targeting agents, including 72 US FDA-approved small molecule kinase inhibitors (SMKIs), along with other ~500 SMKIs in clinical trials [31]. Thus far, the role of kinases has been widely explored in several diseases contexts, reaching a vast number of publications in the last two years (more than 50,000), as shown in panels A-B, Figure 1. However, interest of kinases in the pathogenesis of sepsis and HS have grown over the years, according to an exponential increase in publications in the last two decades (Figure 1, panels A-B). Furthermore, considering that even if only about ~3.5% of sepsis studies and ~2.5% HS studies in the last two years correlate the role of kinases in the course of these clinical conditions, there is still much to be explored/uncovered, making kinases even more attractive as potential pharmacological targets due to the wide range of SMKIs currently available.

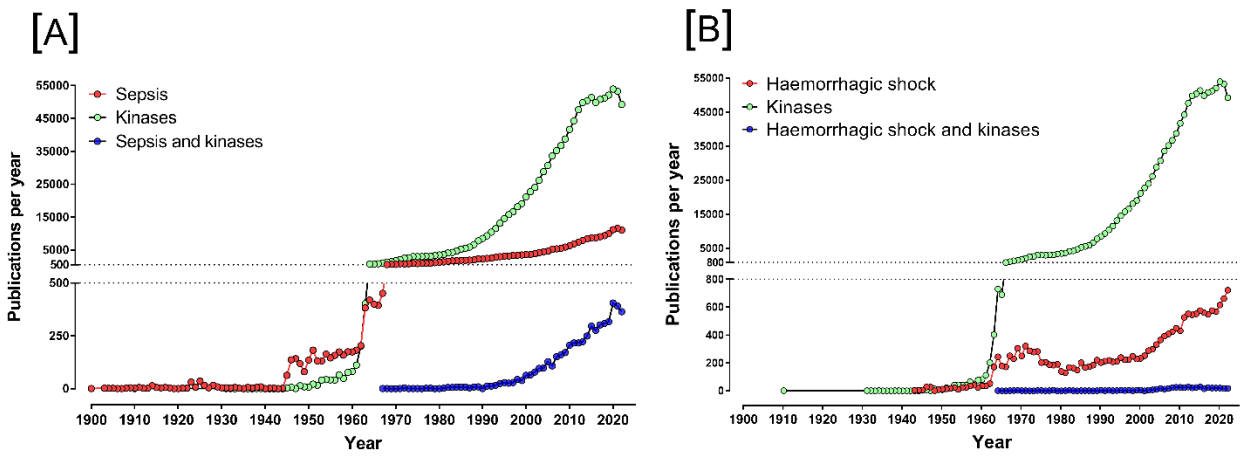

Figure 1. Number of publications related to sepsis, haemorrhagic shock and kinases over the years. *Data were obtained from Pubmed using the word combinations illustrated in the graphs.*

In the following subsections, key kinases widely explored in distinct inflammatory clinical conditions will be described, bringing them into the context of sepsis and HS and their consequently drugability.

3.2.1.1 Focal adhesin kinase (FAK) and Proline-rich tyrosine kinase-2 (Pyk2)

FAK and Pyk2 are two non-receptor proteins tyrosine kinase, belonging to the FAK family, that are activated by a variety of extracellular stimuli. FAK and Pyk2 share the same three-domain organization, with two non-catalytic domains, the band 4.1, ezrin, radixin and moesin (FERM) domain and the focal adhesion targeting (FAT) domain, linked by a central kinase domain, where the highest sequence identity (~60%) is shared among them [32]. Although FAK and Pyk2 possess similar structure, their cell/tissue expression differ. While FAK is ubiquitously expressed, Pyk2 exhibits a more restricted tissue distribution, such as endothelial cells, hematopoietic lineage cells and in the central nervous system. Interestingly, FAK and Pyk2 can synergistically orchestrate downstream signals and despite their homology, the signalling events that lead to kinase activation also differ, while FAK is mainly activated by integrins, growth factor receptors and cytokine receptors, Pyk2 has the unique ability to sense calcium ions ($Ca2^{+}$) [33][34].

The role of FAK-Pyk2 axis has been widely documented as new key players in several inflammatory responses involved in the pathogenesis of endometriosis [35], atherosclerosis [36] and asthma [37] as well as in tumorigenesis and metastasis formation [38][39]. Particularly, FAK has been demonstrated to highly stimulate TNF-α production through the activation of the NF-κB pathway [40]. On the other hand, Pyk2 has been shown to be upregulated following LPS stimulation, thereby inducing monocyte chemotactic protein-1 (MCP-1) production through a p38-MAPK pathway dependent mechanism [41]. In addition, selective inhibition of FAK by using PF573228 reduces abdominal aortic aneurysm (AAA) progression in mice by regulating macrophages polarization [42].

Intriguingly, recent findings have shown that when FAK activity is selectively suppressed (following pharmacological or genetic inhibition), there is a compensatory upregulation in Pyk2 levels [43][44]. These curious findings have suggested that selective inhibition of both proteins

may represent a potential pharmacological approach to counteract FAK-Pyk2-mediated inflammation. Indeed, some interesting studies, both *in vitro* and *in vivo* using selective FAK-Pyk2 dual inhibitor have been shown promising results in metastasis and tumour volume remission of osteosarcomas [45], as well as in the efficacy of reducing IL-1β secretion and also reducing neutrophil and macrophage infiltration in an animal model of monosodium urate (MSU)-induced peritonitis [46]. Additionally, these data corroborate the study designed by Murphy and collaborators (2019), where the authors show that double inhibition of FAK-Pyk2 more efficiently reduces the expression of adhesion molecules after stimulation of TNF-α or IL-1β when compared to selective inhibition of FAK [47]. Figure 2 summarizes the crosstalk between the FAK-PyK2 axis and potential inflammatory pathways.

Overall, so far, there are no clear experimental data reporting the role of FAK-PyK2 axis in the pathogenesis of sepsis or HS, neither potential effect of their pharmacological modulation in these clinical contexts. However, for instance, there are few evidence showing that LPS-induced endotoxemia evokes FAK activation, which contribute to exacerbate the inflammatory response, leading to organ damage and increased mortality [48][49]. Taken together, targeting this axis may represent a promising pharmacological approach in the field of sepsis/HS. In the light of this, a potential canditate for the inhibition of the FAK-PyK2 axis has emerged. PF562271 an ATP-competitive, reversible inhibitor for both FAK and Pyk2 with IC_{50} of 1.5 nmol/L and 13 nmol/L, respectively has been demonstrated effective and safe in several disease contexts [50]. Therefore, PF562271 might be a potential candidate to be repurposed to sepsis/HS since it has successfully completed a phase I clinical trial (NCT00666926) in patients with advanced solid tumors [51][52].

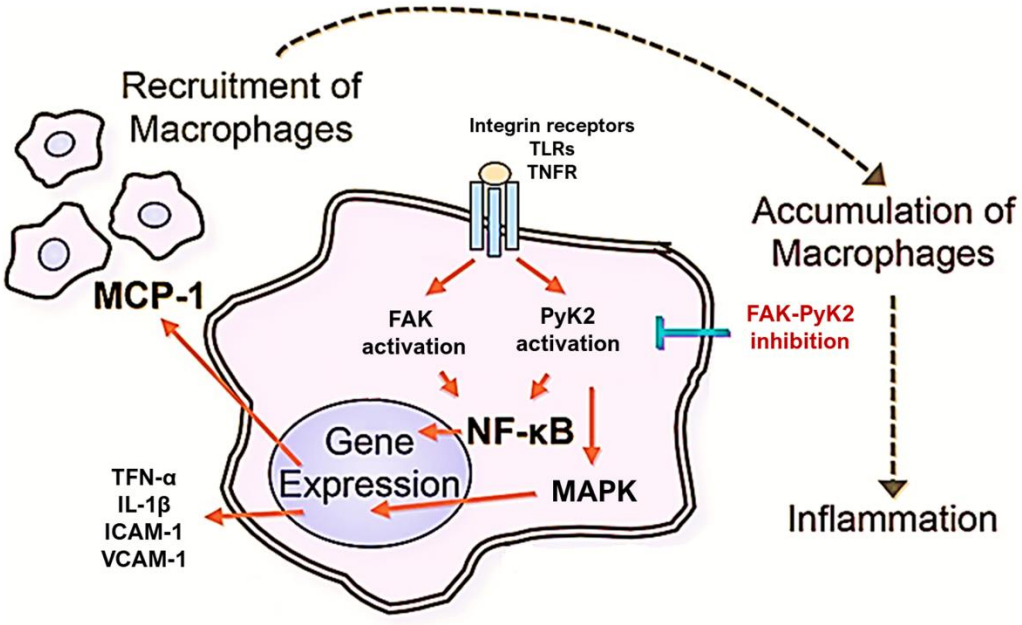

Figure 2: Overall role of FAK and PyK2 in inflammation. *Upon inflammatory stimuli, transmembrane receptors such as (Integrins, TLR, TNFR) activate intracellular FAK and PyK2, leading to activation of NF-κB and MAPK pathways, thus increasing the expression of inflammatory genes that ultimately amplify the inflammatory environment. (Modified from source: Takasuke Harada et al. Macrophage Behavior, (2016)* [42]*).*

3.2.1.2 Bruton's tyrosine kinase (BTK)

In mid-1993, mutations in BTK were first described and correlated to the immunodeficiency disease X-linked agammaglobulinemia (XLA) in humans, which leads to impaired maturation of pre-B cells into mature peripheral B cells [53]. BTK is a cytoplasmatic non-receptor protein tyrosine kinase belonging to the Tec family. In addition, BTK activity is essential in B-cell receptor (BCR)-mediated activation, thus playing a critical role in adaptive immunity. At first, BTK was thought to be expressed only in B cells, nonetheless, its expression comprises all hematopoietic cells (particularly B-lymphocytes) except for plasma cells, natural killer cells and T-lymphocytes [54].

It has been well-described that the aberrant BTK activation in B cells plays a pivotal role in the pathogenesis of B-cell malignancies, autoimmune diseases and inflammation [55][56]. Indeed, great success has been achieved in the development of covalent irreversible BTK inhibitors for the treatment of hematological malignancies, for instance Ibrutinib, a first-generation of BTK inhibitors approved by the FDA in 2013 to control a variety of B-cell tumors [55]. Later on, in 2017, a second-generation irreversible BTK inhibitior, Acalabrutinib, more selective (IC50 of 3 nM) compared to Ibrutinib, has been approved by the FDA for mantle cell lymphoma (MCL) therapy [57]. In these circumstances, driven by the COVID-19 pandemic, Ibrutinib and Acalabrunitib have been extensively evaluated to treat the inflammatory burden triggered by the SARS-CoV-2 infection [58], revealing them as promising candidates to be repurposed to sepsis and HS.

In light of this, a number of BTK inhibitors have shown efficacy in several preclinical models of inflammatory response. For instance, Ibrutinib and Acalabrutinib have already been demonstrated to be proctive against the systemic inflammation and related organ dysfunction in a murine model of sepsis [59]. These findings corroborate consistent data showing that BTK signals downstream TLR4 signaling, in which it binds to its intracellular signaling domain and the adaptor molecules MyD88 (myeloid differentiation primary response 88) and MAL (MyD88-adaptor-like), which, ultimately leads to NF-κB activation [60]. Besides, BTK overactivation contributes to activation/assembly of the NLRP3 inflammasome by directly interacting with its cytoplasmic sensor and adaptor ASC (apoptosis-associated speck like protein containing a caspase recruitment domain) thus, leading to increased caspase-1 activation, which in turn cleaves the pro-IL-1β and pro-IL-18 into their mature conformation [61]. In addition, recently, Fenebrutinib, a highly selective and reversible BTK inhibitor has been shown to be well-tolerated in Phase I clinical studies [62], along with high efficacy in reducing pro-inflammatory cytokines in patients with active rheumatoid arthritis [63]. Taken together, since NF-κB pathway and NLRP3 inflammasome complex play a pivotal role in sepsis and HS, and that BTK inhibitors have attenuated activation of those pathways, along with reducing systemic inflammation in diseases involving excessive inflammation, BTK inhibitors may represent potential candidates to be repurposed for sepsis and HS. Figure 3 summarizes the potential crosstalk between BTK and selective inflammatory pathways.

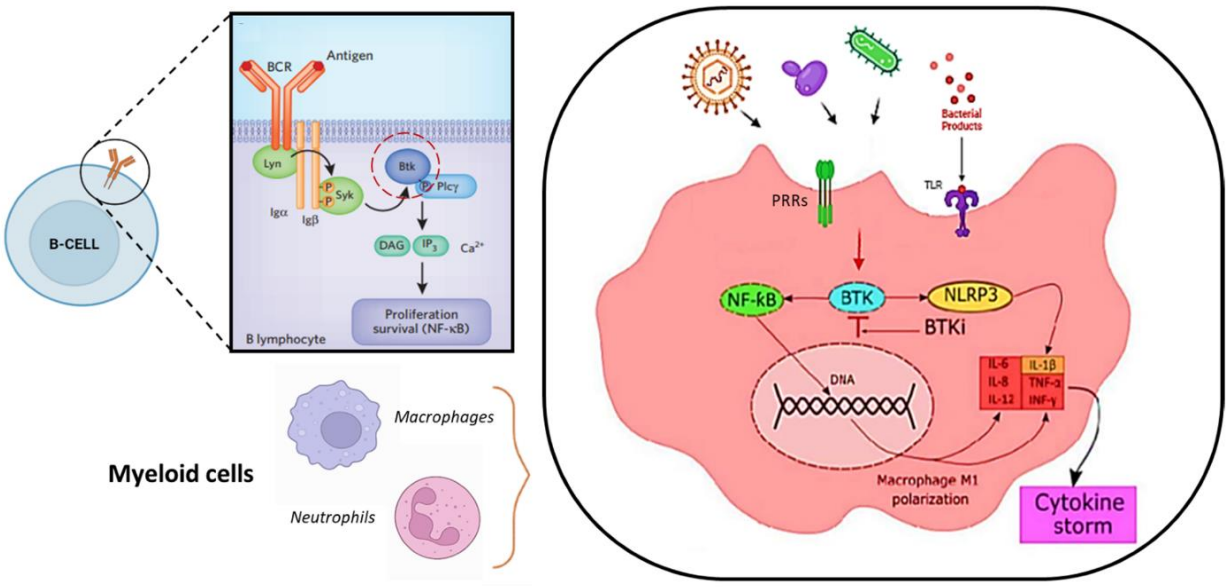

Figure 3: Role of BTK in inflammatory cells. *BTK is a critical mediator of downstream B cell receptor (BCR) signalling, however its role in myeloid cells (macrophages and neutrophils) has been extensively described. Following inflammatory signals (PAMPs and DAMPs) in immune cells, PRRs induce BTK activation, leading to activation of NF-κB and NLRP3 pathways, which then contribute to an overproduction of pro-inflammatory mediators, which ultimately leads to cytokine storm. (Modified from source: Weber A, et al. Frontiers in Immunology. (2017)* [64]*).*

3.2.1.3 Janus kinase/Signal transducer and activator of transcription (JAK/STAT) pathway

Consistent with the cytokine storm seen in sepsis and haemorrhagic shock, targeting signalling pathway downstream cytokine receptors represents an optimistic pharmacological strategy on these clinical disorders. In accordance with this, most cytokines (more than 50) have been identified to signal downstream through the JAK/STAT pathway, except for those mediators which signal through alternative molecular pathways, including TNF-α, IL-1 family members, TGF-β and chemokines [65].

The JAK family is composed of four non-receptor tyrosine protein kinases, named JAK1, JAK2, JAK3, and tyrosin kinase 2 (TYK2), which selectively bind different receptor chains. Whereas seven STAT family members have been identified (STAT1, STAT2, STAT3, STAT4, STAT5a, STAT5b and STAT6). Briefly, upon binding of pro-inflammatory mediators to cell surface receptors, JAKs become activated, leading to the recruitment and phosphorylation of STAT proteins, resulting in their dimerization. Then, dimerized STATs translocate to the nucleus across the nuclear membrane to regulate the expression of related genes [66]. Overall, JAK/STAT signalling pathway is related to various body functions and in some important biological processes, including cell proliferation, differentiation, apoptosis, immune regulation, and haematopoiesis, which in turn plays a crucial role in inflammatory, autoimmune, and myeloproliferative diseases [67]. Notably, JAK/STAT signalling has been shown to be linked to NF-κB [68] and NLRP3 inflammasome pathways during inflammation, thus further propagating pro-inflammatory signals [69][70].

To date, several EMA and/or FDA-approved JAK inhibitors to treat rheumatoid arthritis, psoriatic arthritis, atopic dermatitis, and ulcerative colitis have been clinically used [71]. Among them, a

potential candidate to be repurposed in sepsis and/or HS context is Baricitinib, a powerful JAK1/JAK2 reversible inhibitor (IC50 5.9 and 5.7 nM, respectively) which is an EMA/FDA-approved first-generation small molecule currently used for the treatment of rheumatoid arthritis and atopic dermatitis [72]. In addition, currently, Baricitinib appears to effectively lower systemic inflammation in several ongoing clinical trials in patients with COVID-19.

Besides, Baricitinib has been demonstrated to be protective in other inflammatory conditions. For instance, Collotta et al. (2020), recently showed that JAK/STAT inhibition with Baricitinib counteracts metaflammation, thereby protecting against metabolic abnormalities in mice fed a high-fat diet [73]. Additionally, Lee and collaborators (2021), reported that baricitinib effectively attenuates autoimmune features including renal inflammation in a murine model of systemic lupus erythematosus [74]. In addition to these findings, depending on the ligand and receptor, different combinations of JAK1 and JAK2 are activated with a high degree of specificity. Theses combinations signals through several cytokines/growth factors, including IL-2, -3, -4, -5, -6, -7, -9, -10, -11, -12, -13, -15, -19, -20, -21 -22, -23, -26 IFN-α, -β, -γ, G-CSF, GM-CSF, EPO and TPO [75] (Figure 4), making baricitinib even more attractive for attenuating the cytokine storm due to its similar pattern of potency against JAK1 and JAK2, which in turn amplifies its spectrum of action on inherent cytokine responses.

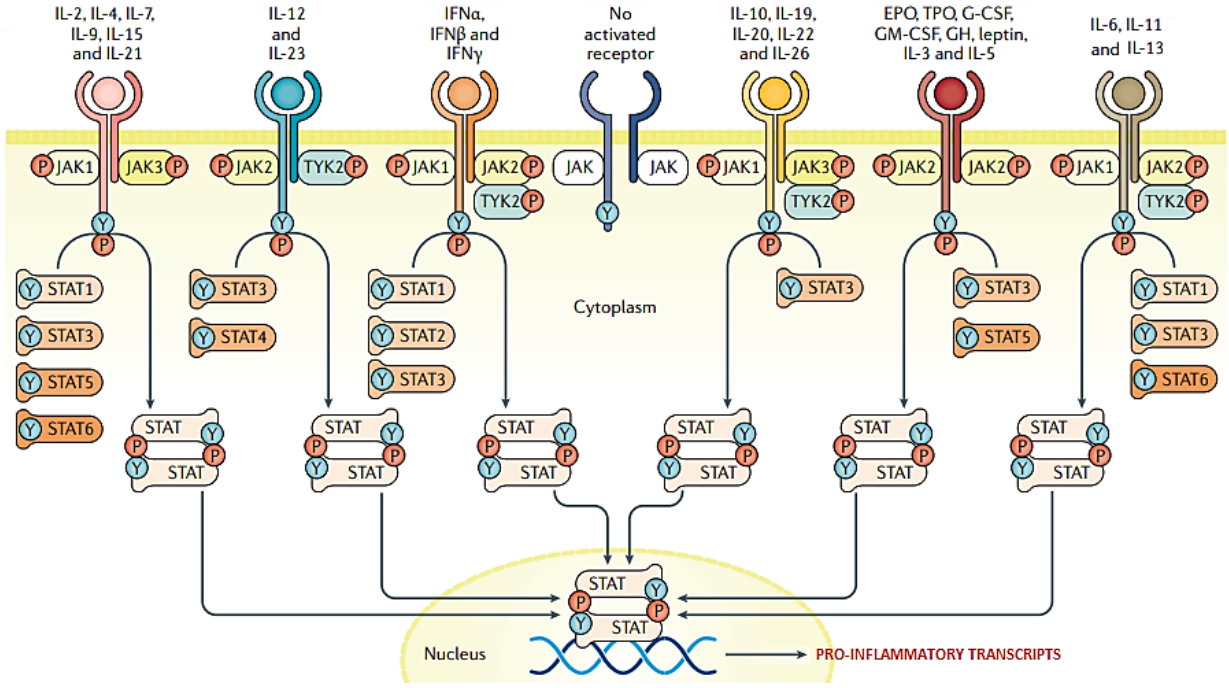

Figure 4: The JAK/STAT pathway. *Cytokines and growth factors bind to their corresponding receptors, leading to receptor dimerization and recruitment of related JAKs, then JAK activation leads to tyrosine phosphorylation of receptors and formation of docking sites for STAT. STATs are phosphorylated by tyrosine, which in turn dissociates from the receptor to form homodimers or heterodimers. Ultimately, STAT dimers enter the nucleus, bind to DNA, and regulate transcription (most pro-inflammatory transcripts). (Modified from source: Salas A, et al. Nature Reviews Gastroenterology & Hepatology (2020)*[76]*).*

3.2.2 Targeting immune cell components

Considering the relevant crosstalk between the immune system and inflammation, particularly the cytokine storm shown during sepsis and HS, which in turn plays a role in the massive recruitment of leukocytes to inflamed tissues, and thus contributing to MOF, alternatives and promising pharmacological strategies to counteract hyper-inflammation-associated MOF will be discussed in the next subsections: targeting immune cell components as a novel and potential approach to be considered in the context of sepsis and HS.

3.2.2.1 Macrophage migration inhibitory factor (MIF)

In line with the development of the cytokine storm and hence MOF during sepsis and HS, a pleiotropic cytokine so-called macrophage migration inhibitory factor (MIF) takes place. MIF is a homo-trimeric protein and has been identified as an inflammatory response potentiator due to its pro-inflammatory and chemokine-like properties [77][78]. Three decades ago, human MIF has been cloned, which contributed to the characterization of its biological activity [79]. To date, MIF has been documented to be secreted/expressed in a wide range of cell-types, including cells of the immune and nervous systems, endothelial cells, epithelial cells, endocrine cells, and macrophages [80][81]. MIF is a ligand for four transmembrane receptors, named Cluster of differentiation 74 (CD74), Chemokine (CXC motif) receptor (CXCR) 2, CXCR4, and CXCR7) which can bind to a single receptor or a complex of receptors thus, jointly activating downstream signalling pathways such as, NF-κB, MAPK and AKT (Figure 5) [82].

In inflammatory conditions, it has been shown that MIF is rapidly expressed and secreted from both immune and non-immune cells in response to several stimuli, including LPS [83], TNF-α [84] and angiotensin-II [85]. In response, MIF increases leukocyte infiltration to the site of infection and/or injury which in turn further contributes to tissue damage [86][87]. When it comes to sepsis, increased plasma levels of MIF have been found in septic patients [88], which appears to be detrimental in the septic context. Indeed, when a recombinant murine form of MIF was given to endotoxemic mice, MIF substantially enhanced the lethality of LPS-mice [89]. In contrast, administration of an anti-MIF antibody to neutralize MIF levels in a murine model of sepsis showed protective results by reducing TNF-α production and neutrophil accumulation [90]. On the contrary, the role of MIF has been poorly investigated in the HS context, however, few evidence have shown elevated plasma levels of MIF in trauma patients [91], and curiously, these high levels are further increased in trauma patients who present MOF [92].

Collectively, pharmacological inhibition of MIF activity represents a potential strategy to be repurposed in the context of HS. In light of this, ISO-1, the most extensively studied MIF inhibitor has emerged as a strong candidate [93]. Recently, ISO-1 has been shown to be protective in several inflammatory diseases, for instance, treatment with ISO-1 attenuates acute kidney injury by reducing activation of the NLRP3 inflammasome complex [94]. Similarly, ISO-1 protected mice from ischemic stroke by reducing neuronal apoptosis [95] Finally, ISO-1 protected septic mice from pro-inflammatory abnormalities and increased mice survival in severe sepsis [96]. Taken all together, ISO-1 potentially could be considered for the treatment of HS.

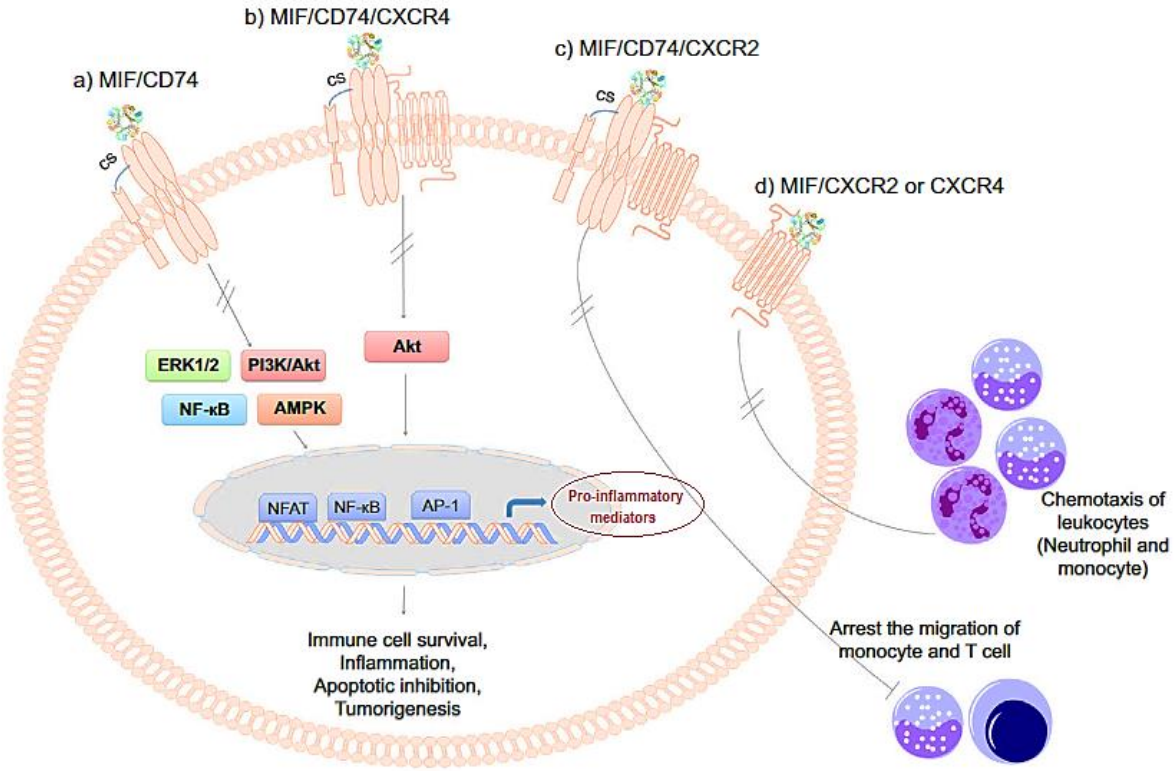

Figure 5: Functional diversity of MIF according to different MIF receptors and receptor complexes. *MIF interacts with different MIF receptors and receptor complexes, which in turn determine the functional diversity of MIF. NF-κB and MAPK are among the main pathways associated with increased expression of pro-inflammatory mediators through CD74 receptors. MIF can also act as a chemotactic cytokine by binding to CXCR2 or CXCR4 receptors. (Modified from source: Sumaiya K, et al. Pharmacology & Therapeutics (2022)* [97]*).*

3.2.2.2 Inducible T cell co-stimulator (ICOS) and ICOS ligand (ICOSL)

The immune checkpoint ICOS, also known as CD278, belongs to the CD28 family of co-stimulatory immunoreceptors. It is a type I transmembrane glycoprotein rapidly induced after T cell receptor (TCR) engagement to deliver a positive co-stimulatory signal [98]. ICOS signalling is initiated upon engagement by its unique ligand (ICOSL, also known as D275, B7-H2, B7h, B7RP-1) which belongs to the B7 family and is expressed on antigen-presenting cells (APCs) and non-hematopoietic cells under inflammatory conditions [99][100]. Over the years, the ICOS-ICOSL axis has been extensively investigated in the immune response as a potential target for the development of cancer immunotherapy.

To date, it is well described that the ICOS-ICOSL axis may display bidirectional effects. On the one hand, ICOS triggering substantially contributes to the differentiation and survival of T regulatory (Treg) cells, which play a key role in immunosuppression by inducing lymphocyte apoptosis [101][102]. On the other hand, ICOSL has been described to interact not only with ICOS, but also with another mediator named osteopontin (OPN). OPN is well known as an inflammatory mediator implicated in the pathogenesis of a variety of disease [103]. However, recently OPN has been identified as a ligand for ICOSL in which OPN binds to ICOSL in a different domain from that used by ICOS, and this interaction is characterized by the opposite effects induced by binding

to ICOS: while ICOS induces anti-inflammatory properties, OPN promotes inflammatory responses, such as increased cell migration [104].

Recent findings have shown that a soluble recombinant form of ICOS (ICOS-Fc) inhibits the adhesion of polymorphonuclear cells to umbilical vascular endothelial cells under IL-1β stimulation [105]. Furthermore, ICOSL triggering by ICOS-Fc has been documented to exert anti-inflammatory effects, such as modulating the maturation and migration of monocyte-derived dendritic cells, due to a rearrangement of inflammatory cytokine secretion [106]. In addition, through a colon carcinoma cell line, ICOS-Fc treatment has been reported to reduce the activation of inflammatory pathways, such as the p38 and ERK (MAPK) signalling pathways [105].

Although the ICOS-ICOSL axis has been extensively explored in the immune response, when it comes to sepsis, its pathological role has been poorly investigated. However, a few evidence have suggested a strict crosstalk between the immunological component and inflammation in septic context. For instance, ICOSL has been shown to be overexpressed in vascular endothelial cell under IL-1β stimuli [105]. On the contrary, septic patients show reduced ICOS expression in whole blood [107], and that reduced ICOS levels are strongly associated with organ dysfunction [108]. In line with these findings, septic patients also display increased serum levels of OPN [109]. On the other hand, in addition to these inflammatory abnormalities, it is suggestive that ICOS triggering may play a role also in the septic immunosuppressive status, where both animals and septic patients have an increased percentage of circulating Treg cells [110][111][112] and consequently, lymphopenia (reduced CD4+ and CD8+ immunocompetent T cells) [113][114]. Figure 6 summarizes the bidirectional effects of ICOS-ICOSL interaction.

Collectively, this evidence supports the hypothesis that pharmacologically modulating the ICOS-ICOSL axis might be an innovative strategy to simultaneously counteract inflammation and immunosuppression states during sepsis. In view of the complex interplay on the ICOS-ICOSL pathway, a soluble recombinant form of ICOS (ICOS-Fc) has emerged as an immunomodulatory drug that acts as antagonist of ICOS and OPN and as agonist of ICOSL. ICOS-Fc has been designed by fusing a cloned extracellular portion of human or mouse ICOS with an Fc IgG1 portion and this molecule has been shown to trigger ICOSL thus promoting downstream responses [115].

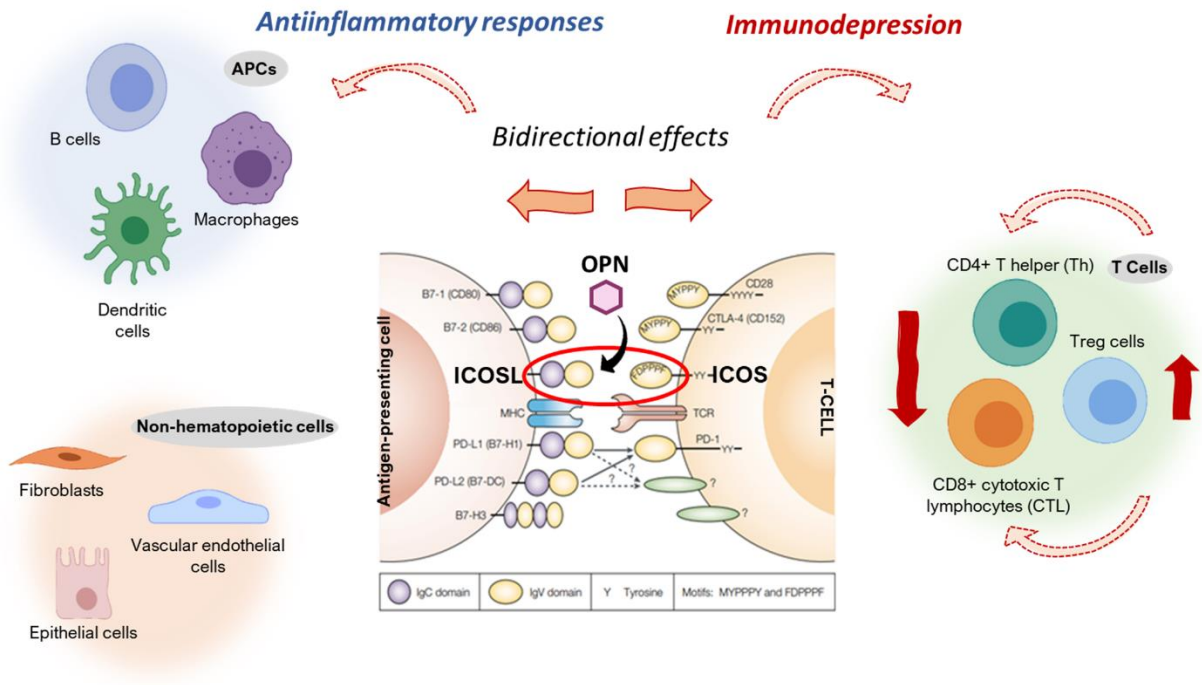

Figure 6: Bidirectional effects of ICOS-ICOSL interaction. *While ICOS is expressed on activated T cells, its unique ligand, ICOSL, is either expressed on antigen-presenting cells and in non-haematopoietic cells. ICOS interacts with ICOSL leading to bidirectional effects. On the one hand, this interaction leads to immunosuppression by reducing the lymphocytes population, on the other hand it has been shown to induce anti-inflammatory responses (reduction of cell migration and expression of pro-inflammatory genes). OPN, a pro-inflammatory cytokine, also interacts with ICOSL, however binding to an alternative domain to that used by ICOS, which in turn leads to opposite effects from those triggered by ICOS. (Modified from source: Sharpe A, et al. Nature Reviews Immunology (2002)* [116]*).*

4 METHODS

4.1 Hypothesis and research strategy

In the overview of the scientific evidence, there is a complex crosstalk involving a multitude of inflammatory and immunological components involved in the molecular mechanisms associated with organ failure in sepsis and haemorrhagic shock. The most relevant pathways whose key role has been suggested by recent findings include FAK, PyK2, BTK, JAK, MIF and ICOS-ICOSL. Thus, the central hypothesis of the present thesis is that pharmacological intervention on these key targets may represent potential treatments to counteract the cytokine storm and related multiorgan dysfunction in sepsis and/or HS.

The research strategies used in this thesis were through rodent models of sepsis and haemorrhagic shock. After the surgeries, mice or rats received selective pharmacological drugs by different routes of administration. All parameters evaluated include *in vivo*, *ex vivo* and *in vitro* analysis in acute and long-term evaluation. An overview of the studies is presented in Table 1.

4.2 Study designs

Table 1: Overview of the studies included in the thesis

	Study design	Follow-up time	Target	Pharmacological intervention
Article I (Sepsis)	**CLP** in 53 male C57BL/6 mice	24/120 h	FAK-PyK2	PF562271
Article II (Sepsis)	**CLP** in 44 male CBA and CBA/CaHN-*Btk*^{xid}/J (Xid) mice	24 h	BTK	Genetic deficiency of the BTK gene/Ibrutinib
Article III (HS)	**HS** in 92 male Wistar rats	4/24 h	BTK	Acalabrutinib/Fenebrutinib
Article IV (HS)	**HS** in 40 male Wistar rats	4 h	JAK1/2	Baricitinib
Article V (HS)	**HS** in 70 male Wistar rats	2/24 h	MIF	ISO-1
Article VI (Sepsis)	**CLP** in 72 male C57BL/6 mice	24 h	ICOSL	ICOS-Fc

Six articles were included in the thesis, comprising 3 sepsis studies (CLP) and 3 haemorrhagic shock studies (HS). Studies were performed using mice or rats, following assessments at established time points (4, 24 and 120 h) evaluations. Each study focused on a selective pharmacological intervention to a specific biological target. CLP – cecal ligation and puncture; HS – haemorrhagic shock; FAK – Focal adhesion kinase; PyK2 – Proline-rich tyrosine kinase 2; BTK – Bruton's tyrosine kinase; JAK – Janus kinase; MIF – Macrophage migration inhibitory factor; ICOSL – Inducible T cell co-stimulator ligand.

4.2.1 Animals and ethical statement

While mice were used to perform sepsis trials, rats were used to carry out haemorrhagic shock model. Thus, male Wild-type (WT, C57BL/6) mice, CBA mice, CBA/CaHN-*BTK*^{xid}/J (*Xid*) mice and Wistar rats were purchased from Envigo laboratories, (IT) and The Jackson Laboratory (Bar Harbor, ME, USA). Mice and rats were housed under standard laboratory conditions, including room temperature (25 ± 2°C) and light-controlled with free access to water and rodent chow for four weeks prior starting the experimental procedures. All animal protocols reported in this study followed the ARRIVE guidelines [117] and the recommendations for preclinical studies of sepsis provided by the MQTiPSS [118]. The procedures were approved by the University's Institutional Ethics Committee as well as the National Authorities (Ethical license numbers: 420/2016-PR, 7936220321, PCF29685, P144E44F2, 7396250219, 312/10 and 855/2021). Details on each ethical statement can be found in the articles included in this thesis.

4.2.2 Polymicrobial sepsis-induced multiple organ failure (MOF)

Articles I, II and VI were based on the septic context. Through pharmacological and/or genetic approaches, these studies were designed to investigate the role of key inflammatory targets potentially related to MOF induction. Briefly, polymicrobial sepsis was induced in male, wild-type or *Xid* mice by the caecal ligation and puncture (CLP) model. Mice were initially anesthetised in an induction chamber at (3% isoflurane delivered in oxygen 0.4 L/min), then kept under anaesthesia throughout surgery *via* nosecone at (2% isoflurane delivered in oxygen 0.4 L/min). Mice's body temperature was maintained at 37°C with a homeothermic blanket and continuously monitored with a rectal thermometer. The abdomen was opened via a mid-line incision (~1.0 cm) and the cecum was externalized. The cecum was ligated just below the ileocecal valve and punctured in a single through-and-through manner. Afterwards, a small amount (droplet ~3 mm) of faecal matter was extruded from both ends and the cecum was placed back in its anatomical position, then the musculature and skin were sutured. Sham-operated mice underwent identical surgical procedure, but without CLP (Figure 7). Immediately after surgery, both resuscitation fluid (0.9% NaCl, 50 mL/kg) at 37°C and analgesic agents (Carprofen 5 mg/kg) were given subcutaneously to all mice. Mice were constantly monitored post-surgical and then placed back into fresh clean cages. One hour after CLP or Sham-operation, mice received either pharmacological treatment or vehicle according to each experimental protocol (see details in the Table 2 and Figure 8).

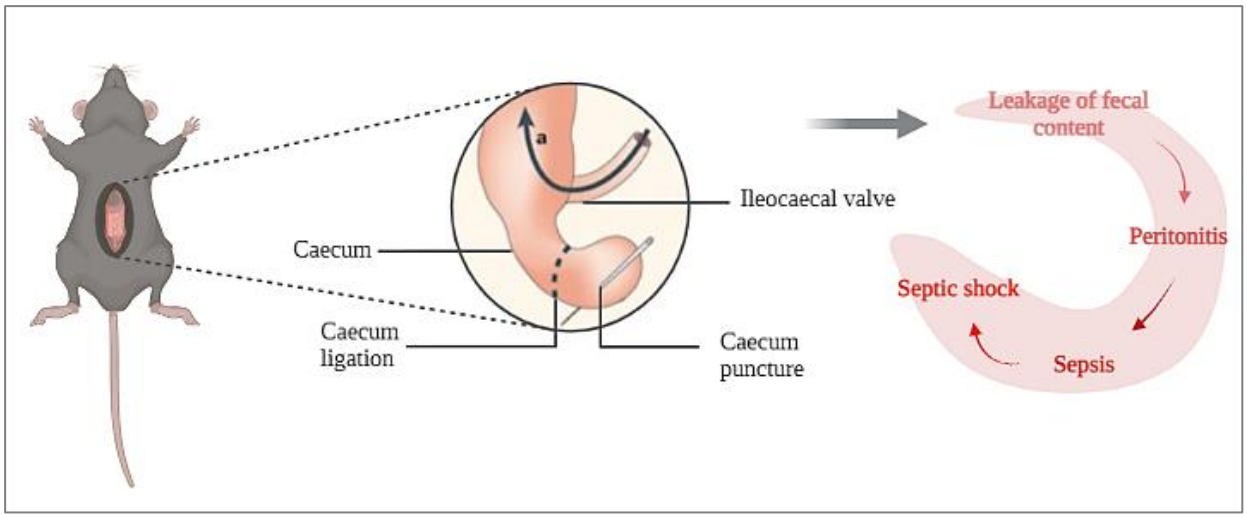

Figure 7: Experimental model of sepsis: caecal ligation and puncture (CLP). *(Modified from source: Buras, Jon A et al. Nature reviews. Drug discovery (2005)*[119]*). Sepsis was induced by CLP surgery in mice. Briefly, the cecum was externalized and ligated just below the ileocaecal valve, then a single through-and-through puncture was performed to squeeze out a small amount of faecal contents to induce local and hence, systemic infection.*

At 24 h, body temperature and a clinical score for monitoring the health of experimental mice were blindly recorded to evaluate the symptoms consistent with murine sepsis. The maximum score of 6 comprised the presence of the following signs: lethargy, piloerection, tremors, periorbital exudates, respiratory distress, and diarrhoea. An observed clinical score >3 was considered as severe sepsis, while a score between 3 and 1 was considered as moderate sepsis. Details on the clinical score are reported in the article I as supplementary material.

Table 2: Treatment schemes (sepsis studies)

	Groups	Target	Drug (dose)	Vehicle (dose)	Frequency and Route of administration
Article I	Sham CLP CLP+PF271	FAK-PyK2	PF562271 (25 mg/kg)	5% DMSO; 40% PEG 300; 5% Tween 80; 50% ddH_2O (5 µL/g)	Once (subcutaneously)
Article II	Sham WT Sham *Xid* CLP WT CLP *Xid* CLP WT+Ibrutinib CLP *Xid*+Ibrutinib	BTK (Genetic deficiency of the BTK gene)	Ibrutinib (30 mg/kg)	5% DMSO + 95% Ringer's Lactate	Once (intravenous)
Article VI	Sham CLP CLP + ICOS-Fc CLP + ^{F119S}ICOS-Fc	ICOS-ICOSL	ICOS-Fc or ^{F119S}ICOS-Fc (100 µg each)	PBS (100 µL/mouse)	Once (intravenous)

Mice were randomly divided into SHAM (false operated) or CLP (septic) groups, then CLP mice were subdivided in groups to receive either vehicle or the drug treatment (intravenous or subcutaneously). DMSO - Dimethyl sulfoxide; PEG - Polyethylene glycol; ddH_2O - double-distilled water; PBS - Phosphate-buffered saline.

4.2.2.1 Survival rate

In **article I**, to evaluate the potential long-term protection by PF271 treatment on sepsis, a survival study was performed at the Federal University of Santa Catarina (Brazil) according to the following protocol: Twenty-eight mice were subjected to CLP-induced sepsis following the same conditions previous described, and then mice were randomly allocated into two groups: CLP + Vehicle (n=14) or CLP + PF271 (received 1 hour after CLP, once subcutaneously, 25 mg/kg) (n=14). Survival rate was assessed every 12 hours over the subsequent 5 days.

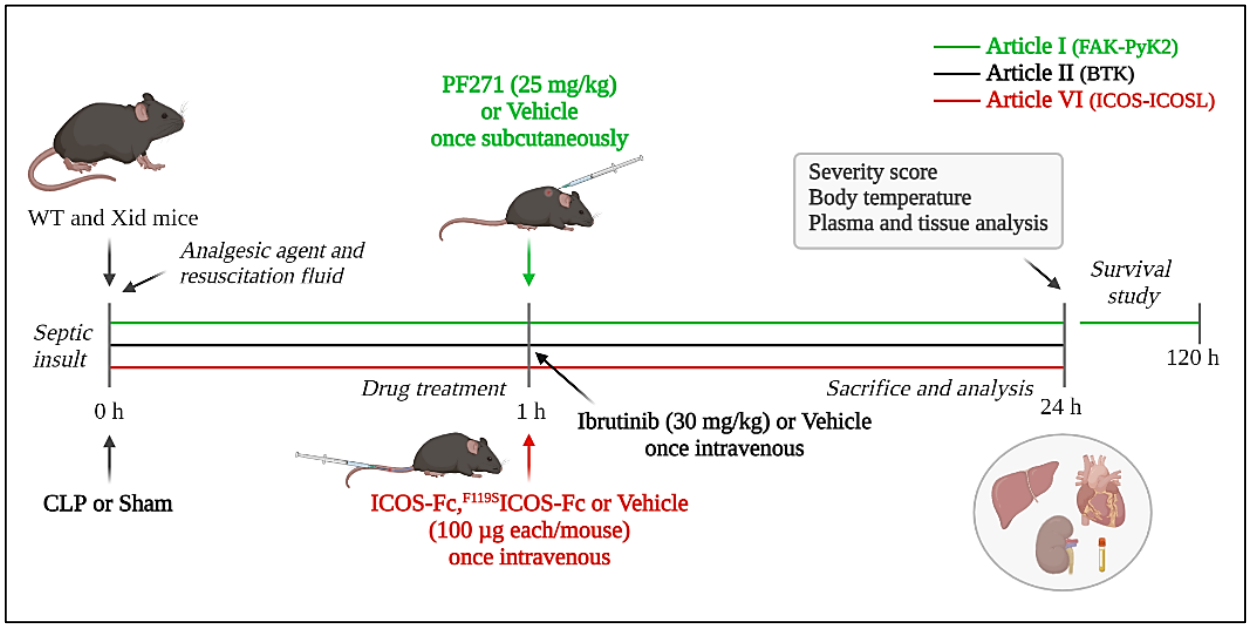

Figure 8. Timeline of the experimental design in sepsis studies. *(Created with biorender.com) sepsis. Wild-type (WT) mice and/or Xid (X-linked immune deficiency) mice were randomly selected to undergo either Sham or CLP surgery. One hour later, mice received once either Vehicle or drug treatment (PF562271 25 mg/kg, Ibrutinib 30 mg/kg, ICOS-Fc 100 µg/mouse or ^{F119S}ICOS-Fc 100 µg/mouse), intravenously or subcutaneously. At 24 h all parameters were analysed. In article I, an additional protocol has been performed following the same initial approach, however, lasting 120 h for mortality rate analysis.*

4.2.3 Haemorrhagic shock-induced multiple organ failure

Articles III, IV and V were based on the haemorrhagic shock context. Through pharmacological approaches, these studies were designed to investigate the role of key inflammatory targets potentially related to MOF induction. Briefly, rats were anesthetized with sodium thiopentone (120 mg/kg i.p. initially and 10 mg/kg i.v. for maintenance as needed). Cannulation with polyethylene catheters (Smiths Medical International Ltd., Kent, UK) of the trachea for facilitation of spontaneous breathing (internal diameter [ID] 1.67 mm), left femoral artery for blood withdrawal and for recording the mean arterial pressure (MAP) (ID 0.40 mm) and left femoral vein for either shed blood or drug administration (ID 0.40 mm) were performed. To prevent tissue desiccation, swabs moistened with PBS were placed over the surgery incision sites. Rats' body temperature was maintained at 37°C with a homeothermic blanket and continuously monitored by a rectal

thermometer. Upon the completion of surgery, the MAP was allowed to stabilize for 15 min. Blood was then withdrawn (up to 1 mL/min into heparinized syringes containing 100 IU/mL heparin mixed with normal saline) through the cannula inserted in the left femoral artery in order to achieve a fall in MAP to 35 ± 5 mmHg, which was recorded with a pressure transducer (attached to the femoral artery cannula, 844-31 Memscap, Durham, USA) and coupled to a PowerLab 8/30 data acquisition system (AD Instruments Pty Ltd., Castle Hill, Australia). Thereafter, MAP was maintained at 35 ± 5 mmHg for a period of 90 min either by further withdrawal of blood during the compensation phase or administration of the shed blood during the decompensation phase. At 90 min after initiation of haemorrhage (or when 25% of the shed blood had to be re-injected to sustain MAP at 35 ± 5 mmHg), resuscitation was performed with the remaining shed blood (mixed with 100 IU/mL heparinized saline) through the left femoral vein over a period of 5 min plus a volume of Ringer's lactate identical to the volume of shed blood (Figure 9). Right after the resuscitation step, drug treatment or vehicle was administered either intravenously or intraperitoneally according to each experimental protocol (see details in the Table 3 and Figure 10). One hour after resuscitation, an infusion of Ringer's lactate (1.5 mL/kg/h) was started as fluid replacement therapy, and it was maintained throughout the experiment for a total of 3 h. Sham-operated rats underwent the same surgical procedures, but without haemorrhage or resuscitation.

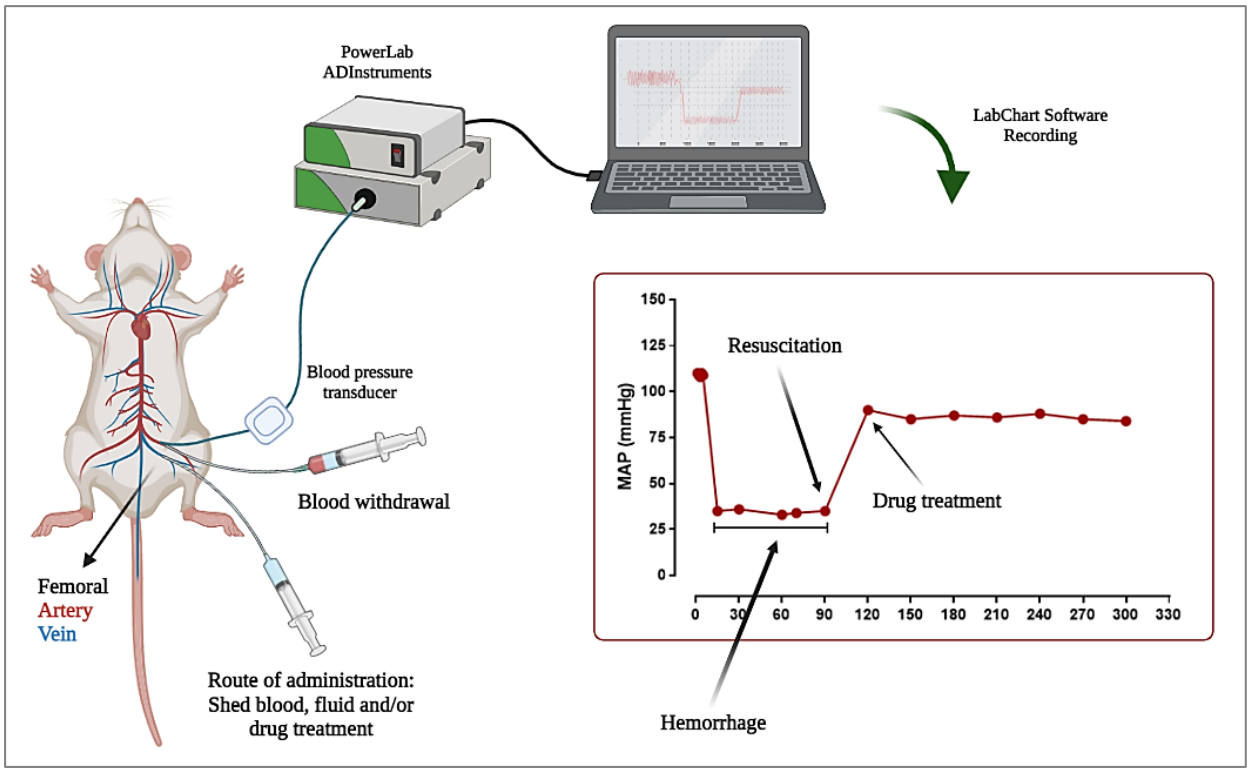

Figure 9: Experimental model of haemorrhagic shock (HS). *(Created with biorender.com) Rats underwent femoral cannulation (artery and vein) to induce haemorrhage by blood withdrawal (duration 90 min) followed by resuscitation (administration of the shed blood). Right after resuscitation, HS-rats received Vehicle or drug treatment by intravenous injection. Femoral arterial access was used to monitor blood pressure throughout the 5 h 30 min procedure.*

Table 3: Treatment schemes (haemorrhagic-shock studies)

	Groups	Target	Drug (dose)	Vehicle (dose)	Frequency and Route of administration
Article III	Sham HS HS + ACA HS + FEN	BTK	Acalabrutinib/Fenebrutinib (3 mg/kg each)	5% DMSO + 95% Ringer's Lactate	Once (intravenously)
Article IV	Sham Sham + BAR HS HS + BAR	JAK1,2	Baricitinib (1 mg/kg)	5% DMSO + 95% Ringer's Lactate	Once (intraperitoneally)
Article V	Sham Sham + ISO-1 HS HS + ISO-1	MIF	ISO-1 (25 mg/kg)	5% DMSO + 95% Ringer's Lactate	Once (intravenously)

Rats were randomly divided into SHAM (false operated) or HS (Haemorrhage) groups, then HS mice were subdivided in groups to receive either vehicle or the drug treatment (intravenous or intraperitoneally*). HS – Haemorrhagic shock; DMSO - Dimethyl sulfoxide; ACA – Acalabrutinib; FEN – Fenebrutinib; BAR – Baricitinib; JAK – Janus kinase; MIF – Macrophage migration inhibitory factor; ISO-1 [(S,R)-3-(4- hydroxyphenyl)-4,5-dihydro-5-isoxazole acetic acid methyl ester].*

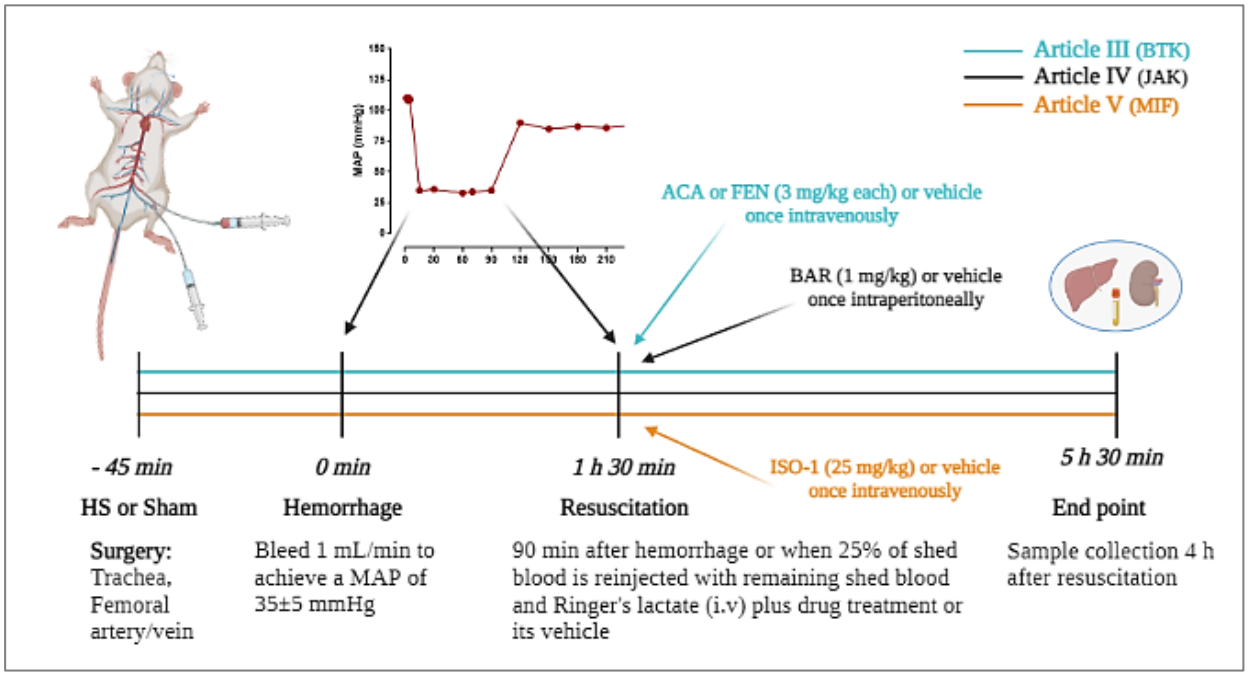

Figure 10. Timeline of the experimental design in haemorrhagic shock studies. *(Created with biorender.com) sepsis. Wistar rats were randomly selected to undergo either Sham or Haemorrhagic shock (HS) protocol. Immediately after resuscitation step, rats received once either Vehicle or drug treatment (Acalabrutinib (ACA) 3 mg/kg, Fenebrutinib (FEN) 3 mg/kg, Baricitinib (BAR) 1 mg/kg or ISO-1 25 mg/kg), intravenously or intraperitoneally. At 4 h post-resuscitation, all parameters were analysed.*

4.2.4 Overall pharmacological aspects of the drugs used in the trials

All trials were designed using potent and selective drugs, for instance PF271 as a potent inhibitor of FAK and PyK2 (IC_{50} of 1.5 and 13 nM, respectively) has been evaluated in a number of kinase screens and panels (cell-free assay), displaying >100 selectivity against all tested enzymes (Table 4) [120]. When it comes to BTK inhibitors, the three drugs tested (Ibrutinib, Acalabrutinib and Fenebrutinib) have similar potency (IC_{50} of 2.4, 10.4 and 5.3 nM, respectively). Curiously, although Ibrutinib shows slightly greater potency compared to Acalabrunitib and Fenebrutinib, it has a lower selectivity profile as shown in Table 4. Acalabrutinib and Fenebrutinib exhibit a selectivity range of 100-1000 x higher against TEC, ITK, BMX, JAK3 and EGFR, while Ibrutinib reaches a selectivity range of 0.5 – 38 x higher for the same kinases [121].

As determined by isolated enzyme assays, Baricitinib inhibits JAK1 and JAK2 almost to an equivalent degree, with IC_{50} values of 5.9 nM and 5.7 nM, respectively. Baricitinib inhibits the JAK3 and TYK2 isoforms to a much lower extent, with IC_{50} values of >500 nM and 53 nM, respectively. The rationale for developing a selective JAK1/2 inhibitor that does not inhibit JAK3 activity was to lower the immunosuppressive effects linked to pan-JAK inhibition [122]. Among the small molecule MIF inhibitors, the best characterized (ISO-1) competitively inhibits tautomerase activity at IC_{50} of 7 μM [93], which has shown similar potency to newly synthesized compounds belonging to the same chemical class, such as Alam-4b (IC_{50} of 7.3 μM) [123] and ISO-66 (IC_{50} of 4.5 μM) [124]. Furthermore, as ISO-1 is still poorly understood in terms of selectivity, an addition group (Sham treated with ISO-1) has been included in the **article V**, in order to avoid false-positive outcomes or toxic effects induced by the dose used in the trial. In the **article VI**, although there is limited information on pharmacodynamic aspects of ICOS-Fc, the dissociation constant for ICOS-Fc (Kd of 24 nM) has been reported [125], suggesting aspects of high affinity by its target. Besides, as no insights into the selectivity of ICOS-Fc has been reported so far, a mutated form of ICOS-Fc has been used at the same dose as ICOS-Fc (100 μg) to overcome potential treatment-induced off-target effects (Table 4).

Table 4: Potency and selectivity aspects of the drugs used in the studies included in the thesis

Compound	Primary target (s) (IC_{50} or Kd in cell-free assay)		Other targets (IC_{50} in cell-free assay)		Reference
PF-562271	FAK PyK2	1.5 nM 13 nM	ABL AuroraA c-SRC CDK2/CyclinA CDK5/p35	>1 μM 145 nM 797 nM 227 nM 120 nM	[120]
Ibrutinib	BTK	2.4 nM	TEC ITK BMX JAK3 EGFR	37.2 nM 91.9 nM 1.2 nM 51.8 nM 30.2 nM	[121]
Acalabrutinib	BTK	10.4 nM	TEC ITK BMX JAK3 EGFR	142.1 nM >1 μM 91.6 nM >1 μM >1 μM	[121]
Fenebrutinib	BTK	5.3 nM	TEC ITK BMX JAK3 EGFR	>1 μM >1 μM 351 nM >1 μM >1 μM	[121]
Baricitinib	JAK1 JAK2	5.9 nM 5.7 nM	JAK3 TYK2	560 nM 53 nM	[126]
ISO-1	MIF	7 μM	-	-	[93]
ICOS-Fc	ICOSL	Kd* 24 nM	-	-	[125]

Potency and selectivity aspects of the inhibitors are listed as IC_{50} values performed in cell-free assays. Kd represents equilibrium dissociation constant for ICOS-Fc. ABL - Tyrosine-protein kinase (Abelson murine leukemia virus); cSRC - Proto-oncogene tyrosine-protein kinase Src; CDK2/5 - Cyclin-dependent kinase 2/5; TEC – tyrosine kinase expressed in hepatocellular carcinoma; ITK - interleukin-2-inducible T-cell kinase; BMX - bone marrow tyrosine kinase on chromosome X; EGFR - Epidermal growth factor receptors; TYK2 - Tyrosine Kinase 2*

4.2.5 Blood collection and organ harvesting

Under deep anaesthesia, mice (24 h post-surgical procedure - sepsis) and rats (4 h post-resuscitation step - HS) were euthanized by exsanguination. Whole blood was withdrawn into vials containing (EDTA 17.1 μM/mL) and plasma content was obtained after centrifugation (13,000 *x* g, 10 min at R.T.). Organs samples (heart, kidneys, liver, and lungs) were quickly harvested and snap frozen in liquid nitrogen, then storage at in freezer at -80 °C. T. *Ex vivo* experiments were then carried out in a blinded fashion.

4.3 Cardiovascular evaluation

In **article II**, septic mice were submitted to cardiac function assessment *in vivo* 24 h after CLP. Briefly, mice were first anesthetised (3% isoflurane delivered in oxygen 0.4 L/min), then kept under anaesthesia throughout procedure *via* nosecone at (2% isoflurane delivered in oxygen 0.4 L/min). Body temperature was monitored/maintained at 37 °C. Cardiac function was assessed by M-mode and B-mode echocardiography using the VisualSonics Vevo 3100 echocardiographic system and a MX550D transducer. Ejection fraction and fractional shortening were recorded. On the other hand, in **article III**, mean arterial pressure (MAP) was recorded in rats that underwent HS insult. Through the femoral artery, a cannula was inserted and then connected to a disposable pressure transducer coupled to the PowerLab 8/30 (AD Instruments Pty Ltd., Castle Hill, Australia). Baseline values of MAP, in mmHg, were recorded in a software (LabChart7®) 4 h after the resuscitation step.

4.4 Measurement of biochemical markers of organ injury

Plasma samples from mice (sepsis) and rats (HS) were used to determine the levels of the transaminase - aspartate aminotransferase (AST) and alanine aminotransferase (ALT) (as biomarkers of liver injury), creatinine (as biomarker of kidney dysfunction), amylase (as biomarker of pancreatic damage) and creatine kinase (CK) (as biomarker of muscle injury). Biochemical markers were measured using commercially available colorimetric clinical assay kits (FAR Diagnostics, Verona, Italy) according to the manufacturer's instructions or samples were sent to an independent veterinary testing laboratory (MRC Harwell Institute, Oxford, UK) to be determined.

4.5 Systemic inflammation determination

In **articles I, II and VI**, systemic cytokine levels were determined in plasma samples using the Luminex suspension bead-based multiplexed Bio-Plex Pro™ Mouse Cytokine. In **articles I and VI** a 6-Plex Th17 panel assay (#M6000007NY) was used to measure the following cytokines (IL-1b, IL-6, TNF-a, IFN-g, IL-17 and IL-10), while in **article II**, a Bio-Plex Pro™ Mouse chemokine 31-Plex panel assay (Bio-Rad, Kabelsketal, Germany) was used to measure the following cytokines (IL-1β, −2, −4, −6, −10, −16, CCL1,−2, −3, −4, −5, −7, −11, −12, −17, −19, −20, −22, −24, −27, IFN-g, TNF-α and the chemokines CX3CL1, CXCL1, −2, −5, −10, −11, −12, −13, −16, and the growth factor GM-CSF). The assay was performed in both panels according to the manufacturer's instructions. However, in the present thesis, only some representative inflammatory cytokines were included, such as TNF-α, IL-1β, IL-6, IL-17 and IL-10.

Briefly, the technique comprises a method for simultaneously detecting multiple biological markers using microspheres (also named as beads) that are dyed with different fluorescent colors. Each color corresponds to a different marker, allowing for up to 50 markers to be distinguished within a single sample. The Bio-plex principle is similar to the traditional ELISA, however based on the fluorescent beads. Capture antibodies directed against the desired biomarker are covalently coupled to the beads. Coupled beads react with the sample containing biomarker of interest. After a series of washes to remove unbound protein, a biotinylated detection antibody is added to create a sandwich complex. The final complex is formed with the addition of streptavidin-phycoerythrin

(SA-PE) conjugate, as a fluorescent indicator. Binding of SA-PE conjugate allows the detection of a fluorescent signal, whose intensity is proportional to the amount of analyte of interest present. The results of the analysis are acquired with the Bio-Plex 200 reader, which allows simultaneous identification of a red laser (at 635 nm) emitted from the beads and of a green laser (at 532 nm) of the fluorescent signal from the phycoerythrin. The concentration of the markers in the samples, expressed in pg/mL, is proportional to the intensity of the signal detected.

In addition, in **article V**, MIF levels was determined in plasma samples from HS-rats. MIF levels were detected by commercially available ELISAs according to the manufacturer's instructions (Cusabio Biotech, Wuhan, China). Detection was read at 450 nm and 540 nm using iMark® microplate absorbance reader (BioRad).

4.6 Western blot analysis

Western blot technique was applied to **all six articles** included in the present thesis.

4.6.1 Sample extraction/preparation

Fifty mg of tissue (heart, liver, kidney) from either mice or rats were homogenized in microtubes containing 500 µL of lysis buffer solution (NaCl 150 mM; Tris-HCl 50 mM pH7.5; EGTA 1 mM; Sodium Deoxycholate 0.25%; NP-40-IGEPAL 1%; Milli-q Water (*quantum sufficit*) + a cocktail of protease inhibitors), on ice using a *Potter-Elvehjem homogenizer*. Subsequently, homogenates were centrifuged (10,000 RPM; 25 min; 4 °C) to obtain a total protein extraction. Total proteins were quantified using Bicinchoninic acid (BCA) Pierce™ assay following the manufacturer's instructions. Homogenates were then stored at -80 °C.

Once total protein extractions were prepared and quantified, 50 µg of proteins were prepared to be separated by electrophoresis. Samples were prepared in microtubes (kept in ice) by adding 50 µg of proteins, 4 µL of sample buffer solution (sample buffer 4x + Dithiothreitol - DTT) and Milli-q water (*quantum sufficit* to reach 15 µL). Samples were heated at 60°C for 10 minutes and then loaded into dodecyl sulphate polyacrylamide gel electrophoresis (SDS-PAGE) (5% stacking gel) and a (8%, 10% or 12% running gel).

4.6.1 Electrophoresis, electro-transfer and immunodetection

After loading 50 µg of proteins into the gels, electrophoresis was performed using (Mini-PROTEAN® Tetra Vertical Electrophoresis Cell, Bio-Rad Laboratories Inc, Hercules, CA, United States), containing running buffer and constant voltage at 200 V, for approximately 35 min (R.T.). At the end of the electrophoresis, proteins from the gels were transferred to a polyvinylidene fluoride (PVDF) membrane (0.45 µM) through an electro-transfer at constant voltage of 100 V for 70 min. Then, membranes were stained with Ponceau solution in order to certify the correct protein transference. The red staining was then removed from the membranes by 3 consecutive washes (5 min each), under agitation, with TBS-T solution (a tris buffered saline 1 x Tween (0,1%) solution). Afterwards, non-specific binding sites on the membranes were blocked with 10% non-fat dry milk (w/v) in TBS-T, for 1 h, at R.T. under agitation. After this step, membranes were quickly washed with TBS-T solution to remove excess blocking solution.

Following the blocking step, membranes were incubated with primary antibodies specific for the targeted protein at the dilution 1:1000 overnight, at 4°C, under agitation. The primary antibodies were prepared by diluting them in TBS 1x solution (TBS 10 x diluted in Milli-Q water) containing NaN_3 as a preservative. The primary antibodies used were: rabbit anti-Thr^{180}/anti-Tyr^{182} p38; rabbit anti-total p38; rabbit anti-Caspase-1; rabbit anti-Tyr^{397} FAK; rabbit anti-total FAK; mouse anti-Tyr^{402} PyK2; rabbit anti-NF-κB; mouse anti-$Ser^{32/36}$ IκBα; mouse anti-total IκBα; rabbit anti-$Tyr^{1007\text{-}1008}$ JAK2; rabbit anti-total JAK2; rabbit anti-Tyr^{705} Stat3; mouse anti-total Stat3; rabbit anti-$Ser^{176/180}$ IKKα/β; rabbit anti-IKKβ; rabbit anti-Tyr^{223} BTK, rabbit anti-total BTK (all purchased from Cell Signaling); mouse anti-NRLP3 (Adipogen); mouse anti-total PyK2 (Santa Cruz). In the following day, membranes were then incubated with a secondary antibody conjugated with horseradish peroxidase (HRP) at the dilution 1:10000 for 1 h at R.T. (anti-mouse or anti-rabbit, purchased from Cell Signaling). Afterwards, the membranes were stripped and incubated with rabbit anti-b-actin (Cell Signaling). Immune complexes were developed using the ECL detection system and visualized by chemiluminescence. Densitometric analysis was performed using Bio-Rad Image Lab Software 6.0.1. Results were normalized to sham bands.

4.7 Immunohistochemical staining

The immunopositivity of iNOS (**article I**) and CD68 (**article IV**) were analysed by immunohistochemistry on 10 µm frozen tissue sections of liver and kidney samples. Slides were fixed (10 min) in acetone post-sectioning. After, endogenous peroxidase activity was blocked using H_2O_2 0.3% (diluted in PBS, 2 min). Then, bovine serum albumin (BSA) 3% (Sigma Aldrich, St. Louis, MO, USA) diluted in PBS was used to block non-specific binding sites per 30 min. While liver and kidney sections (**article I**) were incubated over 2 hours with primary antibodies at room temperature (NOS-2, Santa Cruz, #sc-651, dilution 1:50), renal sections (**article IV**) were incubated with anti-CD68 (1:500; abcam, Cambridge, United Kingdom) in 1% BSA in PBS overnight at 4°C. Subsequently, sections were incubated with HRP-conjugated secondary antibodies or biotinylated anti-rabbit IgG (dilution 1:200; Vector Laboratories, Burlingame, CA, USA) for 1 h. The chromogenic detection was obtained by adding 3,3'-diaminobenzidine (DAB; Vector Laboratories, Burlingame, CA, USA) substrate (2 min of exposition). Finally, the nucleus was counterstained with haematoxylin (10 minutes) and washed in tap water for 7 min. Slides were then immersed in different grades of alcohol for the dehydration: Ethanol 75%, Ethanol 95%, Ethanol 100% (3 min each) and then in Xylol I and Xylol II for 1 minute each. Afterwards, slides were mounted for imaging by using 3-4 drops of the medium (DPX Mountant histology) to attach a cover glass. CD68 staining was quantified by counting positive caskets of a grid (10 x 10) in 20 adjacent cortical areas per section (40x magnification). Images were taken using a KEYENCE BZ-X800 microscope and BZ-X800 viewer after performing white balance and auto exposure.

4.8 Myeloperoxidase (MPO) activity assay

About 100 mg of liver, kidney and lungs samples were homogenised (1:5 w-v) in ice-cold 20 mM sodium phosphate buffer (pH 7.4), and then centrifuged (13,000 g, 10 min, 4 °C). The supernatants were discarded, and the pellets were recovered. Afterward, 500 µL of hexadecyltrimethylammonium bromide buffer (0.5% HTAB in 50 mM sodium phosphate buffer, pH 6.0) was added and the pellets were resuspended. There was an additional step for kidney

tissues, where samples were heated at 60 °C for 2 h in order to remove interfering peroxidases [127]. A second centrifugation (13,000 g, 10 min, 4 °C) for any sort of tissues was again performed. The supernatants (30 µL) were then assessed for myeloperoxidase activity by measuring the H_2O_2-dependent oxidation of 3,3′,5,5′-tetramethylbenzidine (TMB), in which 180 µL of H_2O_2 (final concentration 0.3 mM) diluted in 0.08 M sodium phosphate buffer, pH 5.4, and 20 µL of TMB (final concentration 1.6 mM) dissolved in Milli-q H_2O. In its oxidised form, TMB has a blue colour, which was measured spectrophotometrically. The 96-well plate was incubated for 10 min at 37 °C and the optical density (O.D. 650 nm) was measured every two min. The final supernatant was also used to quantify the protein content, which was determined using a BCA protein assay (Pierce Biotechnology Inc., Rockford, IL, USA) following the manufacturer's instructions. A 5 min incubation time was used, and MPO activity was expressed as optical density at 650 nm per mg of protein.

4.9 (Re)analysis of gene expression in whole blood from critically ill patients

Published datasets were reanalysed on septic and trauma whole blood for targeted genes. In **article II**, BTK gene expression in whole human blood of septic and healthy patients were reanalysed. Original data was obtained from the Gene Expression Omnibus (GEO) under dataset number GDS4971 which was published by Parnell et al [128]. RNA was extracted from whole blood of patients confirmed with sepsis (and healthy participants) over a 5 day time course and analyzed for gene expression via microarray Illumina GenomeStudio V2010.3. Three groups were collected, healthy participants (n = 18), septic survivors (n = 26), and septic non-survivors (n = 9). Besides, in **articles III and IV**, original data were obtained under Gene Expression Omnibus (GEO) accession GSE36809, published by Xiao and colleagues [129]. RNA was extracted from whole blood leukocytes of severe blunt trauma patients (n = 167) over the course of 28 days and healthy controls (n = 37) and hybridized onto an HU133 Plus 2.0 GeneChip (Affymetrix) according to the manufacturer's recommendations. The datasets were reanalysed for BTK (**article III**), JAK2 and STAT3 (**article IV**) gene expression.

4.10 Statistical analysis and data presentation

Statistical analysis is briefly described in this section and detailed in the legends of each figure. Power analysis for the study design through G-Power 3.1™ software [130]. Data were expressed as dot-plots for each animal and as mean ± SD/SEM or median with range of *n* observations, where *n* represents the number of animals/experiments/subjects studied. The standard distribution of data was verified by Shapiro-Wilk normality test and the homogeneity of variances by Bartlett test. The statistical analysis was performed by one/two-way ANOVA, followed by Bonferroni's post-hoc test. Data that were not normally distributed, non-parametric statistical analysis was applied through Kruskal-Wallis followed by Dunn's post hoc-test. Differences in the survival study were determined with a logrank (Mantel-Cox) test. A P value <0.05 was considered significant. Statistical analysis was performed using GraphPad Prism® software version 7.05 (San Diego, California, USA).

In order to achieve the first aim of the present thesis, selective kinases were pharmacologically targeted in both rodent models of sepsis and haemorrhagic shock.

5.1 Targeting kinases as pharmacological strategies to counteract multiorgan dysfunction in sepsis and haemorrhagic shock

FAK and Pyk2, two non-receptor proteins tyrosine kinase, that are activated by a variety of extracellular stimuli, thereby mediating a series of inflammatory cascades, were investigated in the context of sepsis. Through a potent dual inhibitor PF562271, selective inflammatory pathways were analysed as well as the long-term effects of FAK-PyK2 inhibition.

5.1.1 Pharmacological inhibition of the FAK-PyK2 pathway with PF562271 confers organ protection in sepsis by counteracting hyperinflammatory state

The first study design (**article I**), we have shown protective effects of PF271 in a murine model of sepsis. Selective inhibition of FAK and PyK2 proteins attenuated sepsis-induced liver and kidney damage as reported by reduced systemic levels of the biochemical markers AST, ALT (hepatic injury) and creatinine (renal dysfunction) (Figure 11).

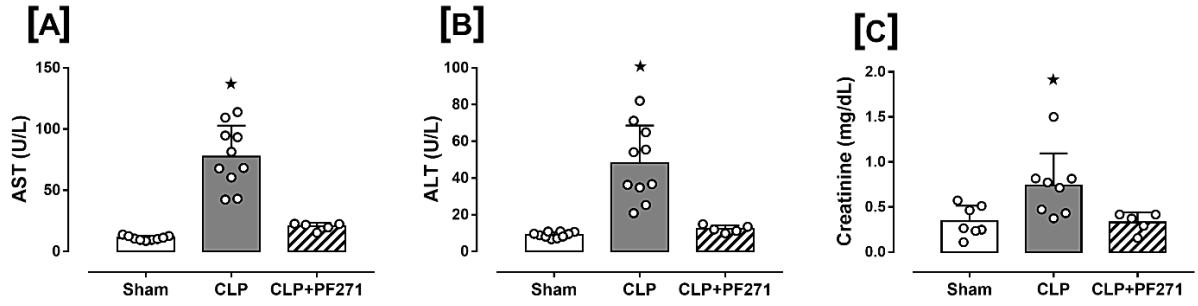

Figure 11: Effect of PF271 Administration on systemic levels of organ damage biomarkers during experimental sepsis. *Mice were randomly selected to undergo Sham or CLP surgery. One hour later, CLP mice were treated once with either vehicle or PF271 (25 mg/kg s.c.). Twenty-four hours after Sham or CLP procedure, the animals' blood was collected and plasma levels of aspartate transaminase (AST)* ***[A]****, alanine transaminase (ALT)* ***[B]*** *and creatinine* ***[C]*** *were determined. Data are expressed as dot plots for each animal and as mean ± SD of 5-10 mice per group. Statistical analysis was performed by one-way ANOVA followed by Bonferroni's post hoc test. *p < 0.05 CLP vs Sham/CLP+PF271.*

We then speculated which might be the possible molecular mechanisms involved in sepsis-induced organ damage. Although consistent evidence suggests a key role of FAK-PyK2 in inflammation [131][132], the role of these two kinases in the septic context remains unclear. We deepened our analyses at the local level (hepatic and renal tissue) and, to be best of our knowledge, we reported here for the first time that, FAK-PyK2 does indeed play a role in the pathogenesis of sepsis, by showing increased phosphorylation of Tyr^{397} on FAK (panels A-B) and Tyr^{402} on PyK2 (panels C-D), suggesting an increased enzyme activation during the septic insult. Furthermore, we confirmed the ability of PF271 to effectively interfere with its pharmacological targets, showed by reduced activation of both FAK and PyK2 in septic mice (Figure 12). Additionally, in septic mice tissues we showed an overactivation of a member of the MAPK pathway (p38) which signals downstream

the FAK-PyK2 pathway (panels E-F, Figure 12). Its activation represents one of the major contributors to a pro-inflammatory status in sepsis, due to an excessive transcription of cytokines [131][133] .

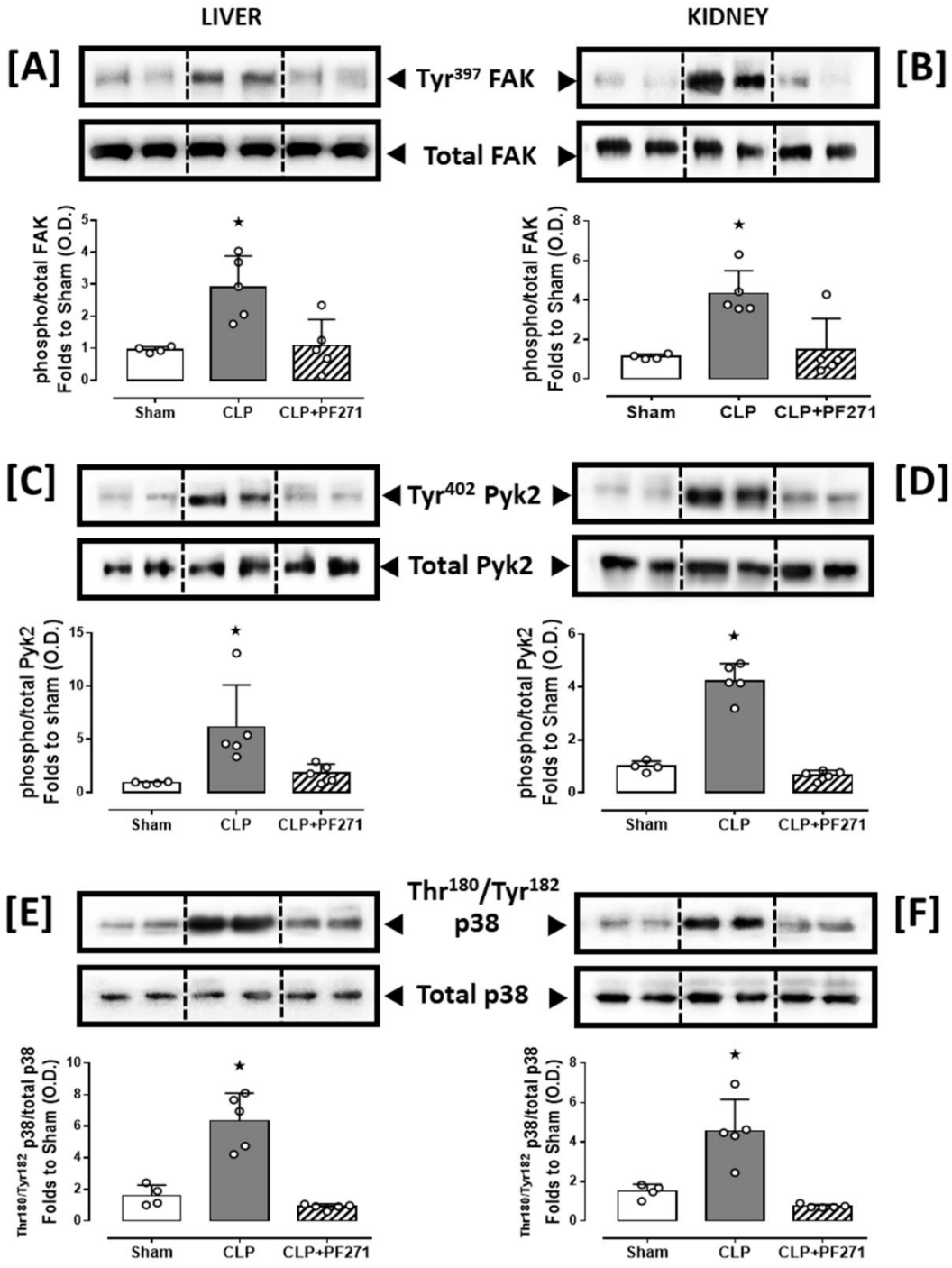

Figure 12: Effect of PF271 on tissue activation of FAK-PyK2 pathway during experimental sepsis. *Mice were randomly selected to undergo Sham or CLP surgery. One hour later, CLP mice were treated once with either Vehicle or PF271 (25 mg/kg s.c.). Twenty-four hours after Sham or CLP procedure, liver and kidney were harvested, and the total protein was extracted from them. Western blotting analysis for phosphorylation of Tyr^{397} on FAK in the liver* ***[A]*** *and kidney* ***[B]*** *were normalized to total FAK; Phosphorylation of Tyr^{402} on PyK2 in the liver* ***[C]*** *and kidney* ***[D]***

*were normalized to total PyK2; Phosphorylation of Thr^{180}/Tyr^{182} on p38 in the liver **[E]** and kidney **[F]** were normalized to total p38. Densitometric analysis of the bands is expressed as relative optical density (O.D.). Data are expressed as dot plots for each animal and as mean ± SD of 4-5 mice per group. Statistical analysis was performed by one-way ANOVA followed by Bonferroni's post hoc test. *p < 0.05 CLP vs Sham/CLP+PF271.*

Indeed, we have confirmed in our experimental model of sepsis a systemically excessive release of several pro-inflammatory cytokines thus, leading to the so-called "cytokine storm", which is one of the main drivers of organ dysfunction associated to sepsis [134]. Interestingly, inhibition of the FAK-PyK2 pathway lowered sepsis-induced cytokines release, revealing a possible central organ protection mechanism triggered by PF271 (Figure 13).

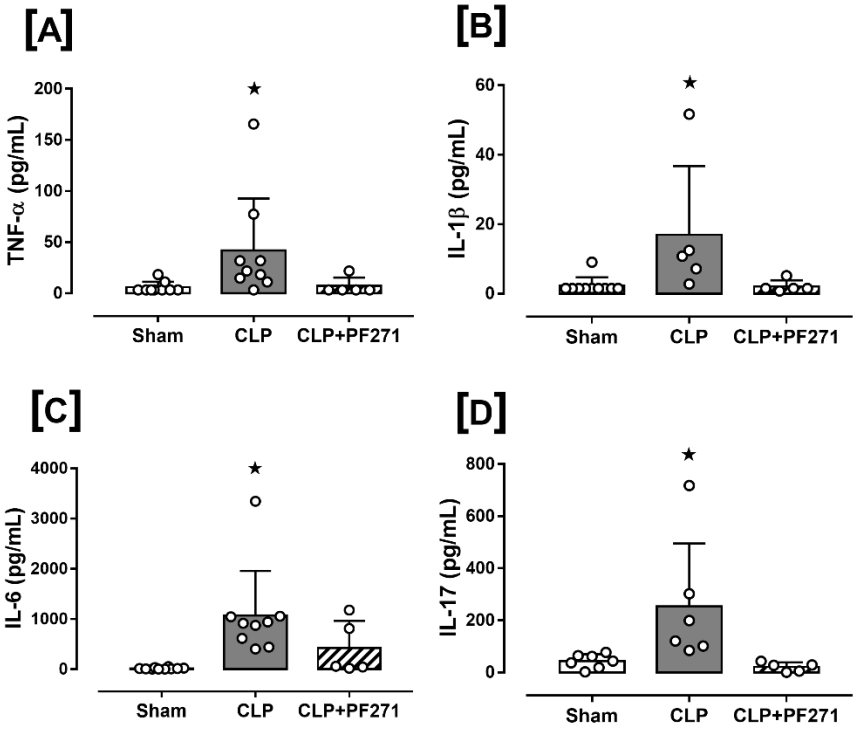

Figure 13: Effect of PF271 on systemic cytokines during experimental sepsis. *Mice were randomly selected to undergo Sham or CLP surgery. One hour later, CLP mice were treated once with either Vehicle or PF271 (25 mg/kg s.c.). Twenty-four hours after Sham or CLP procedure, the animals' blood was collected. Plasma levels of TNF-a **[A]**, IL-1β **[B]**, IL-6 **[C]** and IL-17 **[D]** were determined. Data are expressed as dot plots for each animal and as mean ± SD of 5-10 mice per group. TNF-a, IL-17, and IL-6 were statistically analyzed by one-way ANOVA followed by Bonferroni's post hoc-test, while IL-1β was analyzed by Kruskal-Wallis followed by Dunn's post hoc-test. *p < 0.05 CLP and/or CLP+PF271 vs Sham.*

In line with the detrimental inflammatory markers in sepsis, we have reported an aberrant increase in iNOS expression (Figure 14). Both septic shock and PF271 treatment affected the renal and hepatic expression of iNOS. Interestingly, iNOS expression has been demonstrated to be induced either via the p38 MAPK pathway following LPS stimulation [135] and via FAK and/or PyK2 pathway [136][137], thus suggesting an intriguing cross-talk mechanism linking the FAK/PyK2/p38 axis in inducing iNOS expression during sepsis. This excessive expression of

iNOS in the context of sepsis represents a harmful mediator in the pathogenesis of the disease, being responsible for producing high levels of nitric oxide (NO), which in its excessive concentration, it is directly associated with hypotension and hyporeactivity to vasoconstrictors [138][139], along with events related to cytotoxicity [140]. However, based on these primary findings, such aspects linking the protective effects of PF271 (reduced iNOS expression) and hyporeactivity to vasoconstrictors in sepsis should be deepened considering the relevance of this clinical complication.

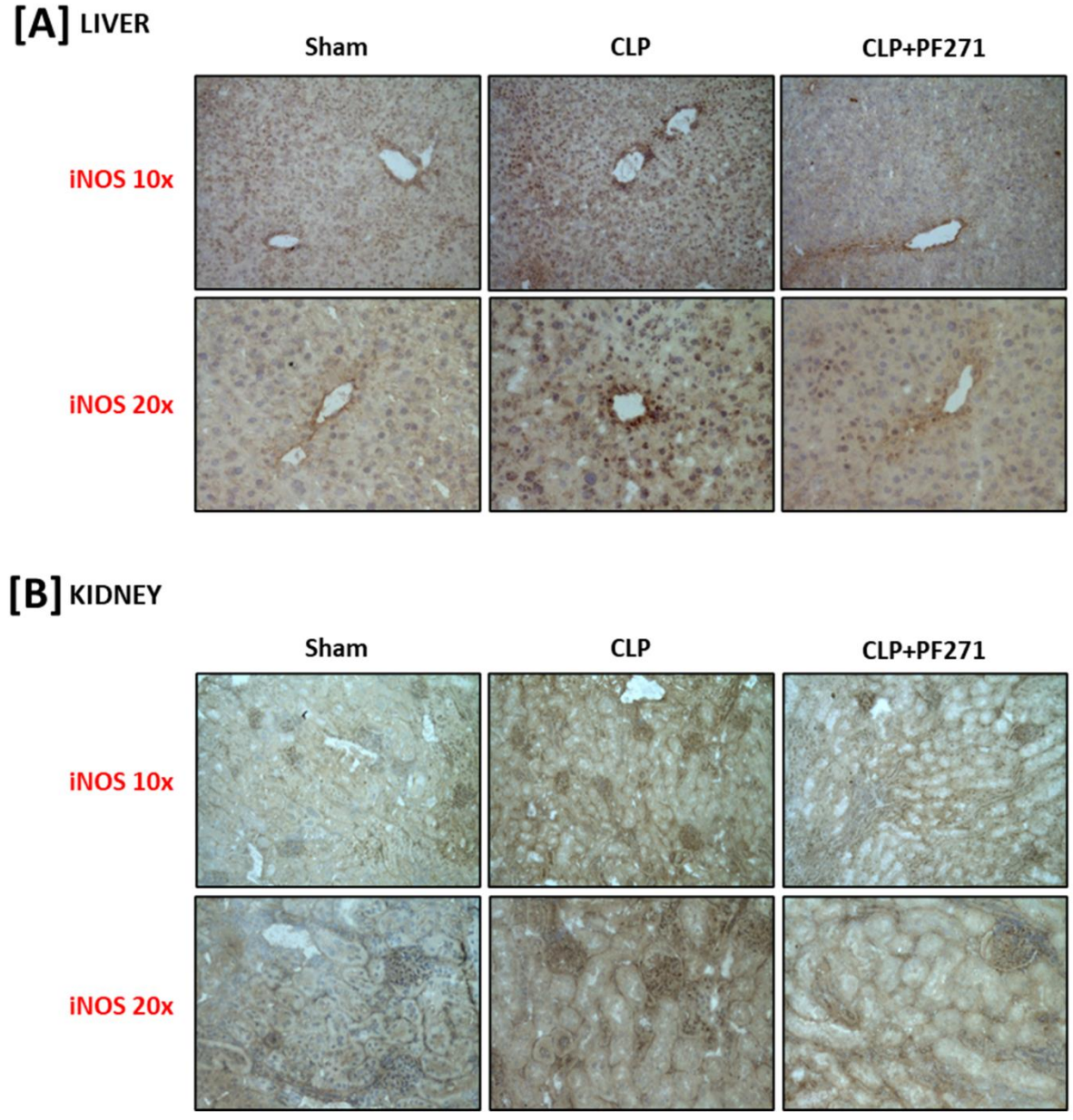

Figure 14: Effect of PF271 on tissue expression of iNOS during experimental sepsis. *Mice were randomly selected to undergo Sham or CLP surgery. One hour later, CLP mice were treated once with either Vehicle or PF271 (25 mg/kg s.c.). Twenty-four hours after Sham or CLP procedure, liver and kidney were harvested. Tissue sections were prepared to identify iNOS expression through immunohistochemistry assay in liver* ***[A]*** *and kidney* ***[B]****. Representative photomicrographs at 10x and 20x magnification were recorded of 5 animals per group.*

The most relevant outcome of this study from a translational point of view is that PF271 confers not solely acute but also long-term protection, demonstrated by the prolonged survival of septic mice treated with FP271 (Figure 15), which provides an opportunity for the repurposing of this small molecule for use in patients with sepsis, since PF271 has already been tested in a phase I clinical trial in oncology (NCT00666926) [51][52].

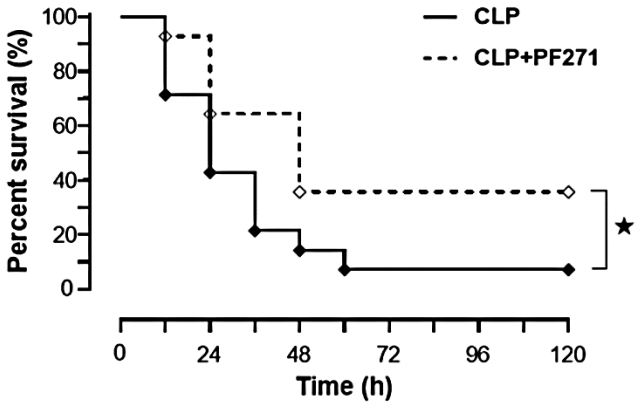

Figure 15: Effect of PF271 on the survival of septic mice. *Mice were randomly selected to undergo Sham or CLP surgery. One hour later, CLP mice were treated once with either Vehicle or PF271 (25 mg/kg s.c.). The mortality rate was recorded over a 5-day period. A log-rank test was used for the comparison of the survival curves (n = 14 mice per group). *p < 0.05 CLP vs CLP+PF271.*

We next investigated the role of Bruton's tyrosine kinase (BTK), a well-known protein kinase critical for the B-cell antigen receptor (BCR) signalling pathway in the septic context. BTK which is also involved in the activation of the TLR signalling pathways and the NLRP3 inflammasome were here investigated through a genetic deficiency of the BTK gene alone in *Xid* mice.

Accordingly, this key protein kinase (BTK), known to be linked with inflammatory disorders has raised wide attention as a potential target in sepsis. Indeed, it has recently been documented that BTK inhibition with Ibrutinib attenuates systemic inflammation and MOF in septic mice [141]. Ibrutinib is an approved drug for the treatment of several diseases, such as chronic lymphatic leukaemia, mantle cell lymphoma, Waldenstrom macroglobulinemia, and graft vs. host disease [142]. However, targeting kinases with selective small molecules has always been a challenge, which in turn, despite the protective effects observed in the previously mentioned study [141], perhaps some of them possibly are due to the well-known off-target effects of Ibrutinib, as it strongly inhibits other kinases, such as Bmx, ErbB4, RIPK2 and TEC. Therefore, the next study (**article II**) has been designed to elucidate these issues.

5.1.2 Selective BTK inhibition protects septic mice from cardiac dysfunction

Firstly, in the present study (**article II**) we have reinforced the relevance of BTK in humans with sepsis, by revealing an impressive increase in BTK expression in whole-blood from non-survivors septic patients, which was not observed in survivors participants (Figure 16). These data strengthen the hypothesis that pharmacological intervention in this pathway during sepsis may be suitable.

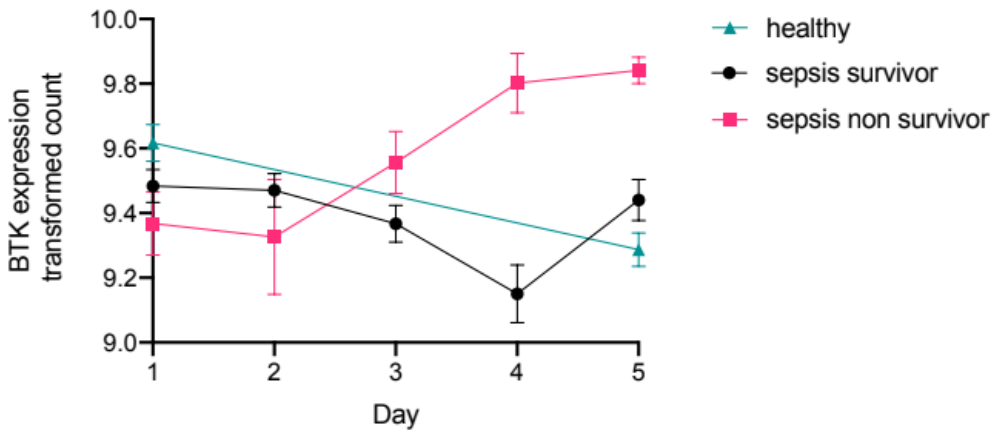

Figure 16: Time course of BTK expression in whole human blood of septic and healthy patients. *Original data was obtained from the gene expression omnibus under dataset number GDS4971 which was published by Parnell et al.* [128]. *Whole blood of patients confirmed with sepsis (and healthy participants) over a 5 day time course. RNA was extracted from whole blood and analyzed for gene expression via microarray Illumina GenomeStudio V2010.3. Three groups were collected, healthy participants, septic survivors, and septic non-survivors. Significance was determined by one-way ANOVA followed by Bonferroni post hoc-test. Data are expressed as mean ± SEM.*

Then, in order to elucidate the role of BTK in sepsis, this study has been conducted through a model of sepsis using X-linked Immunodeficient (*Xid*) mice, (mice with a missense mutation in the BTK gene, resulting in impaired functional BTK).

As the development of cardiac dysfunction affects 40% of septic patients [143], leading to an increased mortality rate of 70–90% in comparison to 20% mortality in patients who do not present cardiac dysfunction [144], here we focused our investigation on the cardiac system as it plays a pivotal role in the pathogenesis of sepsis. We showed that WT-CLP mice developed severe systolic cardiac dysfunction by reducing the ejection fraction (EF, panel B) and fractional shortening (FS, panel C) (Figure 17). Interestingly, when compared with WT-CLP mice, the degree of cardiac dysfunction (EF and FS) measured in CLP-*Xid* mice, WT-CLP mice + Ibrutinib or CLP-*Xid* mice + Ibrutinib were significantly lower following the genetic or pharmacological interventions. In contrast, administration of Ibrutinib to CLP-*Xid* mice had no additional effects on cardiac function, indicating that the beneficial effects of Ibrutinib are not due to off-targets effects of the drug.

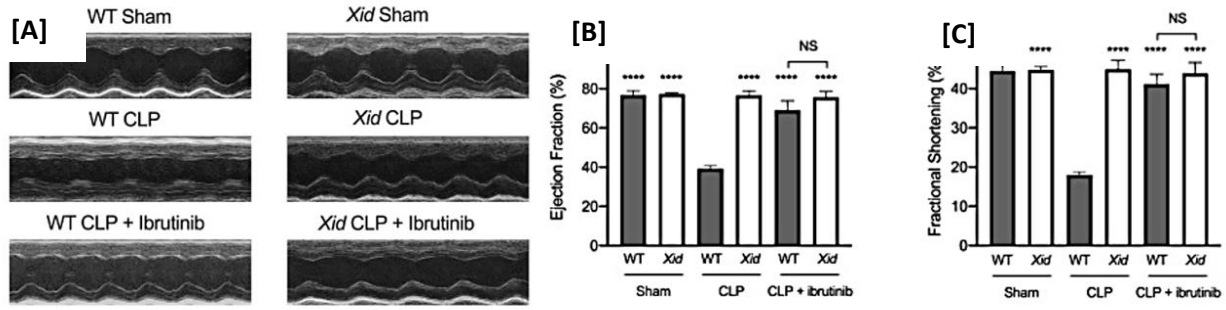

Figure 17: Xid mice are protected from sepsis-induced cardiac dysfunction. *WT and Xid mice were randomly selected to undergo sham or CLP surgery, 1 h later ibrutinib (30 mg/kg) was administered intravenously. At 24 h after CLP, cardiac function was assessed by echocardiography.* ***[A]*** *Representative m-mode images,* ***[B]*** *Ejection Fraction (%) and* ***[C]*** *Fractional shortening (%). The following groups were studied WT sham (n = 5), Xid sham (n = 5), WT-CLP (n = 10), Xid-CLP (n = 10), WT-CLP + ibrutinib (n = 8), and Xid-CLP + ibrutinib (n = 6). Data were expressed as mean ± SEM and analyzed by one-way ANOVA with a Bonferroni post hoc-test. *P < 0.05, **P < 0.01, ***P < 0.001, and ****P < 0.0001 vs. WT-CLP.*

We then speculate what could be the possible molecular mechanisms behind BTK inhibition in cardiac protection. We decided to explore the NLRP3 inflammasome, as its activation has been widely reported as a key player in the pathophysiology of sepsis and septic cardiomyopathy [145]. In addition, several evidence has shown strong involvement of BTK in the activation of NLRP3 complex [141][146][147]. To elucidate these issues, we performed western blot experiments in cardiac tissues from septic mice and reported that experimental sepsis does increase cardiac BTK activation (phosphorylation on Tyr^{223}) leading to an overactivation/expression of the NLRP3 complex and hence, an increase in activated-caspase-1. Impressively, CLP-mice carrying a BTK deficiency were protected from these sepsis-induced abnormalities (Figure 18). This dataset confirms that BTK inhibition contributes to reduced sepsis-related inflammation and organ dysfunction.

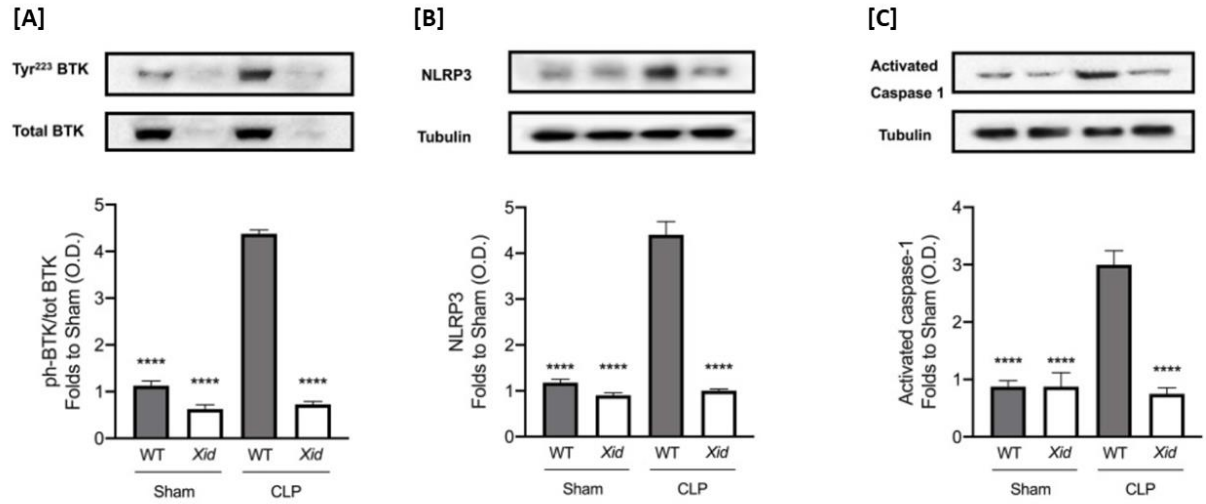

Figure 18: BTK and NLRP3 inflammasome are not activated in Xid mice after experimental sepsis. *Mice underwent sham-operated or CLP surgery and 24 h later signaling pathways in the*

*cardiac tissue were assessed. Densitometric analysis of the bands is expressed as relative optical density (O.D.) of **[A]** phosphorylation of BTK on Tyr223 corrected for the corresponding total BTK and normalized using the related sham bands, **[B]** NLRP3 activation, corrected against tubulin and normalized using the sham related bands and **[C]** Pro-caspase-1 against activated caspase-1 and normalized using the sham related bands. The following groups were studied WT sham, Xid sham, WT-CLP and Xid-CLP (n = 4 per group). Data are expressed as mean ± SEM and analyzed by one-way ANOVA with a Bonferroni post hoc-test. ***P < 0.001 and ****P < 0.0001 vs. WT-CLP.*

Considering the most relevant inflammatory pathways related to BTK activity, we were also able to demonstrate the ability of BTK deficiency/inhibition in reducing the burden of pro-inflammatory cytokines (TNF-α, IL-6 and IL-1β) caused by sepsis, with no additional effects (neither beneficial nor harmful) induced by Ibrutinib in CLP-*Xid* mice (Figure 19).

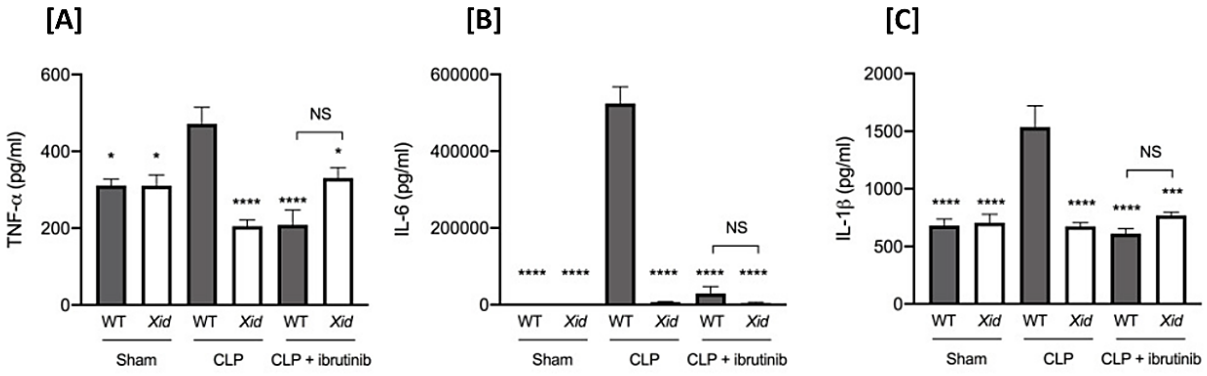

Figure 19: Xid mice do not present with systemic inflammation after polymicrobial sepsis. *Mice underwent sham or CLP surgery, 24 h later cytokines were assessed in serum. **[A]** TNF-α (pg/ml), **[B]** IL-6 (pg/ml) and **[C]** IL-1β (pg/ml). WT sham (n = 5), Xid sham (n = 5), WT-CLP (n = 10), Xid-CLP (n = 10), WT-CLP + ibrutinib (n = 8), and Xid-CLP + ibrutinib (n = 6) were studied. Data are expressed as mean ± SEM and analyzed by one-way ANOVA with a Bonferroni post hoc-test. *P < 0.05, ***P < 0.001, and ****P < 0.0001 vs. WT-CLP.*

In line with these findings, once we have seen the beneficial effects of BTK inhibition in counteracting systemic inflammation in sepsis [141], as well as in other disease contexts [146], BTK inhibitors have emerged as a potential pharmacological strategy to be repurposed for COVID-19 patients, as BTK activity has been found to be increased in whole blood of patients with SARS-CoV-2 infection, who also present systemic cytokine storm [148]. Thus, given the evident protective effects of BTK inhibitors in several inflammatory disease contexts, the next study design (**article III**) has been conducted in an animal model of haemorrhagic shock to explore the potential of repurposing BTK inhibitors in trauma-haemorrhage.

5.1.3 Pharmacological inhibition of BTK activity attenuates haemorrhagic-shock-induced multiple organ dysfunction in rats

To date, the role of BTK in trauma has been poorly investigated, with limited information available [149]. Thus, we start this study (**article III**) providing the clinical relevance of BTK in trauma patients, by reanalysing a dataset already published by Xiao and Colleagues [129]. We showed that BTK expression is elevated in whole blood (leukocytes) of trauma patients, when compared

to healthy controls (Figure 20). This increase starts at Day 1 and remains high until the Day 28. Therefore, suggesting and strengthen BTK as a potential target for new therapeutic strategies in trauma.

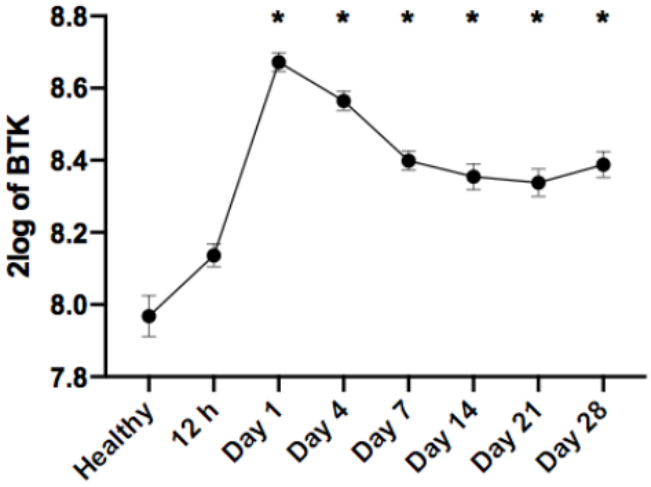

Figure 20: BTK gene expression is elevated in trauma patients. *Original data was obtained from the Gene Expression Omnibus under dataset accession number GSE36809. RNA was extracted from whole blood leukocytes over a 28-day time course from trauma patients (n = 167) and matched healthy controls (n = 37). Data were reanalyzed for BTK gene expression. Data are expressed as mean ± SEM. Statistical analysis was performed using one-way ANOVA followed by a Bonferroni's post- hoc test. * p < 0.05 vs Healthy patients.*

Thus, using a reverse translational approach, we investigated whether pharmacological intervention with two BTK inhibitors would attenuate HS-induced systemic inflammation and organ dysfunction in a rat trial. In this study we used Acalabrutinib (ACA) as a second generation irreversible BTK inhibitor (more selective compared to Ibrutinib – first generation) and Fenebrutinib (FEN) as a reversible BTK inhibitor.

Interestingly, the changes in BTK expression seen in trauma patients corroborate our findings in our animal model of HS. We showed that HS led to an overactivation of BTK (phosphorylation on Tyr ^{223}) in the kidney of rats and that pharmacological inhibition of BTK with both ACA and FEN drugs significantly abolished the increase induced by HS, with no statistical differences between the two treatments (panel A, Figure 21). Then, as there are solid evidence showing that BTK activates the NFκB pathway [150] and in trauma there is a high cytosol-nucleus translocation of NFκB [151]–[153], we also investigate downstream BTK signaling in HS-rats. Thus, as expected, HS led to an overactivation of NFκB pathway, composed by IKKα/β (phosphorylation on Ser$^{176/180}$), IκBα (phosphorylation on Ser$^{32/36}$) and cytosol-nucleus translocation of p65 subunit. Interestingly, inhibition of BTK activity with ACA or FEN equally attenuated NFκB activation in the kidney of HS-rats (panels B-D, Figure 21).

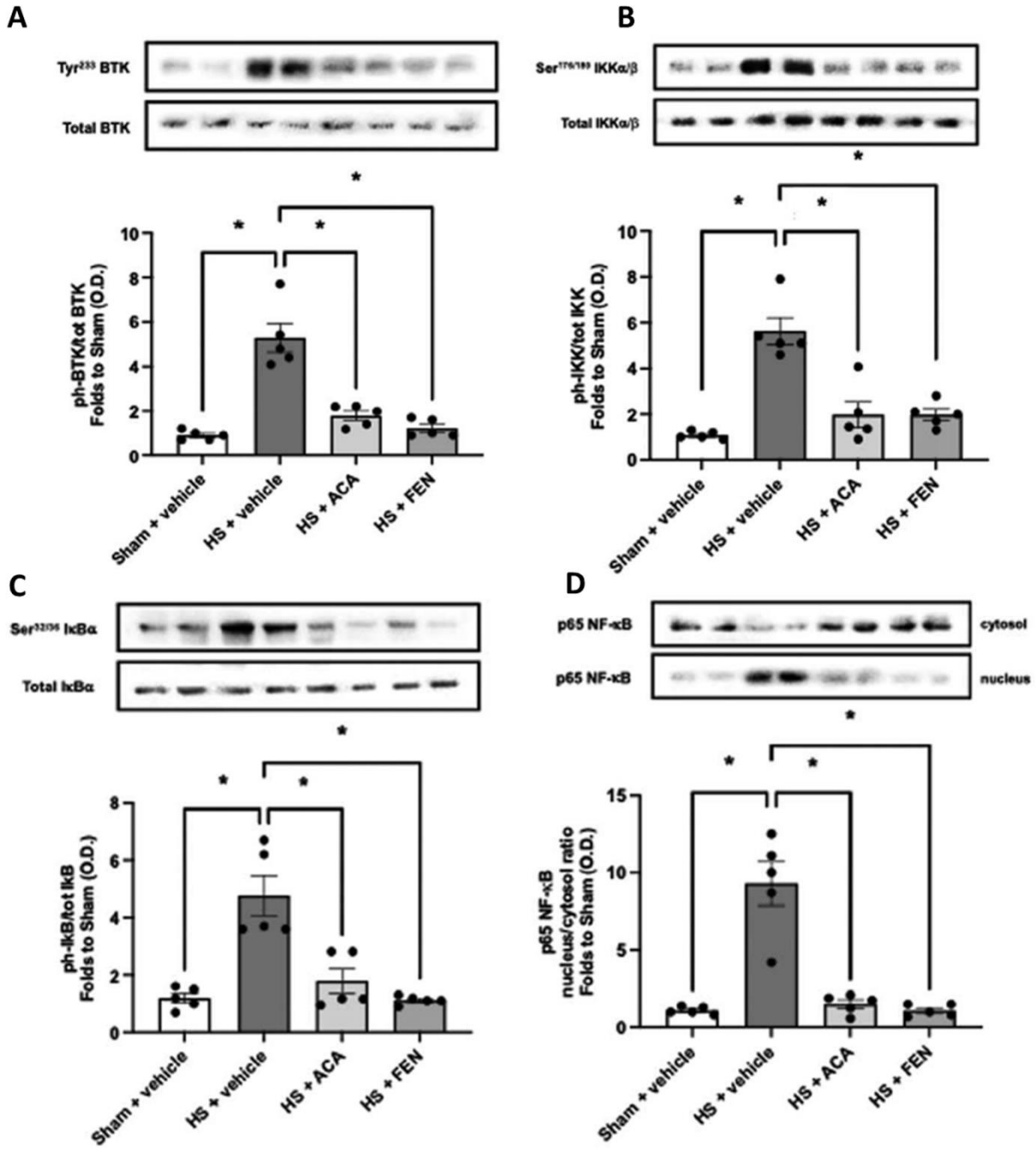

Figure 21: Treatment with BTK inhibitors (Acalabrutinib or Fenebrutinib) attenuates renal BTK and NFκB activation in experimental HS. *[A] The phosphorylation of BTK on Tyr^{223}, [B] the phosphorylation of IKKα/β at Ser$^{176/180}$, [C] the phosphorylation of IκBα at Ser$^{32/36}$ and [D] the Cytosolic-nuclear translocation of p65 subunit of vehicle and BTKi treated (acalabrutinib, ACA; fenebrutinib, FEN) rats were determined by western blotting in the kidney. Protein expression was measured as relative optical density (O.D.) and normalized to the sham band. Data are expressed as mean ± SEM of five animals per group. Statistical analysis was performed using one-way ANOVA followed by a Bonferroni's post-hoc test. *p<0.05 denoted statistical significance.*

NFκB activation starts with pro-inflammatory mediators upstream of its signalling pathway, which then induces the transcription of several pro- and anti-inflammatory cytokines and other

inflammatory mediators [154]. As a result, it functions as a positive feedback loop, further amplifying and perpetuating inflammatory responses, leading to increased endothelial permeability, tissue hypoperfusion/hypoxia, tissue injury, and ultimately organ dysfunction [155]. Thus, as the two BTK inhibitors reduced NFκB activation in HS-rats, we wondered whether the treatments protected against trauma-associated organ dysfunction. Indeed, both drugs improved HS-induced circulatory failure, showing a significantly higher MAP over time post resuscitation when compared to vehicle-treated HS-rats (panels A-B, Figure 22). Simultaneously, HS-rats treated with BTK inhibitors also had attenuated levels of organ damage biomarkers which had been elevated by haemorrhage (ALT, indicating hepatic injury), (Creatinine, indicating renal dysfunction) and (CK, indicating muscular injury) (Figure 23). Collectively, these data suggest that BTK inhibition protects against HS-induced multiorgan dysfunction by reducing the inflammatory burden, with identical efficacy between Acalabrutinib and Fenebrutinib.

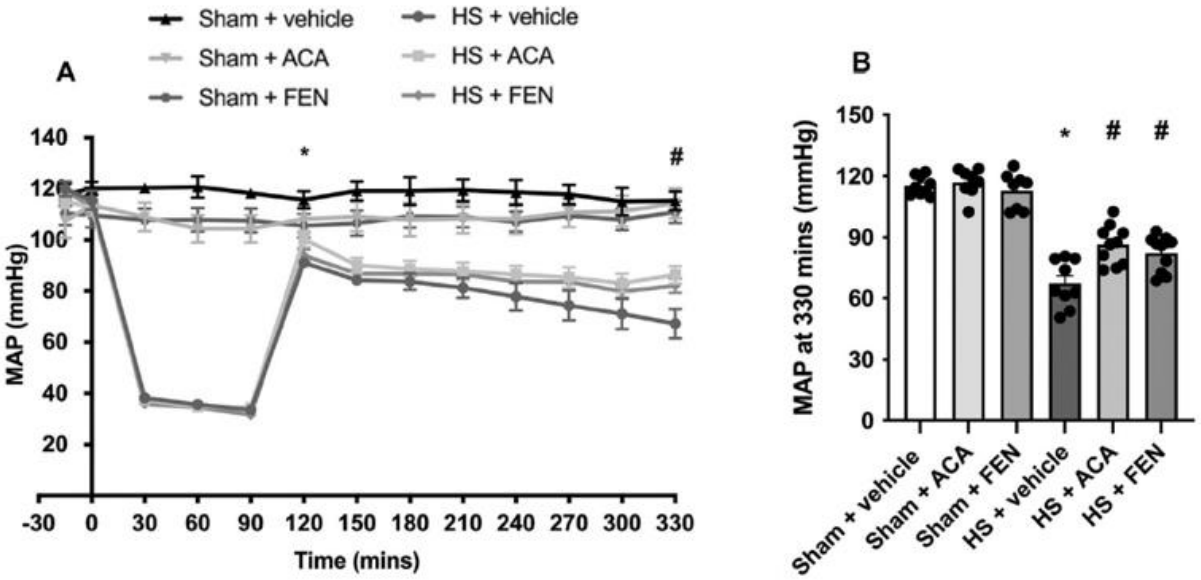

Figure 22: Treatment with BTK inhibitors improves HS-induced circulatory failure. [A] *Mean arterial pressure (MAP) was measured from the completion of surgery to the termination of the experiment for vehicle and BTK inhibitors treated (Acalabrutinib, ACA; Fenebrutinib, FEN) rats.* ***[B]*** *MAP values at the end of the resuscitation period (330 min). Data are expressed as mean ± SEM of 8-10 rats per group. Statistical analysis was performed using two-way ANOVA followed by a Bonferroni's post-hoc test. *p<0.05 Sham + vehicle vs. HS + vehicle; #p<0.05 HS + vehicle vs. HS + BTK inhibitors (ACA or FEN).*

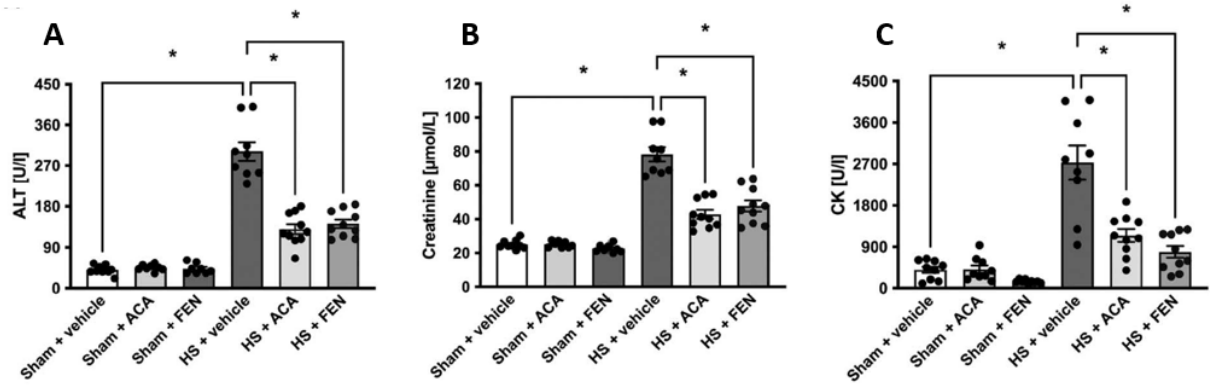

Figure 23: Treatment with BTK inhibitors attenuates HS-induced organ dysfunction. *Rats were subjected to haemorrhagic shock (HS) and 4 h after resuscitation, levels of serum [A] alanine aminotransferase (ALT), [B] creatinine and [E] creatine kinase (CK) were determined in vehicle and BTK inhibitors treated (Acalabrutinib, ACA; Fenebrutinib, FEN) rats. Sham-operated rats were used as control. Data are expressed as mean ± SEM of 8-10 rats per group. Statistical analysis was performed using one-way ANOVA followed by a Bonferroni's post-hoc test. *p<0.05 denoted statistical significance.*

So far, we have shown that both sepsis and haemorrhagic shock trigger an exacerbated inflammatory burden with excessive release of pro-inflammatory cytokines/mediators, which are key drivers of organ dysfunction. Thus, we designed our next animal trial (**article IV)** using a small molecule that targets kinases that directly signal downstream cytokine receptors, thereby seeking for a reduction in the amplification and perpetuation of inflammatory disorders.

JAK-STAT is a well-known intracellular pathway that signals downstream cell-surface cytokine/growth factor receptors, mediating various inflammatory disorders [156], hence, is considered a potential master regulator of many inflammatory signalling processes. However, there is limited information about the role of JAK-STAT pathway in trauma.

5.1.4 Pharmacological inhibition of JAK-STAT pathway reduces multiple organ dysfunction caused by haemorrhagic-shock in rats

Similar to the previous discussed study (**article III**), here (**article IV**) we re-analysed the same dataset already published by Xiao and collaborators [129], where they compared genome-wide gene expression in whole-blood from trauma patients *vs* matched healthy controls. For the present study, the dataset was re-analysed for JAK2 and STAT3 expression. As shown in Figure 24, both JAK2 and STAT3 expression are increased in leukocytes from trauma patients when compared to healthy controls. The increase begins with an initial peak at 12 h for both biomarkers and remains high through Day 28. These datasets highlight that the JAK2-STAT3 pathway may trigger a central role in the pathogenesis of trauma, suggestive of a potential pharmacological target in trauma.

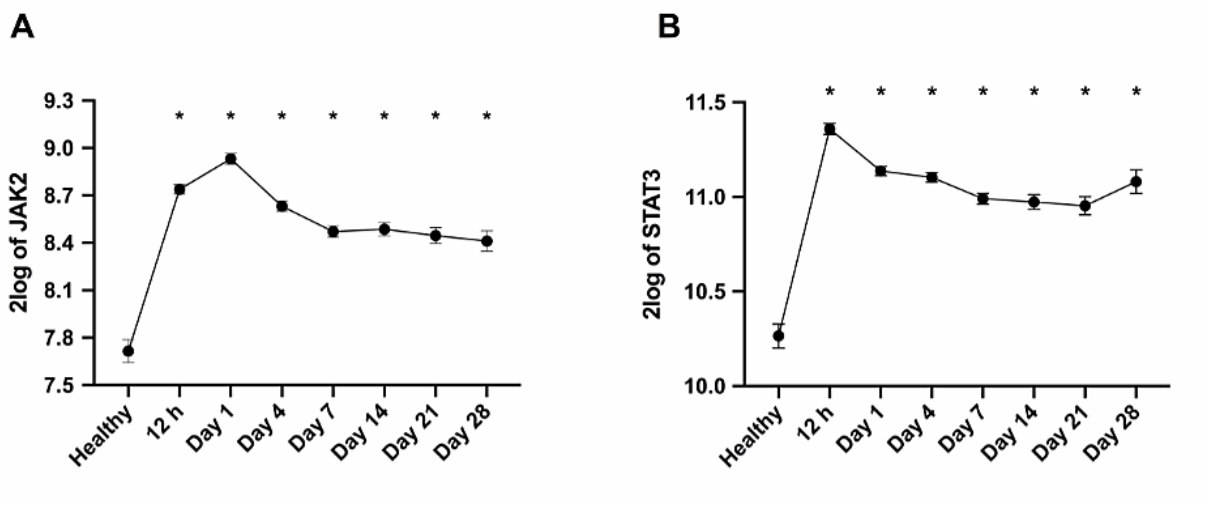

Figure 24: JAK2 and STAT3 gene expression is elevated in trauma patients. *Original data was obtained from the Gene Expression Omnibus under dataset accession number GSE36809. RNA was extracted from whole blood leukocytes over a 28-day time course from trauma patients (n = 167) and matched healthy controls (n = 37). Data were reanalyzed for* ***[A]*** *JAK2 and* ***[B]*** *STAT3 gene expression in trauma patients. Data are expressed as mean ± SEM. Statistical analysis was performed using one-way or two-way ANOVA followed by a Bonferroni's post-hoc test. *p<0.05 denoted statistical significance.*

Again, using a reverse translational approach, we decided to carry out a rat trial using the animal model of haemorrhagic-shock and targeting JAK-STAT pathway with Baricitinib, a selective JAK1/JAK2 inhibitor. Baricitinib is an approved drug for the treatment of inflammatory diseases, including rheumatoid arthritis [157] and atopic dermatitis [158]. Moreover, we have recently demonstrated that JAK-STAT inhibition with Baricitinib ameliorates diet-related metabolic/inflammatory derangements and associated organ damage in a murine model of chronic low-grade inflammation induced by high fat diet [73]. In addition, Baricitinib has gained wide visibility due to its potential inflammation-reducing effects, prompting several clinical trials to investigate the impact of its repurposing for COVID-19 patients (ClinicalTrials.gov Identifier: NCT04320277, NCT04321993, NCT04346147, NCT04381936, NCT04390464, NCT04399798, NCT04640168, NCT04693026, NCT04832880, NCT04890626, NCT04891133, NCT04970719, NCT05056558, NCT05082714, NCT05074420, NCT04393051).

When it comes to an animal model of HS, we have explored the activity of the JAK2-STAT3 using the western blot technique in the kidney and liver of rats that underwent the HS insult. Interestingly, we observed that HS insult led to an overactivation of JAK2 (phosphorylation on $Tyr^{1007\text{-}1008}$) and, consequently, an overactivation of its downstream component STAT3 (phosphorylation on Tyr^{705}) in both organs of HS-rats. These intriguing findings corroborate what has been found in trauma patients. Interestingly, Baricitinib treatment in HS-rats reduced activation of its target (JAK2) to levels similar to those observed in the Sham group and, as a consequence, STAT3 activity was also reduced in HS-rats treated with Baricitinib (panels A-D, Figure 25). We have previously shown that NFκB is highly activated during haemorrhage [151][152]. Curiously, it has been reported that STAT3 prolongs NFκB nuclear retention through an acetyltransferase p300-mediated RelA acetylation mechanism, thereby potentiating NFκB pro-inflammatory responses [159]. Thus, as expected, we showed that HS-rats had a higher p65

(NFκB) cytosolic-nuclear translocation compared to Sham-rats, however, the JAK1/2 inhibitor Baricitinib reduced the increased translocation induced by the HS insult (panels E-F, Figure 25).

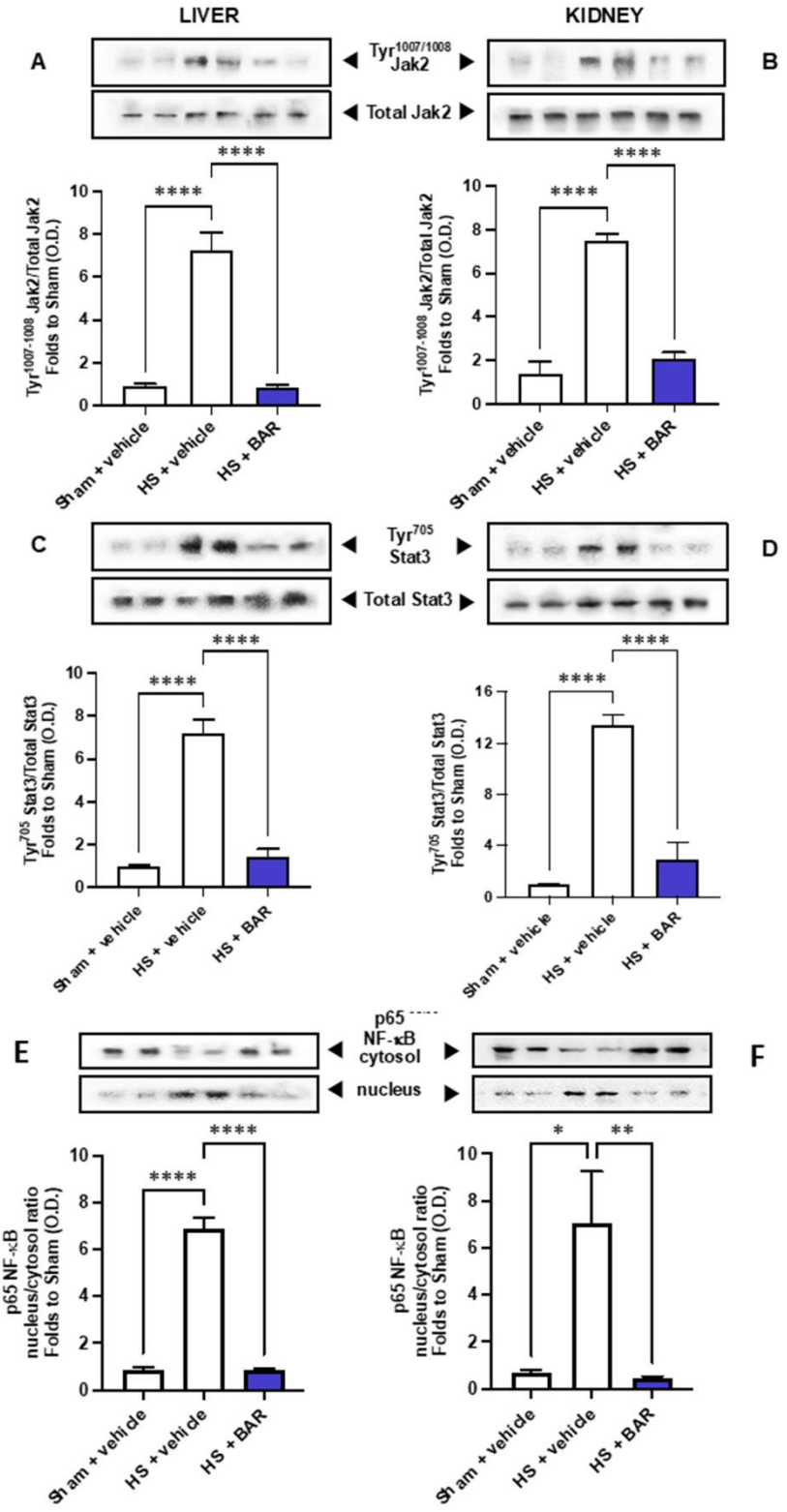

Figure 25: Baricitinib attenuates JAK2/STAT3 and NFκB translocation in HS. [A-B] *The phosphorylation of JAK2 on Tyr$^{1007-1008}$,* ***[C-D]*** *the phosphorylation of STAT3 on Tyr^{705},* ***[E-F]*** *the cytosolic-nuclear translocation of p65 subunit of vehicle and BAR (baricitinib) treated rats were determined by western blot in the liver and kidney. Protein expression was measured as relative*

*optical density (O.D.) and normalized to the sham band. Data are expressed as mean ± SEM of 4-5 animals per group. Statistical analysis was performed using one-way ANOVA followed by a Bonferroni's post-hoc test. *p<0.05 denoted statistical significance.*

The sterile inflammation, as occurs in HS, drives the recruitment of inflammatory cells into tissues to propagate an inflammatory environment, which then contributes to the development of MOF [160][161][162]. In the light of this, endothelial cells play a key role in this mechanism, expressing high levels of adhesion molecules in an NFκB-dependent manner [163]. We then measured CD68 as a biomarker of macrophage infiltration [164]. In our analysis, as shown in Figure 26, CD68 immunopositivity was found to be increased in the kidney of HS-rats treated with vehicle. Specifically, CD68 expression was increased mainly in the renal corpuscles. Interestingly, Baricitinib treatment resulted in substantial reduction in CD68 expression in the kidney of HS-rats, suggesting that pharmacological inhibition of the JAK/STAT pathway prevents macrophage infiltration.

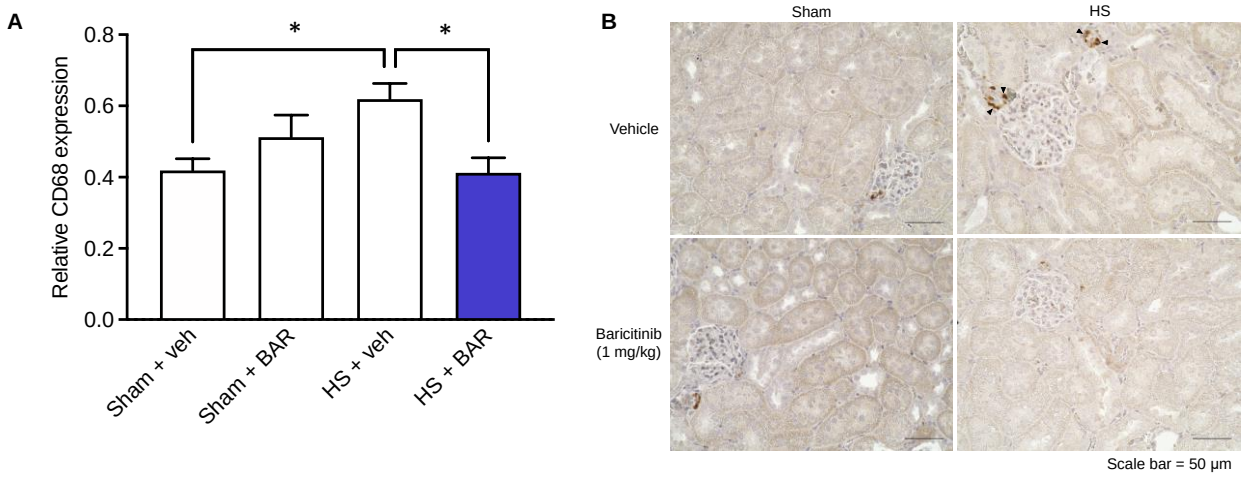

Figure 26: Baricitinib reduces renal macrophage infiltration in experimental HS. *Rats were subjected to hemorrhagic shock (HS) and 4 h after resuscitation,* ***[A]*** *relative CD68 expression in renal tissue of vehicle and BAR (baricitinib) treated rats.* ***[B]*** *Representative images of CD68 staining (40x magnification) are shown. Black arrows highlight* ***[B]*** *sites of positive CD68 staining. Data are expressed as mean ± SEM of eight rats per group. Statistical analysis was performed using* ***[A]*** *one-way ANOVA followed by a Bonferroni's post-hoc test. *p<0.05 denoted statistical significance.*

Sequentially, we have reported, as a result of a reduced inflammation mediated by inhibition of the JAK/STAT pathway with Baricitinib during haemorrhagic shock, a protection against multi-organ failure, including hepatic damage (ALT), renal dysfunction (Creatinine), pancreatic injury (Amylase) and neuromuscular injury (CK) (Figure 27).

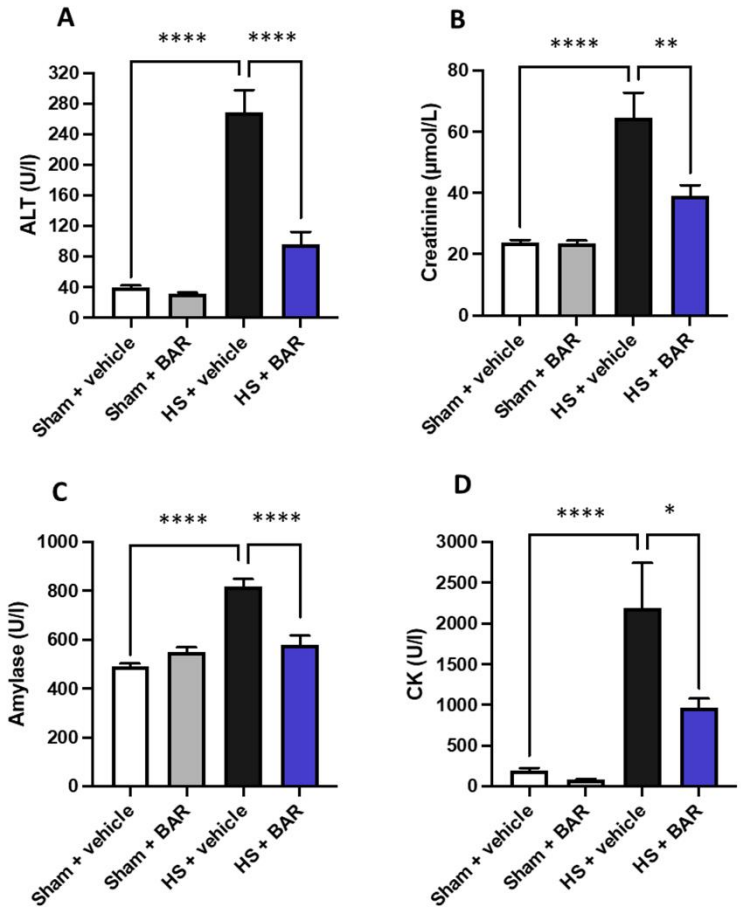

Figure 27: Baricitinib attenuates HS-induced organ injury/dysfunction in HS. *Rats were subjected to haemorrhagic shock (HS) and 4 h after resuscitation, levels of serum* ***[A]*** *alanine aminotransferase (ALT),* ***[B]*** *creatinine,* ***[C]*** *amylase and* ***[D]*** *creatine kinase (CK) were determined in vehicle and BAR (baricitinib) treated rats. Sham-operated rats were used as control. Data are expressed as mean ± SEM of 9-11 rats per group. Statistical analysis was performed using one-way ANOVA followed by a Bonferroni's post-hoc test. *p<0.05 denoted statistical significance.*

Taken together, we have provided consistent data suggesting that JAK inhibitors, such as Baricitinib, may be repurposed to counteract hyperinflammation and associated organ dysfunction induced by haemorrhagic in patients with trauma.

Up to this point, we have seen many determinant molecular aspects/mechanisms that intersect in the pathophysiology of organ dysfunction induced either by trauma or sepsis, and pharmacological strategies targeting kinases have been effective. However, we also have comprehended that the complex interplay between immune system cells and biological tissues represents a key axis in the pathogenesis of inflammatory disorders. We, therefore, decided to target key elements belonging to the immune system to assess whether this innovative pharmacological approach would protect organs from the hyperinflammatory response caused by haemorrhage or sepsis.

5.2 Targeting immune system components as innovative pharmacological approach to counteract multiorgan failure in sepsis and haemorrhagic shock

Macrophage migration inhibitory factor (MIF), a pro-inflammatory cytokine that possesses chemokine-like properties by promoting the expression or production of several pro-inflammatory mediators including IL-1β, IL-2, IL-6, IL-8, IL-12, IFN-g, nitric oxide, TNF-α, cyclooxygenase 2 and matrix metalloproteinases [165]. Consequently, further leukocytes are directed to the site of injury and/or infection [90]. The role of MIF in sepsis and several other inflammatory diseases have already been explored, however its role in haemorrhagic shock has been poorly investigated.

5.2.1 Pharmacological inhibition of macrophage migration inhibitory factor (MIF) activity with ISO-1 confers organ protection in experimental haemorrhagic-shock

As previously discussed, leukocyte recruitment to inflamed tissues is mediated, at least in part, by the NFκB pathway and its transcriptional products, including pro-inflammatory cytokines and chemokines, which in turn contribute to organ dysfunction [166][162]. Among them, MIF, considered the first cytokine activity to be reported [167], a pleiotropic cytokine, with chemokine-like properties, thus promoting the expression of a multitude of pro-inflammatory mediators and therefore intensifying additional leukocytes into inflamed tissues [168]. Interestingly, systemic levels of MIF have been found increased in plasma from trauma patients [169]. Thus, based on this evidence, this study has been designed (**article V**) to investigate the beneficial effects of pharmacological inhibition of MIF activity in a rodent model of haemorrhagic shock.

We report here in our experimental conditions that rats subjected to HS insult showed increased serum levels of MIF (Figure 28), corresponding to what has been found in trauma patients. Interestingly, rats treated with MIF inhibitor (ISO-1) [(S,R)-3-(4- hydroxyphenyl)-4,5-dihydro-5-isoxazole acetic acid methyl ester] significantly reduced MIF levels increased by the HS insult (Figure 28). The reduced MIF levels in HS-rats treated with ISO-1 were associated with multiorgan protection, represented by the biochemical markers of organ damage (ALT, Creatinine, Amylase and CK) (Figure 29).

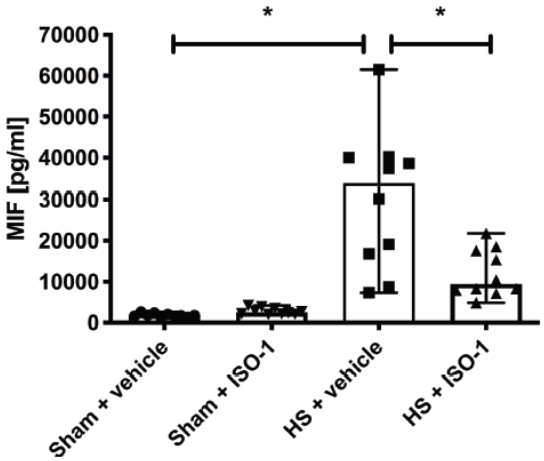

Figure 28: Serum MIF levels are elevated in HS-rats. *Serum MIF levels were detected by ELISA in vehicle or ISO-1 treated rats. Data are expressed as median with range of ten rats per group. Statistical analysis was performed using one-way ANOVA followed by a Bonferroni's post-hoc test. *p < 0.05 vs. HS + vehicle.*

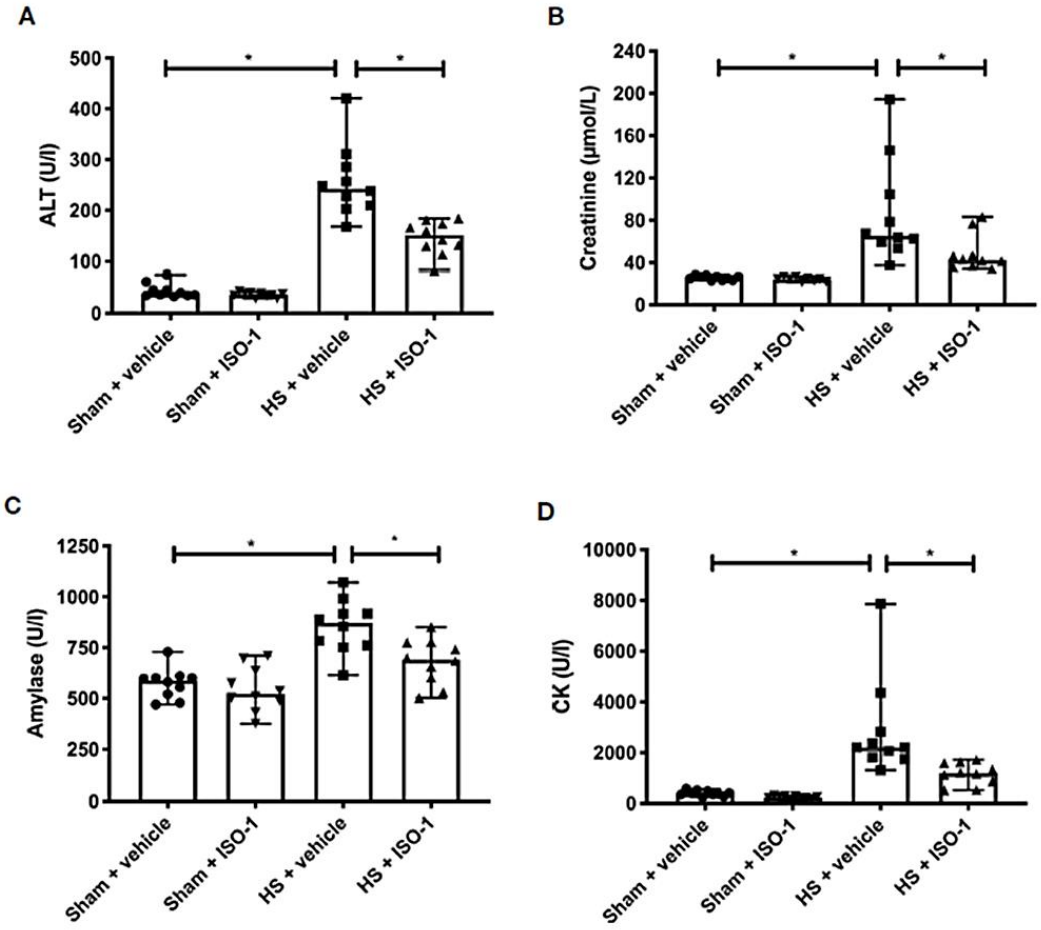

Figure 29: Treatment with ISO-1 attenuates HS-induced organ damage. *Rats were subjected to haemorrhagic shock (HS) and 4 h after resuscitation, levels of serum* ***[A]*** *alanine aminotransferase (ALT),* ***[B]*** *creatinine,* ***[C]*** *amylase and* ***[D]*** *creatine kinase (CK) were determined. Sham-operated rats were used as control. Data are expressed as median with range of ten rats per group. Statistical analysis was performed using one-way ANOVA followed by a Bonferroni's post-hoc test. *p < 0.05 denoted statistical significance.*

Then, in order to uncover the molecular mechanism behind organ protection triggered by ISO-1, we evaluated NLRP3 inflammasome pathway. MIF has been attributed to induce assembly and hence activation of the NLRP3 inflammasome in inflammatory disorders [170][171]. We demonstrated that HS insult led to an increased NLRP3 expression and therefore elevated activated-caspase-1 levels in the liver and kidney, which were prevented by ISO-1 treatment in HS-rats (Figure 30).

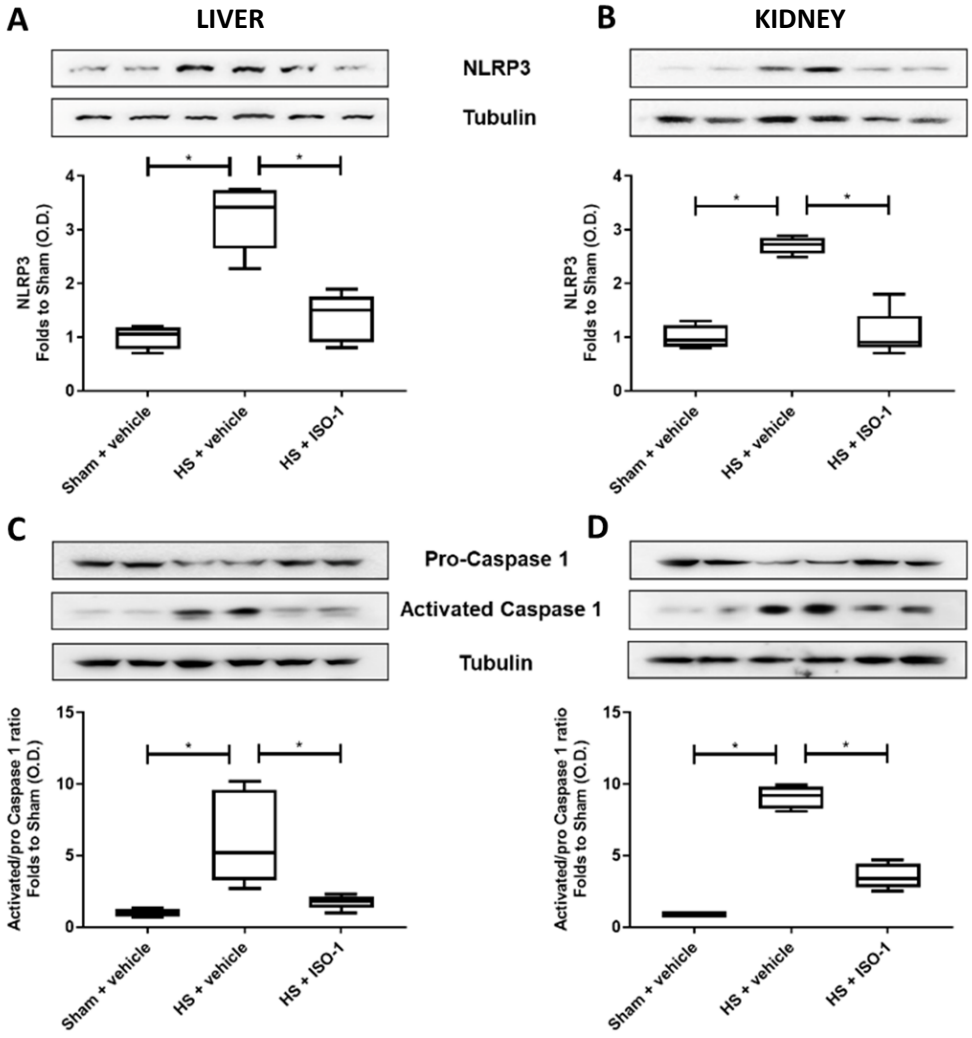

Figure 30: Treatment with ISO-1 attenuates NLRP3 activation in an acute HS model. [A, B] *The activation of NLRP3 and* ***[C, D]*** *the cleavage of pro-caspase 1 of vehicle and ISO-1 treated rats were determined by Western blotting in the liver and kidney. Protein expression was measured as relative optical density (O.D.) and normalized to the sham band. Data are expressed as box and whiskers blotted from min to max of four to five animals per group. Statistical analysis was performed using one-way ANOVA followed by a Bonferroni's post-hoc test. *p<0.05 HS + vehicle vs sham + vehicle or vs. HS + ISO-1.*

In line with these findings, MIF has been demonstrated to increase TLR4 expression, which then potentiates activation of the NFκB pathway, thereby increasing the transcription of inflammatory mediators, including pro-inflammatory cytokines and the NLRP3 components [172]. Furthermore, MIF, along with NFκB-dependent cytokines and NLRP3-dependent IL-1β/IL-18 create a vicious loop, intensifying an inflammatory environment, massively attracting inflammatory cells to damaged tissues. Indeed, our observations reveal that HS-rats had an impressive increase on MPO activity into the lungs and liver, suggesting increased leukocyte infiltration (Figure 31). Intriguingly, treatment with ISO-1 abolished the HS-induced MPO activity. This complex inflammatory interplay may suggest that ISO-1 counteract the inflammatory burden by acting

directly to key targets related to NFκB and NLRP3 pathways, thus reducing local inflammation and hence leukocyte recruitment. Therefore, proposing ISO-1 as a potential therapeutic approach for the prevention of MOF after trauma and/or haemorrhage.

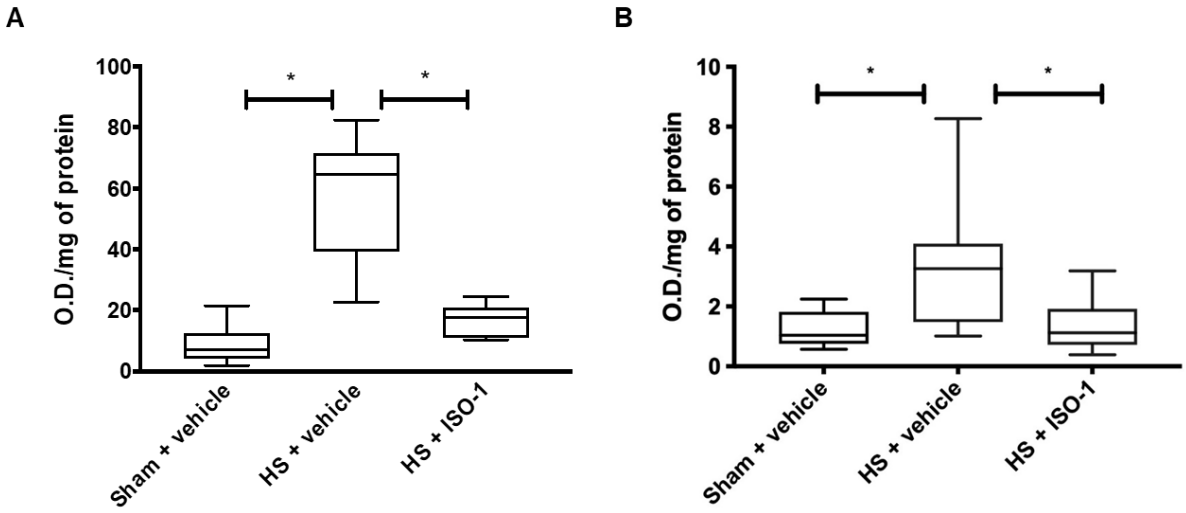

Figure 31: ISO-1 treatment attenuates pulmonary and hepatic MPO activity during experimental HS. *Myeloperoxidase activity was determined in* ***[A]*** *lungs and* ***[B]*** *liver for vehicle and ISO-1 treated rats. Data are expressed as mean ± SEM of n animals per group. Sham + vehicle (n=6); HS + vehicle (n=12); HS + ISO-1 (n=12). Statistical analysis was performed using one-way ANOVA followed by a Bonferroni's post-hoc test. *p<0.05 was considered statistically significant.*

Despite the pivotal role of hyperinflammation in the onset of organ injury in sepsis, the inflammatory response during the early stages appears to be dynamically more complex, as an immunosuppressive response occurs simultaneously, leading to an inflammatory imbalance which then contributes to late deaths and recurrent infections [173]. Accordingly, we wondered how we could concomitantly target hyperinflammation and immunosuppression in sepsis. We went back into the literature and recent findings demonstrate ICOS-ICOSL pathway in mediating several immune responses [174][175].

The two transmembrane proteins which are extensively investigated in the immune response. The immune checkpoint proteins, named as Inducible T cell co-stimulator (ICOS) which is expressed on activated T cells and its unique ligand, ICOSL, which is either expressed on antigen-presenting cells and also in non-haematopoietic cells. ICOS interacts with ICOSL leading to bidirectional effects, where on the one hand it has been shown to induce immunosuppression by reducing lymphocytes population, on the other hand it has been shown to induce anti-inflammatory responses.

ICOS-ICOSL pathway has been poorly investigated in the septic context. Thus, in the next animal trial (**article VI**), we have pharmacologically targeted this immune pathway in CLP-mice to investigate the pathological role of the ICOS-ICOSL axis in the context of sepsis and the potential protective effects of its immunomodulation by administering ICOS-Fc, which is a soluble recombinant form of ICOS that can act as an immunomodulatory drug as both antagonist of ICOS and agonist of ICOSL, modulating cytokine release and cell migration to inflamed tissues.

5.2.2 ICOS-Fc as innovative immunomodulatory strategy to neutralize sepsis-induced inflammation and organ dysfunction

Little information is known about the role of ICOS-ICOSL interaction in sepsis. Nevertheless, recent findings reported that ICOS expression is reduced in whole blood of septic patients [107], and that reduced ICOS levels are strongly associated with organ dysfunction [108]. Indeed, we have shown in our experimental model of polymicrobial sepsis that the administration of exogenous ICOS (ICOS-Fc) to septic mice counteracts systemic inflammation, showed by reduced levels of IL-1β, IL-6, TNF-α and IL-10 increased by sepsis (Figure 32). These findings have been confirmed when septic mice were treated with a mutated form carrying a phenylalanine-to-serine substitution at position 119, therefore unable to bind ICOSL. The observed attenuation in the cytokine storm have been lost in septic mice treated with ^{F119S}ICOS-Fc.

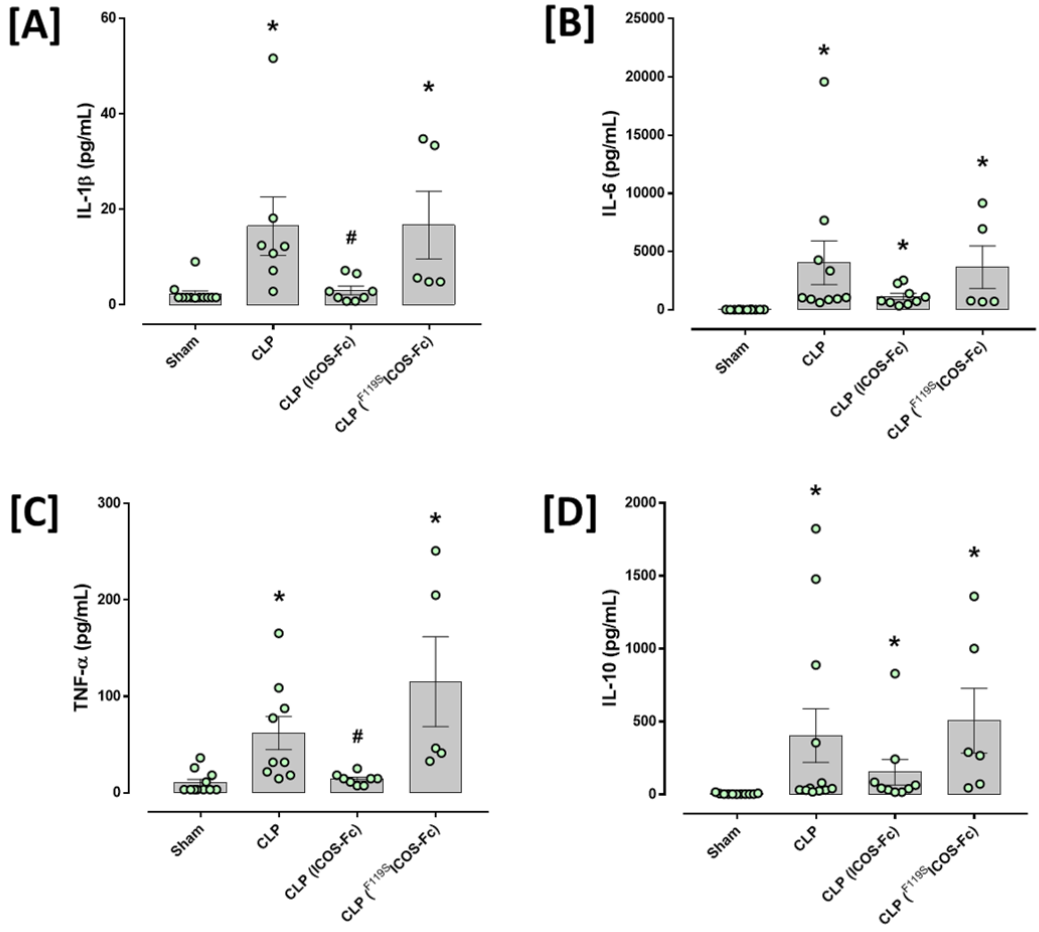

Figure 32: Effect of ICOS-ICOSL axis immunomodulation on systemic cytokines during experimental sepsis. *Wild-type mice were randomly selected to undergo either Sham or CLP surgery. One hour later, mice received once either Vehicle (PBS, 100 µL), ICOS-Fc or ^{F119S}ICOS-Fc (100 µg each) intravenously. At 24 h, blood samples were withdrawn from each mouse and plasma levels of IL-1b **[A]**, IL-6 **[B]**, TNF-a **[C]** and IL-10 **[F]** were determined. Data are expressed as dot plots (for each animal) and as mean ± S.E.M of 9 mice per group. Statistical analysis was performed by one-way ANOVA followed by Bonferroni's post hoc test. *p<0.05 vs Sham; #p<0.05 vs CLP + Vehicle.*

Sepsis-induced unbalanced systemic inflammation triggered augmented leukocyte infiltration into the liver and kidney, represented by increased MPO activity (Figure 33). Intriguingly, treatment of septic mice with ICOS-Fc was able to reduce MPO levels in the kidney. This effect, on the other hand, was absent in the liver of septic mice regardless the drug administration (Figure 33).

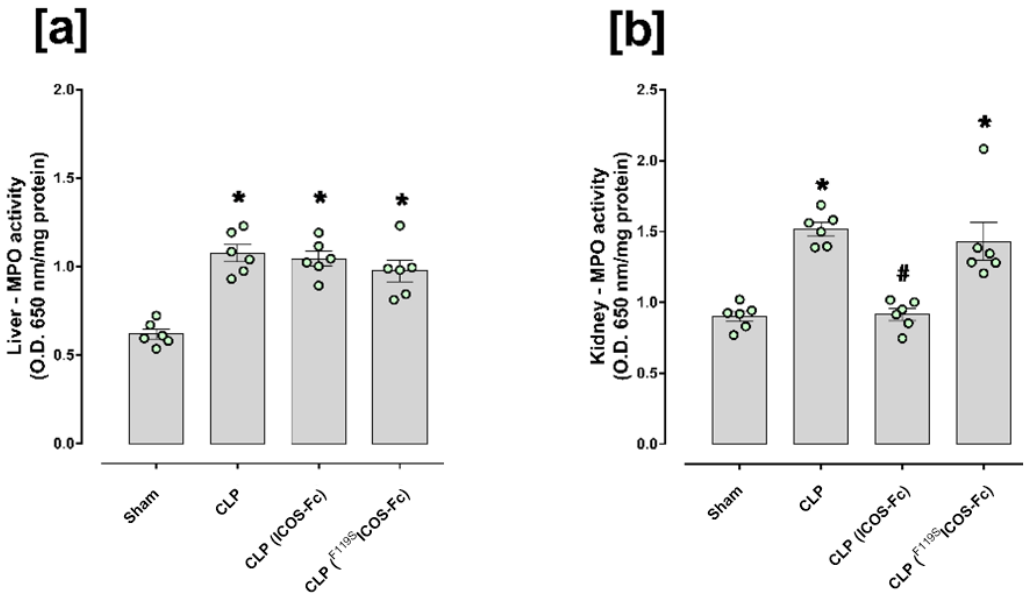

Figure 33: Effects of ICOS-ICOSL axis immunomodulation on sepsis-induced neutrophil (MPO activity) infiltration. *Wild-type mice were randomly selected to undergo either Sham or CLP surgery. One hour later, mice received once either Vehicle (PBS, 100 µL), ICOS-Fc or ^{F119S}ICOS-Fc (100 µg each) intravenously. At 24 h, liver and kidney samples were harvested. Through an in vitro assay, myeloperoxidase (MPO) activity was measured in liver* ***[A]*** *and kidney* ***[B]****. Data are expressed as dot plots (for each animal) and as mean ± S.E.M of 6 mice per group. Statistical analysis was performed by one-way ANOVA followed by Bonferroni's post hoc test. *p<0.05 vs Sham; #p<0.05 vs CLP + Vehicle.*

Reinforcing again our previous findings that the cytokine burden, along with leukocyte infiltration play a part in organ injury, we have shown that septic mice had hepatic and renal damage by raised plasma levels of ALT and Creatinine, which were attenuated in septic mice treated with ICOS-Fc, suggesting then hepatic and renal protection. The protective effects on sepsis-induced organ injury have been further confirmed when the mutated form of ICOS-Fc was given to CLP-mice (Figure 34). However, these divergent outcomes seen in liver and kidney (MPO activity *vs* biomarkers of organ injury) may be the result of varying levels of tissue-dependent ICOSL expression, as it has been reported that hepatocytes did not express ICOSL protein when compared to other tissues, such as the kidney [176]. Furthermore, despite ICOS-Fc has been documented to attenuate leukocyte infiltration into inflamed tissues [177], we hypothesized that the hepatic protection observed in septic mice treated with ICOS-Fc is mainly due to a local and systemic resolution of inflammation rather than an attenuation in leukocytes infiltration.

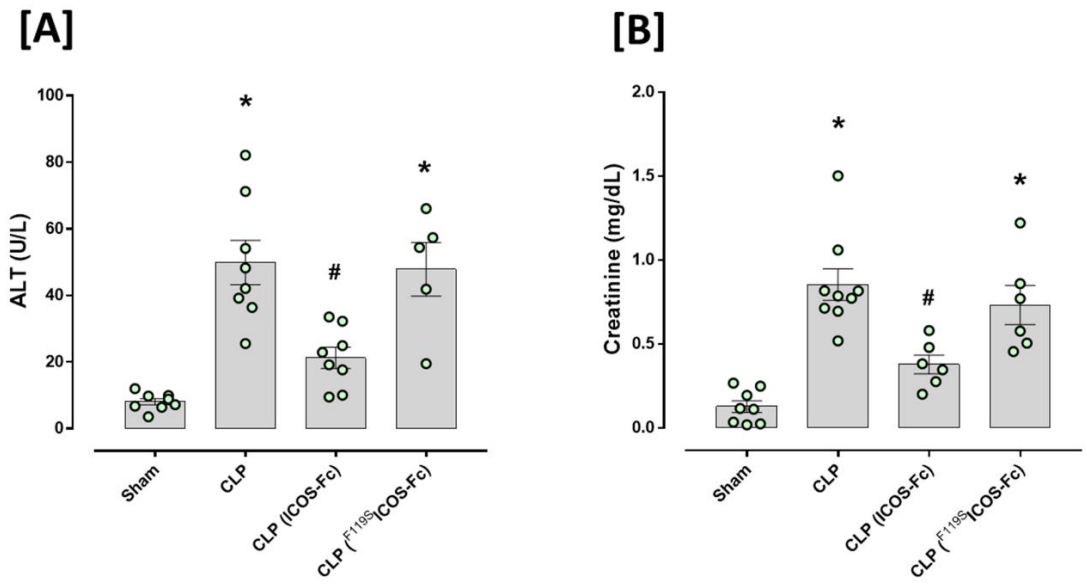

Figure 34: Effect of ICOS-ICOSL axis immunomodulation on sepsis-induced organ damage biomarkers. *Wild-type mice were randomly selected to undergo either Sham or CLP surgery. One hour later, mice received once either Vehicle (PBS, 100 µL), ICOS-Fc or ^{F119S}ICOS-Fc (100 µg each) intravenously. At 24 h, blood samples were withdrawn from each mouse and plasma levels of alanine transaminase (ALT)* ***[A]****, creatinine* ***[B]*** *were determined. Data are expressed as dot plots (for each animal) and as mean ± S.E.M of 9 mice per group. Statistical analysis was performed by one-way ANOVA followed by Bonferroni's post hoc test. *p<0.05 vs Sham; #p<0.05 vs CLP + Vehicle.*

Sequentially, we then decided to go deeper into the molecular mechanisms behind ICOS-Fc-induced organ protection during sepsis. Our starting point was guided by data in the literature demonstrating that tumour cells treated with exogenous ICOS had reduced activation of FAK protein [178]. Besides, as we have previously demonstrated that FAK pathway has a deleterious role in sepsis (**article I**). We, therefore, provide consistent evidence for the first time that sepsis led indeed to an overactivation of the FAK pathway which in turn, led to activation of the downstream p38 MAPK mediator in both organs (liver and kidney) and interestingly, septic mice treated with ICOS-Fc showed significantly reduced activation of FAK-p38 axis in both organs during experimental sepsis (Figure 35).

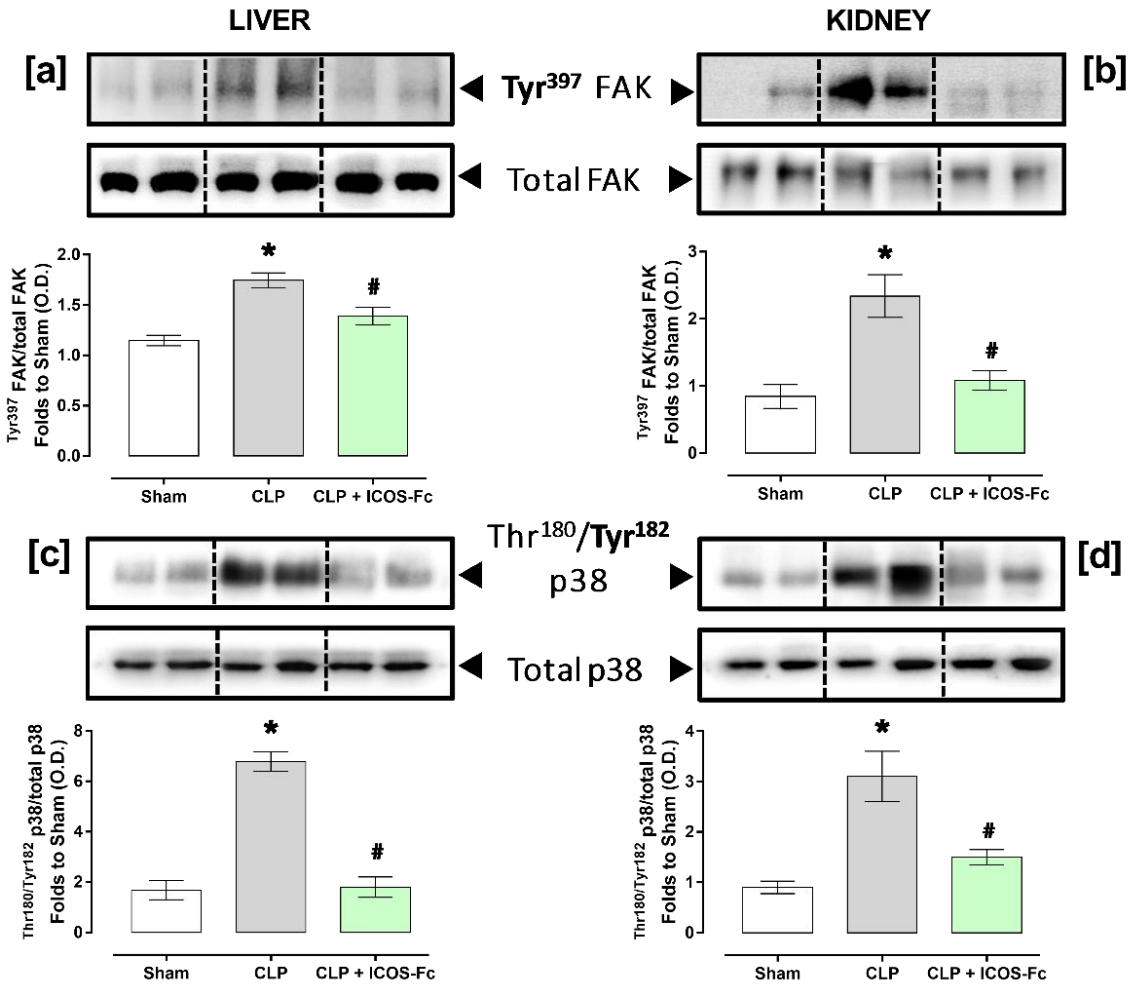

Figure 35: Effects of ICOS-ICOSL axis immunomodulation on tissue inflammatory pathways during experimental sepsis. *Wild-type mice were randomly selected to undergo either Sham or CLP surgery. One hour later, mice received once either Vehicle (PBS, 100 µL) or ICOS-Fc (100 µg) intravenously. At 24 h, liver and kidney samples were harvested, and total proteins were extracted from them. Western blotting analysis for phosphorylation of Tyr397 on FAK in the liver* ***[A]*** *and kidney* ***[B]*** *were normalized to total FAK; Phosphorylation of Thr180/Tyr182 on p38 in the liver* ***[C]*** *and kidney* ***[D]*** *were normalized to total p38, then corrected against β-actin and normalized using the Sham related bands. Densitometric analysis of the bands are expressed as relative optical density (O.D.). Data are expressed as dot plots (for each animal) and as mean ± S.E.M of 4-5 mice per group. Statistical analysis was performed by one-way ANOVA followed by Bonferroni's post hoc test. *p<0.05 vs Sham + Vehicle; #p<0.05 vs CLP + Vehicle.*

We then further explored the NLRP3 inflammasome pathway and we have shown that sepsis induced an overactivation of NLRP3 pathway represented by increased expression of NLRP3 and cleaved caspase-1 and that the treatment with exogenous ICOS was able to reduce their expression in both liver and kidney (Figure 36). These findings further confirmed the systemic plasma levels of IL-1β, which were changed by the septic insult and thus counteracted with ICOS-Fc treatment.

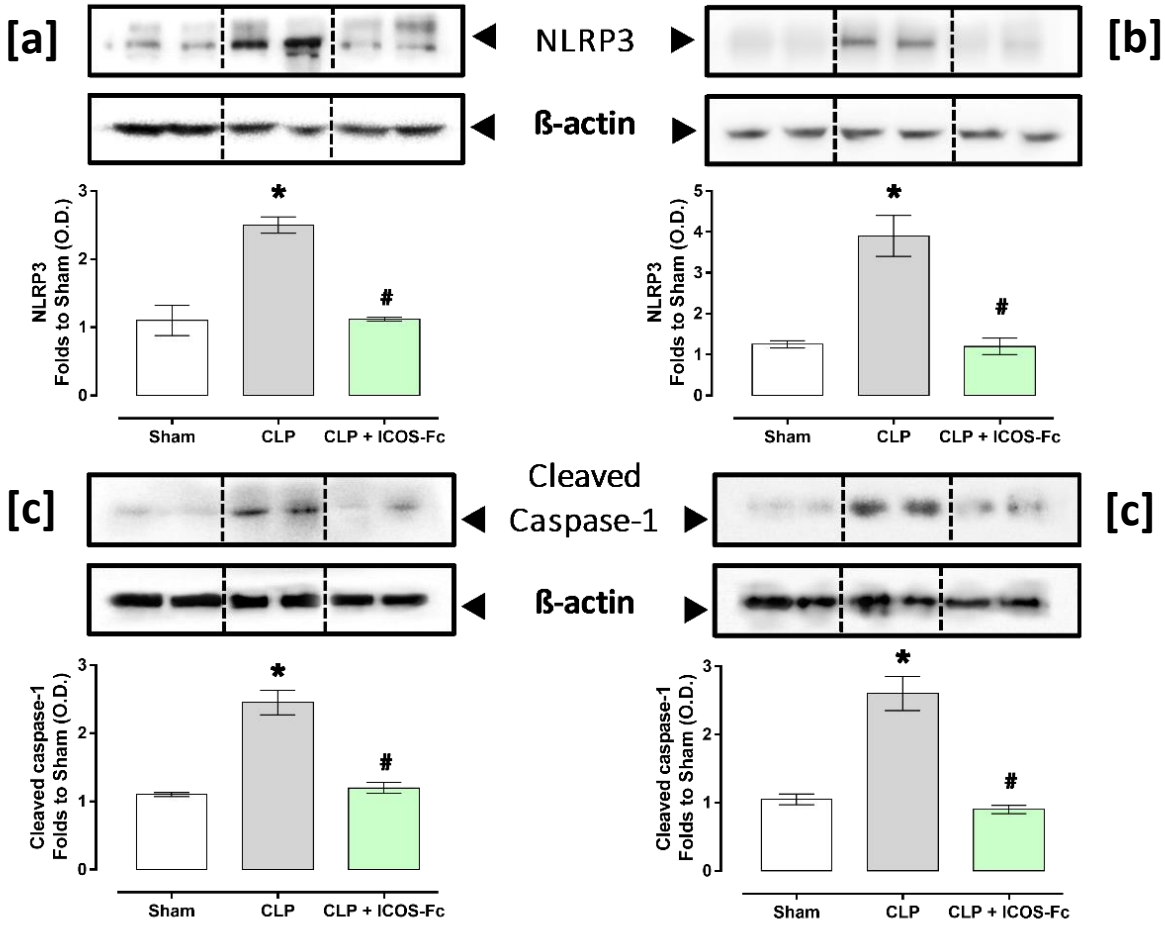

Figure 36: Effects of ICOS-ICOSL axis immunomodulation on sepsis-induced NLRP3 inflammasome activation. *Wild-type mice were randomly selected to undergo either Sham or CLP surgery. One hour later, mice received once either Vehicle (PBS, 100 µL) or ICOS-Fc (100 µg) intravenously. At 24 h, liver and kidney samples were harvested, and total proteins were extracted from them. Western blotting analysis for NLRP3 expression in the liver* ***[A]*** *and kidney* ***[B]*** *were corrected against b-actin and normalized using the Sham related bands; Cleaved caspase-1 expression in the liver* ***[C]*** *and kidney* ***[D]*** *were corrected against β-actin and normalized using the Sham related bands. Densitometric analysis of the bands are expressed as relative optical density (O.D.). Data are expressed as dot plots (for each animal) and as mean ± S.E.M of 4-5 mice per group. Statistical analysis was performed by one-way ANOVA followed by Bonferroni's post hoc test. *p<0.05 vs Sham + Vehicle; #p<0.05 vs CLP + Vehicle.*

In summary, we have shown here that ICOS-ICOSL pathway plays a detrimental role in sepsis. In addition to this, we provide a proof of concept that targeting this pathway with ICOS-Fc represents a powerful immunomodulatory approach for counteracting inflammation and organ injury in sepsis. Moreover, encouraging the development of alternative selective drugs (small molecules) to target ICOS-ICOSL axis to then be repurposed in inflammatory disorders. Furthermore, we are aware that our study has some limitations. Where we believe that the beneficial effects of ICOS-Fc in the septic context do not solely depend on the reduction of the hyper-inflammatory state, but also due to the prevention of the immunosuppressive state, although these aspects still need be uncovered in further studies.

6 GENERAL DISCUSSION

Septic and hemorrhagic shock share several pathological mechanisms in the onset of organ dysfunction, including excessive release of inflammatory cytokines, causing systemic inflammatory response syndrom. Systemic inflammation response can be triggered by PAMPs that are expressed and/or released by invading microorganisms during infection or by DAMPs that are released from host cells during tissue damage [10][179]. While in sepsis there is a mutual action of PAMPs and DAMPs, in hemorrhagic shock (sterile inflammation) the action of DAMPs predominates. However, both PAMPs and endogenous DAMPs are recognized by immune cells through the PRRs, including TLRs receptors, receptors of advanced glycation end products (RAGEs), scavenger receptors and complement receptors [180][181]. After binding the receptors, several signaling pathways are activated, leading to the production of inflammatory mediators such as cytokines, chemokines and vasoactive peptides [10][182]. Within this context, here I highlight the main findings of the present thesis.

First of all, we better elucidated the crucial role of the NFκB-MAPK-NLRP3 axis in the physiopathology of sepsis/HS, and we described a complex cross-talk between distinct mediators in the activation of this axis. Specifically, we documented the role of specific kinases (FAK, PyK2, BTK and JAK) and immunocomponents (ICOSL and MIF) in activation of the NFκB-MAPK-NLRP3 axis. Most notably, we convingly showed that the pharmacological targeting of these key proteins effectively proctect against sepsis/HS-induced systemic inflammation and related-organ dysfunction. An illutrative immage (Figure 37) summarizes this complex interplay we documented in our experimental settings. In adittion to these findings, we carried out another study targeting a key kinase in the context of sepsis (data not yet published). We have explored the role of casein kinase 2 (CK2) in septic mice and we observed that CK2 contributes to the activation of the NFκB and NLRP3 pathways. Additionally, the overactivation of CK2 in sepsis, leads to increased expression of NOS-2, thus producing high levels of NO, which in turn contributes to vascular hyporeactivity to vasoconstrictors (phenylephrine and norepinephrine). Interestingly, the pharmacological inhibition of CK2 attenuated all abdornormalities induced by sepsis. We have also recently demonstrated the deteleterious role of a membrane channel protein (Aquaporin-9, AQP9) in the pathogenesis of sepsis, again showing the complex involvement of NFκB-NLRP3 axis, and that the pharmacological inhibion of AQP9 protects septic mice from inflammatory abdormalities (this article has not been included in the thesis) [183].

In this framework, considering that the activation/regulation of such inflammatory pathways is primarily based in a phosphorilation-dependent manner [28][29], we highlight the role of these powerful pharmacological targets in inflammatory diseases. Kinases are among the most successful drug targets, since they began to be studied in the 1980s [184], where, to date, more than 100 kinase-targeting agents, including 72 US FDA-approved small molecule kinase inhibitors (SMKIs), along with ~500 SMKIs in clinical trials have been explored/used worldwide. Thus, this thesis stands out the powerful use of kinase inhibitors as promising pharmacologocial approach to counteract sepsis/HS-related inflammatory disorders. Furthermore, we have shown here the efficacy of three approved kinase inhibitors (Ibrutinib, Acalabrutinib as BTK inhibitors), (Baricitinib as JAK inhibitor) and (PF562271 as FAK-PyK2 inhibitor), the latter being already tested in a phase I clinical trial [51] in both experimental sepsis and haemorrhagic shock rodent

models. I also highlight the SMKIs-based treatment used in our animal trials constitute another fundamental issue addressed in my thesis, which delimited the concept of drug repurposing/repositioning (identifying, developing and proposing new uses for existing drugs) as a suitable strategy [27], given the urgent need for new therapeutical approches to prevent sepsis and trauma/haemorrhagic shock-associated multiorgan dysfunction.

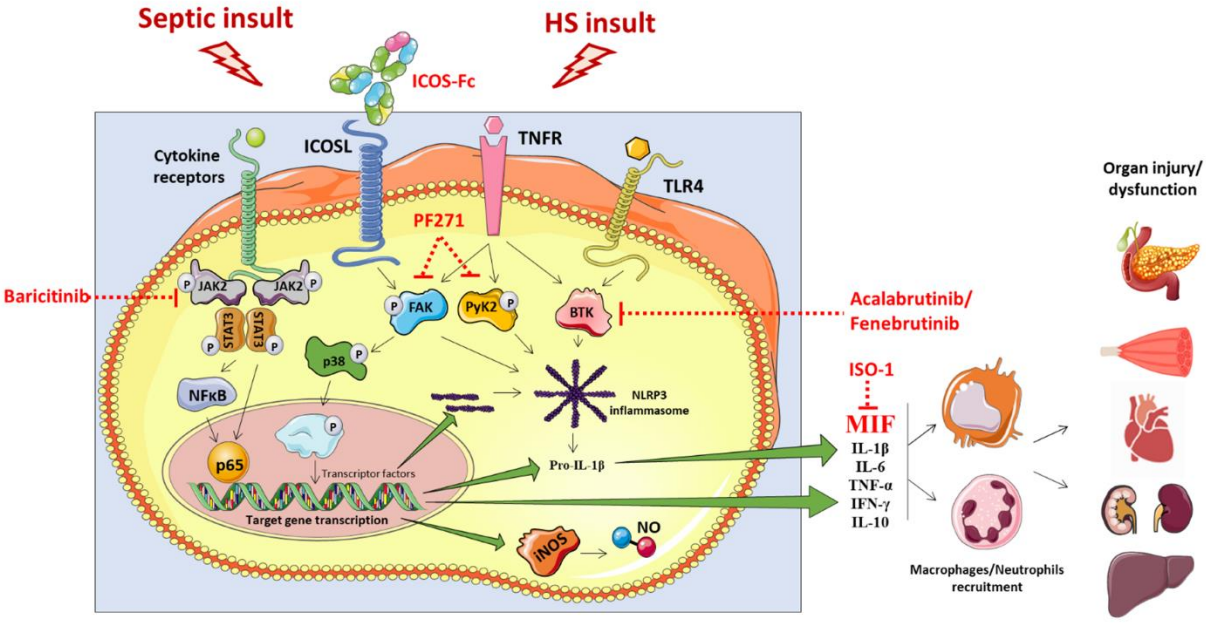

Figure 37: Graphical abstract highlighting the complex molecular interplay displayed by sepsis and/or traumatic injuries. *Sepsis and/or haemorrhage triggers overactivation of the NFkB-MAPK-NLRP3 axis through JAK-STAT, FAK, PyK2, BTK, ICOSL signaling pathways, which leads to an exponential inflammatory response due to increased levels of pro-inflammatory cytokines, including MIF, IL-1β, TNF-α, IL-6. This cytokine storm leads to increased leukocyte recruitment. Excessive systemic inflammation from the combination of cytokine release and innate immune cell recruitment contributes to the onset of multiple organ dysfunct ion syndrome (MODS). Treatment with kinases inhibitors such as baricitinib, PF562271, Acalabrutinib, Fenebrutinib, Ibrutinib or immunomodulators such as ICOS-Fc or ISO-1 may attenuate sepsis/trauma-induced inflammation and thus MODS to improve clinical outcomes and patient prognosis.*

7 CONCLUSIONS

The work in this thesis showed that:

- The FAK, PyK2, BTK, JAK, MIF and ICOS-ICOSL pathways do indeed play a detrimental role in the pathogenesis of sepsis and/or haemorrhagic shock and their pharmacological and genetic inhibition exhibits protection by reducing the cytokine storm and therefore multiple organ failure.

- We highlight that the main molecular mechanism behind organ protection regardless of drug treatment is the attenuation of the inflammatory pathways NFκB and NLRP3 inflammasome. Our findings further corroborate the role of NFκB and NLRP3 as central inflammatory pathways in the development organ dysfunction in sepsis and haemorrhagic shock.

- We emphasize the clinical relevance of a drug repurposing approach, showing that drugs already on the marker such as Ibrutinib, Acalabrutinib, Fenebrutinib and Baricitinib may act as potential candidates to be repositioned for sepsis/haemorrhagic shock.

8 LIMITATIONS AND FUTURE PERSPECTIVES

Limitations:

- Due to ethical reasons, long-term follow-up assessment was not performed in most studies, which is an important outcome for the drug treatment.

- The studies were carried out only in male rodents, which perhaps some finding cannot be directly extrapolated to females.

- The severity of sepsis and haemorrhagic shock depends also the presence of comorbidities, however the studies were conducted in the absence of any of them, which can directly impact development of these clinical conditions.

Future perspectives:

- New studies considering long-term follow-up assessment, gender and comorbidities would be required to confirm and provide more insights into the research field.

- New potential pharmacological targets, either kinases or other key mediators, need to be explored in the septic or haemorrhagic shock context.

- Considering the late diagnosis of sepsis, late treatment might be considered in order to identify a treatment capable of reversing the already established organ damage.

9 ACKNOWLEDGEMENTS

I would first like to thank my supervisors, Professor Massimo Collino and Professor Daniel Fernandes for sharing their immense knowledge and plentiful experience. Thank you for encouraging and guiding me at all the time of my academic research. In particular, I am very thankful to Prof. Massimo Collino for all the opportunities during these years and for the continuous support and patience from the very beginning when I arrived in Italy. I am also very grateful since the first opportunity given by Prof. Daniel Fernandes in 2015 in his laboratory, which was fundamental for me to be concluding this scientific journey today. Working with both of you has been very enjoyable and I have learned and grown a lot. Thank you very much.

I would like to thank all Professors who accepted the invitation to participate in the examining board of my thesis (Prof. Vincenzo Brancaleone, Prof. Antonella de Angelis, Prof. José Eduardo da Silva Santos, Prof. Jamil Assreuy, Prof. Carlo Cifani, Prof. Monica Montagnani, Prof. Michel Fleith Otuki and Prof. Fernando Spiller). A special thanks to Prof. Vincenzo Brancaleone and Prof. José Eduardo da Silva Santos for their willingness to carefully examine my thesis. Thank you so much.

I wanted to thank the researchers I had the opportunity to work with (Prof. Regina de Sordi, Dr. Raffaella Mastrocola, Prof. Fabio Penna, Prof. Umberto Dianzani, Prof. Chiara Dianzani and Prof. Manuela Aragno, Prof. Christoph Thiemermann). Thank you for sharing your knowledge.

I would like to express my deepest gratitude to my dear friend and colleague Eleonora Aimaretti, who, in addition to being an excellent professional, makes this journey much easier. Thank you for your kindness and for everything.

I would also like to extend my thanks to my colleagues at University of Turin, Elisa Porchietto, Giacomo Einaudi, Chiara Rubeo and Debora Collotta for their continuous support and friendship. Thank you for making us a great research team.

In addition, I would like to thank all the students who were part of our day-to-day lab and contributed to the development of this research (Samantha Cannone, Alex Cute, Miquel Cao, Elisa Pettineo, Atefeh Moradi, Maria Semeraro, Alessandra Nela, Patricio Israel, Masiha Aryafar and Giulia Esposito). I am very grateful for your support.

A special thanks to my Brazilian team who also contributed to my research period at UFSC (Junior Garcia de Oliveira, Maria Luisa da Silveira Hahmeyer, Gabrielle Delfrate, Luana Nunes Mariot and Merita Pereira Gonçalves). Thank you for all your help and friendship.

I must thank my dear friends who make my path much easier and happier (Paula Olsen Sorgatto, Nicolò Russo, Davide Bombelli, Mattia Mantovani, João Brondi, Ramon Soltovski, Alex Fissore, Matilde Brunello, Ismaele Di Benedetto and Silvia Domenica). Thanks for always being there.

Lastly, I should extend my thanks to my family in Portuguese. Agradeço imensamente minha mãe, Leoni Ferreira Alves que, apesar da distância, nunca mediu esforços para que eu alcançasse meus objetivos. Muito obrigado por ser a pessoa mais compreensiva e que mais me incentiva a conquistar todos meus ideais e anseios. Um agradecimento especial também aos meus irmãos (Alexandre Ferreira Alves, Felipe Ferreira Alves e Thiago Nahor) e minhas cunhadas (Ingrid Delezuk e Heloiza Rymsza) por todo suporte.

10 REFERENCES

[1] World Health Organization. Link available: "https://www.who.int/news-room/fact-sheets/detail/cardiovascular-diseases-(cvds)."

[2] H. Merdji, V. Schini-Kerth, F. Meziani, and F. Toti, "Long-term cardiovascular complications following sepsis: is senescence the missing link?," *Ann Intensive Care*, vol. 11, no. 1, p. 166, Dec. 2021, doi: 10.1186/s13613-021-00937-y.

[3] S. R. Heckbert *et al.*, "Outcome after Hemorrhagic Shock in Trauma Patients," *The Journal of Trauma: Injury, Infection, and Critical Care*, vol. 45, no. 3, pp. 545–549, Sep. 1998, doi: 10.1097/00005373-199809000-00022.

[4] K. E. Rudd *et al.*, "Global, regional, and national sepsis incidence and mortality, 1990–2017: analysis for the Global Burden of Disease Study," *The Lancet*, vol. 395, no. 10219, pp. 200–211, Jan. 2020, doi: 10.1016/S0140-6736(19)32989-7.

[5] T. Vos *et al.*, "Global burden of 369 diseases and injuries in 204 countries and territories, 1990–2019: a systematic analysis for the Global Burden of Disease Study 2019," *The Lancet*, vol. 396, no. 10258, pp. 1204–1222, Oct. 2020, doi: 10.1016/S0140-6736(20)30925-9.

[6] N. Curry, S. Hopewell, C. Dorée, C. Hyde, K. Brohi, and S. Stanworth, "The acute management of trauma hemorrhage: a systematic review of randomized controlled trials," *Crit Care*, vol. 15, no. 2, p. R92, 2011, doi: 10.1186/cc10096.

[7] M. Singer *et al.*, "The Third International Consensus Definitions for Sepsis and Septic Shock (Sepsis-3)," *JAMA*, vol. 315, no. 8, p. 801, Feb. 2016, doi: 10.1001/jama.2016.0287.

[8] L. Evans *et al.*, "Surviving sepsis campaign: international guidelines for management of sepsis and septic shock 2021," *Intensive Care Med*, vol. 47, no. 11, pp. 1181–1247, Nov. 2021, doi: 10.1007/s00134-021-06506-y.

[9] D. R. Spahn *et al.*, "The European guideline on management of major bleeding and coagulopathy following trauma: fifth edition," *Crit Care*, vol. 23, no. 1, p. 98, Dec. 2019, doi: 10.1186/s13054-019-2347-3.

[10] R. Medzhitov, "Origin and physiological roles of inflammation," *Nature*, vol. 454, no. 7203, pp. 428–435, Jul. 2008, doi: 10.1038/nature07201.

[11] J. M. Lord *et al.*, "The systemic immune response to trauma: an overview of pathophysiology and treatment," *The Lancet*, vol. 384, no. 9952, pp. 1455–1465, Oct. 2014, doi: 10.1016/S0140-6736(14)60687-5.

[12] B. Relja, K. Mörs, and I. Marzi, "Danger signals in trauma," *European Journal of Trauma and Emergency Surgery*, vol. 44, no. 3, pp. 301–316, Jun. 2018, doi: 10.1007/s00068-018-0962-3.

[13] M. J. Delano and P. A. Ward, "The immune system's role in sepsis progression, resolution, and long-term outcome," *Immunol Rev*, vol. 274, no. 1, pp. 330–353, Nov. 2016, doi: 10.1111/imr.12499.

[14] G. Y. Chen and G. Nuñez, "Sterile inflammation: sensing and reacting to damage," *Nat Rev Immunol*, vol. 10, no. 12, pp. 826–837, Dec. 2010, doi: 10.1038/nri2873.

[15] R. Sordi *et al.*, "Resolvin D1 Attenuates the Organ Injury Associated With Experimental Hemorrhagic Shock," *Ann Surg*, vol. 273, no. 5, pp. 1012–1021, May 2021, doi: 10.1097/SLA.0000000000003407.

[16] W. He, H. Dong, C. Wu, Y. Zhong, and J. Li, "The role of NLRP3 inflammasome in sepsis: A potential therapeutic target," *Int Immunopharmacol*, vol. 115, p. 109697, Feb. 2023, doi: 10.1016/j.intimp.2023.109697.

[17] N. Yamada *et al.*, "Novel Synthetic, Host-defense Peptide Protects Against Organ Injury/Dysfunction in a Rat Model of Severe Hemorrhagic Shock," *Ann Surg*, vol. 268, no. 2, pp. 348–356, Aug. 2018, doi: 10.1097/SLA.0000000000002186.

[18] S. A. Emadi, A. G. Baradari, J. Y. Charati, F. Taghavi, and F. H. Kiabi, "SOFA and modified SOFA score for accessing outcomes among trauma patients in intensive care unit," *International Journal of Surgery Open*, vol. 47, p. 100559, Oct. 2022, doi: 10.1016/j.ijso.2022.100559.

[19] Y. Sakr *et al.*, "Patterns and early evolution of organ failure in the intensive care unit and their relation to outcome," *Crit Care*, vol. 16, no. 6, p. R222, 2012, doi: 10.1186/cc11868.

[20] O. Takeuchi and S. Akira, "Pattern Recognition Receptors and Inflammation," *Cell*, vol. 140, no. 6, pp. 805–820, Mar. 2010, doi: 10.1016/j.cell.2010.01.022.

[21] O. O. Nduka and J. E. Parrillo, "The Pathophysiology of Septic Shock," *Crit Care Clin*, vol. 25, no. 4, pp. 677–702, Oct. 2009, doi: 10.1016/j.ccc.2009.08.002.

[22] K. Timmermans, M. Kox, G. J. Scheffer, and P. Pickkers, "Danger in the Intensive Care Unit," *Shock*, vol. 45, no. 2, pp. 108–116, Feb. 2016, doi: 10.1097/SHK.0000000000000506.

[23] K. C. Ma, E. J. Schenck, M. A. Pabon, and A. M. K. Choi, "The Role of Danger Signals in the Pathogenesis and Perpetuation of Critical Illness," *Am J Respir Crit Care Med*, vol. 197, no. 3, pp. 300–309, Feb. 2018, doi: 10.1164/rccm.201612-2460PP.

[24] V. Papayannopoulos, "Neutrophil extracellular traps in immunity and disease," *Nat Rev Immunol*, vol. 18, no. 2, pp. 134–147, Feb. 2018, doi: 10.1038/nri.2017.105.

[25] T. Lawrence, "The Nuclear Factor NF- B Pathway in Inflammation," *Cold Spring Harb Perspect Biol*, vol. 1, no. 6, pp. a001651–a001651, Dec. 2009, doi: 10.1101/cshperspect.a001651.

[26] D. C. Cornelius *et al.*, "NLRP3 inflammasome inhibition attenuates sepsis-induced platelet activation and prevents multi-organ injury in cecal-ligation puncture," *PLoS One*, vol. 15, no. 6, p. e0234039, Jun. 2020, doi: 10.1371/journal.pone.0234039.

[27] J. Langedijk, A. K. Mantel-Teeuwisse, D. S. Slijkerman, and M.-H. D. B. Schutjens, "Drug repositioning and repurposing: terminology and definitions in literature," *Drug Discov Today*, vol. 20, no. 8, pp. 1027–1034, Aug. 2015, doi: 10.1016/j.drudis.2015.05.001.

[28] F. Christian, E. Smith, and R. Carmody, "The Regulation of NF-κB Subunits by Phosphorylation," *Cells*, vol. 5, no. 1, p. 12, Mar. 2016, doi: 10.3390/cells5010012.

[29] N. Song and T. Li, "Regulation of NLRP3 Inflammasome by Phosphorylation," *Front Immunol*, vol. 9, Oct. 2018, doi: 10.3389/fimmu.2018.02305.

[30] G. Manning, D. B. Whyte, R. Martinez, T. Hunter, and S. Sudarsanam, "The Protein Kinase Complement of the Human Genome," *Science (1979)*, vol. 298, no. 5600, pp. 1912–1934, Dec. 2002, doi: 10.1126/science.1075762.

[31] G. L. Goebel, X. Qiu, and P. Wu, “Kinase-targeting small-molecule inhibitors and emerging bifunctional molecules,” *Trends Pharmacol Sci*, vol. 43, no. 10, pp. 866–881, Oct. 2022, doi: 10.1016/j.tips.2022.04.006.

[32] C. A. Lipinski and J. C. Loftus, “Targeting Pyk2 for therapeutic intervention,” *Expert Opin Ther Targets*, vol. 14, no. 1, pp. 95–108, Jan. 2010, doi: 10.1517/14728220903473194.

[33] X. Zhao and J.-L. Guan, “Focal adhesion kinase and its signaling pathways in cell migration and angiogenesis,” *Adv Drug Deliv Rev*, vol. 63, no. 8, pp. 610–615, Jul. 2011, doi: 10.1016/j.addr.2010.11.001.

[34] H. Avraham, S.-Y. Park, K. Schinkmann, and S. Avraham, “RAFTK/Pyk2-mediated cellular signalling,” *Cell Signal*, vol. 12, no. 3, pp. 123–133, Mar. 2000, doi: 10.1016/S0898-6568(99)00076-5.

[35] T. Nagai *et al.*, “Focal Adhesion Kinase-Mediated Sequences, Including Cell Adhesion, Inflammatory Response, and Fibrosis, as a Therapeutic Target in Endometriosis,” *Reproductive Sciences*, vol. 27, no. 7, pp. 1400–1410, Jul. 2020, doi: 10.1007/s43032-019-00044-1.

[36] S. Kim, W. Cho, I. Kim, S.-H. Lee, G. T. Oh, and Y. M. Park, “Oxidized LDL induces vimentin secretion by macrophages and contributes to atherosclerotic inflammation,” *J Mol Med*, vol. 98, no. 7, pp. 973–983, Jul. 2020, doi: 10.1007/s00109-020-01923-w.

[37] Y. Duan, J. Learoyd, A. Y. Meliton, B. S. Clay, A. R. Leff, and X. Zhu, “Inhibition of Pyk2 Blocks Airway Inflammation and Hyperresponsiveness in a Mouse Model of Asthma,” *Am J Respir Cell Mol Biol*, vol. 42, no. 4, pp. 491–497, Apr. 2010, doi: 10.1165/rcmb.2008-0469OC.

[38] R. Naser, A. Aldehaiman, E. Díaz-Galicia, and S. Arold, “Endogenous Control Mechanisms of FAK and PYK2 and Their Relevance to Cancer Development,” *Cancers (Basel)*, vol. 10, no. 6, p. 196, Jun. 2018, doi: 10.3390/cancers10060196.

[39] X. Zhu, Y. Bao, Y. Guo, and W. Yang, “Proline-Rich Protein Tyrosine Kinase 2 in Inflammation and Cancer,” *Cancers (Basel)*, vol. 10, no. 5, p. 139, May 2018, doi: 10.3390/cancers10050139.

[40] J. M. Murphy *et al.*, “Focal Adhesion Kinase Activity and Localization is Critical for TNF-α-Induced Nuclear Factor-κB Activation,” *Inflammation*, vol. 44, no. 3, pp. 1130–1144, Jun. 2021, doi: 10.1007/s10753-020-01408-5.

[41] A. R. Anand, R. Bradley, and R. K. Ganju, “LPS-induced MCP-1 expression in human microvascular endothelial cells is mediated by the tyrosine kinase, Pyk2 via the p38 MAPK/NF-κB-dependent pathway,” *Mol Immunol*, vol. 46, no. 5, pp. 962–968, Feb. 2009, doi: 10.1016/j.molimm.2008.09.022.

[42] T. Harada *et al.*, “Focal Adhesion Kinase Promotes the Progression of Aortic Aneurysm by Modulating Macrophage Behavior,” *Arterioscler Thromb Vasc Biol*, vol. 37, no. 1, pp. 156–165, Jan. 2017, doi: 10.1161/ATVBAHA.116.308542.

[43] F. J. Sulzmaier, C. Jean, and D. D. Schlaepfer, “FAK in cancer: mechanistic findings and clinical applications,” *Nat Rev Cancer*, vol. 14, no. 9, pp. 598–610, Sep. 2014, doi: 10.1038/nrc3792.

[44] S. M. Weis *et al.*, “Compensatory role for Pyk2 during angiogenesis in adult mice lacking endothelial cell FAK,” *Journal of Cell Biology*, vol. 181, no. 1, pp. 43–50, Apr. 2008, doi: 10.1083/jcb.200710038.

[45] C. Hu *et al.*, "Antitumor effect of focal adhesion kinase inhibitor PF562271 against human osteosarcoma *in vitro* and *in vivo*," *Cancer Sci*, vol. 108, no. 7, pp. 1347–1356, Jul. 2017, doi: 10.1111/cas.13256.

[46] I.-C. Chung *et al.*, "Pyk2 activates the NLRP3 inflammasome by directly phosphorylating ASC and contributes to inflammasome-dependent peritonitis," *Sci Rep*, vol. 6, no. 1, p. 36214, Oct. 2016, doi: 10.1038/srep36214.

[47] J. M. Murphy, K. Jeong, Y. A. R. Rodriguez, J.-H. Kim, E.-Y. E. Ahn, and S.-T. S. Lim, "FAK and Pyk2 activity promote TNF-α and IL-1β-mediated pro-inflammatory gene expression and vascular inflammation," *Sci Rep*, vol. 9, no. 1, p. 7617, May 2019, doi: 10.1038/s41598-019-44098-2.

[48] M. C. Guido *et al.*, "Small Interfering RNA Targeting Focal Adhesion Kinase Prevents Cardiac Dysfunction in Endotoxemia," *Shock*, vol. 37, no. 1, pp. 77–84, Jan. 2012, doi: 10.1097/SHK.0b013e31823532ec.

[49] R. C. Petroni *et al.*, "Role of Focal Adhesion Kinase in Lung Remodeling of Endotoxemic Rats," *Shock*, vol. 37, no. 5, pp. 524–530, May 2012, doi: 10.1097/SHK.0b013e31824c7665.

[50] W. G. Roberts *et al.*, "Antitumor Activity and Pharmacology of a Selective Focal Adhesion Kinase Inhibitor, PF-562,271," *Cancer Res*, vol. 68, no. 6, pp. 1935–1944, Mar. 2008, doi: 10.1158/0008-5472.CAN-07-5155.

[51] J. R. Infante *et al.*, "Safety, Pharmacokinetic, and Pharmacodynamic Phase I Dose-Escalation Trial of PF-00562271, an Inhibitor of Focal Adhesion Kinase, in Advanced Solid Tumors," *Journal of Clinical Oncology*, vol. 30, no. 13, pp. 1527–1533, May 2012, doi: 10.1200/JCO.2011.38.9346.

[52] B. Y. Lee, P. Timpson, L. G. Horvath, and R. J. Daly, "FAK signaling in human cancer as a target for therapeutics," *Pharmacol Ther*, vol. 146, pp. 132–149, Feb. 2015, doi: 10.1016/j.pharmthera.2014.10.001.

[53] S. Tsukada *et al.*, "Deficient expression of a B cell cytoplasmic tyrosine kinase in human X-linked agammaglobulinemia," *Cell*, vol. 72, no. 2, pp. 279–290, Jan. 1993, doi: 10.1016/0092-8674(93)90667-F.

[54] C. Liang *et al.*, "The development of Bruton's tyrosine kinase (BTK) inhibitors from 2012 to 2017: A mini-review," *Eur J Med Chem*, vol. 151, pp. 315–326, May 2018, doi: 10.1016/j.ejmech.2018.03.062.

[55] T. Wen, J. Wang, Y. Shi, H. Qian, and P. Liu, "Inhibitors targeting Bruton's tyrosine kinase in cancers: drug development advances," *Leukemia*, vol. 35, no. 2, pp. 312–332, Feb. 2021, doi: 10.1038/s41375-020-01072-6.

[56] L. J. Crofford, L. E. Nyhoff, J. H. Sheehan, and P. L. Kendall, "The role of Bruton's tyrosine kinase in autoimmunity and implications for therapy," *Expert Rev Clin Immunol*, vol. 12, no. 7, pp. 763–773, Jul. 2016, doi: 10.1586/1744666X.2016.1152888.

[57] A. Markham and S. Dhillon, "Acalabrutinib: First Global Approval," *Drugs*, vol. 78, no. 1, pp. 139–145, Jan. 2018, doi: 10.1007/s40265-017-0852-8.

[58] M. Roschewski *et al.*, "Inhibition of Bruton tyrosine kinase in patients with severe COVID-19," *Sci Immunol*, vol. 5, no. 48, Jun. 2020, doi: 10.1126/sciimmunol.abd0110.

[59] C. E. O'Riordan *et al.*, "Bruton's Tyrosine Kinase Inhibition Attenuates the Cardiac Dysfunction Caused by Cecal Ligation and Puncture in Mice," *Front Immunol*, vol. 10, Sep. 2019, doi: 10.3389/fimmu.2019.02129.

[60] R. W. Hendriks, S. Yuvaraj, and L. P. Kil, "Targeting Bruton's tyrosine kinase in B cell malignancies," *Nat Rev Cancer*, vol. 14, no. 4, pp. 219–232, Apr. 2014, doi: 10.1038/nrc3702.

[61] M. Ito *et al.*, "Bruton's tyrosine kinase is essential for NLRP3 inflammasome activation and contributes to ischaemic brain injury," *Nat Commun*, vol. 6, no. 1, p. 7360, Jun. 2015, doi: 10.1038/ncomms8360.

[62] A. E. Herman *et al.*, "Safety, Pharmacokinetics, and Pharmacodynamics in Healthy Volunteers Treated With GDC-0853, a Selective Reversible Bruton's Tyrosine Kinase Inhibitor," *Clin Pharmacol Ther*, vol. 103, no. 6, pp. 1020–1028, Jun. 2018, doi: 10.1002/cpt.1056.

[63] S. Cohen *et al.*, "Fenebrutinib Versus Placebo or Adalimumab in Rheumatoid Arthritis: A Randomized, Double-Blind, Phase <scp>II</scp> Trial," *Arthritis & Rheumatology*, vol. 72, no. 9, pp. 1435–1446, Sep. 2020, doi: 10.1002/art.41275.

[64] A. N. R. Weber, Z. Bittner, X. Liu, T.-M. Dang, M. P. Radsak, and C. Brunner, "Bruton's Tyrosine Kinase: An Emerging Key Player in Innate Immunity," *Front Immunol*, vol. 8, Nov. 2017, doi: 10.3389/fimmu.2017.01454.

[65] R. Morris, N. J. Kershaw, and J. J. Babon, "The molecular details of cytokine signaling via the JAK/STAT pathway," *Protein Science*, vol. 27, no. 12, pp. 1984–2009, Dec. 2018, doi: 10.1002/pro.3519.

[66] J. J. O'Shea, D. M. Schwartz, A. v. Villarino, M. Gadina, I. B. McInnes, and A. Laurence, "The JAK-STAT Pathway: Impact on Human Disease and Therapeutic Intervention," *Annu Rev Med*, vol. 66, no. 1, pp. 311–328, Jan. 2015, doi: 10.1146/annurev-med-051113-024537.

[67] J. J. O'Shea, D. M. Schwartz, A. v. Villarino, M. Gadina, I. B. McInnes, and A. Laurence, "The JAK-STAT Pathway: Impact on Human Disease and Therapeutic Intervention," *Annu Rev Med*, vol. 66, no. 1, pp. 311–328, Jan. 2015, doi: 10.1146/annurev-med-051113-024537.

[68] Y. Fan, R. Mao, and J. Yang, "NF-κB and STAT3 signaling pathways collaboratively link inflammation to cancer," *Protein Cell*, vol. 4, no. 3, pp. 176–185, Mar. 2013, doi: 10.1007/s13238-013-2084-3.

[69] H. Zhu *et al.*, "Janus Kinase Inhibition Ameliorates Ischemic Stroke Injury and Neuroinflammation Through Reducing NLRP3 Inflammasome Activation via JAK2/STAT3 Pathway Inhibition," *Front Immunol*, vol. 12, Jul. 2021, doi: 10.3389/fimmu.2021.714943.

[70] M. Y. Furuya *et al.*, "Tofacitinib inhibits granulocyte–macrophage colony-stimulating factor-induced NLRP3 inflammasome activation in human neutrophils," *Arthritis Res Ther*, vol. 20, no. 1, p. 196, Dec. 2018, doi: 10.1186/s13075-018-1685-x.

[71] P. Xin *et al.*, "The role of JAK/STAT signaling pathway and its inhibitors in diseases," *Int Immunopharmacol*, vol. 80, p. 106210, Mar. 2020, doi: 10.1016/j.intimp.2020.106210.

[72] A. Markham, "Baricitinib: First Global Approval," *Drugs*, vol. 77, no. 6, pp. 697–704, Apr. 2017, doi: 10.1007/s40265-017-0723-3.

[73] D. Collotta *et al.*, "Baricitinib counteracts metaflammation, thus protecting against diet-induced metabolic abnormalities in mice," *Mol Metab*, vol. 39, p. 101009, Sep. 2020, doi: 10.1016/j.molmet.2020.101009.

[74] J. Lee *et al.*, "Baricitinib Attenuates Autoimmune Phenotype and Podocyte Injury in a Murine Model of Systemic Lupus Erythematosus," *Front Immunol*, vol. 12, Aug. 2021, doi: 10.3389/fimmu.2021.704526.

[75] P. J. Murray, "The JAK-STAT Signaling Pathway: Input and Output Integration," *The Journal of Immunology*, vol. 178, no. 5, pp. 2623–2629, Mar. 2007, doi: 10.4049/jimmunol.178.5.2623.

[76] A. Salas *et al.*, "JAK–STAT pathway targeting for the treatment of inflammatory bowel disease," *Nat Rev Gastroenterol Hepatol*, vol. 17, no. 6, pp. 323–337, Jun. 2020, doi: 10.1038/s41575-020-0273-0.

[77] R. A. Mitchell *et al.*, "Macrophage migration inhibitory factor (MIF) sustains macrophage proinflammatory function by inhibiting p53: Regulatory role in the innate immune response," *Proceedings of the National Academy of Sciences*, vol. 99, no. 1, pp. 345–350, Jan. 2002, doi: 10.1073/pnas.012511599.

[78] T. Calandra *et al.*, "MIF as a glucocorticoid-induced modulator of cytokine production," *Nature*, vol. 377, no. 6544, pp. 68–71, Sep. 1995, doi: 10.1038/377068a0.

[79] W. Y. Weiser, L. M. Pozzi, and J. R. David, "Human recombinant migration inhibitory factor activates human macrophages to kill Leishmania donovani.," *J Immunol*, vol. 147, no. 6, pp. 2006–11, Sep. 1991.

[80] T. Calandra, L. A. Spiegel, C. N. Metz, and R. Bucala, "Macrophage migration inhibitory factor is a critical mediator of the activation of immune cells by exotoxins of Gram-positive bacteria," *Proceedings of the National Academy of Sciences*, vol. 95, no. 19, pp. 11383–11388, Sep. 1998, doi: 10.1073/pnas.95.19.11383.

[81] S. S. Jankauskas, D. W. L. Wong, R. Bucala, S. Djudjaj, and P. Boor, "Evolving complexity of MIF signaling," *Cell Signal*, vol. 57, pp. 76–88, May 2019, doi: 10.1016/j.cellsig.2019.01.006.

[82] E. P. C. van der Vorst, Y. Döring, and C. Weber, "Chemokines and their receptors in Atherosclerosis," *J Mol Med*, vol. 93, no. 9, pp. 963–971, Sep. 2015, doi: 10.1007/s00109-015-1317-8.

[83] T. Roger, M. P. Glauser, and T. Calandra, "Macrophage migration inhibitory factor (MIF) modulates innate immune responses induced by endotoxin and Gram-negative bacteria.," *J Endotoxin Res*, vol. 7, no. 6, pp. 456–60, 2001.

[84] H. Y. Lan *et al.*, "TNF-alpha up-regulates renal MIF expression in rat crescentic glomerulonephritis.," *Mol Med*, vol. 3, no. 2, pp. 136–44, Feb. 1997.

[85] E. K. Rice *et al.*, "Induction of MIF synthesis and secretion by tubular epithelial cells: A novel action of angiotensin II," *Kidney Int*, vol. 63, no. 4, pp. 1265–1275, Apr. 2003, doi: 10.1046/j.1523-1755.2003.00875.x.

[86] T. Calandra, J. Bernhagen, R. A. Mitchell, and R. Bucala, "The macrophage is an important and previously unrecognized source of macrophage migration inhibitory factor.," *Journal of Experimental Medicine*, vol. 179, no. 6, pp. 1895–1902, Jun. 1994, doi: 10.1084/jem.179.6.1895.

[87] F. G. Brown *et al.*, "Urine macrophage migration inhibitory factor reflects the severity of renal injury in human glomerulonephritis.," *J Am Soc Nephrol*, vol. 13 Suppl 1, pp. S7-13, Jan. 2002.

[88] A. Beishuizen, L. G. Thijs, C. Haanen, and I. Vermes, "Macrophage Migration Inhibitory Factor and Hypothalamo-Pituitary-Adrenal Function during Critical Illness," *J Clin Endocrinol Metab*, vol. 86, no. 6, pp. 2811–2816, Jun. 2001, doi: 10.1210/jcem.86.6.7570.

[89] J. Bernhagen *et al.*, "MIF is a pituitary-derived cytokine that potentiates lethal endotoxaemia," *Nature*, vol. 365, no. 6448, pp. 756–759, Oct. 1993, doi: 10.1038/365756a0.

[90] T. Calandra *et al.*, "Protection from septic shock by neutralization of macrophage migration inhibitory factor," *Nat Med*, vol. 6, no. 2, pp. 164–170, Feb. 2000, doi: 10.1038/72262.

[91] P. C. Joshi, G. v Poole, V. Sachdev, X. Zhou, and Q. Jones, "Trauma patients with positive cultures have higher levels of circulating macrophage migration inhibitory factor (MIF).," *Res Commun Mol Pathol Pharmacol*, vol. 107, no. 1–2, pp. 13–20, 2000.

[92] M. Hayakawa *et al.*, "Imbalance Between Macrophage Migration Inhibitory Factor and Cortisol Induces Multiple Organ Dysfunction in Patients with Blunt Trauma," *Inflammation*, vol. 34, no. 3, pp. 193–197, Jun. 2011, doi: 10.1007/s10753-010-9223-2.

[93] J. B. Lubetsky *et al.*, "The Tautomerase Active Site of Macrophage Migration Inhibitory Factor Is a Potential Target for Discovery of Novel Anti-inflammatory Agents," *Journal of Biological Chemistry*, vol. 277, no. 28, pp. 24976–24982, Jul. 2002, doi: 10.1074/jbc.M203220200.

[94] Y. Liu *et al.*, "MIF inhibitor ISO-1 alleviates severe acute pancreatitis-associated acute kidney injury by suppressing the NLRP3 inflammasome signaling pathway," *Int Immunopharmacol*, vol. 96, p. 107555, Jul. 2021, doi: 10.1016/j.intimp.2021.107555.

[95] W. Ji, Y. Ren, X. Wei, X. Ding, Y. Dong, and B. Yuan, "Ischemic stroke protected by ISO-1 inhibition of apoptosis via mitochondrial pathway," *Sci Rep*, vol. 13, no. 1, p. 2788, Feb. 2023, doi: 10.1038/s41598-023-29907-z.

[96] Y. Al-Abed *et al.*, "ISO-1 Binding to the Tautomerase Active Site of MIF Inhibits Its Pro-inflammatory Activity and Increases Survival in Severe Sepsis," *Journal of Biological Chemistry*, vol. 280, no. 44, pp. 36541–36544, Nov. 2005, doi: 10.1074/jbc.C500243200.

[97] K. Sumaiya, D. Langford, K. Natarajaseenivasan, and S. Shanmughapriya, "Macrophage migration inhibitory factor (MIF): A multifaceted cytokine regulated by genetic and physiological strategies," *Pharmacol Ther*, vol. 233, p. 108024, May 2022, doi: 10.1016/j.pharmthera.2021.108024.

[98] A. Hutloff *et al.*, "ICOS is an inducible T-cell co-stimulator structurally and functionally related to CD28," *Nature*, vol. 397, no. 6716, pp. 263–266, Jan. 1999, doi: 10.1038/16717.

[99] S. K. Yoshinaga *et al.*, "T-cell co-stimulation through B7RP-1 and ICOS," *Nature*, vol. 402, no. 6763, pp. 827–832, Dec. 1999, doi: 10.1038/45582.

[100] M. M. Swallow, J. J. Wallin, and W. C. Sha, "B7h, a Novel Costimulatory Homolog of B7.1 and B7.2, Is Induced by TNFα," *Immunity*, vol. 11, no. 4, pp. 423–432, Oct. 1999, doi: 10.1016/S1074-7613(00)80117-X.

[101] Y. Burmeister *et al.*, "ICOS Controls the Pool Size of Effector-Memory and Regulatory T Cells," *The Journal of Immunology*, vol. 180, no. 2, pp. 774–782, Jan. 2008, doi: 10.4049/jimmunol.180.2.774.

[102] Q. Chen *et al.*, "ICOS signal facilitates Foxp3 transcription to favor suppressive function of regulatory T cells," *Int J Med Sci*, vol. 15, no. 7, pp. 666–673, 2018, doi: 10.7150/ijms.23940.

[103] S. A. Lund, C. M. Giachelli, and M. Scatena, "The role of osteopontin in inflammatory processes," *J Cell Commun Signal*, vol. 3, no. 3–4, pp. 311–322, Dec. 2009, doi: 10.1007/s12079-009-0068-0.

[104] D. Raineri *et al.*, "Osteopontin binds ICOSL promoting tumor metastasis," *Commun Biol*, vol. 3, no. 1, p. 615, Oct. 2020, doi: 10.1038/s42003-020-01333-1.

[105] C. Dianzani *et al.*, "B7h Triggering Inhibits Umbilical Vascular Endothelial Cell Adhesiveness to Tumor Cell Lines and Polymorphonuclear Cells," *The Journal of Immunology*, vol. 185, no. 7, pp. 3970–3979, Oct. 2010, doi: 10.4049/jimmunol.0903269.

[106] S. Occhipinti *et al.*, "Triggering of B7h by the ICOS Modulates Maturation and Migration of Monocyte-Derived Dendritic Cells," *The Journal of Immunology*, vol. 190, no. 3, pp. 1125–1134, 2013, doi: 10.4049/jimmunol.1201816.

[107] P. Möhnle *et al.*, "MicroRNAs 143 and 150 in whole blood enable detection of T-cell immunoparalysis in sepsis," *Molecular Medicine*, vol. 24, no. 1, p. 54, Dec. 2018, doi: 10.1186/s10020-018-0056-z.

[108] Menéndez *et al.*, "Simultaneous Depression of Immunological Synapse and Endothelial Injury is Associated with Organ Dysfunction in Community-Acquired Pneumonia," *J Clin Med*, vol. 8, no. 9, p. 1404, Sep. 2019, doi: 10.3390/jcm8091404.

[109] L. M. Castello *et al.*, "The role of osteopontin as a diagnostic and prognostic biomarker in sepsis and septic shock," *Cells*, vol. 8, no. 2, pp. 1–12, 2019, doi: 10.3390/cells8020174.

[110] Y. Luan, C. Yin, Q. Qin, N. Dong, X. Zhu, and Z. Sheng, "Effect of Regulatory T Cells on Promoting Apoptosis of T Lymphocyte and Its Regulatory Mechanism in Sepsis," *JOURNAL OF INTERFERON & CYTOKINE RESEARCH*, vol. 35, no. 12, pp. 969–980, 2015, doi: 10.1089/jir.2014.0235.

[111] K. SAITO *et al.*, "Sepsis is Characterized by the Increases in Percentages of Circulating CD4 + CD25 + Regulatory T Cells and Plasma Levels of Soluble CD25," *Journal of Experimental Medicine*, vol. 216, pp. 61–68, 2008, doi: 10.1620/tjem.216.61.

[112] F. Leng, J. Liu, Z. Liu, J. Yin, and H.-P. Qu, "Increased proportion of CD4 D CD25 D Foxp3 D regulatory T cells during early-stage sepsis in ICU patients," *Journal of Microbiology, Immunology and Infection*, vol. 46, no. 5, pp. 338–344, 2013, doi: 10.1016/j.jmii.2012.06.012.

[113] F. Venet *et al.*, "Increased circulating regulatory T cells (CD4+CD25+CD1272) contribute to lymphocyte anergy in septic shock patients," *Intensive Care Med*, vol. 35, pp. 678–686, 2009, doi: 10.1007/s00134-008-1337-8.

[114] S. Inoue *et al.*, "Reduction of Immunocompetent T Cells Followed by Prolonged Lymphopenia in Severe Sepsis in the Elderly*," *Clin Investig (Lond)*, vol. 41, no. 3, pp. 810–819, 2013, doi: 10.1097/CCM.0b013e318274645f.

[115] R. di Niro *et al.*, "Construction of miniantibodies for the in vivo study of human autoimmune diseases in animal models," *BMC Biotechnol*, vol. 7, pp. 1–10, 2007, doi: 10.1186/1472-6750-7-46.

[116] A. H. Sharpe and G. J. Freeman, "The B7–CD28 superfamily," *Nat Rev Immunol*, vol. 2, no. 2, pp. 116–126, Feb. 2002, doi: 10.1038/nri727.

[117] N. Percie du Sert *et al.*, "The ARRIVE guidelines 2.0: Updated guidelines for reporting animal research," *PLoS Biol*, vol. 18, no. 7, p. e3000410, Jul. 2020, doi: 10.1371/journal.pbio.3000410.

[118] M. F. Osuchowski *et al.*, "Minimum Quality Threshold in Pre-Clinical Sepsis Studies (MQTiPSS): An International Expert Consensus Initiative for Improvement of Animal Modeling in Sepsis," *Shock*, vol. 50, no. 4, pp. 377–380, Oct. 2018, doi: 10.1097/SHK.0000000000001212.

[119] J. A. Buras, B. Holzmann, and M. Sitkovsky, "Animal Models of sepsis: setting the stage," *Nat Rev Drug Discov*, vol. 4, no. 10, pp. 854–865, Oct. 2005, doi: 10.1038/nrd1854.

[120] W. G. Roberts *et al.*, "Antitumor Activity and Pharmacology of a Selective Focal Adhesion Kinase Inhibitor, PF-562,271," *Cancer Res*, vol. 68, no. 6, pp. 1935–1944, Mar. 2008, doi: 10.1158/0008-5472.CAN-07-5155.

[121] G. E. Ringheim, M. Wampole, and K. Oberoi, "Bruton's Tyrosine Kinase (BTK) Inhibitors and Autoimmune Diseases: Making Sense of BTK Inhibitor Specificity Profiles and Recent Clinical Trial Successes and Failures," *Front Immunol*, vol. 12, Nov. 2021, doi: 10.3389/fimmu.2021.662223.

[122] Whittaker M, "Center for Drug Evaluation and Research Application Number: 207924orig1s000 Pharmacology Review(s) Pharmacology/Toxicology Review Labeling Review Memo. Published online 2018."

[123] A. Alam *et al.*, "Synthesis and bio-evaluation of human macrophage migration inhibitory factor inhibitor to develop anti-inflammatory agent," *Bioorg Med Chem*, vol. 19, no. 24, pp. 7365–7373, Dec. 2011, doi: 10.1016/j.bmc.2011.10.056.

[124] K. IOANOU *et al.*, "ISO-66, a novel inhibitor of macrophage migration inhibitory factor, shows efficacy in melanoma and colon cancer models," *Int J Oncol*, vol. 45, no. 4, pp. 1457–1468, Oct. 2014, doi: 10.3892/ijo.2014.2551.

[125] M. Maeda *et al.*, "Regulation of T cell response by blocking the ICOS signal with the B7RP-1-specific small antibody fragment isolated from human antibody phage library," *MAbs*, vol. 1, no. 5, pp. 453–461, Sep. 2009, doi: 10.4161/mabs.1.5.9633.

[126] J. S. Fridman *et al.*, "Selective Inhibition of JAK1 and JAK2 Is Efficacious in Rodent Models of Arthritis: Preclinical Characterization of INCB028050," *The Journal of Immunology*, vol. 184, no. 9, pp. 5298–5307, May 2010, doi: 10.4049/jimmunol.0902819.

[127] C. Schierwagen, A.-C. Bylund-Fellenius, and C. Lundberg, "Improved method for quantification of tissue PMN accumulation measured by myeloperoxidase activity," *J Pharmacol Methods*, vol. 23, no. 3, pp. 179–186, May 1990, doi: 10.1016/0160-5402(90)90061-O.

[128] G. P. Parnell *et al.*, "Identifying Key Regulatory Genes in the Whole Blood of Septic Patients to Monitor Underlying Immune Dysfunctions," *Shock*, vol. 40, no. 3, pp. 166–174, Sep. 2013, doi: 10.1097/SHK.0b013e31829ee604.

[129] W. Xiao *et al.*, "A genomic storm in critically injured humans," *Journal of Experimental Medicine*, vol. 208, no. 13, pp. 2581–2590, Dec. 2011, doi: 10.1084/jem.20111354.

[130] F. Faul, E. Erdfelder, A.-G. Lang, and A. Buchner, "G*Power 3: A flexible statistical power analysis program for the social, behavioral, and biomedical sciences," *Behav Res Methods*, vol. 39, no. 2, pp. 175–191, May 2007, doi: 10.3758/BF03193146.

[131] A. R. Anand, R. Bradley, and R. K. Ganju, “LPS-induced MCP-1 expression in human microvascular endothelial cells is mediated by the tyrosine kinase, Pyk2 via the p38 MAPK/NF-κB-dependent pathway,” *Mol Immunol*, vol. 46, no. 5, pp. 962–968, Feb. 2009, doi: 10.1016/j.molimm.2008.09.022.

[132] J. M. Murphy *et al.*, “Focal Adhesion Kinase Activity and Localization is Critical for TNF-α-Induced Nuclear Factor-κB Activation,” *Inflammation*, vol. 44, no. 3, pp. 1130–1144, Jun. 2021, doi: 10.1007/s10753-020-01408-5.

[133] A. D. Bachstetter and L. J. van Eldik, “The p38 MAP Kinase Family as Regulators of Proinflammatory Cytokine Production in Degenerative Diseases of the CNS,” 2010.

[134] Chaudhry H *et al.*, “Role of cytokines as a double-edged sword in sepsis,” *In Vivo (Brooklyn)*, vol. 27, pp. 669–684, 2013.

[135] J. Zhan, Z. Zhang, C. Chen, K. Chen, and Y. Wang, “Penehyclidine hydrochloride attenuates LPS-induced iNOS production by inhibiting p38 MAPK activation in endothelial cells,” *Mol Biol Rep*, vol. 39, no. 2, pp. 1261–1265, Feb. 2012, doi: 10.1007/s11033-011-0857-4.

[136] M. Chu, Y. Koshman, R. Iyengar, T. Kim, B. Russell, and A. M. Samarel, “Contractile Activity Regulates Inducible Nitric Oxide Synthase Expression and NO ¡ Production in Cardiomyocytes via a FAK-Dependent Signaling Pathway,” *J Signal Transduct*, vol. 2012, pp. 1–11, Jul. 2012, doi: 10.1155/2012/473410.

[137] R. Liu, F. Lioté, D. M. Rose, D. Merz, and R. Terkeltaub, “Proline-rich tyrosine kinase 2 and Src kinase signaling transduce monosodium urate crystal-induced nitric oxide production and matrix metalloproteinase 3 expression in chondrocytes,” *Arthritis Rheum*, vol. 50, no. 1, pp. 247–258, Jan. 2004, doi: 10.1002/art.11486.

[138] C. Thiemermann and J. Vane, “Inhibition of nitric oxide synthesis reduces the hypotension induced by bacterial lipopolysaccharides in the rat in vivo,” *Eur J Pharmacol*, vol. 182, no. 3, pp. 591–595, Jul. 1990, doi: 10.1016/0014-2999(90)90062-B.

[139] C. Szabó, J. A. Mitchell, C. Thiemermann, and J. R. Vane, “Nitric oxide-mediated hyporeactivity to noradrenaline precedes the induction of nitric oxide synthase in endotoxin shock,” *Br J Pharmacol*, vol. 108, no. 3, pp. 786–792, Mar. 1993, doi: 10.1111/j.1476-5381.1993.tb12879.x.

[140] J.-L. VINCENT, H. ZHANG, C. SZABO, and J.-C. PREISER, “Effects of Nitric Oxide in Septic Shock,” *Am J Respir Crit Care Med*, vol. 161, no. 6, pp. 1781–1785, Jun. 2000, doi: 10.1164/ajrccm.161.6.9812004.

[141] C. E. O’Riordan *et al.*, “Bruton’s Tyrosine Kinase Inhibition Attenuates the Cardiac Dysfunction Caused by Cecal Ligation and Puncture in Mice,” *Front Immunol*, vol. 10, Sep. 2019, doi: 10.3389/fimmu.2019.02129.

[142] D. S. Sanford, W. G. Wierda, J. A. Burger, M. J. Keating, and S. M. O’Brien, “Three Newly Approved Drugs for Chronic Lymphocytic Leukemia: Incorporating Ibrutinib, Idelalisib, and Obinutuzumab into Clinical Practice,” *Clin Lymphoma Myeloma Leuk*, vol. 15, no. 7, pp. 385–391, Jul. 2015, doi: 10.1016/j.clml.2015.02.019.

[143] J. D. Hunter and M. Doddi, “Sepsis and the heart,” *Br J Anaesth*, vol. 104, no. 1, pp. 3–11, Jan. 2010, doi: 10.1093/bja/aep339.

[144] J. E. Parrillo, “Septic Shock in Humans,” *Ann Intern Med*, vol. 113, no. 3, p. 227, Aug. 1990, doi: 10.7326/0003-4819-113-3-227.

[145] V. Kumar, “Inflammasomes: Pandora’s box for sepsis,” *J Inflamm Res*, vol. Volume 11, pp. 477–502, Dec. 2018, doi: 10.2147/JIR.S178084.

[146] G. S. D. Purvis *et al.*, “Inhibition of Bruton’s TK regulates macrophage NF-κB and NLRP3 inflammasome activation in metabolic inflammation,” *Br J Pharmacol*, p. bph.15182, Aug. 2020, doi: 10.1111/bph.15182.

[147] M. Ito *et al.*, “Bruton’s tyrosine kinase is essential for NLRP3 inflammasome activation and contributes to ischaemic brain injury,” *Nat Commun*, vol. 6, no. 1, p. 7360, Jun. 2015, doi: 10.1038/ncomms8360.

[148] M. Roschewski *et al.*, “Inhibition of Bruton tyrosine kinase in patients with severe COVID-19,” *Sci Immunol*, vol. 5, no. 48, Jun. 2020, doi: 10.1126/sciimmunol.abd0110.

[149] X. Liu *et al.*, “Inhibition of BTK protects lungs from trauma-hemorrhagic shock-induced injury in rats,” *Mol Med Rep*, vol. 16, no. 1, pp. 192–200, Jan. 2017, doi: 10.3892/mmr.2017.6553.

[150] C. A. Jefferies *et al.*, “Bruton’s Tyrosine Kinase Is a Toll/Interleukin-1 Receptor Domain-binding Protein That Participates in Nuclear Factor κB Activation by Toll-like Receptor 4,” *Journal of Biological Chemistry*, vol. 278, no. 28, pp. 26258–26264, Jul. 2003, doi: 10.1074/jbc.M301484200.

[151] R. Sordi *et al.*, “Resolvin D1 Attenuates the Organ Injury Associated With Experimental Hemorrhagic Shock,” *Ann Surg*, vol. 273, no. 5, pp. 1012–1021, May 2021, doi: 10.1097/SLA.0000000000003407.

[152] R. Sordi *et al.*, “Artesunate Protects Against the Organ Injury and Dysfunction Induced by Severe Hemorrhage and Resuscitation,” *Ann Surg*, vol. 265, no. 2, pp. 408–417, Feb. 2017, doi: 10.1097/SLA.0000000000001664.

[153] N. Yamada *et al.*, “Novel Synthetic, Host-defense Peptide Protects Against Organ Injury/Dysfunction in a Rat Model of Severe Hemorrhagic Shock,” *Ann Surg*, vol. 268, no. 2, pp. 348–356, Aug. 2018, doi: 10.1097/SLA.0000000000002186.

[154] U. Senftleben and M. Karin, “The IKK/NF-kappa B pathway.,” *Crit Care Med*, vol. 30, no. 1 Suppl, pp. S18-26, Jan. 2002.

[155] S. F. Liu and A. B. Malik, “NF-κB activation as a pathological mechanism of septic shock and inflammation,” *American Journal of Physiology-Lung Cellular and Molecular Physiology*, vol. 290, no. 4, pp. L622–L645, Apr. 2006, doi: 10.1152/ajplung.00477.2005.

[156] W. J. Leonard and J. J. O’Shea, “JAKS AND STATS: Biological Implications,” *Annu Rev Immunol*, vol. 16, no. 1, pp. 293–322, Apr. 1998, doi: 10.1146/annurev.immunol.16.1.293.

[157] “CHMP. ANNEX I SUMMARY OF PRODUCT CHARACTERISTICS.”

[158] “Overview | Baricitinib for treating moderate to severe atopic dermatitis | Guidance | NICE.”

[159] H. Lee *et al.*, “Persistently Activated Stat3 Maintains Constitutive NF-κB Activity in Tumors,” *Cancer Cell*, vol. 15, no. 4, pp. 283–293, Apr. 2009, doi: 10.1016/j.ccr.2009.02.015.

[160] C. C. Chen and A. M. Manning, “Transcriptional Regulation of Endothelial Cell Adhesion Molecules: A Dominant Role for NF-κB,” in *Inflammation: Mechanisms and Therapeutics*, Basel: Birkhäuser Basel, 1995, pp. 135–141. doi: 10.1007/978-3-0348-7343-7_12.

[161] S. J. Campbell *et al.*, “Hepatic Nuclear Factor κB Regulates Neutrophil Recruitment to the Injured Brain,” *J Neuropathol Exp Neurol*, vol. 67, no. 3, pp. 223–230, Mar. 2008, doi: 10.1097/NEN.0b013e3181654957.

[162] Y. Zhao *et al.*, “Blockade of ICAM-1 Improves the Outcome of Polymicrobial Sepsis via Modulating Neutrophil Migration and Reversing Immunosuppression,” *Mediators Inflamm*, vol. 2014, pp. 1–10, 2014, doi: 10.1155/2014/195290.

[163] M. S. Hayden and S. Ghosh, “NF-κB in immunobiology,” *Cell Res*, vol. 21, no. 2, pp. 223–244, Feb. 2011, doi: 10.1038/cr.2011.13.

[164] D. A. Chistiakov, M. C. Killingsworth, V. A. Myasoedova, A. N. Orekhov, and Y. v Bobryshev, “CD68/macrosialin: not just a histochemical marker,” *Laboratory Investigation*, vol. 97, no. 1, pp. 4–13, Jan. 2017, doi: 10.1038/labinvest.2016.116.

[165] M. Bacher *et al.*, “An essential regulatory role for macrophage migration inhibitory factor in T-cell activation.,” *Proceedings of the National Academy of Sciences*, vol. 93, no. 15, pp. 7849–7854, Jul. 1996, doi: 10.1073/pnas.93.15.7849.

[166] T. Collins, M. A. Read, A. S. Neish, M. Z. Whitley, D. Thanos, and T. Maniatis, “Transcriptional regulation of endothelial cell adhesion molecules: NF-κB and cytokine-inducible enhancers,” *The FASEB Journal*, vol. 9, no. 10, pp. 899–909, Jul. 1995, doi: 10.1096/fasebj.9.10.7542214.

[167] J. R. David, “Delayed hypersensitivity in vitro: its mediation by cell-free substances formed by lymphoid cell-antigen interaction.,” *Proceedings of the National Academy of Sciences*, vol. 56, no. 1, pp. 72–77, Jul. 1966, doi: 10.1073/pnas.56.1.72.

[168] M. S. Hayden and S. Ghosh, “NF-κB in immunobiology,” *Cell Res*, vol. 21, no. 2, pp. 223–244, Feb. 2011, doi: 10.1038/cr.2011.13.

[169] C.-C. Chuang, C.-J. Hung, M.-C. Tsai, T.-M. Yeh, and Y.-C. Chuang, “High concentrations of circulating macrophage migration inhibitory factor in patients with severe blunt trauma: Is serum macrophage migration inhibitory factor concentration a valuable prognostic factor?,” *Crit Care Med*, vol. 32, no. 3, pp. 734–739, Mar. 2004, doi: 10.1097/01.CCM.0000117170.13320.F4.

[170] T. Lang *et al.*, “Macrophage migration inhibitory factor is required for NLRP3 inflammasome activation,” *Nat Commun*, vol. 9, no. 1, p. 2223, Jun. 2018, doi: 10.1038/s41467-018-04581-2.

[171] M. S. Shin *et al.*, “Macrophage Migration Inhibitory Factor Regulates U1 Small Nuclear RNP Immune Complex–Mediated Activation of the NLRP3 Inflammasome,” *Arthritis & Rheumatology*, vol. 71, no. 1, pp. 109–120, Jan. 2019, doi: 10.1002/art.40672.

[172] T. Roger, J. David, M. P. Glauser, and T. Calandra, “MIF regulates innate immune responses through modulation of Toll-like receptor 4,” *Nature*, vol. 414, no. 6866, pp. 920–924, Dec. 2001, doi: 10.1038/414920a.

[173] R. S. Hotchkiss, G. Monneret, and D. Payen, “Sepsis-induced immunosuppression: from cellular dysfunctions to immunotherapy,” *Nat Rev Immunol*, vol. 13, no. 12, pp. 862–874, Dec. 2013, doi: 10.1038/nri3552.

[174] S. A. Lund, C. M. Giachelli, and M. Scatena, “The role of osteopontin in inflammatory processes,” *J Cell Commun Signal*, vol. 3, no. 3–4, pp. 311–322, Dec. 2009, doi: 10.1007/s12079-009-0068-0.

[175] C. Dianzani *et al.*, “B7h Triggering Inhibits Umbilical Vascular Endothelial Cell Adhesiveness to Tumor Cell Lines and Polymorphonuclear Cells,” *The Journal of Immunology*, vol. 185, no. 7, pp. 3970–3979, Oct. 2010, doi: 10.4049/jimmunol.0903269.

[176] C. Wahl, P. Bochtler, L. Chen, R. Schirmbeck, and J. Reimann, “B7-H1 on Hepatocytes Facilitates Priming of Specific CD8 T Cells But Limits the Specific Recall of Primed Responses,” *Gastroenterology*, vol. 135, no. 3, pp. 980–988, Sep. 2008, doi: 10.1053/j.gastro.2008.05.076.

[177] C. Dianzani *et al.*, “B7h Triggering Inhibits Umbilical Vascular Endothelial Cell Adhesiveness to Tumor Cell Lines and Polymorphonuclear Cells,” *The Journal of Immunology*, vol. 185, no. 7, pp. 3970–3979, Oct. 2010, doi: 10.4049/jimmunol.0903269.

[178] C. Dianzani *et al.*, “B7h Triggering Inhibits the Migration of Tumor Cell Lines,” *The Journal of Immunology*, vol. 192, no. 10, pp. 4921–4931, May 2014, doi: 10.4049/jimmunol.1300587.

[179] J. J. Oppenheim and D. Yang, “Alarmins: chemotactic activators of immune responses,” *Curr Opin Immunol*, vol. 17, no. 4, pp. 359–365, Aug. 2005, doi: 10.1016/j.coi.2005.06.002.

[180] X. Zhang and D. Mosser, “Macrophage activation by endogenous danger signals,” *J Pathol*, vol. 214, no. 2, pp. 161–178, Jan. 2008, doi: 10.1002/path.2284.

[181] T. Kawai and S. Akira, “The role of pattern-recognition receptors in innate immunity: update on Toll-like receptors,” *Nat Immunol*, vol. 11, no. 5, pp. 373–384, May 2010, doi: 10.1038/ni.1863.

[182] G.-Y. Chen, J. Tang, P. Zheng, and Y. Liu, “CD24 and Siglec-10 Selectively Repress Tissue Damage–Induced Immune Responses,” *Science (1979)*, vol. 323, no. 5922, pp. 1722–1725, Mar. 2009, doi: 10.1126/science.1168988.

[183] S. Mohammad *et al.*, “RG100204, A Novel Aquaporin-9 Inhibitor, Reduces Septic Cardiomyopathy and Multiple Organ Failure in Murine Sepsis,” *Front Immunol*, vol. 13, Jun. 2022, doi: 10.3389/fimmu.2022.900906.

[184] P. Cohen, “Protein kinases — the major drug targets of the twenty-first century?,” *Nat Rev Drug Discov*, vol. 1, no. 4, pp. 309–315, Apr. 2002, doi: 10.1038/nrd773.

PHD ACTIVITIES

Attended courses – 2019-2022 (Italy)

- Advances in Pharmacology - 2019/2020
- Advances in Phytochemistry - 2019/2020
- Advances in Pharmaceutical Technology (nanomedicine and drug delivery) - 2019/2020
- Green and Sustainable Chemical Processes - 2020/2021
- Molecular Imaging - 2020/2021
- Biosensors - 2020/2021
- Environmental pollution and health – 2021/2022
- Drug Design – 2021/2022
- Advances in Nanotechnology 2021/2022

Attended courses – 2019-2022 (Brazil)

- FMC510016 – General seminars in Pharmacology - 2019
- FMC510048 - Advanced Topics in Research - 2020
- FMC510049 – Endocrine Pharmacology - 2020
- EST510009 - Teaching internship – Pharmacology - 2020
- EST510008 - Teaching internship – Pharmacology - 2021
- FMC510038 – Biochemical and Molecular Pharmacology - 2021
- FMC510054 - Advanced Topics in Cardiovascular Research - 2021
- FMC3121000 - Recent Advances in Cardiovascular Pharmacology, pain, inflammation and study of drug action mechanisms – 2022
- FMC510053 - Interventions in the Inflammatory Response - 2022
- FMC3123000 - Advanced Seminars: Nitric Oxide – 2022

Poster/Conferences – 2019/2022

- **(June-2022)** 15th World Congress on Inflammation (**WCI**), Rome - Italy.
  Poster and oral communication

- **(Oct-2022)** 54th Brazilian Congress of Pharmacology and Experimental Therapeutics (**SBFTE**)– Florianópolis – SC – BR – Virtual format.
  Poster Presentation

- **(Nov-2022)** 41° Congresso Nazionale della Società Italiana di Farmacologia (**SIF**)- Il Valore Scientifico e L'uso Appropriato Del Farmaco – Roma, Italy.
  Poster and oral communication

- **(Oct-2022)** 29° Congresso Nazionale della Società Italiana di Diabetologia (SID) – Rimini, Italy.
  Oral communication

- **(Nov-2021)** Recenti Sviluppi in Immunofarmacologia - 1° Meeting del GdL Immunofarmacologia della (**SIF**) (Società Italiana di Farmacologia).
  Poster Presentation
- **(Oct-2021)** Summer School – The skin barrier – University of Copenhagen, Hornbæk, Denmark. **(72 h).**
  Poster presentation
- **(Mar-2021)** Virtual Summer School - Exploring Pathways to Impact training – EIT FOOD – (**40 h**)
- **(Mar-2021)** 40° Congresso Nazionale della Societa' Italiana di Farmacologia - Il Valore Scientifico e L'uso Appropriato del Farmaco.
  Poster presentation
- EU SUMMIT on inflammation resolution
- MINDinGUT summer School

Article I

frontiers in Immunology

ORIGINAL RESEARCH
published: 01 February 2022
doi: 10.3389/fimmu.2022.837180

Pharmacological Inhibition of FAK-Pyk2 Pathway Protects Against Organ Damage and Prolongs the Survival of Septic Mice

*Gustavo Ferreira Alves[1,2], Eleonora Aimaretti[3], Giacomo Einaudi[4], Raffaella Mastrocola[3], Junior Garcia de Oliveira[2], Debora Collotta[1], Elisa Porchietto[4], Manuela Aragno[3], Carlo Cifani[4], Regina Sordi[2], Christoph Thiemermann[5], Daniel Fernandes[2] and Massimo Collino[1]**

[1] Department of Neurosciences (Rita Levi Montalcini), University of Turin, Turin, Italy, [2] Department of Pharmacology, Federal University of Santa Catarina, Florianópolis, Brazil, [3] Department of Clinical and Biological Sciences, University of Turin, Turin, Italy, [4] Pharmacology Unit, School of Pharmacy, University of Camerino, Camerino, Italy, [5] William Harvey Research Institute, Bart's and The London School of Medicine and Dentistry, Queen Mary University of London, London, United Kingdom

OPEN ACCESS

Edited by:
Rudolf Lucas,
Augusta University, United States

Reviewed by:
Marcin Filip Osuchowski,
Ludwig Boltzmann Institute for Experimental and Clinical Traumatology, Austria
Jonathan Steven Alexander,
Louisiana State University Health Shreveport, United States

***Correspondence:**
Massimo Collino
massimo.collino@unito.it

Specialty section:
This article was submitted to Inflammation, a section of the journal Frontiers in Immunology

Received: 16 December 2021
Accepted: 14 January 2022
Published: 01 February 2022

Citation:
Alves GF, Aimaretti E, Einaudi G, Mastrocola R, de Oliveira JG, Collotta D, Porchietto E, Aragno M, Cifani C, Sordi R, Thiemermann C, Fernandes D and Collino M (2022) Pharmacological Inhibition of FAK-Pyk2 Pathway Protects Against Organ Damage and Prolongs the Survival of Septic Mice. Front. Immunol. 13:837180. doi: 10.3389/fimmu.2022.837180

Sepsis and septic shock are associated with high mortality and are considered one of the major public health concerns. The onset of sepsis is known as a hyper-inflammatory state that contributes to organ failure and mortality. Recent findings suggest a potential role of two non-receptor protein tyrosine kinases, namely Focal adhesion kinase (FAK) and Proline-rich tyrosine kinase 2 (Pyk2), in the inflammation associated with endometriosis, cancer, atherosclerosis and asthma. Here we investigate the role of FAK-Pyk2 in the pathogenesis of sepsis and the potential beneficial effects of the pharmacological modulation of this pathway by administering the potent reversible dual inhibitor of FAK and Pyk2, PF562271 (PF271) in a murine model of cecal ligation and puncture (CLP)-induced sepsis. Five-month-old male C57BL/6 mice underwent CLP or Sham surgery and one hour after the surgical procedure, mice were randomly assigned to receive PF271 (25 mg/kg, s.c.) or vehicle. Twenty-four hours after surgery, organs and plasma were collected for analyses. In another group of mice, survival rate was assessed every 12 h over the subsequent 5 days. Experimental sepsis led to a systemic cytokine storm resulting in the formation of excessive amounts of both pro-inflammatory cytokines (TNF-α, IL-1β, IL-17 and IL-6) and the anti-inflammatory cytokine IL-10. The systemic inflammatory response was accompanied by high plasma levels of ALT, AST (liver injury), creatinine, (renal dysfunction) and lactate, as well as a high, clinical severity score. All parameters were attenuated following PF271 administration. Experimental sepsis induced an overactivation of FAK and Pyk2 in liver and kidney, which was associated to p38 MAPK activation, leading to increased expression/activation of several pro-inflammatory markers, including the NLRP3 inflammasome complex, the adhesion molecules ICAM-1, VCAM-1 and E-selectin and the enzyme NOS-2 and

myeloperoxidase. Treatment with PF271 inhibited FAK-Pyk2 activation, thus blunting the inflammatory abnormalities orchestrated by sepsis. Finally, PF271 significantly prolonged the survival of mice subjected to CLP-sepsis. Taken together, our data show for the first time that the FAK-Pyk2 pathway contributes to sepsis-induced inflammation and organ injury/dysfunction and that the pharmacological modulation of this pathway may represents a new strategy for the treatment of sepsis.

Keywords: sepsis, NLRP3 inflammasome, inflammation, Focal adhesion kinase (FAK), proline-rich tyrosine kinase 2 (PYK2)

INTRODUCTION

Sepsis is a major public health concern, responsible for high mortality and morbidity rates, followed by a reduced quality of life for survivors (1–3). The latest data on the global sepsis burden reported 48.9 million incident cases and 11.0 million sepsis-related deaths, representing 19.7% of all deaths worldwide (4). Despite the progress in clinical and basic research, the prognosis of septic patients remains remarkably poor, prompting the World Health Organization and World Health Assembly to recognize sepsis as a global health priority and, thus, adopting a resolution to improve the prevention, diagnosis and management of sepsis (5). The morbidity and mortality in sepsis are driven by organ dysfunction (6) and, among the multitude of triggering mechanisms, acute hyperinflammation has a substantial impact on host responses, which in turn contributes to sepsis-related multiple organ failure (MOF) (7). Very recently, two non-receptor proteins tyrosine kinase, belonging to the Focal adhesion kinase (FAK) family, namely FAK and Proline-rich tyrosine kinase 2 (Pyk2), have been identified as new key players in mediating the inflammatory response involved in the pathogenesis of endometriosis (8), atherosclerosis (9) and asthma (10) as well as in tumorigenesis and metastasis formation (11, 12). FAK and Pyk2 are ubiquitously expressed and they share the same three-domain organization, with two non-catalytic domains, the band 4.1, ezrin, radixin and moesin (FERM) domain and the focal adhesion targeting (FAT) domain, linked by a central kinase domain (13). In addition to the kinase function, both FAK and Pyk2 act as scaffold proteins and play a crucial role in downstream integrin signaling (14, 15). Despite their homology, the signaling events that lead to activation of these two kinases differ. FAK is mainly activated by integrins, growth factor receptors and cytokine receptors, leading to overproduction of several pro-inflammatory mediators and cytokines (16). In contrast, Pyk2 has the exclusive ability to sense calcium ions and it can be overactivated under lipopolysaccharide (LPS) stimulation resulting in overproduction of chemokines that regulate migration and infiltration of monocytes/macrophages, including monocyte chemotactic protein-1 (MCP-1), through a p38-MAPK pathway dependent mechanism (17, 18). Besides, a compensatory upregulation in Pyk2 levels has been documented following pharmacological or genetic inhibition of FAK (19, 20). Thus, the selective and simultaneous inhibition of both proteins may represent an innovative pharmacological approach to counteract FAK-Pyk2-mediated inflammatory response and recently published papers have demonstrated the efficacy of a FAK-Pyk2 dual inhibitor, PF562271 (PF271), to counteract leukocyte infiltration and vascular inflammation in both *in vitro* and *in vivo* conditions (21, 22). Despite few studies have shown that LPS-induced endotoxemia evokes FAK activation, which contributes to exacerbate the inflammatory response, leading to organ damage and increased mortality (23, 24), so far, no experimental data have been reported on the potential effects of pharmacological modulation of the FAK-Pyk2 signaling pathway against sepsis. Thus, the present study was designed to address this issue by investigating the potential beneficial effects of a potent reversible dual inhibitor of both FAK and Pyk2 (PF271) in a murine model of polymicrobial sepsis.

PF271 is an ATP-competitive, reversible inhibitor for both FAK and Pyk2 with IC_{50} of 1.5 nmol/L and 13 nmol/L, respectively (25), which has completed a phase I clinical trial (NCT00666926) in patients with advanced solid tumors (26, 27).

MATERIAL AND METHODS

Animals and Ethical Statement

Male, five-month-old C57BL/6 mice (from Envigo laboratories, IT), weighing 30-35 g were used and kept under standard laboratory conditions. The animals were housed in an environment with temperature (25 ± 2°C) and light/dark cycle (12/12 h) automatically controlled, as well as *ad libitum* access to food and water. The animals were kept under standard laboratory conditions for four weeks before the start of the experimental procedures. The animal protocols are reported in compliance with the ARRIVE guidelines (28) and the MQTiPSS recommendations for preclinical sepsis studies (29) and they were approved by the local Animal Use and Care Committees as well as the National Authorities (Ethical number approvals: 420/2016-PR, Italy and 7936220321 Brazil).

Polymicrobial Sepsis

Sepsis was induced through the cecal ligation and puncture (CLP) introduced by Wichterman and co-workers (1980) (30) with slight modifications. Mice were anesthetized with 3% isoflurane (IsoFlo, Abbott Laboratories) together with 0.4 L/min oxygen in an anaesthesia chamber. Once mice were sedated,

they were kept anesthetized by administration of 2% isoflurane (via nosecone) together with 0.4 L/min oxygen throughout the surgical procedure. Through a thermal blanket, the body temperature was maintained at 37°C and constantly monitored using a rectal thermometer. Mice were submitted to a mid-line laparotomy of approximately 1.0 cm and, after location and exposure, the cecum was ligated with a cotton thread right below the ileocecal valve. A single through-and-through puncture of the cecum was carried out with a sterile 21 G needle and the cecum was lightly compressed to leak a small amount (droplet) of feces. Then, the cecum was carefully relocated into peritoneal cavity, which was sutured with silk thread. Sham-operated mice underwent the same procedure, but without CLP. Immediately after the surgical procedures, each mouse received an analgesic agent (Carprofen, 5 mg/kg, s.c.) and resuscitation fluid (37°C, 0.9% NaCl, 50 mL/kg, s.c.) in order to support the hemodynamic situation of the animals and to induce a hyperdynamic shock phase (31, 32). Mice were left on a homeothermic blanket, being constantly monitored until they recover from anesthesia and then placed back into fresh clean cages.

Twenty-four hours post-CLP, the body temperature was recorded, and a blinded assessment of a clinical score was performed to evaluate the symptoms consistent with murine sepsis. The 6 following signs were used to score the health of experimental mice: lethargy, piloerection, tremors, periorbital exudates, respiratory distress, and diarrhea. An observed clinical score >3 was defined as developing severe sepsis, while a score ≤3 indicated the development of moderate sepsis (33). Details on the clinical score are reported as supplementary material.

Drug Treatment

Twenty-five mice were randomly distributed into three groups and subjected to either Sham or CLP procedure: Sham (Vehicle), CLP (Vehicle) and CLP+PF271. One hour after surgeries, mice received once either Vehicle (5 µl/g) (5% DMSO; 40% PEG 300; 5% Tween 80; 50% ddH2O) or PF562271 (PF271) (#PF562271, Selleck Chemicals, Sylvanfield Dr, Houston, USA) subcutaneously at the dose of 25 mg/kg, based on previous *in vivo* studies (21, 34).

Survival Study

To evaluate the potential therapeutic effect of PF271 on sepsis, 28 mice were subjected to CLP-induced sepsis and then randomly allocated into two groups, receiving either Vehicle or PF271 (25 mg/kg) once subcutaneously, one hour after CLP; n = 14 for each group. Survival rates were assessed every 12 h over the subsequent 5 days.

Plasma and Organ Collection

Twenty-four hours after surgery, mice were anesthetized using isoflurane and euthanized by cardiac exsanguination. Blood samples were collected in microtubes containing EDTA (17.1 µM/mL of blood) and then centrifuged at 13,000 *g* at R.T. to obtain plasma content. Liver and kidney samples were harvested and conserved in cryotubes containing or not optimal cutting temperature (OCT) compound and frozen in liquid nitrogen. Samples were stored at -80°C until analysis, which were performed blindly.

Biochemical Analysis

Plasma levels of aspartate aminotransferase (AST) (#7036), Alanine aminotransferase (ALT) (#7018), creatinine (#7075), urea (#7144) and lactate (#7170) were measured using commercially available clinical assay kits (FAR Diagnostics, Verona, Italy) following the manufacturer's instructions.

Cytokine and Hormone Analysis

Cytokines were determined in plasma by using the Luminex suspension bead-based multiplexed Bio-Plex Pro™ Mouse Cytokine Th17 Panel A 6-Plex (#M6000007NY) assay (Bio-Rad, Kabelsketal, Germany). The cytokines IFN-γ, IL-1β, IL-6, IL-10, IL-17 and TNF-α were measured according to the manufacturer's instructions. Plasma hormone levels of PAI-1 (#ab197752) and Resistin (#ab205574) were measured through conventional enzyme-linked immunosorbent assays (ELISA) according to the manufacturer's instructions.

Myeloperoxidase (MPO) Activity Assay

MPO activity assay has been described previously (35). About 100 mg of liver and kidney samples were homogenized, centrifuged and assayed for MPO activity by measuring the H_2O_2-dependent oxidation of 3,3′,5,5′-tetramethylbenzidine (TMB). MPO activity was expressed as optical density (O.D.) at 650 nm per mg of protein.

Immunohistochemistry

MPO and NOS-2 immunopositivity were analyzed by immunohistochemistry on 10 µm frozen tissue sections of liver and kidney samples. Slides were fixed (10 min) in acetone post-sectioning. Sections were incubated over 2 h with primary antibodies at room temperature (MPO, Abcam, #ab9535, dilution 1:25; iNOS, Santa Cruz, #sc-651, dilution 1:50) and subsequently for 1 h with horseradish peroxidase (HRP)-conjugated secondary antibodies (dilution 1:200). The chromogenic detection was obtained by adding 3,3'-diaminobenzidine (DAB) substrate (2 min of exposition). Finally, the nucleus was counterstained with hematoxylin (10 min).

qRT-PCR

Total RNA was extracted from the liver (15 mg) and kidney (17 mg) using Animal Tissue RNA Purification Kit (#25700 Norgen Biotek Corporation, Thorold, ON, Canada) according to manufacturer's instructions. The RNA concentration and purity were measured using a nanodrop (Titertek-Berthold) machine and 200 ng/µL (liver) or 120 ng/µL (kidney) were reverse transcripted. cDNA was prepared using the SensiFAST™ cDNA Synthesis Kit 50 reactions (#BIO-65053 Meridian Bioscience, USA) according to manufacturer's instructions. Real time qPCR was performed using 100 ng of cDNA (liver and kidney) through the SensiFAST™ SYBR® No-ROX Kit (#BIO-98005 Meridian Bioscience, USA) according to manufacturer's instructions. PCR reaction was carried out on the CFX Connect Real-Time PCR Detection System (Bio-Rad). Relative gene

expression was obtained after normalization to housekeeping genes (β-actin and GAPDH) using the formula $2^{-\Delta\Delta CT}$ as previously described (36) and folds change was determined by comparison to Sham group. The QuantiTect primers β-actin (#QT00095242, Mm_Actb_1_SG), GAPDH (#QT01658692, Mm_Gapdh_3_SG), ICAM1 (#QT00155078, Mm_Icam1_1_SG), VCAM1 (#QT00128793, Mm_Vcam1_1_SG), E-Selectin (#QT00114338, Mm_Sele_1_SG) used in this study were purchased from QIAGEN (Germantown, MD, EUA).

Western Blot Analysis

About 50 mg of liver and kidney samples were homogenized and centrifuged (13,000 *g*, 10 min, 4°C). Supernatants were collected and the protein content was determined using a BCA protein assay following the manufacturer's instructions. 50 μg of total proteins were loaded for immunoblot experiments. Proteins were separated by either 8% or 10% sodium dodecyl sulphate-polyacrylamide gel electrophoresis (SDS-PAGE) and transferred to a polyvinylidene difluoride (PVDF) membrane, which was then incubated with primary antibodies (dilution 1:1000). The antibodies used were: rabbit anti-Thr^{180}/anti-Tyr^{182} p38 (Cell Signaling #9211); rabbit anti-total p38 (Cell Signaling #9212); mouse anti-NRLP3 (Adipogen- AG-20B-0014-C100); rabbit anti-Caspase-1 (Cell Signaling #24232); rabbit anti-Tyr^{397} FAK (Cell Signaling #3283); rabbit anti-total FAK (Cell Signaling #3285); mouse anti-Tyr^{402} PyK2 (Cell Signaling #3291); mouse anti-total PyK2 (Santa Cruz #sc-393181); rabbit anti-β-actin (Cell Signaling #4970). Blots were then incubated with a secondary antibody (Cell Signaling - anti-mouse #7076; anti-rabbit #7074) conjugated with HRP (dilution 1:10000) and developed using the ECL detection system. The immunoreactive bands were analyzed by the Bio-Rad Image Lab SoftwareTM 6.0.1 and results were normalized to sham.

Statistical Analysis

Power analysis for the study design through G-Power 3.1™ software (37). Data are expressed as dot plots for each animal and as mean ± SD of 5-10 mice. The standard distribution of data was verified by Shapiro-Wilk normality test and the homogeneity of variances by Bartlett test. The statistical analysis was performed by one-way ANOVA, followed by Bonferroni's *post-hoc* test. Data that were not normally distributed, non-parametric statistical analysis was applied through Kruskal-Wallis followed by Dunn's *post hoc*-test. Differences in the survival study were determined with a log-rank (Mantel-Cox) test. A P value <0.05 was considered significant. Statistical analysis was performed using GraphPad Prism® software version 7.05 (San Diego, California, USA).

Materials

Unless otherwise stated, all reagents were purchased from the Sigma-Aldrich Company Ltd. (St. Louis, Missouri, USA). The BCA Protein Assay kit was from Pierce Biotechnology Inc. (Rockford, IL, USA). Antibodies were from Cell-Signaling Technology (Beverly, MA, USA).

RESULTS

PF271 Improves Severity Score and Prolongs Survival of Septic Mice

Mice that underwent CLP surgery developed clinical signals of severe sepsis (score >3) (**Figure 1A**) associated with hypothermia (24.51 ± 0.24°C) at 24 h after the onset of experimental sepsis (**Figure 1B**). Interestingly, treatment with PF271 demonstrated a protective effect in septic mice, as the severity score (score=0) and body temperature (36.0 ± 0.29°C) did not differ (P>0.05) from those observed in the Sham group (**Figures 1A, B**). To further determine the overall long-term effect of PF271 treatment, we performed a survival study in septic mice. As shown in **Figure 1C**, the median survival was 24 h in the CLP-mice treated with vehicle and 48 h in the CLP-mice treated with PF271. PF271 significantly prolonged the survival time of septic mice since 93% of the CLP+Vehicle mice died within 120 h, while the CLP-mice treated with PF271 had significantly reduced mortality of 64% (hazard ratio: 0.33; 95% confidence interval: 0.12–0.89; P < 0.05).

PF271 Administration Reduces Plasma Levels of Biomarkers of Organ Damage in CLP-Induced Sepsis

CLP-mice treated with vehicle exhibited a significant increase in their plasma levels of lactate (74.91 ± 6.31 mg/dL), AST (77.5 ± 8.02 U/L), ALT (48.19 ± 6.47 U/L) and creatinine (0.74 ± 0.13 mg/dL) compared to Sham animals (42.86 ± 4.55; 11.0 ± 0.57; 9.09 ± 0.48; 0.34 ± 0.06, respectively), hence, suggesting poor tissue perfusion (lactate), hepatic (AST and ALT) and renal (creatinine) dysfunction. When plasma samples of septic mice exposed to the FAK-PyK2 inhibitor were evaluated, the concentrations of the same biomarkers were found at levels similar to those detected in the sham group (49.04 ± 5.49; 20.48 ± 1.37; 12.3 ± 0.86; 0.33 ± 0.05, respectively) (**Figures 2A–D**). Additionally, a slight increase in plasma urea levels was recorded in septic mice (81.65 ± 25.6), when compared to Sham animals (53.48 ± 4.6), but not in the CLP+PF271 group (35.5 ± 8.7) (**Figure 2E**).

PF271 Administration Counteracts the Cytokine Storm Evoked by Experimental Sepsis

Twenty-four h after surgery, septic control mice developed a systemic cytokine storm, with a massive increase in the levels of pro-inflammatory cytokines, specifically TNF-α, IL-1β, IL-17, IL-6, and the proteins PAI-1 and Resistin, when compared to Sham animals. Most notably, treatment with PF271 completely abolished the CLP-induced increase in these markers (**Figures 3A–D, G, H**). Interestingly, sepsis also evoked a robust increase in plasma level of the anti-inflammatory cytokine IL-10, whose systemic concentration was not significantly affected by PF271 treatment (**Figure 3E**). On the contrary, neither the intervention (CLP) nor the PF271treatment significantly affected the systemic levels of IFN-γ (**Figure 3F**).

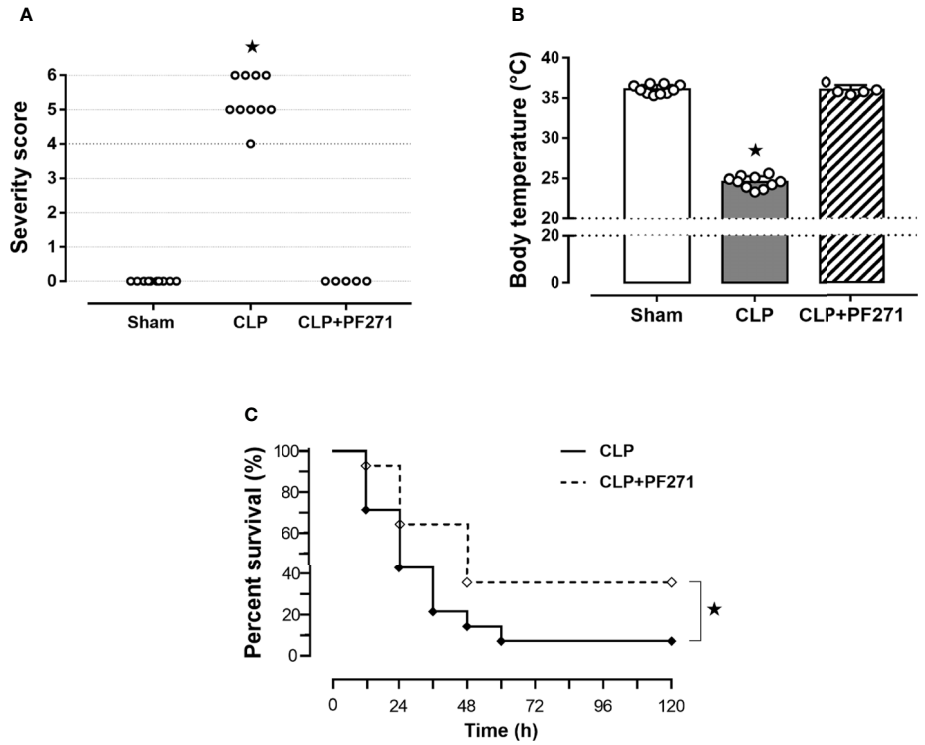

FIGURE 1 | Effect of PF271 on severity and survival in experimental sepsis. Mice were randomly selected to undergo Sham or CLP surgery. One hour later, CLP mice were treated once with either Vehicle or PF271 (25 mg/kg s.c.). Twenty-four hours after Sham or CLP procedure, severity score **(A)** and body temperature **(B)** were recorded. Data are expressed as dot plots for each animal and as mean ± SD of 5-10 mice per group. The Kruskal-Wallis followed by Dunn's *post hoc*-test was applied to assess the severity score, whereas for body temperature, one-way ANOVA followed by Bonferroni's *post hoc*-test was used. *p < 0.05 CLP *vs* Sham/CLP+PF271. The mortality rate was recorded over a 5-day period **(C)**. A log-rank test was used for the comparison of the survival curves (n = 14 mice per group). *p < 0.05 CLP *vs* CLP+PF271.

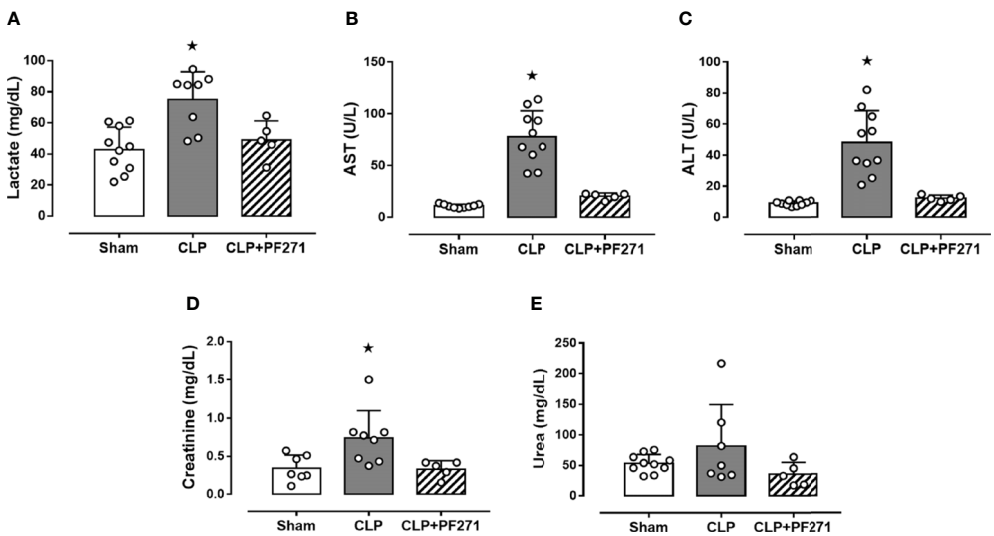

FIGURE 2 | Effect of PF271 on plasma CLP-induced organ damage markers. Mice were randomly selected to undergo Sham or CLP surgery. One hour later, CLP mice were treated once with either vehicle or PF271 (25 mg/kg s.c.). Twenty-four hours after Sham or CLP procedure, the animals' blood was collected. Plasma levels of lactate **(A)**, aspartate transaminase (AST) **(B)**, alanine transaminase (ALT) **(C)**, creatinine **(D)** and urea **(E)** were determined. Data are expressed as dot plots for each animal and as mean ± SD of 5-10 mice per group. Statistical analysis was performed by one-way ANOVA followed by Bonferroni's *post hoc* test. *p < 0.05 CLP *vs* Sham/CLP+PF271.

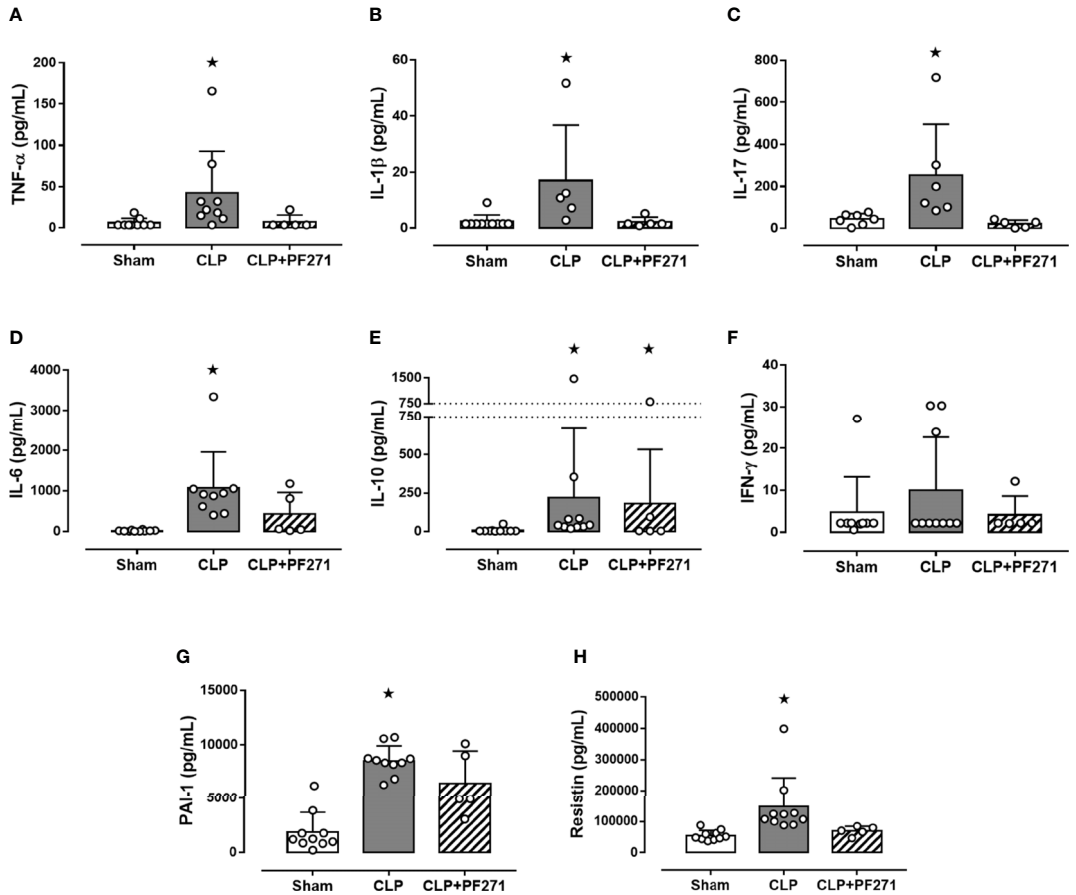

FIGURE 3 | Effect of PF271 on plasma cytokines/hormones during experimental sepsis. Mice were randomly selected to undergo Sham or CLP surgery. One hour later, CLP mice were treated once with either Vehicle or PF271 (25 mg/kg s.c.). Twenty-four hours after Sham or CLP procedure, the animals' blood was collected. Plasma levels of TNF-α **(A)**, IL-1β **(B)**, IL-17 **(C)**, IL-6 **(D)** IL-10 **(E)**, IFN-γ **(F)**, PAI-1 **(G)** and Resistin **(H)** were determined. Data are expressed as dot plots for each animal and as mean ± SD of 5-10 mice per group. TNF-α, IL-17, IL-6, IL-10 and Resistin and were statistically analyzed by one-way ANOVA followed by Bonferroni's *post hoc*-test, while IL-1β, IFN-γ and PAI-1 were analyzed by Kruskal-Wallis followed by Dunn's *post hoc*-test. *$p < 0.05$ CLP and/or CLP+PF271 *vs* Sham.

PF271 Reverses Local Neutrophil Infiltration and Inflammation Evoked by Sepsis

As PF271 displayed protective effects against CLP-induced liver and kidney dysfunctions, we next investigated the possible underlying mechanisms. CLP injury doubled MPO activity in liver and kidney when compared to Sham mice, suggesting an increase in local polymorphonuclear cells (mainly neutrophils) infiltration. In contrast, the degree of MPO activity in CLP-mice treated with PF271 was similar to those recorded in sham mice (**Figures 4A, B**). The dramatic increase in MPO activity in liver (0.445 ± 0.02 *vs* 1.015 ± 0.10) and kidney (0.487 ± 0.02 *vs* 0.855 ± 0.05) following CLP injury was confirmed by immunohistochemistry analysis. While MPO immunopositivity was widely detected in the liver (**Figure 4C**) the increase in staining for MPO in the kidney was restricted to the renal corpuscles (**Figure 4D**). Interestingly, in both organs, treatment with PF271 abolished the increase in MPO-staining induced by experimental sepsis (**Figures 4C, D**). The increase in MPO-activity/staining seen in animals with CLP-sepsis and the prevention of this effect by PF271 treatment were mirrored by similar effects of CLP and PF271 on iNOS expression. As shown in **Figure 5**, iNOS immunopositivity was found to be increased in both liver (panel A) and kidney (panel B) of septic mice. Specifically, a high and wide expression/distribution of iNOS was observed in liver, being predominant in the periphery of blood vessels, whereas renal iNOS immunopositivity was increased mainly in the renal corpuscles and in the cortical tubules. Interestingly, PF271 treatment resulted in substantial reduction of the iNOS expression in both liver and kidney of septic mice (**Figures 5A, B**). The impact of the septic insult and the drug treatment on local inflammation was also confirmed by the gene-expression analysis of the adhesion molecules ICAM-1, VCAM-1 and E-Selectin, whose levels were drastically increased following the sepsis injury and significantly reduced by PF271 administration (**Figures 6A–F**).

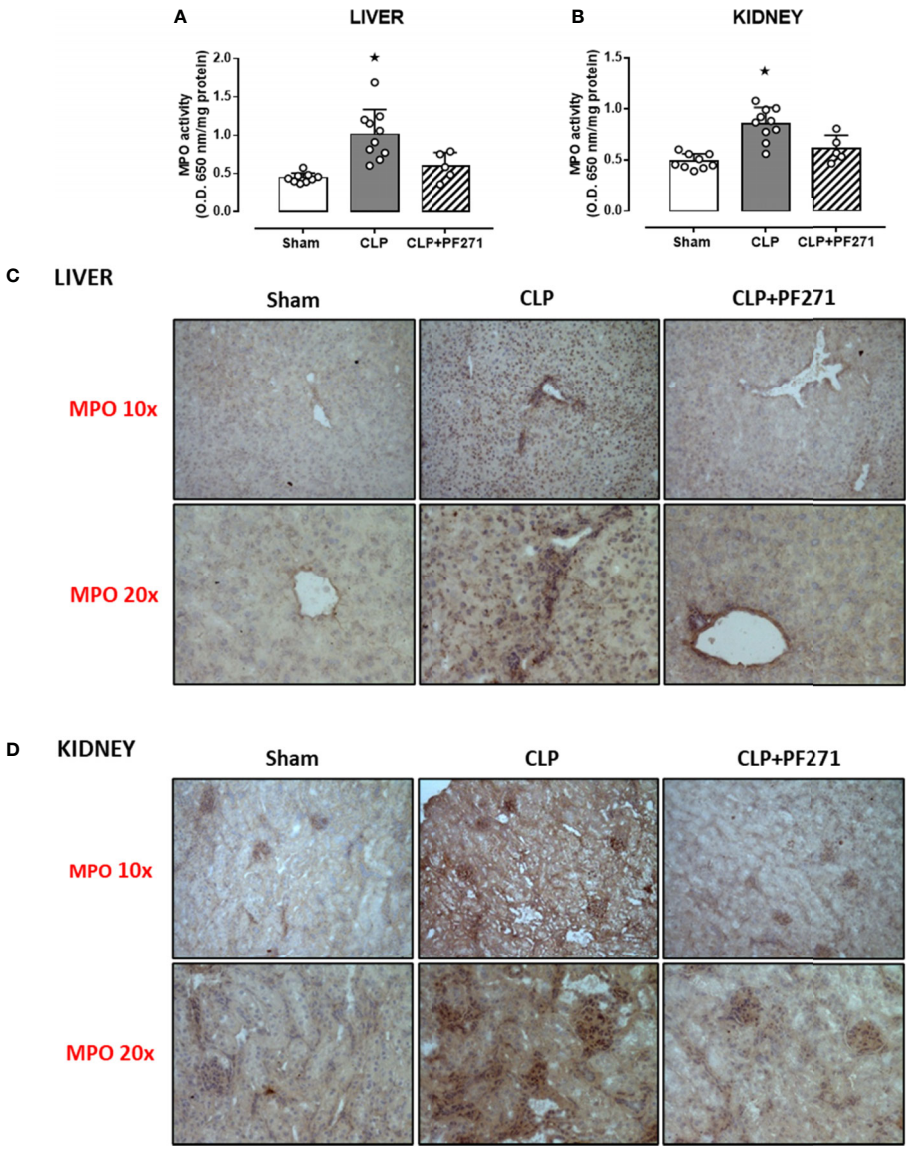

FIGURE 4 | Effect of PF271 on neutrophil tissue infiltration during experimental sepsis. Mice were randomly selected to undergo Sham or CLP surgery. One hour later, CLP mice were treated once with either Vehicle or PF271 (25 mg/kg s.c.). Twenty-four hours after Sham or CLP procedure, liver and kidney were harvested. Through an *in vitro* assay, myeloperoxidase (MPO) activity was measured in liver **(A)** and kidney **(B)**. Tissue sections were prepared to identify MPO through immunohistochemistry assay in liver **(C)** and kidney **(D)**. Representative photomicrographs at 10x and 20x magnification were recorded of 5 animals per group. Data are expressed as dot plots for each animal and as mean ± SD of 5-10 mice per group for MPO activity. Statistical analysis was performed by one-way ANOVA followed by Bonferroni's *post hoc*-test. *p < 0.05 CLP *vs* Sham/CLP+PF271.

PF271 Reduces Local FAK-PyK2 Activity in Septic Mice

To demonstrate that the above-mentioned effects were correlated with modulation of the pharmacological targets, we evaluated the local activation of FAK-PyK2 pathway. As shown in **Figure 7**, in liver and kidney both the septic insult and the drug treatment did not significantly modify the total expression of the FAK and PyK2 proteins. However, tissue homogenates of mice that underwent CLP exhibited a significant increase in both phosphorylation of Tyr^{397} on FAK (panels A-B) and Tyr^{402} on PyK2 (panels C-D), suggestive of increased enzyme activation. Furthermore, an overactivation of the downstream p38 MAPK protein triggered by FAK-PyK2 was also documented, as shown by a robust increase in the phosphorylation of Thr^{180}/Tyr^{182} on p38 MAPK in liver (**Figure 7E**) and kidney (**Figure 7F**) of septic mice. As expected, mice treated with PF271 showed reduced activation of either FAK-PyK2 and its downstream effector p38 MAPK, confirming the ability of PF271 to interfere with its

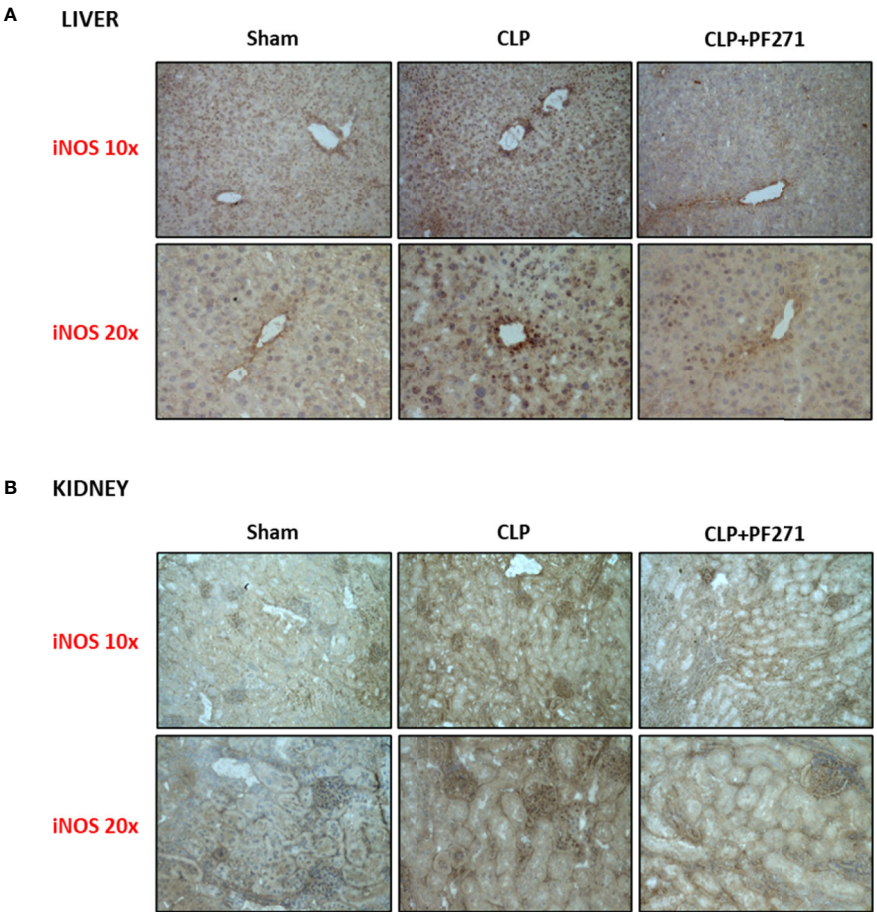

FIGURE 5 | Effect of PF271 on tissue expression of iNOS during experimental sepsis. Mice were randomly selected to undergo Sham or CLP surgery. One hour later, CLP mice were treated once with either Vehicle or PF271 (25 mg/kg s.c.). Twenty-four hours after Sham or CLP procedure, liver and kidney were harvested. Tissue sections were prepared to identify iNOS expression through immunohistochemistry assay in liver **(A)** and kidney **(B)**. Representative photomicrographs at 10x and 20x magnification were recorded of 5 animals per group.

pharmacological targets in our experimental conditions (**Figures 7A–F**).

NLRP3 Inflammasome Expression and Activity Are Attenuated by FAK-PyK2 Inhibition During Polymicrobial Sepsis

We and others (33, 38, 39) have previously documented a pivotal role of the NLRP3 inflammasome pathway in mediating deleterious effects in sepsis. We, therefore, explored a potential cross-talk mechanism linking FAK-PyK2 inhibition to impaired NLRP3 activity. As shown in **Figure 8**, experimental sepsis evoked a robust increase in the assembly of the NLRP3 complex in liver and kidney, which was associated with a subsequent increase in the cleavage of caspase-1, when compared to animals in the Sham group. In contrast, mice subjected to CLP and treated with PF271 showed a significant reduction in the renal and hepatic expression and activation of the NLRP3 inflammasome complex.

DISCUSSION

Preliminary *in vitro* and *in vivo* studies have previously suggested a role of the FAK-Pyk2 pathways in inflammation and, ultimately, organ damage caused by LPS (23, 24, 40, 41). Here we show, for the first time, that administration of PF271, a selective dual inhibitor of both FAK and Pyk2, ameliorates the severity score and prolongs the survival in a murine model of CLP-sepsis. Mice subjected to sepsis (and treated with vehicle) developed local and systemic inflammation, severe organ injury/dysfunction and this was associated with a high mortality. In contrast, administration of the reversible inhibitor for both FAK and Pyk2, PF271, counteracted all these abnormalities caused by sepsis and resulted in long-term protection and improved survival. In this study, we confirmed that sepsis does, indeed, lead to phosphorylation and, hence, activation of both FAK and Pyk2 and we show that PF271 attenuates FAK-Pyk2 phosphorylation, and thus activation, in septic mice. In addition, we explored the molecular mechanisms involved in the deleterious effects

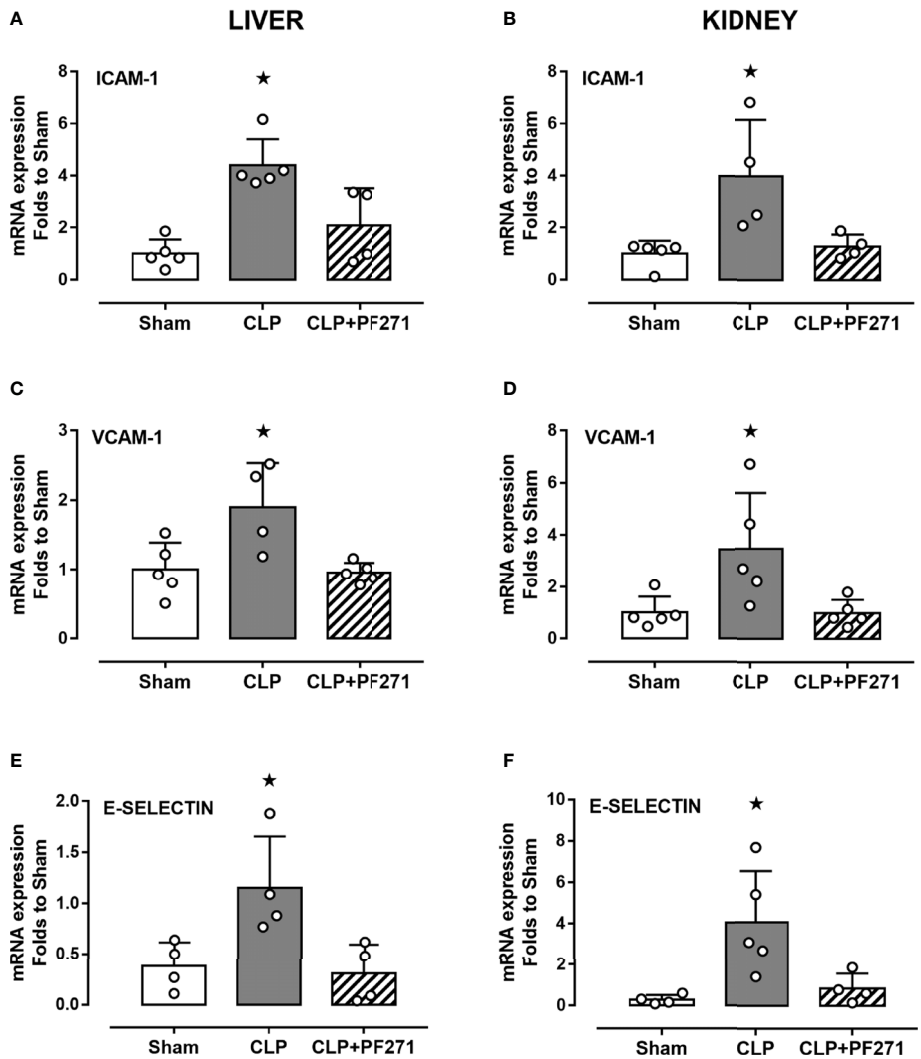

FIGURE 6 | Effect of PF271 on tissue expression of adhesion molecules during experimental sepsis. Mice were randomly selected to undergo Sham or CLP surgery. One hour later, CLP mice were treated once with either Vehicle or PF271 (25 mg/kg s.c.). Twenty-four hours after Sham or CLP procedure, liver and kidney were harvested, and the total mRNA was extracted from them. Real time qPCR was performed for the following genes: ICAM-1 in liver **(A)** and kidney **(B)** extractions; VCAM-1 in liver **(C)** and kidney **(D)** extractions; E-Selectin in liver **(E)** and kidney **(F)** extractions. Relative gene expression was obtained after normalization to housekeeping genes (β-actin and GAPDH) using the formula $2^{-\Delta\Delta CT}$ and folds change was determined by comparison to Sham group. Data are expressed as dot plots for each animal and as mean ± SD of 4-5 mice per group. Statistical analysis was performed by one-way ANOVA followed by Bonferroni's *post hoc* test. *$p < 0.05$ CLP *vs* Sham/CLP+PF271.

attributed to FAK-Pyk2 overactivation during sepsis. In the liver and kidney of septic mice, we documented that PF271 attenuated the upregulation of the cellular adhesion molecules (CAMs) VCAM-1, ICAM-1 and E-Selectin, which exert a pivotal role in driving leukocyte infiltration and the following excessive inflammatory response, which ultimately lead to the development of MOF (42–44). We also documented that PF271 administration was associated with a significant reduction in local (liver and kidney) expression and activity of either MPO, a well-known biomarker of neutrophil infiltration (45), and iNOS, which is detectable in neutrophils, leading to overproduction of nitric oxide (NO) and the following generation of other reactive species (46). Our study does not allow the identification of the specific cell types involved in PF271-mediated responses. Nevertheless, it is well described that cells of the innate immune system and endothelial cells are the most prominent type involved in the exorbitant release of inflammatory cytokines, which in turn drives septic inflammation (47) and the same cells express the FAK-PyK2 cascade, whose role in the cellular production of inflammatory mediators has been clearly demonstrated (17, 22, 40, 48–50). We may, thus, speculate that the beneficial effects of PF271, including those related to the preservation of organ function in sepsis, are due, at least in part, to a direct effect of PF271 on both leukocytes and endothelial cells.

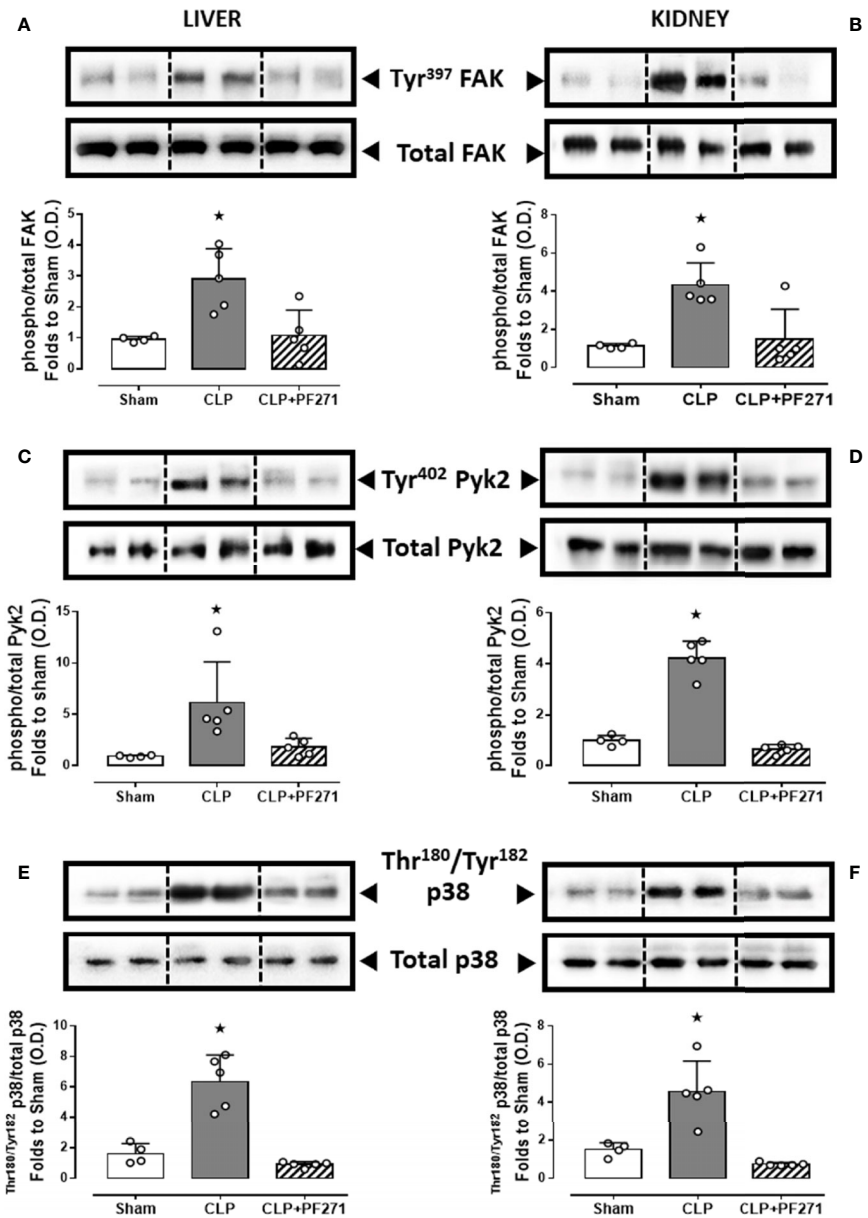

FIGURE 7 | Effect of PF271 on tissue activation of FAK-PyK2 pathway during experimental sepsis. Mice were randomly selected to undergo Sham or CLP surgery. One hour later, CLP mice were treated once with either Vehicle or PF271 (25 mg/kg s.c.). Twenty-four hours after Sham or CLP procedure, liver and kidney were harvested, and the total protein was extracted from them. Western blotting analysis for phosphorylation of Tyr^{397} on FAK in the liver **(A)** and kidney **(B)** were normalized to total FAK; Phosphorylation of Tyr^{402} on PyK2 in the liver **(C)** and kidney **(D)** were normalized to total PyK2; Phosphorylation of Thr^{180}/Tyr^{182} on p38 in the liver **(E)** and kidney **(F)** were normalized to total p38. Densitometric analysis of the bands is expressed as relative optical density (O.D.). Data are expressed as dot plots for each animal and as mean ± SD of 4-5 mice per group. Statistical analysis was performed by one-way ANOVA followed by Bonferroni's *post hoc* test. *$p < 0.05$ CLP *vs* Sham/CLP+PF271.

One of the most relevant downstream signaling events directly activated by FAK-Pyk2 is the MAPK p38-dependent signaling pathway, which in turn activates the NF-κB transcription factor, leading to cytokines overproduction and, thus, the cytokine storm typical of the systemic inflammation and organ dysfunction associated to sepsis (17, 40, 50, 51). Here we confirmed a local overactivation of the p38 MAPK signaling during experimental sepsis, which was significantly reduced by PF271 treatment. The sepsis-induced activation of p38 MAPK was paralleled by a massive increase in the systemic levels of proinflammatory cytokines, such as TNF-α, IL-1β, IL-17 and IL-6, as well as the anti-inflammatory cytokine IL-10. Most notably, we report that all pro-inflammatory cytokines had an impressive reduction when mice were treated with PF271, whereas high

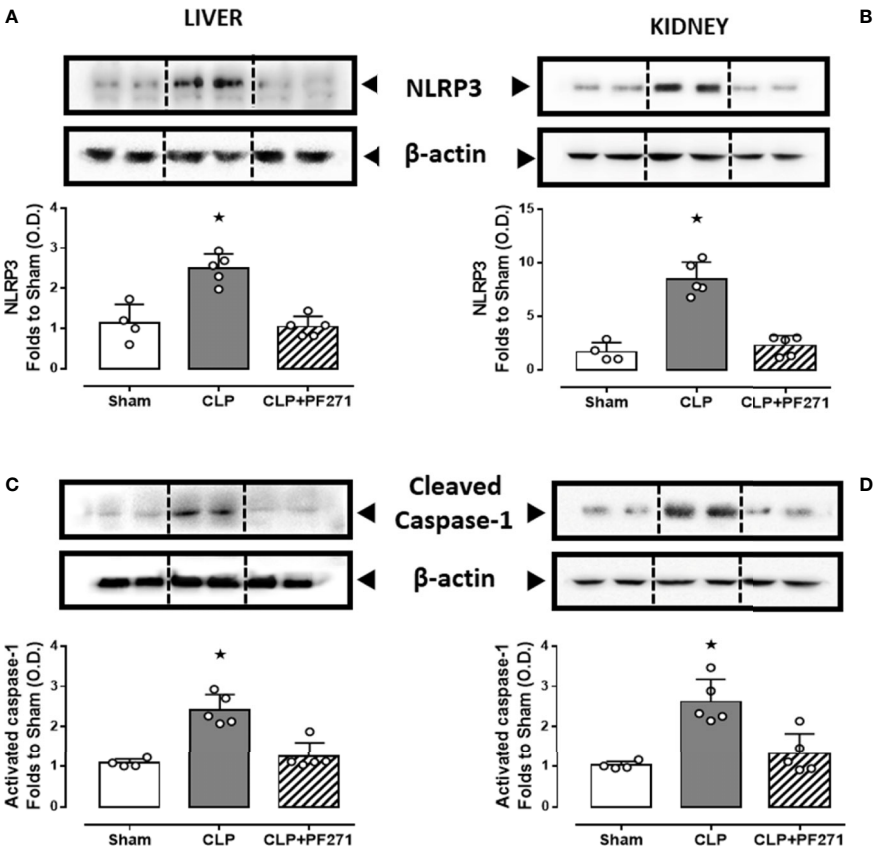

FIGURE 8 | Effect of PF271 on tissue activation of the NLRP3 inflammasome during experimental sepsis. Mice were randomly selected to undergo Sham or CLP surgery. One hour later, CLP mice were treated once with either Vehicle or PF271 (25 mg/kg s.c.). Twenty-four hours after Sham or CLP procedure, liver and kidney were harvested, and the total protein was extracted from them. Western blotting analysis for NLRP3 in the liver **(A)** and kidney **(B)** were corrected against β-actin and normalized using the Sham related bands; Cleaved caspase-1 in the liver **(C)** and kidney **(D)** were corrected against β-actin and normalized using the Sham related bands. Densitometric analysis of the bands is expressed as relative optical density (O.D.). Data are expressed as dot plots for each animal and as mean ± SD of 4-5 mice per group. Statistical analysis was performed by one-way ANOVA followed by Bonferroni's *post hoc* test. *$p < 0.05$ CLP *vs* Sham/CLP+PF271.

levels of the anti-inflammatory cytokine IL-10 were unaffected by treatment. In keeping with clinical studies (52, 53), we also documented a significant sepsis-induced upregulation of the recently discovered inflammatory cytokine resistin and, most notably, we demonstrated here, for the first time, that its systemic concentrations may be affected by the pharmacological modulation of the FAK-Pyk2 pathway. The reduction in resistin levels caused by PF271 in sepsis could contribute, at least in part, to the prolonged survival of septic mice following drug treatment, as recent findings have demonstrated that resistin significantly impairs neutrophil killing of Gram-positive and Gram-negative organisms, thus contributing to the development of immunosuppression, which is central to sepsis-related morbidity and mortality (54). However, further studies are needed to support this hypothesis. One of the cytokines showing a relevant modulation by either sepsis and PF271 was IL-1β. IL-1β is primarily released from the activated NLRP3 inflammasome, which plays a pivotal role in the pathogenesis of sepsis (55). We thus evaluated the potential impact of the FAK-Pyk2 pharmacological modulation on the NLRP3 complex formation and activation showing that the treatment with PF271 abolished the NLRP3 overexpression and caspase-1 overactivation secondary to sepsis, which was paralleled by systemic reduction in IL-1β. Our data strengthen previously published experimental data demonstrating that Pyk2 directly phosphorylates monomeric apoptosis-associated speck-like protein containing CARD (ASC) subunits of the NLRP3 inflammasome, bringing ASC into an oligomerization-competent state to then activate caspase-1 and trigger IL-1β secretion (21).

During experimental sepsis, we also documented a significant overproduction of plasminogen activator inhibitor-1 (PAI-1), the serum levels of which have been reported to rapidly increase in the early stages of sepsis and are positively correlated to sepsis severity in humans (56). PAI-1 overproduction may also contribute to the FAK activation observed in our experimental model as PAI-1 has been demonstrated to induce FAK phosphorylation leading to processes of macrophage infiltration (57). The slight reduction in PAI-1 levels observed in septic mice following PF271 administration could be due, at

least in part, to the reduced systemic concentrations of cytokines, mainly IL-6, which has been reported to exert a key role in regulating PAI-1 expression in vascular endothelial cells (58). We also found high plasmatic levels of lactate, a marker of tissue perfusion, during experimental sepsis and we reported the treatment with PF271 brought its levels to values not different from the control group. Plasma lactate is not only a marker of tissue perfusion, but it is currently used as a diagnostic criterion to determine whether a patient is in septic shock (1). Thus, our findings also demonstrate the ability of PF271 to improve hemodynamic factors during sepsis. However, we must acknowledge that the lack of direct measurements of hemodynamic parameters does not allow us to reach a solid conclusion on this specific issue.

Our study has further limitations, including the lack of evidence of any effects of PF271 on other important organs involved in MOF associated with sepsis, such as the lungs and the heart, as well as the use of only male mice, which does not allow to get a better understanding of the role of gender dimorphism in the effects of PF271. Although the experimental procedures reported here are in keeping with most of the recommendations reported in the MQTiPSS consensus guidelines (29), we did not consider the use of repeated analgesic and antimicrobial treatments as well as continuous fluid resuscitation. Furthermore, all efficacy endpoints that we evaluated, and the overall survival were assessed only at day 1 and day 5 post-CLP, respectively, and multiple and longer kinetics are needed for a better understanding of the overall efficacy of PF271 on the dynamic changes taking place in sepsis. Thus, future studies are required to improve the clinical relevance of our findings as well as to gain a better insight into the safety profile of the proposed drug treatment.

CONCLUSIONS

This study shows for the first time that the development of organ dysfunction induced by a clinically relevant polymicrobial sepsis model is associated with activation of the FAK-Pyk2 pathway, while the pharmacological inhibition of this pathway results in protective effects and prolonged survival. This beneficial effect is likely to be due to the prevention of leukocyte infiltration and related excessive local inflammation through the modulation of FAK-Pyk2 downstream inflammatory cascades, including p38-MAPK and NLRP3 inflammasome. As PF271 has already been tested in a phase I clinical trial in oncology, our finding may provide an opportunity for the repurposing of this compound for the use in patients with sepsis.

DATA AVAILABILITY STATEMENT

The raw data supporting the conclusions of this article will be made available by the authors, without undue reservation.

ETHICS STATEMENT

The animal study was reviewed and approved by Ministero della Salute, UFFICIO VI, Tutela del benessere animale, igiene zootecnica e igiene urbana veterinaria.

AUTHOR CONTRIBUTIONS

GA, DF, and MC conceived and designed the experiments. GA, EA, GE, RM, JG, DC, and EP performed the experiments. GA, EA, RM, JG, MA, CC, RS, CT, DF, and MC analyzed the data. GA, MA, CC, RS, CT, DF, and MC contributed to the writing of the manuscript. All authors reviewed the manuscript before submission.

FUNDING

This work was supported and funded by the Università degli Studi di Torino (Ricerca Locale 2020 and 2021) and by the Foundation for Research and Innovation of the State of Santa Catarina (2021TR000318).

SUPPLEMENTARY MATERIAL

The Supplementary Material for this article can be found online at: https://www.frontiersin.org/articles/10.3389/fimmu.2022.837180/full#supplementary-material

REFERENCES

1. Singer M, Deutschman CS, Seymour CW, Shankar-Hari M, Annane D, Bauer M, et al. The Third International Consensus Definitions for Sepsis and Septic Shock (Sepsis-3). *Jama* (2016) 315(8):801–10. doi: 10.1001/jama.2016.0287
2. Vincent JL, Marshall JC, Ñamendys-Silva SA, François B, Martin-Loeches I, Lipman J, et al. Assessment of the Worldwide Burden of Critical Illness: The Intensive Care Over Nations (ICON) Audit. *Lancet Respir Med* (2014) 2 (5):380–6. doi: 10.1016/S2213-2600(14)70061-X
3. Iwashyna TJ, Ely EW, Smith DM, Langa KM. Long-Term Cognitive Impairment and Functional Disability Among Survivors of Severe Sepsis. *Jama* (2010) 304(16):1787–94. doi: 10.1001/jama.2010.1553
4. Rudd KE, Johnson SC, Agesa KM, Shackelford KA, Tsoi D, Kievlan DR, et al. Global, Regional, and National Sepsis Incidence and Mortality, 1990–2017: Analysis for the Global Burden of Disease Study. *Lancet* (2020) 395 (10219):200–11. doi: 10.1016/S0140-6736(19)32989-7
5. Reinhart K, Daniels R, Kissoon N, Machado FR, Schachter RD, Finfer S. Recognizing Sepsis as a Global Health Priority—a WHO Resolution. *N Engl J Med* (2017) 377(5):414–7. doi: 10.1056/NEJMp1707170
6. Pool R, Gomez H, Kellum JA. Mechanisms of Organ Dysfunction in Sepsis. *Crit Care Clin* (2018) 34(1):63–80. doi: 10.1016/j.ccc.2017.08.003
7. Lelubre C, Vincent JL. Mechanisms and Treatment of Organ Failure in Sepsis. *Nat Rev Nephrol* (2018) 14(7):417–27. doi: 10.1038/s41581-018-0005-7
8. Nagai T, Ishida C, Nakamura T, Iwase A, Mori M, Murase T, et al. Focal Adhesion Kinase-Mediated Sequences, Including Cell Adhesion, Inflammatory Response, and Fibrosis, as a Therapeutic Target in Endometriosis. *Reprod Sci* (2020) 27(7):1400–10. doi: 10.1007/s43032-019-00044-1

9. Kim S, Cho W, Kim I, Lee SH, Oh GT, Park YM. Oxidized LDL Induces Vimentin Secretion by Macrophages and Contributes to Atherosclerotic Inflammation. *J Mol Med* (2020) 98:973–83. doi: 10.1007/s00109-020-01923-w
10. Duan Y, Learoyd J, Meliton AY, Clay BS, Leff AR, Zhu X. Inhibition of Pyk2 Blocks Airway Inflammation and Hyperresponsiveness in a Mouse Model of Asthma. *Am J Respir Cell Mol Biol* (2010) 42(4):491–7. doi: 10.1165/rcmb.2008-0469OC
11. Naser R, Aldehaiman A, Díaz-Galicia E, Arold ST. Endogenous Control Mechanisms of FAK and PYK2 and Their Relevance to Cancer Development. *Cancers* (2018) 10(6):196. doi: 10.3390/cancers10060196
12. Zhu X, Bao Y, Guo Y, Yang W. Proline-Rich Protein Tyrosine Kinase 2 in Inflammation and Cancer. *Cancers* (2018) 10(5):139. doi: 10.3390/cancers10050139
13. Lipinski CA, Loftus JC. Targeting Pyk2 for Therapeutic Intervention. *Expert Opin Ther Targets* (2010) 14(1):95–108. doi: 10.1517/14728220903473194
14. Orr AW, Murphy-Ullrich JE. Regulation of Endothelial Cell Function BY FAK and PYK2. *Front Biosci* (2004) 9(1):1254–66. doi: 10.2741/1239
15. Zhao X, Guan JL. Focal Adhesion Kinase and Its Signaling Pathways in Cell Migration and Angiogenesis. *Adv Drug Deliv Rev* (2011) 63(8):610–5. doi: 10.1016/j.addr.2010.11.001
16. Murphy JM, Jeong K, Cioffi DL, Campbell PM, Jo H, Ahn EYE, et al. Focal Adhesion Kinase Activity and Localization Is Critical for TNF-α-Induced Nuclear Factor-κb Activation. *Inflammation* (2021) 44(3):1130–44. doi: 10.1007/s10753-020-01408-5
17. Anand AR, Bradley R, Ganju RK. LPS-Induced MCP-1 Expression in Human Microvascular Endothelial Cells Is Mediated by the Tyrosine Kinase, Pyk2 *via* the P38 MAPK/NF-κb-Dependent Pathway. *Mol Immunol* (2009) 46(5):962–8. doi: 10.1016/j.molimm.2008.09.022
18. Avraham H, Park SY, Schinkmann K, Avraham S. RAFTK/Pyk2-Mediated Cellular Signalling. *Cell Signal* (2000) 12(3):123–33. doi: 10.1016/s0898-6568(99)00076-5
19. Sulzmaier FJ, Jean C, Schlaepfer DD. FAK in Cancer: Mechanistic Findings and Clinical Applications. *Nat Rev Cancer* (2014) 14(9):598–610. doi: 10.1038/nrc3792
20. Weis SM, Lim ST, Lutu-Fuga KM, Barnes LA, Chen XL, Göthert J, et al. Compensatory Role for Pyk2 During Angiogenesis in Adult Mice Lacking Endothelial Cell FAK. *J Cell Biol* (2008) 181(1):43–50. doi: 10.1083/jcb.200710038
21. Chung IC, OuYang CN, Yuan SN, Li HP, Chen JT, Shieh HR, et al. Pyk2 Activates the NLRP3 Inflammasome by Directly Phosphorylating ASC and Contributes to Inflammasome-Dependent Peritonitis. *Sci Rep* (2016) 6(1):1–13. doi: 10.1038/srep36214
22. Murphy JM, Jeong K, Rodriguez YA, Kim JH, Ahn EYE, Lim STS. FAK and Pyk2 Activity Promote TNF-α and IL-1β-Mediated Pro-Inflammatory Gene Expression and Vascular Inflammation. *Sci Rep* (2019) 9(1):1–14. doi: 10.1038/s41598-019-44098-2
23. Guido MC, Clemente CF, Moretti AI, Barbeiro HV, Debbas V, Caldini EG, et al. Small Interfering RNA Targeting Focal Adhesion Kinase Prevents Cardiac Dysfunction in Endotoxemia. *Shock* (2012) 37(1):77–84. doi: 10.1097/SHK.0b013e31823532ec
24. Petroni RC, Teodoro WR, Guido MC, Barbeiro HV, Abatepaulo F, Theobaldo MC, et al. Role of Focal Adhesion Kinase in Lung Remodeling of Endotoxemic Rats. *Shock* (2012) 37(5):524–30. doi: 10.1097/shk.0b013e31824c7665
25. Roberts WG, Ung E, Whalen P, Cooper B, Hulford C, Autry C, et al. Antitumor Activity and Pharmacology of a Selective Focal Adhesion Kinase Inhibitor, PF-562,271. *Cancer Res* (2008) 68(6):1935–44. doi: 10.1158/0008-5472.CAN-07-5155
26. Infante JR, Camidge DR, Mileshkin LR, Chen EX, Hicks RJ, Rischin D, et al. Safety, Pharmacokinetic, and Pharmacodynamic Phase I Dose-Escalation Trial of PF-00562271, an Inhibitor of Focal Adhesion Kinase, in Advanced Solid Tumors. *J Clin Oncol* (2012) 30(13):1527–33. doi: 10.1200/JCO.2011.38.9346
27. Lee BY, Timpson P, Horvath LG, Daly RJ. FAK Signaling in Human Cancer as a Target for Therapeutics. *Pharmacol Ther* (2015) 146:132–49. doi: 10.1016/j.pharmthera.2014.10.001
28. Percie du Sert N, Hurst V, Ahluwalia A, Alam S, Avey MT, Baker M, et al. The ARRIVE Guidelines 2.0: Updated Guidelines for Reporting Animal Research. *J Cereb Blood Flow Metab* (2020) 40(9):1769–77. doi: 10.1371/journal.pbio.3000410
29. Osuchowski MF, Ayala A, Bahrami S, Bauer M, Boros M, Cavaillon JM, et al. Minimum Quality Threshold in Pre-Clinical Sepsis Studies (MQTiPSS): An International Expert Consensus Initiative for Improvement of Animal Modeling in Sepsis. *Intensive Care Med Exp* (2018) 6(1):1–6. doi: 10.1097/SHK.0000000000001212
30. Wichterman KA, Baue AE, Chaudry IH. Sepsis and Septic Shock—A Review of Laboratory Models and a Proposal. *J Surg Res* (1980) 29(2):189–201. doi: 10.1016/0022-4804(80)90037-2
31. Hubbard WJ, Choudhry M, Schwacha MG, Kerby JD, Rue LWIII, Bland KI, et al. Cecal Ligation and Puncture. *Shock* (2005) 24:52–7. doi: 10.1097/01.shk.0000191414.94461.7e
32. Rittirsch D, Huber-Lang MS, Flierl MA, Ward PA. Immunodesign of Experimental Sepsis by Cecal Ligation and Puncture. *Nat Protoc* (2009) 4(1):31–6. doi: 10.1038/nprot.2008.214
33. O'Riordan CE, Purvis GS, Collotta D, Krieg N, Wissuwa B, Sheikh MH, et al. X-Linked Immunodeficient Mice With No Functional Bruton's Tyrosine Kinase Are Protected From Sepsis-Induced Multiple Organ Failure. *Front Immunol* (2020) 11:581758. doi: 10.3389/fimmu.2020.581758
34. Sun H, Pisle S, Gardner ER, Figg WDII. Bioluminescent Imaging Study: FAK Inhibitor, PF-562,271, Preclinical Study in PC3M-Luc-C6 Local Implant and Metastasis Xenograft Models. *Cancer Biol Ther* (2010) 10(1):38–43. doi: 10.4161/cbt.10.1.11993
35. Kovalski V, Prestes AP, Oliveira JG, Alves GF, Colarites DF, Mattos JE, et al. Protective Role of cGMP in Early Sepsis. *Eur J Pharmacol* (2017) 807:174–81. doi: 10.1016/j.ejphar.2017.05.012
36. Livak KJ, Schmittgen TD. Analysis of Relative Gene Expression Data Using Real-Time Quantitative PCR and the 2– ΔΔCT Method. *Methods* (2001) 25(4):402–8. doi: 10.1006/meth.2001.1262
37. Faul F, Erdfelder E, Lang AG, Buchner A. G* Power 3: A Flexible Statistical Power Analysis Program for the Social, Behavioral, and Biomedical Sciences. *Behav Res Methods* (2007) 39(2):175–91. doi: 10.3758/bf03193146
38. O'Riordan CE, Purvis GS, Collotta D, Chiazza F, Wissuwa B, Al Zoubi S, et al. Bruton's Tyrosine Kinase Inhibition Attenuates the Cardiac Dysfunction Caused by Cecal Ligation and Puncture in Mice. *Front Immunol* (2019) 10:2129. doi: 10.3389/fimmu.2019.02129
39. Chen YL, Xu G, Liang X, Wei J, Luo J, Chen GN, et al. Inhibition of Hepatic Cells Pyroptosis Attenuates CLP-Induced Acute Liver Injury. *Am J Trans Res* (2016) 8(12):5685.
40. Anand AR, Cucchiarini M, Terwilliger EF, Ganju RK. The Tyrosine Kinase Pyk2 Mediates Lipopolysaccharide-Induced IL-8 Expression in Human Endothelial Cells. *J Immunol* (2008) 180(8):5636–44. doi: 10.4049/jimmunol.180.8.5636
41. Duan Y, Learoyd J, Meliton AY, Leff AR, Zhu X. Inhibition of Pyk2 Blocks Lung Inflammation and Injury in a Mouse Model of Acute Lung Injury. *Respir Res* (2012) 13(1):1–10. doi: 10.1186/1465-9921-13-4
42. Zhao YJ, Yi WJ, Wan XJ, Wang J, Tao TZ, Li JB, et al. Blockade of ICAM-1 Improves the Outcome of Polymicrobial Sepsis *via* Modulating Neutrophil Migration and Reversing Immunosuppression. *Mediators Inflamm* (2014) 2014:1–10. doi: 10.1155/2014/195290
43. Yu X, Wang Y, Yang D, Tang X, Li H, Lv X, et al. α 2A-Adrenergic Blockade Attenuates Septic Cardiomyopathy by Increasing Cardiac Norepinephrine Concentration and Inhibiting Cardiac Endothelial Activation. *Sci Rep* (2018) 8(1):1–15. doi: 10.1038/s41598-018-23304-7
44. Zhang F, Brenner M, Yang WL, Wang P. A Cold-Inducible RNA-Binding Protein (CIRP)-Derived Peptide Attenuates Inflammation and Organ Injury in Septic Mice. *Sci Rep* (2018) 8(1):1–11. doi: 10.1038/s41598-017-13139-z
45. Yu H, Liu Y, Wang M, Restrepo RJ, Wang D, Kalogeris TJ, et al. Myeloperoxidase Instigates Proinflammatory Responses in a Cecal Ligation and Puncture Rat Model of Sepsis. *Am J Physiol-Heart Circ Physiol* (2020) 319(3):H705–21. doi: 10.1152/ajpheart.00440.2020
46. Jyoti A, Singh AK, Dubey M, Kumar S, Saluja R, Keshari RS, et al. Interaction of Inducible Nitric Oxide Synthase With Rac2 Regulates Reactive Oxygen and Nitrogen Species Generation in the Human Neutrophil Phagosomes: Implication in Microbial Killing. *Antioxid Redox Signaling* (2014) 20(3):417–31. doi: 10.1089/ars.2012.4970

47. Delano MJ, Ward PA. The Immune System's Role in Sepsis Progression, Resolution, and Long-Term Outcome. *Immunol Rev* (2016) 274(1):330–53. doi: 10.1111/imr.12499
48. Chapman NM, Houtman JC. Functions of the FAK Family Kinases in T Cells: Beyond Actin Cytoskeletal Rearrangement. *Immunol Res* (2014) 59(1):23–34. doi: 10.1007/s12026-014-8527-y
49. Paone C, Rodrigues N, Ittner E, Santos C, Buntru A, Hauck CR. The Tyrosine Kinase Pyk2 Contributes to Complement-Mediated Phagocytosis in Murine Macrophages. *J Innate Immun* (2016) 8(5):437–51. doi: 10.1159/000442944
50. Chang M, Guo F, Zhou Z, Huang X, Yi L, Dou Y, et al. HBP Induces the Expression of Monocyte Chemoattractant Protein-1 *via* the FAK/PI3K/AKT and P38 MAPK/NF-κb Pathways in Vascular Endothelial Cells. *Cell Signal* (2018) 43:85–94. doi: 10.1016/j.cellsig.2017.12.008
51. Chaudhry H, Zhou J, Zhong YIN, Ali MM, McGuire F, Nagarkatti PS, et al. Role of Cytokines as a Double-Edged Sword in Sepsis. *Vivo* (2013) 27 (6):669–84.
52. Macdonald SP, Bosio E, Neil C, Arendts G, Burrows S, Smart L, et al. Resistin and NGAL Are Associated With Inflammatory Response, Endothelial Activation and Clinical Outcomes in Sepsis. *Inflamm Res* (2017) 66(7):611–9. doi: 10.1007/s00011-017-1043-5
53. Sundén-Cullberg J, Nyström T, Lee ML, Mullins GE, Tokics L, Andersson J, et al. Pronounced Elevation of Resistin Correlates With Severity of Disease in Severe Sepsis and Septic Shock. *Crit Care Med* (2007) 35(6):1536–42. doi: 10.1097/01.CCM.0000266536.14736.03
54. Miller L, Singbartl K, Chroneos ZC, Ruiz-Velasco V, Lang CH, Bonavia A. Resistin Directly Inhibits Bacterial Killing in Neutrophils. *Intensive Care Med Exp* (2019) 7(1):1–12. doi: 10.1186/s40635-019-0257-y
55. Danielski LG, Della Giustina A, Bonfante S, Barichello T, Petronilho F. The NLRP3 Inflammasome and Its Role in Sepsis Development. *Inflammation* (2020) 43(1):24–31. doi: 10.1007/s10753-019-01124-9
56. Zeerleder S, Schroeder V, Hack CE, Kohler HP, Wuillemin WA. TAFI and PAI-1 Levels in Human Sepsis. *Thromb Res* (2006) 118(2):205–12. doi: 10.1016/j.thromres.2005.06.007
57. Thapa B, Koo BH, Kim YH, Kwon HJ, Kim DS. Plasminogen Activator Inhibitor-1 Regulates Infiltration of Macrophages Into Melanoma *via* Phosphorylation of FAK-Tyr925. *Biochem Biophys Res Commun* (2014) 450 (4):1696–701. doi: 10.1016/j.bbrc.2014.07.070
58. Kang S, Tanaka T, Inoue H, Ono C, Hashimoto S, Kioi Y, et al. IL-6 Trans-Signaling Induces Plasminogen Activator Inhibitor-1 From Vascular Endothelial Cells in Cytokine Release Syndrome. *Proc Natl Acad Sci* (2020) 117(36):22351–6. doi: 10.1073/pnas.2010229117

Conflict of Interest: The authors declare that the research was conducted in the absence of any commercial or financial relationships that could be construed as a potential conflict of interest.

Article II

frontiers in Immunology

ORIGINAL RESEARCH
published: 07 October 2020
doi: 10.3389/fimmu.2020.581758

X-Linked Immunodeficient Mice With No Functional Bruton's Tyrosine Kinase Are Protected From Sepsis-Induced Multiple Organ Failure

Caroline E. O'Riordan[1], Gareth S. D. Purvis[2], Debora Collotta[3], Nadine Krieg[4,5], Bianka Wissuwa[4,5], Madeeha H. Sheikh[1], Gustavo Ferreira Alves[3], Shireen Mohammad[1], Lauren A. Callender[1], Sina M. Coldewey[4,5], Massimo Collino[3], David R. Greaves[2†] and Christoph Thiemermann[1*†]*

[1] William Harvey Research Institute, Queen Mary University of London, London, United Kingdom, [2] Sir William Dunn School of Pathology, University of Oxford, Oxford, United Kingdom, [3] Department of Drug Science and Technology, University of Turin, Turin, Italy, [4] Department of Anesthesiology and Intensive Care Medicine, Jena University Hospital, Jena, Germany, [5] Septomics Research Center, Jena University Hospital, Jena, Germany

We previously reported the Bruton's tyrosine kinase (BTK) inhibitors ibrutinib and acalabrutinib improve outcomes in a mouse model of polymicrobial sepsis. Now we show that genetic deficiency of the BTK gene *alone* in *Xid* mice confers protection against cardiac, renal, and liver injury in polymicrobial sepsis and reduces hyperimmune stimulation ("cytokine storm") induced by an overwhelming bacterial infection. Protection is due in part to enhanced bacterial phagocytosis *in vivo*, changes in lipid metabolism and decreased activation of NF-κB and the NLRP3 inflammasome. The inactivation of BTK leads to reduced innate immune cell recruitment and a phenotypic switch from M1 to M2 macrophages, aiding in the resolution of sepsis. We have also found that BTK expression in humans is increased in the blood of septic non-survivors, while lower expression is associated with survival from sepsis. Importantly no further reduction in organ damage, cytokine production, or changes in plasma metabolites is seen in *Xid* mice treated with the BTK inhibitor ibrutinib, demonstrating that the protective effects of BTK inhibitors in polymicrobial sepsis are mediated solely by inhibition of BTK and not by off-target effects of this class of drugs.

Keywords: X-linked immunodeficient mice, Bruton's tyrosine kinase (BTK), sepsis, ibrutinib, cytokine storm, phagocytosis, NF-κB, NLRP3 inflammasome

OPEN ACCESS

Edited by:
Manuela Mengozzi, Brighton and Sussex Medical School, United Kingdom

Reviewed by:
Masahiko Hatano, Chiba University, Japan
Basilia Zingarelli, Cincinnati Children's Hospital Medical Center, United States

****Correspondence:***
Caroline E. O'Riordan
c.e.oriordan@qmul.ac.uk
Christoph Thiemermann
c.thiemermann@qmul.ac.uk

† These authors share last authorship

Specialty section:
This article was submitted to Inflammation, a section of the journal Frontiers in Immunology

Received: *09 July 2020*
Accepted: *26 August 2020*
Published: *07 October 2020*

Citation:
O'Riordan CE, Purvis GSD, Collotta D, Krieg N, Wissuwa B, Sheikh MH, Ferreira Alves G, Mohammad S, Callender LA, Coldewey SM, Collino M, Greaves DR and Thiemermann C (2020) X-Linked Immunodeficient Mice With No Functional Bruton's Tyrosine Kinase Are Protected From Sepsis-Induced Multiple Organ Failure. Front. Immunol. 11:581758. doi: 10.3389/fimmu.2020.581758

INTRODUCTION

Sepsis is a common and life-threatening condition caused by a dysregulated host response to an infection, either bacterial, fungal, or viral (1). Sepsis is a major public health problem leading to multiple organ dysfunction and death. Globally there are 50 million cases of sepsis resulting in the death of 11 million people every year representing 20% of all deaths worldwide (2). Despite intensive, supportive care, and current treatments (antibiotic therapy and fluid resuscitation), no targeted therapies have proven effective at reducing mortality (3, 4). There is an urgent need for the

development of pharmacological treatments for sepsis-induced organ dysfunction (5).

Bruton's tyrosine kinase (BTK) is well-known as a critical component of the B-cell antigen receptor (BCR) signaling pathway (6). BTK is also involved in the activation of the toll-like receptor (TLR) signaling pathways (by binding to the TIR domain of TLR4 and TLR's adaptor molecules MyD88, and Mal) and the NLRP3 inflammasome (by binding to the ASC component) (7–9). Activation of both the TLR signaling pathway and the NLRP3 inflammasome play a pivotal role in the pathophysiology of sepsis (10, 11). The expression of BTK is not restricted to B cells, as BTK is also expressed in cells of myeloid lineage, including macrophages and neutrophils (12, 13), activation of which contributes to the pathophysiology of sepsis.

We have recently shown that the BTK inhibitors ibrutinib (first generation) and acalabrutinib (more selective, second generation) attenuate the systemic inflammation ("cytokine storm") and the multiple organ failure caused by sepsis in mice (14). Ibrutinib is already approved for the use in chronic lymphatic leukemia, mantle cell lymphoma, Waldenstrom macroglobulinemia, and graft vs. host disease (15) and acalabrutinib in mantle cell lymphoma (16). The recent COVID-19 pandemic has driven the search for drugs that can be repurposed to either reduce virus load and/or the cytokine storm in patients with severe COVID-19 infections. It has been found that BTK activation and IL-6 production is increased in COVID-19 patients and the effects of acalabrutinib are currently being evaluated in these patients (17). Roschewski et al. (17) showed that some severe COVID-19 patients receiving acalabrutinib had improved oxygenation and reduced CRP and plasma IL-6, suggesting that BTK inhibitors could be repurposed for diseases involving excessive inflammation.

Although we have proposed that the inhibition of BTK is the key driver of the observed beneficial effects of BTK inhibitors in sepsis, it is possible that some of the well-known off-target effects of these compounds account for or, at least, contribute to the beneficial effects observed (14). For instance, we identified that both ibrutinib and acalabrutinib strongly inhibit five different kinases: BTK, Bmx, ErbB4, RIPK2, and TEC. Our discovery that acalabrutinib and ibrutinib reduce inflammation and organ dysfunction in sepsis has triggered three important questions: (1) Does inhibition of BTK activity alone account for the observed beneficial effects? And (2) Does inhibition of systemic inflammation reduce the host response to infection and ultimately cause increased harm? (3) What effect does BTK inactivation have on the metabolomic profile of septic mice? Interest in metabolomic profiling is growing, as the metabolome is the result of expression and function of a multitude of proteins and, hence, has been suggested to be a sensitive readout of drug responses (18, 19). The present study was designed to address these questions by inducing polymicrobial sepsis in mice with X-linked immunodeficiency (*Xid*). *Xid* mice have a missense mutation within the BTK gene [arginine to cysteine at position 28 (R28C)] in the N-terminally located pleckstrin homology domain, resulting in expression of a BTK protein that is functionally inactive (20, 21). Having developed a model of sepsis in *Xid* mice (and wild-type mice, CBA background), we have investigated the impact of impaired BTK function on organ dysfunction, systemic inflammation (cytokine storm), changes in plasma metabolites, and bacterial clearance.

METHODS

Ethical Statement

The Animal Welfare Ethics Review Boards of Queen Mary University of London and The Dunn School of Pathology in the University of Oxford approved all experiments in accordance with the Home Office guidance on the operation of Animals (Scientific Procedures Act 1986) published by Her Majesty's Stationery Office and the Guide for the Care and Use of Laboratory Animals of the National Research Council. Work was conducted under U.K. Home Office project license number PCF29685 and P144E44F2.

Mice

This study was carried out on twenty-three 10 week-old, male CBA mice (Charles River Laboratories UK Ltd., Kent, UK) and twenty-one 10 week-old, male CBA/CaHN-*Btk*^{xid}/J (*Xid)* mice (from Jackson laboratory), weighing 25–30 g and kept under standard laboratory conditions. Six mice were housed together (in each cage) with access to a chow diet and water *ad libitum*. They were subjected to a 12 h light and dark cycle with a temperature maintained at 19–23°C. Group sizes for each experiment were calculated following power calculations based on previous studies (14).

Polymicrobial Sepsis

Cecal ligation and puncture (CLP) was performed in 10 week-old male CBA (wild type) or *Xid* mice as previously described (14, 22). Mice were randomly assigned to undergo CLP or sham-operated surgery, the surgeon was blinded to the genotype of the mouse. Briefly, mice were anesthetised with isoflurane (2% delivered in O_2) and the cecum was fully ligated below the ileocecal valve. A double puncture was made with a 18G needle into the cecum and a small amount of feces was squeezed out after which the cecum was returned to its anatomical position, then the laparotomy was closed. All animals received fluids (5 ml/kg saline into abdomen before closure and 10 ml/kg saline s.c., immediately after surgery), antibiotics (Imipenem/Cilastatin; 20 mg/kg dissolved in 7.5 ml/kg of saline s.c.), and analgesics (buprenorphine; 0.05 mg/kg i.p.) at 6 and 18 h after surgery. Sham-operated mice underwent the same procedure, but without CLP. At 1 h after CLP, WT or *Xid* mice received 30 mg/kg ibrutinib (Selleck Chemicals) intravenously.

A clinical score for monitoring the health of experimental mice was used to evaluate the symptoms consistent with murine sepsis. The maximum score of six comprised the presence of the following signs: lethargy, piloerection, tremors, periorbital exudates, respiratory distress, and diarrhea. Mice with a clinical score >3 were defined as exhibiting severe sepsis, against a moderate sepsis for a score ≤ 3. Animals were culled at 24 h after the onset of sepsis (CLP).

Assessment of Cardiac Function *in vivo*

At 24 h post CLP, mice were anesthetised (0.5–2% isoflurane in O_2); body temperature was maintained at 37°C and heart rate was maintained at 450 bpm. Then, cardiac function was assessed by M-mode and B-mode echocardiography using the VisualSonics Vevo 3100 echocardiographic system and a MX550D transducer. The following parameters were measured: left ventricular ejection fraction, fractional shortening, fractional area change, cardiac output, stroke volume, and myocardial performance index, as described previously (14).

Kidney Dysfunction and Hepatocellular Injury

After 24 h, mice were sacrificed by terminal cardiac puncture, where terminal blood samples were immediately decanted into 1.3 ml serum gel tubes (Sarstedt, Nürnbrecht, Germany). Blood was allowed to coagulate for at least 10 min at room temperature, then samples were centrifuged at 9,000 rpm for 3 min to separate the serum. Then 100 µl of serum was snap frozen in liquid nitrogen and sent to an independent veterinary testing laboratory (MRC Harwell Institute, Oxford, UK) to evaluate the following biomarkers in a blinded fashion: Urea and creatinine (as markers of renal dysfunction), alanine aminotransferase (ALT), aspartate transaminase (AST) (markers of hepatocellular injury), and lactate dehydrogenase (LDH) (marker of cell injury).

Quantification of Immune Cells After Peritoneal Lavage

Peritoneal lavage exudate was collected by injecting 5 ml of 2 mM of EDTA in PBS into the peritoneal cavity. After gentle massaging, ∼4 ml of exudate was removed with an 18G needle. Cells were washed in FACS buffer (0.05 % BSA, 2 mM EDTA in PBS pH 7.4) and then blocked using anti-CD16/32 (Biolegend) for 10 min at 4°C. Peritoneal cells were analyzed using anti-CD45 (clone 30-F11; BioLegend), anti-CD11b (clone M1/70; BioLegend), anti-F4/80 (clone BM8; BioLegend), anti-Ly6G (clone 1A8; BioLegend), anti-CD206 (clone C068C2; BioLegend), and anti-MHCII (clone. M5/114.15.2; BioLegend) antibodies. Absolute cell count was calculated by the addition of counting beads (BioLegend). Data were acquired using BD LSR II Fortessa (Becton Dickinson) and analyzed using FlowJo analysis software (version 10.6, Treestar Inc.). The gating strategy is depicted in **Figure S1**.

Cytokine Analysis

The principle of multiplex flow immunoassay technology has been reviewed previously (23, 24). Cytokines, chemokines, and a growth factor were determined in serum by Bio-Plex Pro Mouse Chemokine 31-Plex panel assay (Bio-Rad, Kabelsketal, Germany). The cytokines IL-1ß, −2, −4, −6, −10, −16, CCL1, −2, −3, −4, −5, −7, −11, −12, −17, −19, −20, −22, −24, −27, IFN-γ, TNF-α and the chemokines CX3CL1, CXCL1, −2, −5, −10, −11, −12, −13, −16, and the growth factor GM-CSF were measured according to the manufacturer's instructions.

Bacteria Counting

Accurate evaluation of the number of bacteria in peritoneal lavage fluid and blood samples was performed by flow cytometry using the SYTO BC bacteria counting kit (Thermo Fischer Scientific).

Phagocytic Ability

Peritoneal lavage exudate containing neutrophils and macrophages was obtained 24 h after CLP as described above. pHrodo™ red *E. Coli* bioparticles™ (Thermo Fischer Scientific) were resuspended in live cell imagining solution (BioLegend) at 10 mg/ml and 10 µL of bioparticles were opsonised with 20 µL of fresh serum for 1 h at 37°C under gentle agitation, after which they were washed and resuspended in 10 µL of live cell imagining solution. 1×10^6 cells of peritoneal exudate were collected by centrifugation (300 g × 5 min) and resuspended in 890 µL of live cell imaging solution, after which 100 µl of fresh serum and 10 µL of optimized bioparticles were added and incubated for 45 min at 37°C under gentle agitation in the dark. Cells were washed and then blocked using anti-CD16/32 (Biolegend) for 10 min at 4°C followed by staining with surface markers anti-CD11b (clone M1/70; BioLegend), anti-Ly6G (clone 1A8; BioLegend), and anti-F4/80 (clone BM8; BioLegend) for 30 min at 4°C. 10,000 $CD11b^+$ cells were collected by Amnis® ImageStream®^{X} Mk II Imaging Flow Cytometer (Luminex) at a magnification of x40 and analyzed by IDEAS software for each experimental sample. Neutrophils were identified as ($CD11b^+$, $Ly6G^+$, $F4/80^-$) and macrophages were identified as ($CD11b^+$, $Ly6G^-$, $F4/80^+$). This equated to ∼7,000 neutrophils and 2,000 macrophages for both WT and *Xid* mice to undergo phagocytosis analysis via IDEAS software. For WT mice the average number of cells positive with pHrodo *E. coli* BioParticles were 4,200 neutrophils and 1,200 macrophages. For *Xid* mice the average number of cells positive with pHrodo *E. coli* BioParticles were neutrophils 5,600 and 1,200 macrophages.

Western Blots

Immunoblot analyses of cardiac tissue samples were carried out using a semi-quantitative western blotting analysis. The antibody used were: 1:1,000 rabbit anti-$Ser^{176/180}$-IKKα/β, 1:1,000 rabbit anti-total IKKα/β, mouse anti-$Ser^{32/36}$-IκBα, mouse anti-total IκBα, rabbit anti-Tyr^{223}-BTK, rabbit anti-total BTK, rabbit anti-Tyr^{1217} PLCγ, rabbit anti-total PLCγ (from Cell Signaling), 1:5,000 rabbit anti NLRP3 inflammasome (from Abcam), mouse anti-caspase 1 (p20) (from Adipogen). The apex of the heart was taken and homogenized. Proteins were then extracted as previously described (25) and concentrations were quantified by bicinchoninic acid (BCA) protein assay (Thermo Fisher Scientific Rockford, IL). Proteins were separated by 8% sodium dodecyl sulfate (SDS)-PAGE and transferred to polyvinylidene fluoride membranes. Membranes were blocked in 10% milk solution with TBS-Tween and then incubated with the primary antibody overnight at 4°C. The next day the secondary antibody was added for 30 min at room temperature and visualized using the ECL detection system. Tubulin was used as loading control. The immunoreactive bands were analyzed by the Bio-Rad Image Lab Software™ 6.0.1 and results were normalized to the sham bands.

BTK Gene Expression in Whole Human Blood

Original data was obtained from the gene expression omnibus under dataset number GDS4971 which was published by Parnell et al. (26). RNA isolated from whole-blood samples of survivors ($n = 26$) and non-survivors ($n = 9$) of sepsis as well as healthy participants ($n = 18$) over the course of 5 days was assayed on the Illumina HT-12 gene expression microarray consisting of 48,804 probes. The dataset was analyzed for expression of BTK gene in these three groups. The figure was generated using R software (ver 4.0.2), gene expression is quantile normalization and log transformation of the data was applied. Significance was determined by a one-way ANOVA followed by a Bonferroni *post hoc*-test.

Metabolomic Analysis

Metabolites were analyzed by liquid chromatography coupled to triple quadrupole mass spectrometry (LC-MS/MS) using an ultra-high-performance liquid chromatography (UHPLC) system (Nexera LC-40 series) and the triple quadrupole mass spectrometer LCMS-8050, both from Shimadzu Deutschland GmbH (Duisburg, Germany). Samples were analyzed with a method for sphingosine-1-phosphate and sphingosine and the supplied method packages "primary metabolites," "phospholipids," and "lipid mediators" according to the manufacturer's protocols (Shimadzu Deutschland GmbH, Duisburg, Germany) with the following modifications: 20 μL of serum sample were precipitated by addition of 200 μL of methanol (LCMS-grade) in vials. Prior to processing, the methanol was spiked with internal standard (IS) solution in a final concentration of 45.45 nM. The supernatant was taken for analysis after 4 days of incubation at −80°C and subsequent centrifugation at 14,000 rcf for 10 min at 4°C. Primary metabolites were analyzed using the HPLC Column Discovery® HS F5, 3 μm, 150 × 2.1 mm from Sigma-Aldrich Chemie GmbH (Munich, Germany). For phospholipids and lipid mediators, the 2.1 × 150 mm 2.6 μm particle size C8 Kinetex LC Column (Phenomenex Inc., Torrance, USA) was used. Sphingosine-1-phosphate and sphingosine were separated using a MultoHigh 100 RP 18-3μ 60 × 2 mm column (Chromatographie Service GmbH, Langerwehe, Germany) with intermittent runs for equilibration. Mass spectrometric detection was performed by multiple reactions monitoring (MRM) after injection of 10 μl sample, unless stated otherwise. Further information on HPLC programs and solvents (**Table S1**), LCMS-8050 settings (**Table S2**), and recorded mass transitions of identified significantly changed analytes (**Tables S3–S6**) are listed in the Supplement. Metabolome primary data were analyzed and further processed with LabSolutions 5.91 and LabSolutions Insight 3.10 (Shimadzu Deutschland GmbH, Duisburg, Germany).

Statistics

Statistical differences were determined using a one-way ANOVA, followed by Bonferroni *post hoc*-test or unpaired Student's *t*-test as appropriate (GraphPad Prism 8.0; significant when $P < 0.05$). Results are expressed as mean ± SEM of n observations, where *n* represents the number of animals studied.

Metabolome data were determined by calculating area ratios for each analyte by dividing peak area of each analyte by peak area of the related IS. Data analysis for metabolome data was performed as follows: Readings below detection level were set to half of detection level for each analyte separately. Metabolome data was log2 transformed and normalized by subtracting median metabolite abundance per sample from all abundances of each sample. Normalization was carried out separately for primary metabolites, phospholipids, and lipid mediators. *Z* scores were calculated using mean and standard deviation of all samples. Contrasts were analyzed pairwise between selected sample groups by unpaired *t*-tests. *P*-values were Benjamini Hochberg adjusted (27). Analytes with adjusted *P*-values below 0.05 were considered significantly different. For a first exploratory overview a principal component analysis (PCA) was carried out using the normalized and scaled metabolome data. Data analysis was carried out using R version 3.4.4 (28).

RESULTS

Xid Mice Have 100% Predicted Survival Rate

When compared to sham-operated mice, WT mice subjected to cecal ligation and puncture (CLP) showed clinical signs of severe sepsis (80%; score >3). In contrast, all *Xid* mice subjected to CLP had a score of ≤3 indicating only moderate sepsis (**Figure 1A**). All mice in the WT-CLP group which received ibrutinib had a score of ≤3 indicating moderate sepsis and all mice in the *Xid*-CLP + ibrutinib group had a score ≤3. When compared to sham-operated mice, WT mice subjected to CLP experienced hypothermia (a rectal temperature of <30°C) at 24 h after the onset of CLP, whereas the rectal temperature of *Xid*-CLP, WT-CLP + ibrutinib and *Xid*-CLP + ibrutinib remained at 37°C (**Figure 1B**). A reduction in temperature to <30°C or a change of 5°C over time in each animal has been reported to predict death in mice with CLP (29). As mortality of animals is not an acceptable routine endpoint in the UK, we used the reduction in rectal temperature <30°C as a surrogate marker for mortality. Using this surrogate marker, we would predict the mortality of WT-CLP mice to be 90% (confirming that our model is a model of severe sepsis), while the predicted mortality of *Xid*-CLP mice would be 0% (e.g., 100% predicted survival; **Figure 1C**). WT-CLP mice receiving ibrutinib had a predicted mortality of 15%, whereas *Xid*-CLP mice receiving ibrutinib had a predicted mortality of 0%. When compared to sham-operated mice, WT mice subjected to CLP showed a decrease in heart rate, whereas the heart rate of *Xid*-CLP remained similar to that of sham-operated animals (**Figure 1D**). When compared to WT-CLP mice, the administration of ibrutinib 1 h after CLP attenuated the decline in heart rate in WT mice. Mice in the *Xid*-CLP + ibrutinib group had a similar heart rate to mice in the *Xid*-CLP group. *Xid*-CLP mice receiving

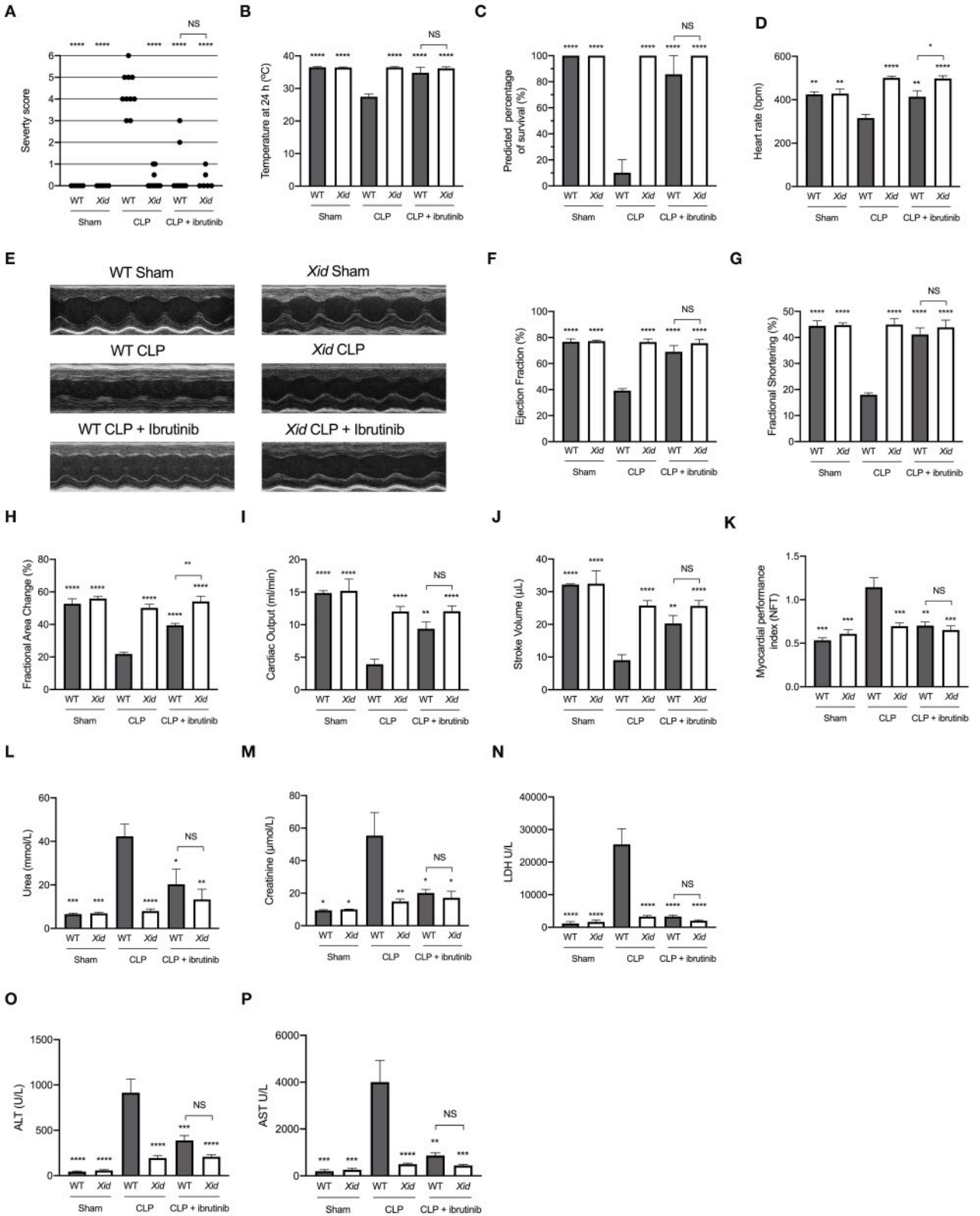

FIGURE 1 | *Xid* mice are protected from sepsis-induced multiple organ failure. WT and *Xid* mice were randomly selected to undergo sham or CLP surgery, 1 h later ibrutinib (30 mg/kg) was administered intravenously. At 24 h after CLP, cardiac function was assessed by echocardiography and parameters of renal and liver function were assessed in serum. **(A)** Severity Score 24 h after CLP. **(B)** Temperature 24 h after CLP (°C). **(C)** Predicted percentage of survival (%). **(D)** Heart rate 24 h after CLP

(Continued)

FIGURE 1 | (bmp). **(E)** Representative m-mode images. **(F)** Ejection Fraction (%). **(G)** Fractional shortening (%). **(H)** Fractional area change (%). **(I)** Cardiac output (ml/min). **(J)** Stroke volume (μL). **(K)** Myocardial performance index (NFT). **(L)** Urea (mmol/L). **(M)** Creatinine (μmol/L). **(N)** Lactate dehydrogenase (U/L). **(O)** ATL (U/L). **(P)** AST (U/L). The following groups were studied WT sham ($n = 5$), *Xid* sham ($n = 5$), WT-CLP ($n = 10$), *Xid*-CLP ($n = 10$), WT-CLP + ibrutinib ($n = 8$), and *Xid*-CLP + ibrutinib ($n = 6$). Data are expressed as mean ± SEM and analyzed by one-way ANOVA with a Bonferroni *post hoc*-test. $^{*}P < 0.05$, $^{**}P < 0.01$, $^{***}P < 0.001$, and $^{****}P < 0.0001$ vs. WT-CLP.

ibrutinib had a higher heart rate than WT-CLP mice treated with ibrutinib.

Xid Mice Are Protected From Sepsis-Induced Cardiac Dysfunction

Cardiac function was assessed *in vivo* by echocardiography. **Figure 1E** shows representative M-mode images in the short axis in sham-operated mice, CLP mice, and CLP + ibrutinib mice of both genotypes. When compared to sham-operated mice, WT mice subjected to CLP showed a reduction in ejection fraction (EF), fractional shortening (FS), fractional area change (FAC), cardiac output (CO), stroke volume (SV), and an increase in myocardial performance index (MPI), indicating severe global, systolic cardiac dysfunction. In contrast, *Xid* mice subjected to CLP had only a very minor cardiac dysfunction and all indices of cardiac performance (EF, FS, FAC, CO, SV, and MPI) were significantly improved from those measured in WT-CLP (**Figures 1F–K**). Thus, the degree of cardiac dysfunction caused by CLP in *Xid* mice is significantly reduced when compared to that observed in WT-mice. When compared to WT-CLP mice (CBA background) treatment of WT-mice with ibrutinib 1 h after CLP attenuated the sepsis-induced cardiac dysfunction. In contrast, administration of ibrutinib to *Xid*-CLP mice had no effect on cardiac function (**Figures 1F–K**), indicating that the addition of ibrutinib in *Xid* mice with CLP results in no beneficial or deleterious effects due to off target actions of the drug.

Xid Mice Are Protected From Sepsis-Induced Kidney Dysfunction and Hepatocellular Injury

Kidney dysfunction and hepatocellular injury was assessed by measuring serum creatinine, urea, ALT, AST, and LDH. When compared to sham-operated mice, WT mice subjected to CLP had significant renal dysfunction (rise in urea and creatinine), hepatocellular injury (rise in ALT and AST) and cell injury (rise in LDH). In contrast, in *Xid* mice subjected to CLP, the degree of kidney dysfunction, hepatocellular injury and cell injury was significantly reduced when compared to WT-CLP mice (**Figures 1L–P**). When compared to WT-CLP, treatment of WT-CLP mice with ibrutinib (1 h after CLP) significantly attenuated the rise of plasma/serum urea, creatinine, ALT, AST, and LDH. In contrast, administration of ibrutinib in *Xid*-CLP mice had no significant effect on organ dysfunction (as this was prevented in *Xid*-mice). No significant difference was observed between WT-CLP + ibrutinib and *Xid*-CLP + ibrutinib for any of the parameters of organ dysfunction measured.

Xid Mice Do Not Present With Systemic Inflammation After Polymicrobial Sepsis

Using a multiplex array, we analyzed 31 cytokines and chemokines in the serum of all animals. When compared to sham-operated mice, WT mice subjected to CLP sepsis showed a significant increase in the serum levels of pro-inflammatory cytokines TNF-α, IL-6, and IL-1β, the anti-inflammatory cytokine IL-10, neutrophils chemoattractant chemokines (KC & ENA-78), monocyte chemoattractant chemokines (MCP-1, MIP-1α, and MIP-1β) and G-CSF. In contrast, the levels of these cytokines and chemokines in the serum of *Xid*-CLP were significantly reduced when compared to WT-CLP mice (**Figures 2A–J**). When compared to WT-CLP, treatment of WT-CLP mice with ibrutinib (1 h after CLP) significantly attenuated the rise in cytokines and chemokines. In contrast, administration of ibrutinib in *Xid*-CLP-mice had no significant effect on the production of cytokines and chemokines (as this was prevented in *Xid*-mice). No significant difference was observed between WT-CLP + ibrutinib and *Xid*-CLP + ibrutinib for any cytokines and chemokines. The alterations of a further 21 cytokines and chemokines can be seen in **Figure 2K** and absolute values in **Table S7**.

Xid Mice Have Fewer Infiltrating Immune Cells in the Peritoneum and Enhanced Polarization to M2 Macrophages in Sepsis

We also evaluated the cell composition and phenotype in the peritoneal exudates of all animals by flow cytometry gating strategy seen in **Figure S1**. When compared to sham-operated mice, WT mice subjected to CLP showed a significant increase in neutrophils and macrophages into the peritoneum. In contrast, *Xid*-CLP mice exhibited a significant reduction in the number of infiltrating neutrophils and macrophages when compared to WT-CLP mice (**Figures 3A–C**). Upon further analysis of the subsets of macrophages, we found that the macrophages obtained from WT-CLP mice are predominately of the pro-inflammatory M1 phenotype (60% M1 and 40% M2), while the macrophages of *Xid*-CLP are of the pro-resolving (anti-inflammatory) M2 phenotype (40% M1 and 60% M2) (**Figures 3D,E**).

Xid Mice Have Fewer Bacteria in Peritoneum and Blood Due to Increased Phagocytosis in Sepsis

In order to determine the mechanism that accounts for the improved outcome of BTK deficient mice, we investigated bacterial clearance *in vivo* in WT and *Xid*-mice at 24 h after

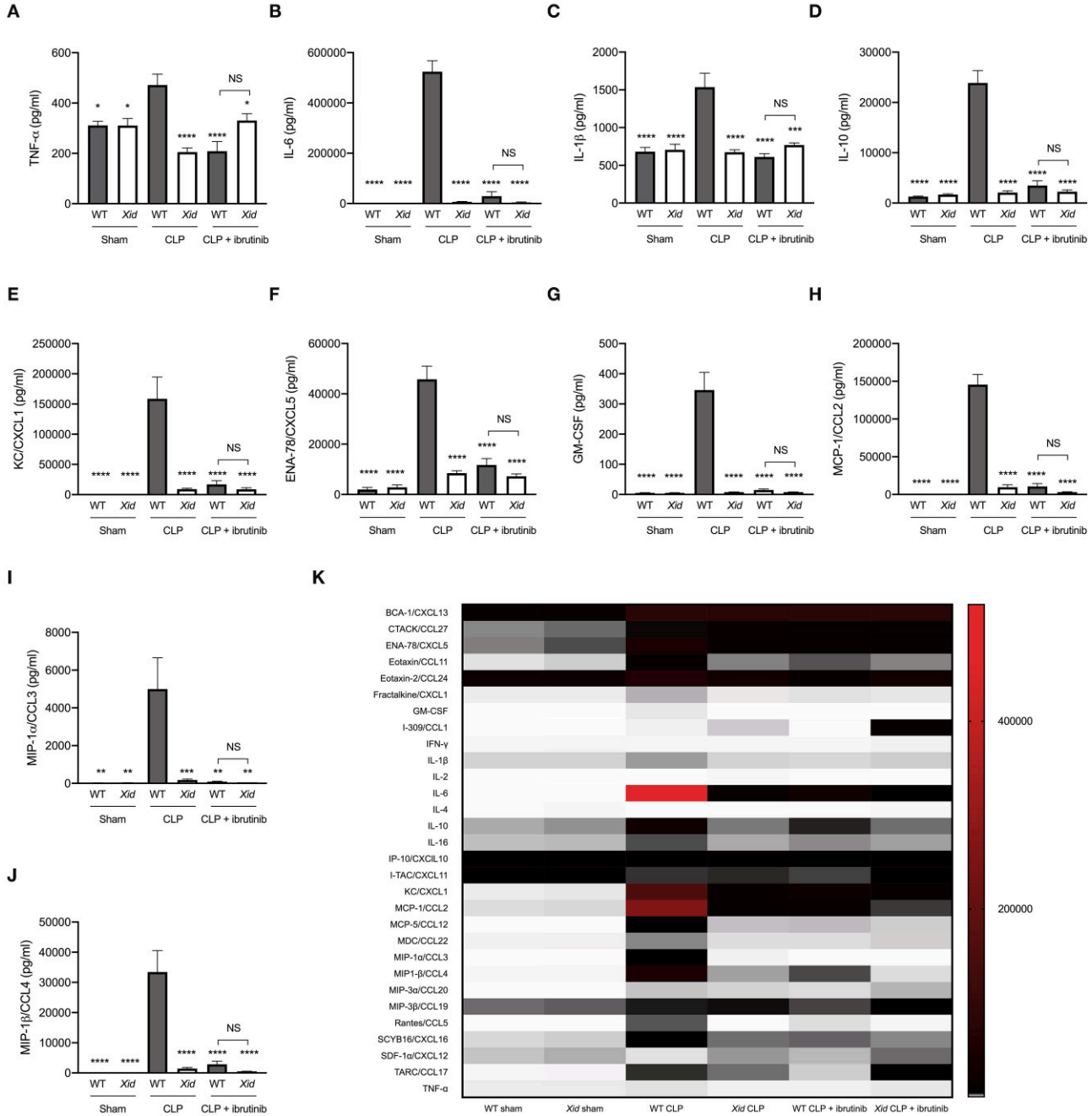

FIGURE 2 | *Xid* mice do not present with systemic inflammation after polymicrobial sepsis. Mice underwent sham or CLP surgery, 24 h later cytokines and chemokines were assessed in serum. **(A)** TNF-α serum concentration (pg/ml). **(B)** IL-6 serum concentration (pg/ml). **(C)** IL-1β serum concentration (pg/ml). **(D)** IL-10 serum concentration (pg/ml). **(E)** KC/CXCL1 serum concentration (pg/ml). **(F)** ENA-78/CXCL5 serum concentration (pg/ml). **(G)** GM-CSF serum concentration (pg/ml). **(H)** MCP-1/CCL2 serum concentration (pg/ml). **(I)** MIP-1α/CCL3 serum concentration (pg/ml). **(J)** MIP-1β/CCL4 serum concentration (pg/ml). **(K)** Heat-map of 31 cytokines/chemokines serum concentration (pg/ml). The following groups were studied WT sham ($n = 5$), *Xid* sham ($n = 5$), WT-CLP ($n = 10$), *Xid*-CLP ($n = 10$), WT-CLP + ibrutinib ($n = 8$), and *Xid*-CLP + ibrutinib ($n = 6$). Data are expressed as mean ± SEM and analyzed by one-way ANOVA with a Bonferroni *post hoc*-test. $^{*}P < 0.05$, $^{**}P < 0.01$, $^{***}P < 0.001$, and $^{****}P < 0.0001$ vs. WT-CLP.

the onset of CLP, as the survival of sepsis is dependent on the ability to clear bacteria. When compared to sham-operated mice, WT mice subjected to CLP exhibited elevated peritoneal and blood bacteria counts (**Figures 4A–D**). However, *Xid*-CLP mice had significantly fewer bacteria in the peritoneal cavity and blood than WT-CLP mice,

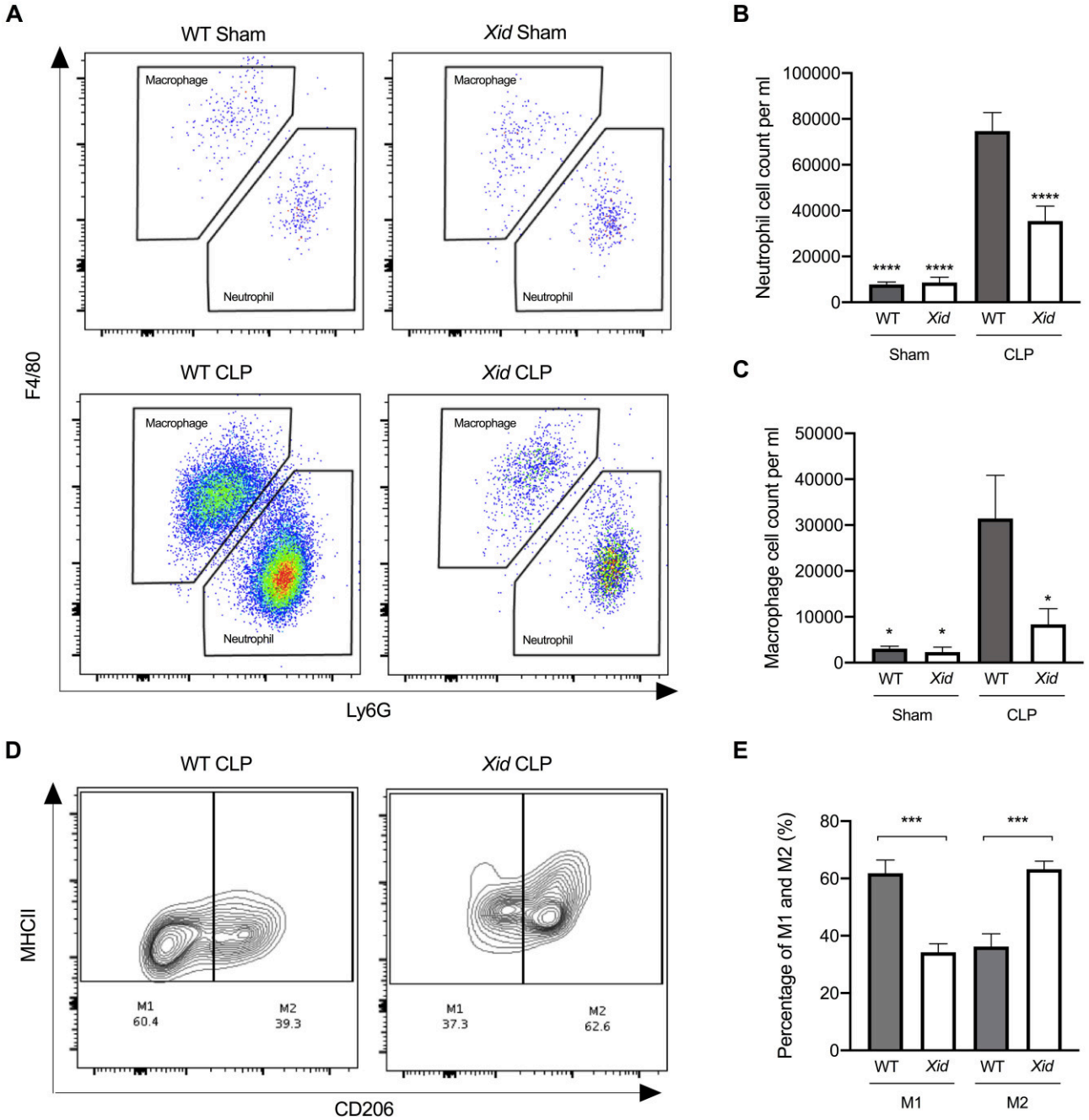

FIGURE 3 | *Xid* mice have fewer infiltrating immune cells in the peritoneum and enhanced polarization to M2 macrophages. Mice underwent sham or CLP surgery, 24 h later peritoneal lavage fluid was analyzed. **(A)** Scattergrams illustrating macrophage (identified as $F4/80^{+}Ly6G^{-}$) and neutrophils (identified as $F4/80^{-}Ly6G^{+}$). **(B)** Peritoneal neutrophil ($F4/80^{-}Ly6G^{+}$) cell count per ml. **(C)** Peritoneal macrophage ($F4/80^{+}Ly6G^{-}$) cell count per ml. **(D)** Contour plot illustrating percentage of M1 and M2 macrophages in WT and *Xid* mice, M1 identified as $MHCII^{+}CD206^{-}$ and M2 identified as $MHCII^{+}CD206^{+}$. **(E)** Percentage of M1 and M2 macrophages in WT mice and *Xid* mice (%). The following groups were studied WT sham ($n = 5$), *Xid* sham ($n = 5$), WT-CLP ($n = 10$), and *Xid*-CLP ($n = 10$). Data are expressed as mean ± SEM and analyzed by one-way ANOVA with a Bonferroni *post hoc*-test. $^{*}P < 0.05$, $^{***}P < 0.001$, and $^{****}P < 0.0001$ vs. WT-CLP.

showing that *Xid*-mice clear bacteria more efficiently than WT mice.

Clearance of bacteria is secondary to phagocytosis of bacteria in neutrophils and macrophages. *Xid* mice subjected to CLP presented with a reduced number of infiltrating immune cells, but also reduced bacterial counts at 24 h post CLP. This raises the question as to how fewer infiltrating immune cells are able to clear more bacteria? To address this question, we investigated

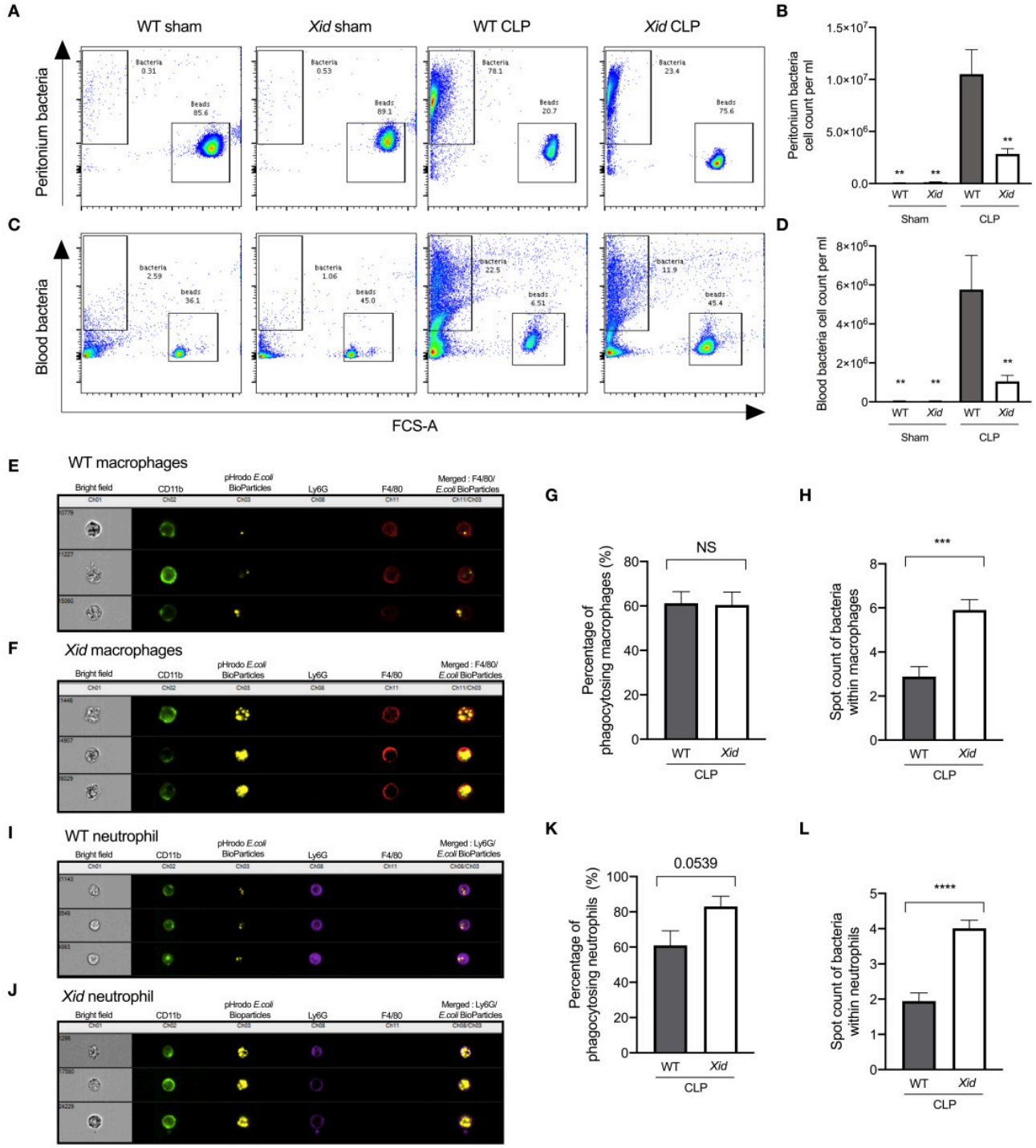

FIGURE 4 | *Xid* mice result in enhanced bacterial clearance in peritoneum and blood due to increased phagocytosis in sepsis. Mice underwent sham or CLP surgery, 24 h later peritoneal lavage fluid and blood were analyzed. Macrophages identified as ($CD11b^+$, $F4/80^+$, and $Ly6G^-$) and neutrophils identified as ($CD11b^+$, $F4/80^-$, and $Ly6G^+$). **(A)** Representative images of peritoneal bacteria cell count. **(B)** Peritoneum bacteria cell count per ml. **(C)** Representative images of blood bacteria cell count. **(D)** Blood bacteria cell count per ml. **(E)** Representative images of WT-CLP macrophages phagocytosis on the imagestream. **(F)** Representative images of *Xid*-CLP macrophages phagocytosis on the imagestream. **(G)** Percentage of phagocytosing macrophages (%). **(H)** Average number of pHrodo red *E. coli* BioParticles within macrophages. **(I)** Representative images of WT-CLP neutrophil phagocytosis on the imagestream. **(J)** Representative images of *Xid*-CLP neutrophil phagocytosis on the imagestream. **(K)** Percentage of phagocytosing neutrophils (%). **(L)** Average number of pHrodo red *E. coli* BioParticles within neutrophils. The following groups were studied WT sham ($n = 5$), *Xid* sham ($n = 5$,) WT-CLP ($n = 10$), and *Xid*-CLP ($n = 10$). Data are expressed as mean ± SEM and analyzed by one-way ANOVA with a Bonferroni *post hoc*-test or a two-tailed Students *t*-test as appropriate. $^{**}P < 0.01$, $^{***}P < 0.001$, and $^{****}P < 0.0001$ vs. WT-CLP.

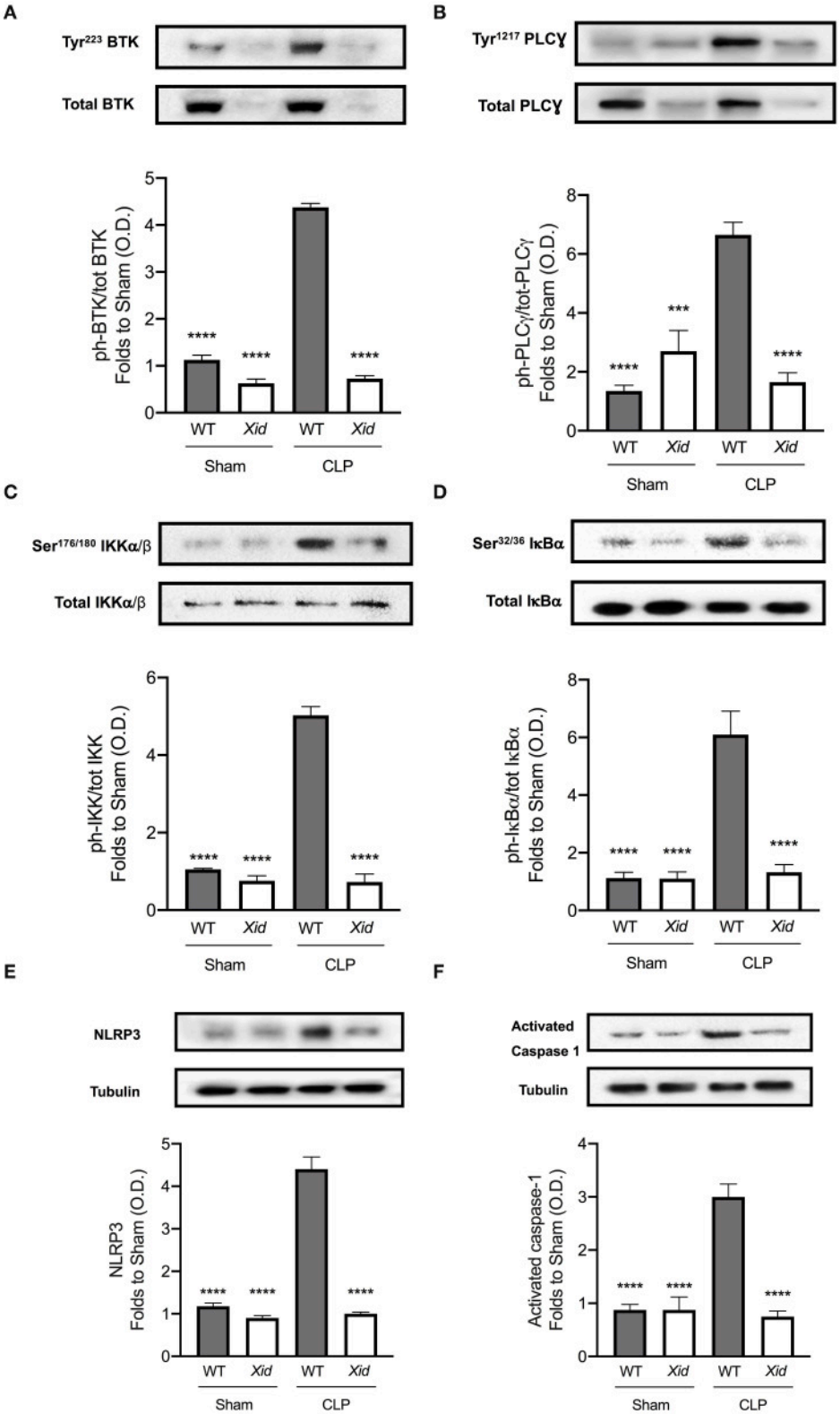

FIGURE 5 | BTK, NF-κB, and NLRP3 inflammasome are not activated in *Xid* mice after polymicrobial sepsis. Mice underwent sham-operated or CLP surgery and 24 h later signaling events in the cardiac tissue were assessed. Densitometric analysis of the bands is expressed as relative optical density (O.D.) of **(A)** phosphorylation of BTK at Tyr^{223} corrected for the corresponding total BTK and normalized using the related sham bands. **(B)** Phosphorylation of PLCγ at Tyr^{1217}

(Continued)

FIGURE 5 | corrected for the corresponding total PLCγ and normalized using the related sham bands. **(C)** Phosphorylation of IKKα/β at $Ser^{176/180}$ corrected for the corresponding total IKKα/β and normalized using the sham related bands. **(D)** Phosphorylation of IκBα at $Ser^{32/36}$ corrected for the corresponding total IκBα and normalized using the related sham band. **(E)** NLRP3 activation, corrected against tubulin and normalized using the sham related bands. **(F)** Pro-caspase-1 against activated caspase-1 and normalized using the sham related bands. The following groups were studied WT sham ($n = 4$), *Xid* sham ($n = 4$), WT-CLP ($n = 4$), and *Xid*-CLP ($n = 4$). Data are expressed as mean ± SEM and analyzed by one-way ANOVA with a Bonferroni *post hoc*-test. $^{***}P < 0.001$ and $^{****}P < 0.0001$ vs. WT-CLP.

whether *Xid* neutrophils and macrophages have increased phagocytic ability *in vivo*. We found that the percentage of neutrophils and macrophages, which are phagocytosing bacteria, are similar in WT-CLP and *Xid*-CLP mice. However, neutrophils and macrophages of *Xid*-CLP mice contain more bacteria per immune cell than WT-CLP mice, showing a 100% increase in phagocytic ability of both neutrophils and macrophages (**Figures 4E–L**). Collectively, this data clearly demonstrates that *Xid* mice with a deficiency in BTK show enhanced phagocytosis *in vivo* resulting in improved clearance of bacteria during a septic episode.

BTK, NF-κB, and NLRP3 Inflammasome Are Not Activated in *Xid* Mice After Polymicrobial Sepsis

To understand the signaling mechanism associated with the observed cardiac dysfunction in CLP-sepsis, we investigated the effect of BTK deficiency in *Xid* mice on the activation of key signaling pathways of inflammation: BTK, NF-κB, and NLRP3 inflammasome activation (**Figure 5**). When compared to sham-operated mice, WT mice subjected to CLP showed an increase of BTK activation as demonstrated by significant increases in the phosphorylation of cardiac BTK at Tyr^{223} and the phosphorylation of PLCγ at Tyr^{1217}. No activation of BTK was detected in *Xid* mice, even after CLP injury and the phosphorylation of cardiac BTK at Tyr^{223} and the phosphorylation of PLCγ at Tyr^{1217} in *Xid*-CLP mice were similar to that of sham-operated animals (**Figures 5A,B**).

NF-κB activation plays a key role in the pathophysiology of sepsis. When compared to sham-operated mice, WT-CLP mice exhibit a significant increase in NF-κB activation as demonstrated by significant increases in the phosphorylation of IKKα/β at $Ser^{176/180}$ and the phosphorylation of IκBα at $Ser^{32/36}$. When compared to WT-CLP mice, *Xid*-CLP mice the phosphorylation of IKKα/β at $Ser^{176/180}$ and IκBα at $Ser^{32/36}$ was significantly reduced, indicating that the degree of activation of NF-κB caused by sepsis in the heart was significantly lower in *Xid*-mice than in WT-mice (**Figures 5C,D**).

When compared to sham-operated mice, WT mice subjected to CLP showed an increase in the activation of the NLRP3 inflammasome, demonstrated by an increase in the expression of the NLRP3 inflammasome and cleavage of pro-caspase-1 to caspase-1 in the heart (**Figures 5E,F**) as well as an increase the production of IL-1β in serum (**Figure 2C**). In contrast, *Xid*-CLP mice showed reduced activation of NLRP3 inflammasome as demonstrated by a decrease in the expression of the NLRP3 inflammasome, cleavage of pro-caspase-1 to caspase-1 (**Figures 5E,F**) and IL-1β when compared to WT-CLP mice (**Figure 2C**).

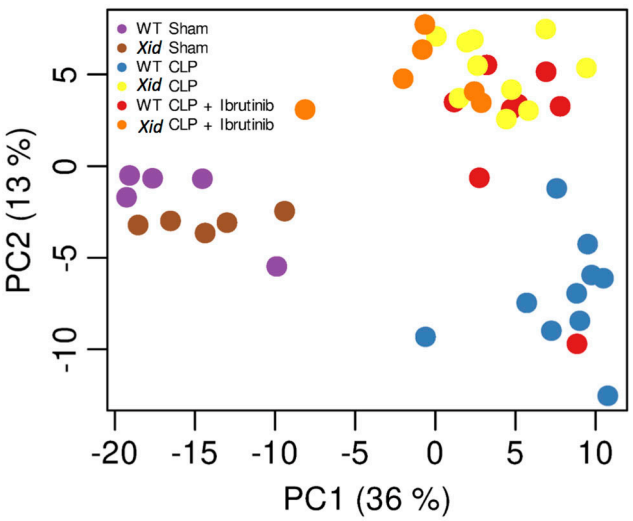

FIGURE 6 | Principal component analysis (PCA). Principal component analysis (PCA) of the normalized and scaled metabolome data. Plot shows first two principal components (PC), which account for almost half of the total variance in the data set. Variance between replicates is far less than between different experimental conditions. Contrasts between main experimental conditions are visible in the shown PCs. Each dot represents a sample and each color represents a mice group.

Xid Mice Show Lower Levels of Sepsis-Dysregulated Metabolites

Using a targeted metabolomic approach, we detected 240 analytes in murine plasma. A two-dimensional principal component analysis (PCA) of all detected analytes (**Figure 6**), revealed a clear distinction between the two sham-operated mice groups (WT sham and *Xid* sham), the WT-CLP mice group and the three treated and/or *Xid* CLP-induced mice groups (*Xid* CLP, WT CLP + Ibrutinib, and *Xid* CLP + Ibrutinib). The first principal component explained about 36% of total variation among the six mice groups and separated the sham-operated mice from the CLP-induced mice groups. The second principal component explained about 13% of total variation of all metabolites and achieved the same effect as PC2, but further it separated the CLP-induced WT mice group from the three mice groups *Xid* CLP, WT CLP + ibrutinib, and *Xid* CLP + ibrutinib. Significant changes in analytes were identified and analyzed via hierarchical clustered *z* score heatmaps and their significant log2-fold changes of selected group comparisons were shown in log2-fold change heatmaps (**Figures S2–S5**). The heatmaps illustrate 55 significant primary metabolites (**Figure S2**), 138 significant phospholipids

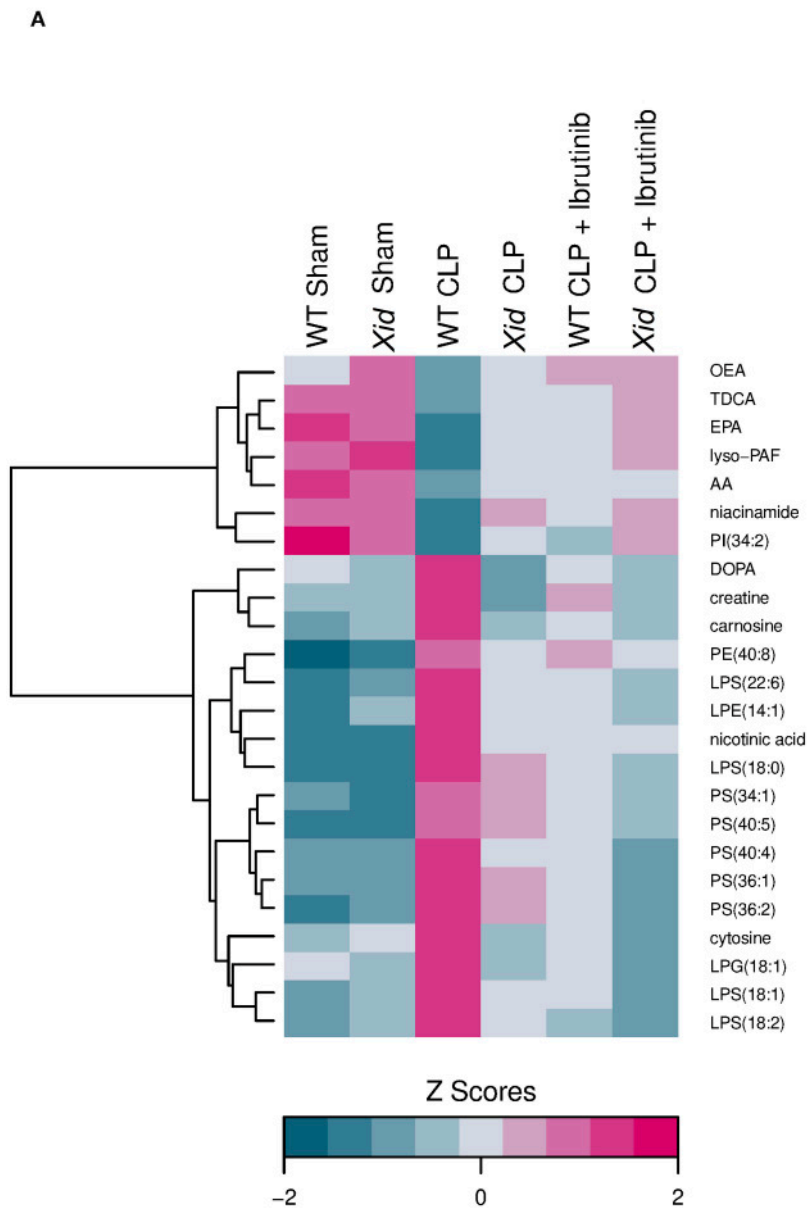

FIGURE 7 | Heatmap of significant restored metabolites in the groups XID CLP, WT CLP + Ibrutinib, and XID CLP + Ibrutinib. **(A)** Hierarchical clustered z score heatmaps showed significantly changed analytes and **(B)** log2-fold change heatmaps showed their significant log2-fold changes for selected groupwise comparisons. The heatmap shows analytes which, compared to the WT CLP group ($n = 10$), restored in all three groups [*Xid*-CLP ($n = 10$), WT-CLP + ibrutinib ($n = 8$), and *Xid*-CLP + ibrutinib ($n = 6$)] to the level of the two sham groups [WT Sham ($n = 5$), *Xid* Sham ($n = 5$)]. Each column in a *z* score heatmap represented the mean value of all animals in a group, each column in a log2-fold change heatmap represented a groupwise comparison and each row defined an analyte. Analytes were hierarchically clustered using Ward's minimum variance method (76) and an euclidian distance between log2-fold changes. Dendrograms provide information about distances between clusters. AA, arachidonic acid; AEA, arachidonoylethanolamide; DHA, docosahexaenoic acid; DOPA, dihydroxyphenylalanine; EPA, eicosapentaenoic acid; LPE, lysophosphatidylethanolamine; LPG, lysophosphatidylglycerol; LPS, lysophosphatidylserine; lyso-PAF, lyso-platelet activating factor; OEA, oleoylethanolamine; PE, phosphatidylethanolamine; PI, phosphatidylinositol; PS, phosphatidylserine; TDCA, taurodeoxycholic acid.

and their derivatives (**Figures S3,S4**), and 6 significant lipid mediators (**Figure S5**).

Figure 7 shows a sorting of 24 analytes that were significantly restored in the three mice groups *Xid*-CLP, WT-CLP + ibrutinib, and *Xid*-CLP + ibrutinib to the initial levels of both sham-operated groups compared to the WT-CLP mice group. The ibrutinib treatment or the BTK inactivation or the combination of both restored 7 significant decreased and 17 significant increased analytes in CLP-induced WT-mice. The decreased analytes belonged predominantly to the lipid

mediator's docosahexaenoic acid (DHA), eicosapentaenoic acid (EPA), lyso-platelet activating factor (lyso-PAF), and oleoylethanolamine (OEA). The bile acid taurodeoxycholic acid (TDCA), the phosphatidylinositol (PI) (34:2) and the primary metabolite niacinamide were also reduced. The increased analytes included five primary metabolites (dihydroxyphenylalanine (DOPA), creatine, carnosine, nicotinic acid, cytosine), four lysophosphatidylserines, five phosphatidylserines, one lysophosphatidylethanolamine, one lysophaphatidylglycerol and one phosphytidylethanolamine.

Sorting by analytes that were only significantly restored in *Xid*-CLP (**Figure S6**) showed five analytes. One analyte was increased, the primary metabolite kynurenine, and four analytes were decreased in the WT-CLP group and this included the primary metabolite uridine and one the phospholipids phosphatidylserine, phosphatidylethanolamine, and phosphatidylinositol. Twenty-three analytes showed the sorting by significantly restored analytes in the mice groups *Xid* CLP and *Xid* CLP + Ibrutinib (**Figure S7**). The levels of 10 analytes (cGMP, creatinine, ursodeoxycholic acid (UDCA), deoxycholic acid (DCA), adenine, one lysophosphatidylserine, one lysophosphatidylglycerol, three lysophosphatidylethanolamines) were upregulated and 13 analytes (one sphingomyelin, six phosphatidylcholines, three phosphatidylethanolamines, two phosphatidylserines, one phosphatidylinositol) were downregulated in CLP-induced wildtype mice. Analytes that were only restored in the mice group WT-CLP + ibrutinib could not be determined. The heatmap with analytes that were significantly restored in the mice groups WT-CLP + ibrutinib and *Xid*-CLP + ibrutinib (**Figure S8**) showed one increased primary metabolite (cholesterol) and three decreased phospholipids (two phosphatidylserines and one lysophosphatidylserine).

Expression of BTK Is Increased in Whole Human Blood of Septic Non-survivors

Parnell et al. (26) collected whole blood of patients confirmed with sepsis (and healthy participants) over a 5 day time course with the first day of collection being within the initial 24 h of admission to the ICU. RNA was extracted from whole blood and gene expression was analyzed by microarray. Three groups were collected, healthy participants, septic survivors and septic non-survivors. Dataset is available on the gene expression omnibus under GDS4791. We reanalysed this dataset for BTK expression in these three groups and found that at day 1 there is no significant differences in gene expression between healthy, septic survivors, and septic non-survivors (**Figures 8A,B**). However, over the course of 5 days BTK expression increases in septic non-survivors and a significant difference between non-survivors and healthy participants as well as a significant difference between non-survivors and survivors is observed at day 5 (**Figure 8C**). There was no significant difference in BTK expression between septic survivors and healthy volunteers (**Figures 8A–C**).

DISCUSSION

Sepsis is the overwhelming host response to infection (bacterial, fungal, or viral) leading to shock and multiple organ dysfunction. We have previously reported that BTK inhibitors (ibrutinib, acalabrutinib) significantly attenuate sepsis-induced cardiac dysfunction and reduced inflammatory cytokine production, but BTK inhibitors have many off target effects (14). In the present study we investigated whether the beneficial effects are exclusively due to inhibition of BTK and how a reduction in systemic inflammation due to BTK loss of function mutation affects bacterial clearance *in vivo*. We addressed these questions by conducting a model of polymicrobial sepsis in *Xid* mice (which have a missense mutation in the BTK gene, resulting in BTK to be functionally impaired). We report here for the first time that *Xid* mice are protected from sepsis-induced multiple organ dysfunction (cardiac, renal, and hepatocellular) due to increased bacterial clearance and suppression of systemic inflammation (cytokine storm) (please see **Figure 9** for schematic diagram of the role of BTK in the pathophysiology of sepsis).

BTK Inactivation Prevents Sepsis-Induced Multiple Organ Dysfunction

Sepsis results in multiple organ failure including cardiac dysfunction, renal dysfunction and hepatocellular injury. We report here for the first time that *Xid* mice subjected to sepsis are protected from developing cardiac dysfunction, hepatocellular injury, and renal dysfunction. Most notably, ibrutinib significantly reduced sepsis-induced multiple organ failure in WT-mice but had no further beneficial effect in *Xid*-mice subjected to CLP-indicating that the observed beneficial effect of ibrutinib in WT-mice can solely be explained by inhibition of BTK-activity. We have previously reported that inhibition of BTK by ibrutinib or acalabrutinib attenuate sepsis-induced cardiac and renal dysfunction in C57Bl/6 mice (14) and additionally we have now shown that delayed administration of ibrutinib in WT-CLP (CBA background) also attenuates sepsis-induced cardiac dysfunction, renal dysfunction, and hepatocellular injury, confirming that BTK inhibitors work in two different genetic backgrounds of mice. Furthermore, in this study we find that administration of ibrutinib (which inhibits a significant number of kinases in addition to BTK, more than acalabrutinib) in *Xid*-CLP mice neither results in further beneficial effects nor any adverse effects on cardiac, renal, or liver (dys)function. Inhibition of BTK reduces disease severity in animal models of sepsis-induced lung injury (30, 31), warm liver ischemia and reperfusion (32) and spontaneous lupus nephritis (33). Thus, we here provide evidence that inhibition of BTK alone is sufficient to prevent sepsis-induced multiple organ injury.

BTK Inactivation Results in Enhanced Bacterial Phagocytosis

We then investigated the mechanism(s) by which inactivation of BTK protects mice against sepsis-induced multiple organ failure. In septic patients, an essential treatment is early source

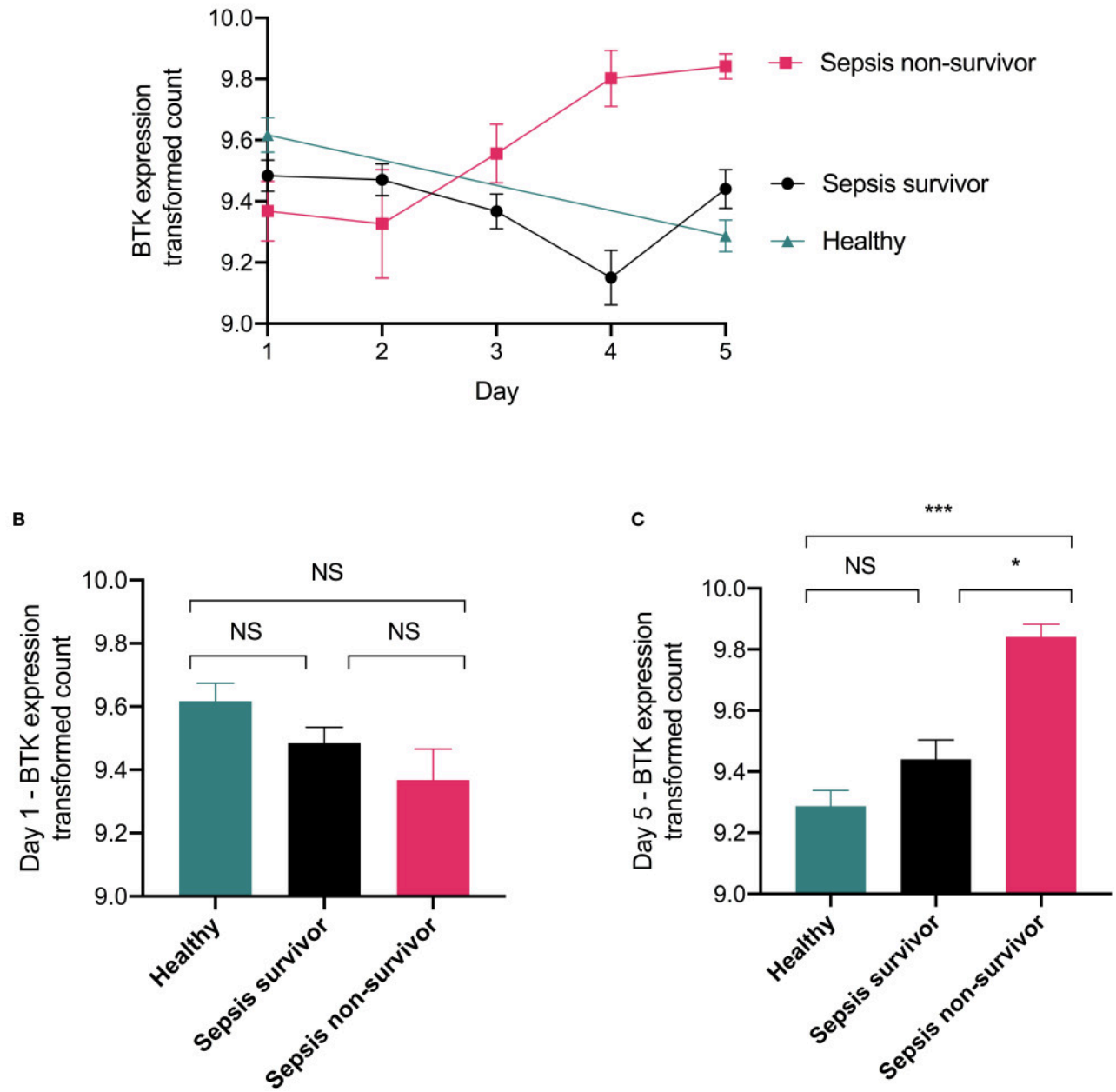

FIGURE 8 | Expression of BTK is increased in whole human blood of septic non-survivor's Original data was obtained from the gene expression omnibus under dataset number GDS4971 which was published by Parnell et al. (26). Whole blood of patients confirmed with sepsis (and healthy participants) over a 5 day time course. RNA was extracted from whole blood and analyzed for gene expression via microarray Illumina GenomeStudio V2010.3. Three groups were collected, healthy participants, septic survivors, and septic non-survivors. **(A)** Time course of BTK expression. **(B)** Day 1 BTK expression. **(C)** Day 5 BTK expression. Data was reanalysed looking for expression of BTK gene in their dataset and generated the figure using the software R, gene expression was quantile normalization and log transformation of the data was applied. Significance was determined by one-way ANOVA followed by Bonferroni *post hoc*-test and a value of $^{*}P < 0.05$ and $^{***}P < 0.001$ were considered significant. Data are expressed as mean ± SEM. Day 1 healthy ($n = 18$), septic survivors ($n = 26$), septic non-survivors ($n = 9$). Day 2 septic survivors ($n = 24$), septic non-survivors ($n = 7$). Day 3 septic survivors ($n = 22$), septic non-survivors ($n = 7$). Day 4 septic survivors ($n = 13$), septic non-survivors ($n = 5$). Day 5 healthy ($n = 18$), septic survivors ($n = 11$), septic non-survivors ($n = 3$).

control (removal of infection), which is associated with improved outcomes (34). We found that CLP in *Xid* mice results in a reduction of the number of bacteria in both peritoneum and blood (at 24 h after onset of CLP) when compared to WT-CLP mice. This may well be due to an increase in bacterial phagocytosis in *Xid* mice. Macrophages obtained from

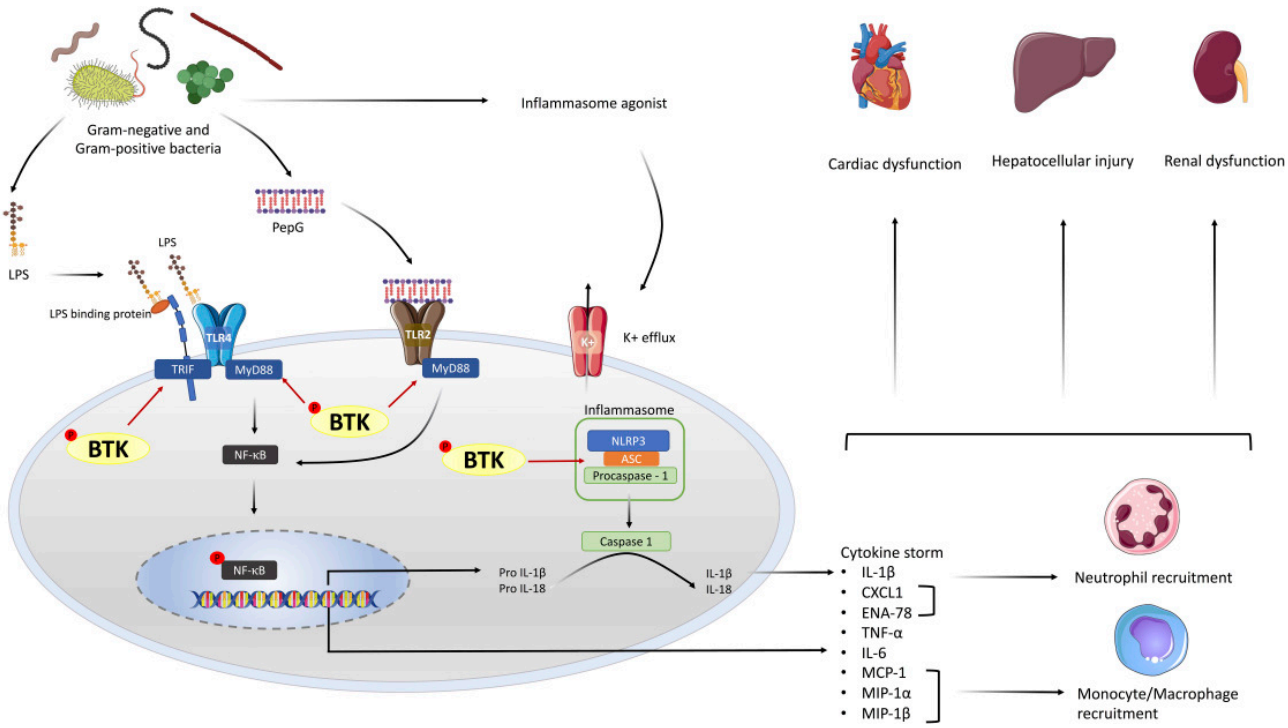

FIGURE 9 | Schematic diagram representing the role of Bruton's tyrosine kinase (BTK) in the pathophysiology of sepsis. LPS is released from Gram-negative bacteria which activate the TLR4 signaling pathway and the release of PepG from Gram-positive bacteria activate the TLR2 signaling pathway. BTK is involved in the activation of TLR4 and TLR2 by binding to MyD88 and TRIF thus activating their representative signaling cascades. The activation of the MyD88 signaling pathway, leads to the activation of NF-κB and the production of pro-inflammatory cytokines. Additionally, BTK activates the NLRP3 inflammasome by binding to the ASC component of the inflammasome. Once active the NLRP3 inflammasome cleaves pro-IL-1β to active IL-1β. The production of chemokines from NF-κB activation results in the recruitment of neutrophils and macrophages. Excessive inflammation from the cytokine storm and innate immune cells results in multiple organ failure/injury. The use of BTK inhibitors such as ibrutinib or acalabrutinib supress sepsis-induced inflammation and thus multiple-organ failure/injury.

Xid-mice do not show defects in in phagocytosis (35, 36) and we found that the percentage of phagocytosing cells are similar in both WT and *Xid* mice. We discovered, however, that macrophages obtained from *Xid*-mice with sepsis had taken up a significantly larger number of bacteria. This was also true for neutrophils from *Xid*-mice. We believe that the increase in phagocytosis by macrophages and neutrophils from *Xid*-mice *in vivo* could explain the observed increase in clearance of bacteria in peritoneum and blood. Beguem et al. (37) found that monocytes from healthy volunteers stimulated with LPS and treated with evobrutinib resulted in an increased rate of phagocytosis *in vitro* due to a switch of macrophages from the pro-inflammatory M1 to the pro-resolving M2 phenotype and this was associated with reduced secretion of TNF-α. In addition, *Xid* mice infected with *Francisella tularensis* showed enhanced bacterial clearance from the lung and spleen, which correlated with a significant improvement of survival when compared to wild-type controls (38).

This raises the question of the underlying mechanisms that enables or drives increased phagocytosis in *Xid*-mice? Neither inhibition of BTK activity with ibrutinib nor inactivation of BTK in *Xid* mice affects monocyte FcγR-mediated phagocytosis, but it does supress FcγR-mediated cytokine production. The decrease of calcium flux due to BTK inhibition also does not affect phagocytosis, but does decrease cytokine production (35). BTK inhibition results in the polarization to M2 macrophages [which have greater phagocytic ability (39)], demonstrated by increased expression of CD206. CD206 is involved in phagocytosis of a number of bacterial strains. For example, monocyte-derived macrophages that express high levels of CD206 phagocytosed 78% of *E. coli*, while monocyte-derived macrophages that express low levels of CD206 only phagocytosed 30% of *E. coli* (40). Excessive activation of neutrophils is known to decrease survival and enhance susceptibility to subsequent bacterial infections (41). One mechanism that may contribute to the pathology of sepsis is the release of neutrophil extracellular traps as they contain the beneficial antimicrobial nuclear proteins but also damaging citrullinated histones, elastase, myeloperoxidase and MMP-3 (42, 43). The release of neutrophil extracellular traps results in ineffective phagocytosis (44). Florence et al. (31) showed that BTK was increased in the lung neutrophils and inhibiting BTK protected mice against lethal influenza by reducing the release of neutrophil extracellular traps. The decrease of neutrophil extracellular traps was also observed in human peripheral blood neutrophils

incubated with influenza and BTK inhibitor (31). However, the exact molecular mechanisms underlying this phenomenon are yet to be elucidated. Future studies are required to increase our understanding as to how *Xid* macrophages and neutrophils phagocytose more bacteria per immune cell.

BTK Inactivation Results in Reduced Infiltration of the Peritoneum With Innate Immune Cells

BTK plays a fundamental role in signaling and function of B cells, but BTK is also highly expressed in myeloid cells such as macrophages and neutrophils (9) and inactivation of BTK results in reduced cell-mediated inflammatory responses (45, 46). We report here that *Xid*-CLP mice have reduced infiltrating innate immune cells (macrophages and neutrophils) in the peritoneum (site of infection). We propose that this may lead to a reduction of the formation of cytokines/chemokines in the serum and, hence, will prevent the cytokines storm.

BTK Inactivation Results in M2 Polarization

Macrophages play an important role in the two phases of sepsis (early pro-inflammatory phase and the later anti-inflammatory phase), as they can have either pro-inflammatory or anti-inflammatory properties. Initially, M1 macrophages (pro-inflammatory) activate inflammation by secreting TNF-α, IL-1β, IL-6, and IL-12 to promote the removal of the pathogen, then M2 macrophages repair tissue and resolve inflammation by secreting cytokines including IL-10 (47, 48). If the M1 macrophage-driven pro-inflammatory response cannot be controlled, the resultant cytokine storm can be a key driver of the severity of sepsis leading to organ failure and death (49). From our experiments we conclude that a loss of function or inhibition of BTK drives the switch from the pro-inflammatory M1 phenotype to pro-resolving M2 phenotype in response to LPS (50). Here we report that macrophages obtained from septic *Xid*-mice have a pro-resolving M2 phenotype, whereas macrophages obtained from septic WT-mice have the M1 phenotype. Most notably, macrophages of the M2 phenotype have a greater phagocytotic function resulting in increased clearance of apoptotic cells and an acceleration of resolution (39). Indeed, M2 macrophages protect against sepsis-induced lung injury (51) and sepsis-induced acute kidney injury (52). Transplantation of M2 macrophages has been suggested as a potential therapeutic approach for sepsis-induced lung injury (51).

BTK Inactivation Reduces the Activation of NF-κB

BTK plays a pivotal role in the activation of TLRs and, hence, the signaling steps leading to the activation of NF-κB (7), which plays a key role in the pathophysiology of septic cardiomyopathy (53). Here we report that *Xid* mice subjected to polymicrobial sepsis have a reduced activation of BTK and NF-κB (measured as phosphorylation of IKKα/β and IκBα) in the heart. We have previously reported that BTK inhibitors ibrutinib or acalabrutinib reduce the activation of cardiac BTK and NF-κB in mice subjected to sepsis (14). Furthermore, we have shown that inhibition of NF-κB activation with an inhibitor of IKK also attenuates the cardiac dysfunction associated with polymicrobial sepsis (53). Purvis et al. (46) showed that ibrutinib treatment attenuated the activation of NF-κB and gene expression of cytokines in the diabetic kidney and liver. Thus, we propose that an impairment in the activation of BTK in *Xid* mice leads to reduced activation of NF-κB in the heart, which contributes to or accounts for the observed reduction in organ injury and dysfunction observed in *Xid*-mice with sepsis.

BTK Inactivation Prevents the Cytokine Storm

Activation of NF-κB leads to an increase in the production of cytokines and chemokines such as the pro-inflammatory cytokines TNF-α, IL-6, IL-1β, and the anti-inflammatory cytokine IL-10, neutrophils chemoattractant chemokines (KC & ENA-78), monocyte chemoattractant chemokines (MCP-1, MIP-1α, and MIP-1β) and G-CSF, all of which contribute to the systemic inflammation and organ dysfunction associated with sepsis (54). Out of all these cytokines, the ones increased most in our model of murine sepsis were IL-6, KC, and MCP-1. The levels of IL-8 and monocyte chemoattractant protein-1 (MCP-1) are associated with early 48 h and 28 day mortality in sepsis patients (55). Most notably, we report that in *Xid*-mice subjected to CLP-sepsis, all of these cytokines and chemokines are markedly reduced. WT-CLP mice treated with ibrutinib also show reduced production of sepsis-associated cytokines and chemokines and no difference is observed with the addition of ibrutinib to *Xid*-CLP mice. Thus, an impairment of BTK activation in *Xid*-mice prevents NF-κB and NLRP3-dependent, systemic inflammation (cytokine storm) resulting in a reduction in organ injury/dysfunction.

BTK Inactivation Reduces the Activation of the NLRP3 Inflammasome

BTK is also involved in the assembly/activation of the NLRP3 inflammasome in both mice and humans (8, 56). The activation of the NLRP3 inflammasome also plays a role in the pathophysiology of sepsis and septic cardiomyopathy (57). Pharmacological inhibition of NLRP3 activation with MCC950 (NLRP3 inflammasome inhibitor) reduced the neurological and cognitive impairment in septic animals (58). It has also been reported that genetic deficiency of NLRP3 promotes resolution of inflammation in polymicrobial sepsis (59). We report here that the activation of the NLRP3 inflammasome (measured as NLRP3 activation, caspase-1 activation and IL-1β release) was largely reduced in *Xid*-mice subjected to CLP when compared to WT-mice with sepsis. We previously reported that BTK inhibitors (ibrutinib or acalabrutinib) inhibit the activation of the NLRP3 inflammasome and production of IL-1β in septic animals (14). Purvis et al. (46) showed that ibrutinib treatment also attenuated the activation NLRP3 inflammasome in the diabetic kidney and liver. Thus, we propose that prevention of the activation of the NLRP3 inflammasome secondary to reduced activation of BTK importantly contributes to the reduction in inflammation and organ dysfunction observed in septic *Xid*-mice.

BTK Inactivation Restores Dysregulated Metabolites

PCA showed that 49% of the total variance of all metabolites formed three well separable clusters. The metabolomic profiles of CLP-induced WT mice formed one cluster and was clearly distinguishable from a second cluster (WT sham-operated and *Xid* sham-operated) and a third cluster consisting of the three groups *Xid*-CLP, WT-CLP + ibrutinib, and *Xid*-CLP + ibrutinib. The common clustering of the latter three groups supports the assumption that the inhibition of BTK alone is responsible for the partial restoration of dysregulated metabolites in sepsis.

Host defense toward bacterial infection is a complex interplay of several mechanisms including inflammation, coagulation, immune activation, hypoxia, and metabolic reprogramming. Specifically, the regulation and impact of the metabolic changes is known to play an important role in the pathophysiology of sepsis (60). We demonstrated in this study that deregulated members of lipid mediators, phospholipids, primary metabolites and bile acids in CLP-induced WT-mice were restored by ibrutinib (in WT-mice) and/or by inactivation of the BTK gene (*Xid*-mice). The elevated and reduced plasma levels of some restored metabolites in the WT CLP group were already shown. For example, an increased metabolism of the lipid mediators AA and EPA could be found in plasma of sepsis patients (61). In addition, two other lipid mediators, OEA and lyso-PAF, were decreased in CLP-induced WT mice. Platelet-activating factor (PAF) is a proinflammatory mediator in systemic inflammation and its known to be upregulated in sepsis (62). Degradation of the immediate precursor lyso-PAF is probably a result of its increased transformation to PAF (63). The decreased levels of the lipid-amide OEA are probably a compensatory mechanism in sepsis-related weight loss and disturbed energy balance, because OEA is a modulator in food consumption and weight management and actually leads to satiation or meal termination (64). Even the restoration of the reduced bile acid TDCA and the elevated amino acid DOPA seems to be a positive regulatory mechanism. TDCA ameliorates systemic inflammation, normalizes blood pressure, prevents kidney injury, and prolongs survival in a mouse sepsis model (65). DOPA has anti-neuro inflammation effects and improved neuroplasticity in septic mice (66). The plasma of the WT-CLP group showed also increased levels of isoforms of the phospholipids species lysophaphatidylserine and PS, probably due to their procoagulant activity in sepsis (67, 68). Some primary metabolites were also enhanced in septic mice and restored by ibrutinib administration and BTK inactivation such as the dysregulated precursors (cytosine, niacinamide, nicotinic acid) of nucleotide or nicotinate and nicotinamide metabolism (69, 70). The restoration also included the loss of carnosine to plasma due to skeletal muscle wasting in sepsis (71) and the elevated levels of creatine presumably because of the known higher activity of creatine kinase to catalyze the urgently required ATP in developing sepsis (72). This data of restored metabolites demonstrates that *Xid* mice with a deficiency in BTK have a similar metabolomic profile in sepsis than WT-CLP-mice treated with ibrutinib.

In addition, the data in **Figures S5,S6** reveal that *Xid* mice restored metabolites 7 times more than ibrutinib-treated mice (**Figure S7**). Many of the additionally restored metabolites in *Xid* mice are known to be deregulated in sepsis such as adenine (73) creatinine (74), and kynurenine (75). An explanation for the different magnitude of restored metabolites in *Xid* mice in comparison with ibrutinib-treated mice could be the different number of inhibited kinases. Thus, the *Xid* mice seem to benefit from the inhibition of only one kinase, namely BTK, which in addition to reducing cytokine storm restores the sepsis-related dysregulation of specific metabolites.

BTK Expression Is Increased in Whole Human Blood of Septic Non-survivors

Currently the expression and/or activation of BTK in septic patients has not been reported. There are datasets available on the GEO and we reanalysed microarray data (GDS4971) of the time course of gene expression in healthy, septic survivors, and septic non-survivors published by Parnell et al. (26). Interestingly, our analysis revealed an increase in expression of BTK in septic non-survivors, whereas BTK expression in septic survivors does not increase and is not different from healthy volunteers. Thus, increases in BTK expression in septic patients correlate with mortality, while lower levels of BTK expression are associated with survival from sepsis. There were no clear differences between cytokine expression of TNF-α, IL-6, MCP-1, CXCL1 in the three groups, expression of BTK was a better predictor of mortality rather than with the expression of any one cytokine. We have previously shown in septic mouse hearts that activation of BTK correlates with cardiac dysfunction (14). BTK activation also increases in whole blood of COVID-19 patients which, like septic patients, also present with excessive systemic inflammation (cytokine storm) (17).

LIMITATIONS OF THE STUDY

We have shown that *Xid*-mice subjected to CLP have increased bacterial clearance and reduced systemic inflammation (secondary to reduced activation of the NLRP3 inflammasome and NF-κB) and cardiac (organ) dysfunction. There is good evidence that mortality of patients with sepsis increases with an increase in the number of organs failing (SOFA scores). In the UK survival studies in septic models are not routinely conducted due to ethical reasons. Thus, we were unable to investigate the survival of *Xid* mice undergoing sepsis. It has been reported that a reduction in temperature $<30^{\circ}$C or a change of temperature of 5°C over time predicts mortality in animals with sepsis (29). Using this more humane surrogate marker, we found that *Xid* mice with sepsis have a predicted mortality of 0% (100% survival), while WT-mice with sepsis would have a predicted mortality of 90% (10% survival). We found that ibrutinib does not affect predicted mortality in *Xid*-CLP resulting in a predicted mortality of 0% (100% survival) and that delayed administration of ibrutinib in WT-CLP mice led to a predicated mortality of 15% (85% survival). It would be useful to confirm the impact

of an impairment in BTK function in *Xid*-mice on outcome (mortality) in a more long-term sepsis model.

CONCLUSION

We report here for the first time that genetic inactivation of BTK is responsible for conferring protection against multiple organ failure in a clinically relevant model of sepsis. Most importantly we have shown that the inactivation of BTK in *Xid* mice results in an increase of bacterial phagocytosis in macrophages and neutrophils, thus, increasing bacterial clearance in both peritoneum and blood. Inactivation of BTK also results in a phenotypic switch of macrophages from M1 to the M2 phenotype, which aids in the resolution of sepsis. The suppression of the immune system by inactivated BTK leads to reduced activation of NF-κB and the NLRP3 inflammasome, therefore, preventing the induction of the cytokine storm. Metabolomic analysis revealed a dysregulation of metabolites in WT septic mice. Most notably, we found that inactivation of BTK in *Xid*-mice or administration of ibrutinib in WT mice is responsible for the (partial) restoration of dysregulated metabolites in sepsis. As the administration of ibrutinib to *Xid*-CLP mice did not result in any additional (beneficial) effects on the alterations in organ dysfunction, cytokine/chemokines formation and changes in metabolites caused by sepsis, our data strongly suggest that BTK inactivation is responsible for the observed effects of ibrutinib. Lastly, we have found that BTK expression in humans is increased in the blood of septic non-survivors, while lower expression is associated with survival from sepsis. Taken together our work suggests that BTK inhibitors maybe repurposed for the use in sepsis (or other conditions associated with excessive local or systemic inflammation including COVID-19) due to their ability to reduce systemic inflammation (cytokine storm), their ability to enhance the phagocytosis of macrophages and switch macrophages from the pro-inflammatory M1 to the anti-inflammatory M2 phenotype.

DATA AVAILABILITY STATEMENT

The raw data supporting the conclusions of this article will be made available by the authors, without undue reservation.

ETHICS STATEMENT

The animal study was reviewed and approved by The Animal Welfare Ethics Review Boards of Queen Mary University of London and The Dunn School of Pathology in the University of Oxford approved all experiments in accordance with the Home Office guidance on the operation of Animals (Scientific Procedures Act 1986) published by Her Majesty's Stationery Office and the Guide for the Care and Use of Laboratory Animals of the National Research Council. Work was conducted under U.K. Home Office project license number PCF29685 and P144E44F2. All *in vivo* experiments are reported in accordance to ARRIVE guidelines.

AUTHOR CONTRIBUTIONS

CO'R, GP, SC, MC, DG, and CT conceived and designed the experiments. CO'R, GP, DC, NK, BW, MS, GF, SM, and LC performed the experiments. CO'R, GP, MC, SC, NK, BW, DG, and CT analyzed the data. CO'R, DG, and CT contributed to the writing of the manuscript. All authors reviewed the manuscript before submission.

FUNDING

CO'R was sponsored by Barts and The London School of Medicine and Dentistry, Queen Mary University of London. This work was, in part, supported by William Harvey Research Limited and the William Harvey Research Foundation, the British Heart Foundation (Award number: RG/15/10/23915 to DG), the Oxford BHF Centre of Research Excellence (Award number: RE/13/1/30181 to GP and DG), the Federal Ministry of Education and Research (BMBF), Germany [Award number: 03Z22JN12 to SC, Research Group Translational Septomics, Centre for Innovation Competence (ZIK) Septomics].

ACKNOWLEDGMENTS

We would like to thank Hira Bahadur Ale for their technical assistance on the Amnis® ImageStream®X Mk II Imaging Flow Cytometer. We thank Dominik Driesch (BioControl Jena GmbH, Jena, Germany) for statistical advice with respect to metabolome analysis.

SUPPLEMENTARY MATERIAL

The Supplementary Material for this article can be found online at: https://www.frontiersin.org/articles/10.3389/fimmu.2020.581758/full#supplementary-material

REFERENCES

1. Singer M, Deutschman CS, Seymour CW, Shankar-Hari M, Annane D, Bauer M, et al. The third international consensus definitions for sepsis and septic shock (sepsis-3). *JAMA*. (2016) 315:801–10. doi: 10.1001/jama.2016.0287
2. Rudd KE, Johnson SC, Agesa KM, Shackelford KA, Tsoi D, Kievlan DR, et al. Global, regional, and national sepsis incidence and mortality, 1990-2017: analysis for the Global Burden of Disease Study. *Lancet*. (2020) 395:200–11. doi: 10.1016/S0140-6736(19)32989-7
3. Marshall JC. Why have clinical trials in sepsis failed? *Trends Mol Med*. (2014) 20:195–203. doi: 10.1016/j.molmed.2014.01.007
4. Cavaillon J, Singer M, Skirecki T. Sepsis therapies: learning from 30 years of failure of translational research to propose new leads. *EMBO Mol Med*. (2020) 12:e10128. doi: 10.15252/emmm.201810128

5. Martin L, Derwall M, Al Zoubi S, Zechendorf E, Reuter DA, Thiemermann C, et al. The septic heart: current understanding of molecular mechanisms and clinical implications. *Chest*. (2019) 155:427–37. doi: 10.1016/j.chest.2018.08.1037
6. Tsukada S, Saffran DC, Rawlings DJ, Parolini O, Allen RC, Klisak I, et al. Deficient expression of a B cell cytoplasmic tyrosine kinase in human X-linked agammaglobulinemia. *Cell*. (1993) 72:279–90. doi: 10.1016/0092-8674(93)90667-F
7. Jefferies CA, Doyle S, Brunner C, Dunne A, Brint E, Wietek C, et al. Bruton's tyrosine kinase is a Toll/interleukin-1 receptor domain-binding protein that participates in nuclear factor kappaB activation by Toll-like receptor 4. *J Biol Chem*. (2003) 278:26258–64. doi: 10.1074/jbc.M301484200
8. Ito M, Shichita T, Okada M, Komine R, Noguchi Y, Yoshimura A, et al. Bruton's tyrosine kinase is essential for NLRP3 inflammasome activation and contributes to ischaemic brain injury. *Nat Commun*. (2015) 6:7360. doi: 10.1038/ncomms8360
9. Weber ANR, Bittner Z, Liu X, Dang T-M, Radsak MP, Brunner C. Bruton's tyrosine kinase: an emerging key player in innate immunity. *Front Immunol*. (2017) 8:1454. doi: 10.3389/fimmu.2017.01454
10. Danielski LG, Della GA, Bonfante S, Barichello T, Petronilho F. The NLRP3 inflammasome and its role in sepsis development. *Inflammation*. (2020) 43:24–31. doi: 10.1007/s10753-019-01124-9
11. Deng M, Scott MJ, Loughran P, Gibson G, Sodhi C, Watkins S, et al. Lipopolysaccharide clearance, bacterial clearance, and systemic inflammatory responses are regulated by cell type-specific functions of TLR4 during sepsis. *J Immunol*. (2013) 190:5152–60. doi: 10.4049/jimmunol.1300496
12. Brunner C, Müller B, Wirth T. Bruton's tyrosine kinase is involved in innate and adaptive immunity. *Histol Histopathol*. (2005) 20:945–55. doi: 10.14670/HH-20.945
13. Pal Singh S, Dammeijer F, Hendriks RW. Role of Bruton's tyrosine kinase in B cells and malignancies. *Mol Cancer*. (2018) 17:57. doi: 10.1186/s12943-018-0779-z
14. O'Riordan CE, Purvis GSD, Collotta D, Chiazza F, Wissuwa B, Al Zoubi S, et al. Bruton's tyrosine kinase inhibition attenuates the cardiac dysfunction caused by cecal ligation and puncture in mice. *Front Immunol*. (2019) 10:2129. doi: 10.3389/fimmu.2019.02129
15. Sanford DS, Wierda WG, Burger JA, Keating MJ, O'Brien SM. Three newly approved drugs for chronic lymphocytic leukemia: incorporating ibrutinib, idelalisib, and obinutuzumab into clinical practice. *Clin Lymphoma Myeloma Leuk*. (2015) 15:385–91. doi: 10.1016/j.clml.2015.02.019
16. Markham A, Dhillon S. Acalabrutinib: first global approval. *Drugs*. (2018) 78:139–45. doi: 10.1007/s40265-017-0852-8
17. Roschewski M, Lionakis MS, Sharman JP, Roswarski J, Goy A, Monticelli MA, et al. Inhibition of Bruton tyrosine kinase in patients with severe COVID-19. *Sci Immunol*. (2020) 5:eabd0110. doi: 10.1126/sciimmunol.abd0110
18. Cambiaghi A, Pinto BB, Brunelli L, Falcetta F, Aletti F, Bendjelid K, et al. Characterization of a metabolomic profile associated with responsiveness to therapy in the acute phase of septic shock. *Sci Rep*. (2017) 7:9748. doi: 10.1038/s41598-017-09619-x
19. Leite HP, de Lima LFP. Metabolic resuscitation in sepsis: a necessary step beyond the hemodynamic? *J Thorac Dis*. (2016) 8:552–7. doi: 10.21037/jtd.2016.05.37
20. Rawlings DJ, Saffran DC, Tsukada S, Largaespada DA, Grimaldi JC, Cohen L, Mohr RN, et al. Mutation of unique region of Bruton's tyrosine kinase in immunodeficient XID mice. *Science*. (1993) 261:358–61. doi: 10.1126/science.8332901
21. Thomas J, Sideras P, Smith C, Vorechovsky I, Chapman V, Paul W. Colocalization of X-linked agammaglobulinemia and X-linked immunodeficiency genes. *Science*. (1993) 261:355–8. doi: 10.1126/science.8332900
22. Zechendorf E, O'Riordan CE, Stiehler L, Wischmeyer N, Chiazza F, Collotta D, et al. Ribonuclease 1 attenuates septic cardiomyopathy and cardiac apoptosis in a murine model of polymicrobial sepsis. *JCI insight*. (2020) 5:e131571. doi: 10.1172/jci.insight.131571
23. Morgan E, Varro R, Sepulveda H, Ember JA, Apgar J, Wilson J, et al. Cytometric bead array: a multiplexed assay platform with applications in various areas of biology. *Clin Immunol*. (2004) 110:252–66. doi: 10.1016/j.clim.2003.11.017
24. Varro R, Chen R, Sepulveda H, Apgar J. Bead-based multianalyte flow immunoassays. In: Clifton NJ, editor. *Methods in Molecular Biology*. Totowa, NJ: Humana Press (2007). p. 125–52. doi: 10.1007/978-1-59745-323-3_9
25. Collino M, Pini A, Mugelli N, Mastroianni R, Bani D, Fantozzi R, et al. Beneficial effect of prolonged heme oxygenase 1 activation in a rat model of chronic heart failure. *Dis Model Mech*. (2013) 6:1012–20. doi: 10.1242/dmm.011528
26. Parnell GP, Tang BM, Nalos M, Armstrong NJ, Huang SJ, Booth DR, et al. Identifying key regulatory genes in the whole blood of septic patients to monitor underlying immune dysfunctions. *Shock*. (2013) 40:166–74. doi: 10.1097/SHK.0b013e31829ee604
27. Benjamini Y, Hochberg Y. Controlling the false discovery rate: a practical and powerful approach to multiple testing. *J R Stat Soc Ser B*. (1995) 57:289–300. doi: 10.1111/j.2517-6161.1995.tb02031.x
28. R Core Team (2018). *R: A Language and Environment for Statistical Computing*. Vienna: R Foundation for Statistical Computing. Available online at: https://www.R-project.org/
29. Mai SHC, Sharma N, Kwong AC, Dwivedi DJ, Khan M, Grin PM, et al. Body temperature and mouse scoring systems as surrogate markers of death in cecal ligation and puncture sepsis. *Intensive Care Med Exp*. (2018) 6:20. doi: 10.1186/s40635-018-0184-3
30. Zhou P, Ma B, Xu S, Zhang S, Tang H, Zhu S, et al. Knockdown of Burton's tyrosine kinase confers potent protection against sepsis-induced acute lung injury. *Cell Biochem Biophys*. (2014) 70:1265–75. doi: 10.1007/s12013-014-0050-1
31. Florence JM, Krupa A, Booshehri LM, Davis SA, Matthay MA, Kurdowska AK. Inhibiting Bruton's tyrosine kinase rescues mice from lethal influenza-induced acute lung injury. *Am J Physiol Lung Cell Mol Physiol*. (2018) 315:L52. doi: 10.1152/ajplung.00047.2018
32. Palumbo T, Nakamura K, Lassman C, Kidani Y, Bensinger SJ, Busuttil R, et al. Bruton tyrosine kinase inhibition attenuates liver damage in a mouse warm ischemia and reperfusion model. *Transplantation*. (2017) 101:322–31. doi: 10.1097/TP.0000000000001552
33. Chalmers SA, Glynn E, Garcia SJ, Panzenbeck M, Pelletier J, Dimock J, et al. BTK inhibition ameliorates kidney disease in spontaneous lupus nephritis. *Clin Immunol*. (2018) 197:205–18. doi: 10.1016/j.clim.2018.10.008
34. Rhodes A, Evans LE, Alhazzani W, Levy MM, Antonelli M, Ferrer R, et al. Surviving sepsis campaign: international guidelines for management of sepsis and septic shock: 2016. *Intensive Care Med*. (2017) 43:304–77. doi: 10.1007/s00134-017-4683-6
35. Ren L, Campbell A, Fang H, Gautam S, Elavazhagan S, Fatehchand K, et al. Analysis of the effects of the Bruton's tyrosine kinase (Btk) inhibitor ibrutinib on monocyte Fcγ receptor (FcγR) function. *J Biol Chem*. (2016) 291:3043–52. doi: 10.1074/jbc.M115.687251
36. Mangla A, Khare A, Vineeth V, Panday NN, Mukhopadhyay A, Ravindran B, et al. Pleiotropic consequences of Bruton tyrosine kinase deficiency in myeloid lineages lead to poor inflammatory responses. *Blood*. (2004) 104:1191–7. doi: 10.1182/blood-2004-01-0207
37. Beguem Alankus Y, Grenningloh R, Haselmayer P, Bender A, Bruttger J. *Inhibition of Bruton's Tyrosine Kinase (BTK) Prevents Inflammatory Macrophage Differentiation: A Potential Role in RA and SLE - ACR Meeting Abstracts*. Chicago, IL: *American College of Rheumatology* (2018).
38. Crane DD, Griffin AJ, Wehrly TD, Bosio CM. B1a cells enhance susceptibility to infection with virulent Francisella tularensis via modulation of NK/NKT cell responses. *J Immunol*. (2013) 190:2756–66. doi: 10.4049/jimmunol.1202697
39. Roszer T. Understanding the mysterious M2 macrophage through activation markers and effector mechanisms. *Mediators Inflamm*. (2015) 2015:1–16. doi: 10.1155/2015/816460
40. Schulz D, Severin Y, Zanotelli VRT, Bodenmiller B. In-depth characterization of monocyte-derived macrophages using a mass cytometry-based phagocytosis assay. *Sci Rep*. (2019) 9:1925. doi: 10.1038/s41598-018-38127-9
41. Liu F-C, Chuang Y-H, Tsai Y-F, Yu H-P. Role of neutrophil extracellular traps following injury. *Shock*. (2014) 41:491–8. doi: 10.1097/SHK.0000000000000146
42. Czaikoski PG, Mota JMSC, Nascimento DC, Sônego F, Castanheira FV, Melo PH, et al. Neutrophil extracellular traps induce organ

damage during experimental and clinical sepsis. *PLoS ONE*. (2016) 11:e0148142. doi: 10.1371/journal.pone.0148142
43. Colón DF, Wanderley CW, Franchin M, Silva CM, Hiroki CH, Castanheira FVS, et al. Neutrophil extracellular traps (NETs) exacerbate severity of infant sepsis. *Crit Care*. (2019) 23:113. doi: 10.1186/s13054-019-2407-8
44. Manfredi AA, Ramirez GA, Rovere-Querini P, Maugeri N. The neutrophil's choice: phagocytose vs make neutrophil extracellular traps. *Front Immunol*. (2018) 9:288. doi: 10.3389/fimmu.2018.00288
45. de Porto AP, Liu Z, de Beer R, Florquin S, de Boer OJ, Hendriks RW, et al. Btk inhibitor ibrutinib reduces inflammatory myeloid cell responses in the lung during murine pneumococcal pneumonia. *Mol Med*. (2019) 25:3. doi: 10.1186/s10020-018-0069-7
46. Purvis GSD, Collino M, Aranda-Tavio H, Chiazza F, O'Riordan CE, Zeboudj L, et al. Inhibition of Bruton's tyrosine kinase regulates macrophage NF-κB and NLRP3 inflammasome activation in metabolic inflammation. *Br J Pharmacol*. (2020) 1–17. doi: 10.1111/bph.15182
47. Liu Y-C, Zou X-B, Chai Y-F, Yao Y-M. Macrophage polarization in inflammatory diseases. *Int J Biol Sci*. (2014) 10:520–9. doi: 10.7150/ijbs.8879
48. Atri C, Guerfali FZ, Laouini D. Role of human macrophage polarization in inflammation during infectious diseases. *Int J Mol Sci*. (2018) 19:1801. doi: 10.3390/ijms19061801
49. Stearns-Kurosawa DJ, Osuchowski MF, Valentine C, Kurosawa S, Remick DG. The pathogenesis of sepsis. *Annu Rev Pathol*. (2011) 6:19. doi: 10.1146/annurev-pathol-011110-130327
50. Ní Gabhann J, Hams E, Smith S, Wynne C, Byrne JC, Brennan K, et al. Btk regulates macrophage polarization in response to lipopolysaccharide. *PLoS ONE*. (2014) 9:e85834. doi: 10.1371/journal.pone.0085834
51. Shen Y, Song J, Wang Y, Chen Z, Zhang L, Yu J, et al. M2 macrophages promote pulmonary endothelial cells regeneration in sepsis-induced acute lung injury. *Ann Transl Med*. (2019) 7:142. doi: 10.21037/atm.2019.02.47
52. Li X, Mu G, Song C, Zhou L, He L, Jin Q, et al. Role of M2 macrophages in sepsis-induced acute kidney injury. *Shock*. (2018) 50:233–9. doi: 10.1097/SHK.0000000000001006
53. Chen J, Kieswich JE, Chiazza F, Moyes AJ, Gobbetti T, Purvis GSD, et al. IκB kinase inhibitor attenuates sepsis-induced cardiac dysfunction in CKD. *J Am Soc Nephrol*. (2017) 28:94–105. doi: 10.1681/ASN.2015060670
54. Chaudhry H, Zhou J, Zhong Y, Ali MM, McGuire F, Nagarkatti PS, et al. Role of cytokines as a double-edged sword in sepsis. *In Vivo*. (2013) 27:669–84.
55. Bozza FA, Salluh JI, Japiassu AM, Soares M, Assis EF, Gomes RN, et al. Cytokine profiles as markers of disease severity in sepsis: a multiplex analysis. *Crit Care*. (2007) 11:R49. doi: 10.1186/cc5783
56. Liu X, Pichulik T, Wolz O-O, Dang T-M, Stutz A, Dillen C, et al. Human NACHT, LRR, and PYD domain–containing protein 3 (NLRP3) inflammasome activity is regulated by and potentially targetable through Bruton tyrosine kinase. *J Allergy Clin Immunol*. (2017) 140:1054–67. doi: 10.1016/j.jaci.2017.01.017
57. Kumar V. Inflammasomes: Pandora's box for sepsis. *J Inflamm Res*. (2018) 11:477–502. doi: 10.2147/JIR.S178084
58. Fu Q, Wu J, Zhou X-Y, Ji M-H, Mao Q-H, Li Q, et al. NLRP3/caspase-1 pathway-induced pyroptosis mediated cognitive deficits in a mouse model of sepsis-associated encephalopathy. *Inflammation*. (2019) 42:306–18. doi: 10.1007/s10753-018-0894-4
59. Lee S, Nakahira K, Dalli J, Siempos II, Norris PC, Colas RA, et al. NLRP3 inflammasome deficiency protects against microbial sepsis via increased lipoxin B_4 synthesis. *Am J Respir Crit Care Med*. (2017) 196:713–26. doi: 10.1164/rccm.201604-0892OC
60. Van Wyngene L, Vandewalle J, Libert C. Reprogramming of basic metabolic pathways in microbial sepsis: therapeutic targets at last? *EMBO Mol Med*. (2018) 10:e8712. doi: 10.15252/emmm.201708712
61. Yamaguchi J, Kinoshita K, Ihara S, Furukawa M, Sakurai A. The clinical significance of low serum arachidonic acid in sepsis patients with hypoalbuminemia. *Intern Med*. (2018) 57:1833–40. doi: 10.2169/internalmedicine.9124-17
62. Yost CC, Weyrich AS, Zimmerman GA. The platelet activating factor (PAF) signaling cascade in systemic inflammatory responses. *Biochimie*. (2010) 92:692–7. doi: 10.1016/j.biochi.2010.02.011
63. Baker RR. Lipid acetylation reactions and the metabolism of platelet-activating factor. *Neurochem Res*. (2000) 25:667–683. doi: 10.1023/A:1007567205078
64. Tutunchi H, Saghafi-Asl M, Ostadrahimi A. A systematic review of the effects of oleoylethanolamide, a high-affinity endogenous ligand of PPAR-α, on the management and prevention of obesity. *Clin Exp Pharmacol Physiol*. (2020) 47:543–52. doi: 10.1111/1440-1681.13238
65. Chang S, Kim Y-H, Kim Y-J, Kim Y-W, Moon S, Lee YY, et al. Taurodeoxycholate increases the number of myeloid-derived suppressor cells that ameliorate sepsis in mice. *Front Immunol*. (2018) 9:1984. doi: 10.3389/fimmu.2018.01984
66. Li F, Zhang B, Duan S, Qing W, Tan L, Chen S, et al. Small dose of L-dopa/Benserazide hydrochloride improved sepsis-induced neuroinflammation and long-term cognitive dysfunction in sepsis mice. *Brain Res*. (2020) 1737:146780. doi: 10.1016/j.brainres.2020.146780
67. Stone MD, Nelsestuen GL. Efficacy of soluble phospholipids in the prothrombinase reaction. *Biochemistry*. (2005). 44:4037–41. doi: 10.1021/bi047655n
68. Zhang Y, Meng H, Ma R, He Z, Wu X, Cao M, et al. Circulating microparticles, blood cells, and endothelium induce procoagulant activity in sepsis through phosphatidylserine exposure. *Shock*. (2016) 45:299–307. doi: 10.1097/SHK.0000000000000509
69. Audrito V, Messana VG, Deaglio S. NAMPT and NAPRT: two metabolic enzymes with key roles in inflammation. *Front Oncol*. (2020) 10:358. doi: 10.3389/fonc.2020.00358
70. Tsalik EL, Willig LK, Rice BJ, van Velkinburgh JC, Mohney RP, McDunn JE, et al. Renal systems biology of patients with systemic inflammatory response syndrome. *Kidney Int*. (2015) 88:804–14. doi: 10.1038/ki.2015.150
71. Callahan LA, Supinski GS. Sepsis-induced myopathy. *Crit Care Med*. (2009) 37:S354. doi: 10.1097/CCM.0b013e3181b6e439
72. Baranwal AK, Deepthi G, Rohit MK, Jayashree M, Angurana SK, Kumar-M P. Longitudinal study of CPK-MB and echocardiographic measures of myocardial dysfunction in pediatric sepsis: are patients with shock different from those without? *Indian J Crit Care Med*. (2020) 24:109–15. doi: 10.5005/jp-journals-10071-23340
73. Miller SG, Hafen PS, Brault JJ. Increased adenine nucleotide degradation in skeletal muscle atrophy. *Int J Mol Sci*. (2019) 21:88. doi: 10.3390/ijms21010088
74. Vanmassenhove J, Lameire N, Dhondt A, Vanholder R, Van Biesen W. Prognostic robustness of serum creatinine based AKI definitions in patients with sepsis: a prospective cohort study. *BMC Nephrol*. (2015) 16:112. doi: 10.1186/s12882-015-0107-4
75. Lögters TT, Laryea MD, Altrichter J, Sokolowski J, Cinatl J, Reipen J, et al. Increased plasma kynurenine values and kynurenine-tryptophan ratios after major trauma are early indicators for the development of sepsis. *Shock*. (2009) 32:29–34. doi: 10.1097/SHK.0b013e31819714fa
76. Murtagh F, Legendre P. Ward's hierarchical agglomerative clustering method: which algorithms implement ward's criterion? *J Classif*. (2014) 31:274–95. doi: 10.1007/s00357-014-9161-z

Conflict of Interest: The authors declare that the research was conducted in the absence of any commercial or financial relationships that could be construed as a potential conflict of interest.

Article III

OPEN

Inhibition of Bruton's Tyrosine Kinase Activity Attenuates Hemorrhagic Shock-Induced Multiple Organ Dysfunction in Rats

Nikita M. Patel, MSci,✉ Filipe R. M. B. Oliveira, MSc,† Hanna Pillmann Ramos,†*
Eleonora Aimaretti, MSc,‡ Gustavo Ferreira Alves, MSc,§
Sina M. Coldewey, MD, PhD,¶‖ Massimo Collino, PhD,§ Regina Sordi, PhD,†
*and Christoph Thiemermann, MD, PhD**

Objective: The aim of this study was to investigate (a) the potential of the Bruton's tyrosine kinase (BTK) inhibitors acalabrutinib and fenebrutinib to reduce multiple organ dysfunction syndrome (MODS) in acute (short-term and long-term follow-up) hemorrhagic shock (HS) rat models and (b) whether treatment with either acalabrutinib or fenebrutinib attenuates BTK, NF-κB and NLRP3 activation in HS.

Background: The MODS caused by an excessive systemic inflammatory response following trauma is associated with a high morbidity and mortality. The protein BTK is known to play a role in the activation of the NLRP3 inflammasome, which is a key component of the innate inflammatory response. However, its role in trauma-hemorrhage is unknown.

Methods: Acute HS rat models were performed to determine the influence of acalabrutinib or fenebrutinib on MODS. The activation of BTK, NF-κB and NLRP3 pathways were analyzed by western blot in the kidney.

Results: We demonstrated that (a) HS caused organ injury and/or dysfunction and hypotension (post-resuscitation) in rats, while (b) treatment of HS-rats with either acalabrutinib or fenebrutinib attenuated the organ injury and dysfunction in acute HS models and (c) reduced the activation of BTK, NF- kB and NLRP3 pathways in the kidney.

Conclusion: Our results point to a role of BTK in the pathophysiology of organ injury and dysfunction caused by trauma/hemorrhage and indicate that BTK inhibitors may be repurposed as a potential therapeutic approach for MODS after trauma and/or hemorrhage.

Keywords: acalabrutinib, Bruton's tyrosine kinase, fenebrutinib hemorrhagic shock, ischemia-reperfusion, multiple organ dysfunction syndrome, trauma

(*Ann Surg* 2023;277:e624–e633)

Trauma is one of the leading causes of death and disability in those aged under 44 and exceeds the number of deaths caused by HIV, tuberculosis and malaria combined.[1] Globally there are approximately 6 million trauma-related deaths each year. Trauma-associated hemorrhage accounts for almost 40% of all trauma mortalities[2] and is a key driver of multiple organ dysfunction (MODS).[3] The mechanisms contributing to MODS include a) an excessive systemic inflammatory response secondary to the release of damage-associated molecular patterns from extensive tissue damage and b) ische-mia-reperfusion (I/R) injury.[4] There are no specific pharmacological interventions that prevent the onset of MODS associated with HS.

Bruton's tyrosine kinase (BTK) is a cytoplasmic, non-receptor protein tyrosine kinase first discovered in X-linked agammaglobu-linemia.[5] All cells of hematopoietic origin except plasma cells, natural killer cells and T-lymphocytes express BTK.[6] Whilst BTK was initially known for its critical role in B-lymphocyte development and, thus, adaptive immunity, more recent studies point to a pivotal role for BTK in innate immunity.[7]

Trauma leads to a so-called 'genomic storm' that results in a change in >80% of cellular functions and pathways[8] including an increased expression of B-lymphocyte receptor signaling. Inhibition of BTK activity reduces multiple organ injury/dysfunction, activation of NF-κB and NLRP3 inflammasome as well as the release of cytokines and chemokines caused by cecum-ligation and puncture (CLP).[9] Mice with inactive BTK (X-Linked immunodeficient) are protected from sepsis-induced MODS.[10] Prevention of NF-κB activation reduces the MODS and improves survival rate in rodent models of septic shock[11,12] and HS.[13]

Driven by the COVID-19 pandemic, there has been a significant focus on repurposing strategies that dampen the cytokine storm and pulmonary injury linked to severe acute respiratory syndrome corona-virus 2 (SARS–CoV–2). Interestingly, there is a positive correlation between disease severity and BTK activity following SARS–CoV–2 infection.[14–16] Thus, BTK inhibitors (BTKi) appear to reduce systemic inflammation and ongoing clinical trials will assess the potential impact of this repurposing strategy on outcome in COVID–19 patients (ClinicalTrials.gov Identifier: NCT04382586, NCT04665115, NCT04439006, NCT04375397, NCT04528667 and NCT04440007).

From the *William Harvey Research Institute, Barts and The London School of Medicine and Dentistry, Queen Mary University of London, London, United Kingdom; †Department of Pharmacology, Universidade Federal de Santa catarina, Sc, Brazil; ‡Department of clinical and Biological Sciences, University of Turin, Turin, Italy; §Department of Neurosciences "Rita Levi Montalcini", University of Turin, Turin, Italy; ¶Department of Anesthesiology and Intensive Care Medicine, Jena University Hospital, Jena, Germany; and ‖Septomics Research Center, Jena University Hospital, Jena, Germany.

✉n.m.patel@qmul.ac.uk.

Sources of support: NMP was funded by the William Harvey Research Foundation, FRMBO and HPR were funded by National Council for Scientific and Technological Development (CNPq) fellowship. National Council for Scientific and Technological Development to RS (CNPq, Brazil, Grant 409018/ 2018–0).

Author Contributions: Conception and design: NMP, RS, and CT;
Acquisition of data: NMP, FRMBO, HPR and RS;
Analysis and interpretation of data: NMP, FRMBO, HPR, EA, GFA, SMC, MC, RS, CT
Drafting the manuscript for important intellectual content: NMP and CT All authors reviewed and approved the manuscript. The authors report no conflicts of interest.

Supplemental digital content is available for this article. Direct URL citations appear in the printed text and are provided in the HTML and PDF versions of this article on the journal's website, www.annalsofsurgery.com.

ISSN: 0003-4932/23/27703-e624
DOI: 10.1097/SLA.0000000000005357

BTKi are commonly used in patients with B-lymphocyte malignancies (chronic lymphocytic leukemia, mantle cell lymphoma) and have received approval by the FDA for patients with marginal zone lymphoma, small lymphocytic lymphoma, Waldenstrom's macroglobulinemia and chronic graft versus host disease.[17] Given the evident protective effects of BTKi administration in sepsis and COVID-19, we wished to explore the potential of repurposing BTKi in trauma-hemorrhage. Currently, there is limited information about the role of BTK in trauma.[18]

METHODS

BTK Gene Expression in Human Whole Blood

Original data was obtained under Gene Expression Omnibus (GEO) accession GSE36809, published by Xiao and colleagues.[8] RNA was extracted from whole blood leukocytes of severe blunt trauma patients (n = 167) over the course of 28 days and healthy controls (n = 37) and hybridized onto an HU133 Plus 2.0 GeneChip (Affymetrix) according to the manufacturer's recommendations. The dataset was reanalyzed for BTK gene expression.

Use of Experimental Animals - Ethical Statement

For the short-term follow-up acute HS model, all animal procedures were approved by the Animal Welfare Ethics Review Board of Queen Mary University of London and by the Home Office (License number PC5F29685). For the long-term follow-up acute HS model, all animal procedures were approved by the Universidade Federal de Santa Catarina Institutional Committee for Animal Use in Research (License number 7396250219) in accordance with the Brazilian Government Guidelines for Animal Use in Research.

Experimental Design

Male Wistar rats (for short-term follow-up acute model: Charles River Laboratories Ltd., UK; for long-term follow-up acute model: Universidade Federal de Santa Catarina, Brazil) weighing 250–350 g were kept under standard laboratory conditions and received a chow diet and water *ad libitum.* Acalabrutinib (3 mg/ kg; Insight Biotechnology, UK) and fenebrutinib (3 mg/kg; Insight Biotechnology, UK) were separately diluted in 5% DMSO + 95% Ringer's Lactate (vehicle) and rats were treated (i.v. in short-term follow-up and i.p. in long-term follow-up) upon resuscitation. Further information about acalabrutinib and fenebrutinib can be found in the supplemental, http://links.lww.com/SLA/D600.

Acute Hemorrhagic Shock Model (Short-Term Follow-up)

The short-term follow-up acute HS model was performed as previously described in this journal.[19–21] Briefly, fifty-four rats were anesthetized with sodium thiopentone (120 mg/kg i.p. initially and 10 mg/kg i.v. for maintenance as needed) and randomized into six groups: Sham + vehicle (n = 9); Sham + acalabrutinib (3 mg/kg; n = 8), Sham + fenebrutinib (3 mg/kg; n = 8), HS + vehicle (n = 9); HS + acalabrutinib (3 mg/kg; n = 10); HS + fenebrutinib (3 mg/kg; n = 10). Blood was withdrawn to achieve a fall in mean arterial pressure (MAP) to 35 ± 5 mmHg, which was maintained for 90 minutes. At 90 minutes after initiation of hemorrhage (or when 25% of the shed blood had to be reinjected to sustain MAP), resuscitation was performed. At 4 hours post-resuscitation, blood was collected for the measurement of biomarkers of organ injury/dysfunction (MRC Harwell Institute, Oxfordshire, UK). Sham-operated rats were used as control and underwent identical surgical procedures, but without hemorrhage or resuscitation. Detailed description of the short-term follow-up model can be found in the supplemental (Supplemental Digital Content Figure 1A, http://links.lww.com/SLA/D600).

Acute Hemorrhagic Shock Model (Long-Term Follow-Up)

Thirty-eight rats were administered analgesia with tramadol (10 mg/kg i.p.) 15 minutes prior to anesthesia induction with ketamine and xylazine (100 mg/kg and 10 mg/kg i.m. respectively) and randomized into four groups: Sham + vehicle (n = 9); Sham + acalabrutinib (3 mg/kg; n = 10); HS + vehicle (n = 10); HS + acalabrutinib (3 mg/kg; n = 9). Blood was withdrawn to achieve a fall in MAP to 40 ± 2 mm Hg, which was maintained for 90 minutes. At 90 minutes after initiation of hemorrhage (or when 25% of the shed blood had to be reinjected to sustain MAP), resuscitation was performed. At 24 hours post-resuscitation, blood was collected for the measurement of organ injury/dysfunction parameters. Sham-operated rats were used as control and underwent identical surgical procedures, but without hemorrhage or resuscitation. Detailed description of the long-term follow-up model can be found in the supplemental (Supplemental Digital Content Figure 1B, http://links.lww.com/SLA/D600).

Western Blot Analysis

Semi-quantitative immunoblot analysis was carried out in kidney samples as previously described.[22] Detailed description of the method can be found in the Supplemental Digital Content, http://links.lww.com/SLA/D600.

Quantification of Myeloperoxidase Activity

Determination of myeloperoxidase activity in lung and liver tissue samples was performed. Detailed description of the method can be found in the Supplemental Digital Content, http://link-s.lww.com/SLA/D600.

Statistical Analysis

All figures are expressed as mean ± SEM of *n* observations, where *n* represents the number of animals/experiments/subjects studied. Measurements obtained from the patient groups and vehicle and BTKi treated animal groups were analyzed by one-way ANOVA followed by a Bonferroni's post-hoc test on GraphPad Prism 8.0 (GraphPad Software, Inc., La Jolla, CA). The distribution of the data was verified by Shapiro-Wilk normality test, and the homogeneity of variances by Bartlett test. When necessary, values were transformed into logarithmic values to achieve normality and homogeneity of variances. $P < 0.05$ was considered statistically significant.

RESULTS

BTK Gene Expression is Elevated in Trauma Patients

Xiao and colleagues[8] compared genome-wide expression in leukocytes from trauma patients against matched healthy controls. We reanalyzed this dataset for BTK expression. When compared to healthy controls, BTK expression was significantly elevated at all time points except 12 hours ($P < 0.05$; Supplemental Digital Content Figure 2, http://links.lww.com/SLA/D600). An initial peak was observed at Day 1 followed by a

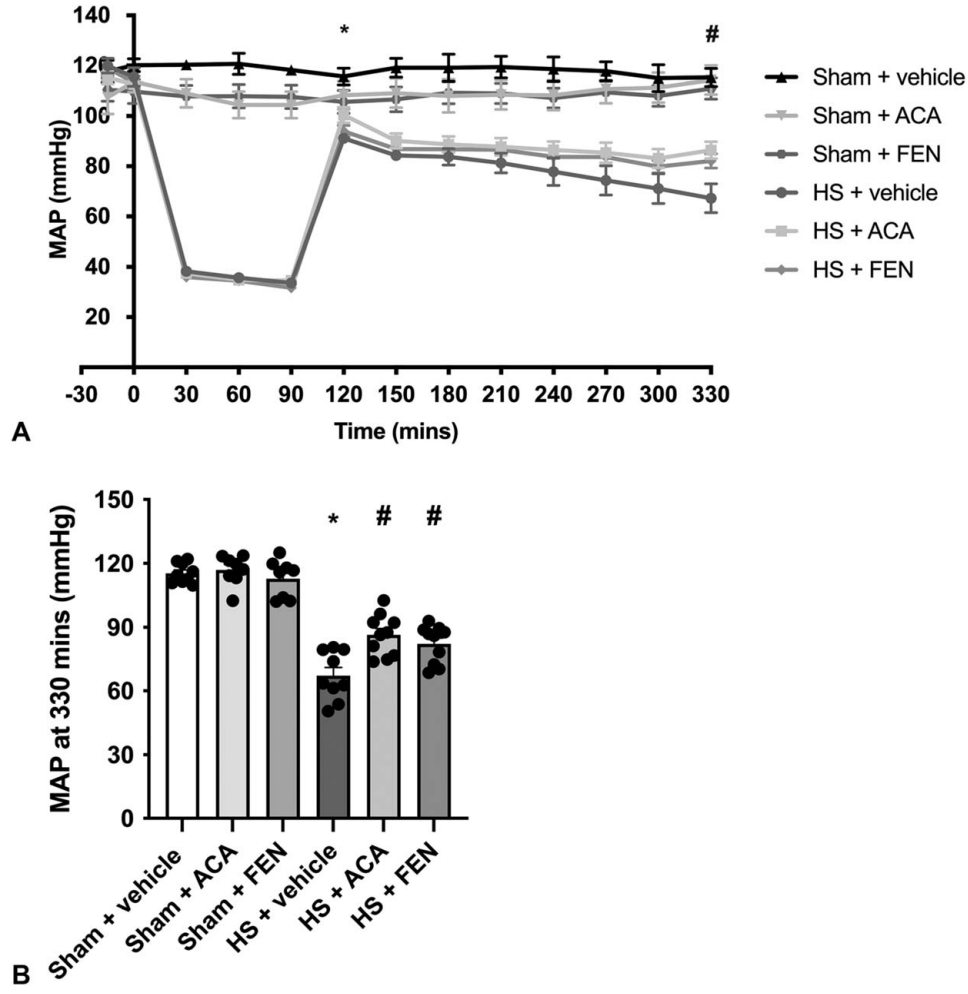

FIGURE 1. Treatment with BTKi improves HS-induced circulatory failure in a short-term follow-up acute HS model. (A) Mean arterial pressure (MAP) was measured from the completion of surgery to the termination of the experiment for vehicle and BTKi treated (acalabrutinib, ACA;fenebrutinib, FEN) rats. (B) MAP values at the end of the resuscitation period (330 min). Data are expressed as mean ± SEM of 8–10 animals per group. Statistical analysis was performed using two-way ANOVA followed by a Bonferroni's post-hoc test. $^{*}P < 0.05$ Sham + vehicle vs. HS + vehicle; $\#P < 0.05$ HS + vehicle vs. HS + BTKi (ACA or FEN).

gradual decrease, however, BTK expression remained elevated at Day 28.

BTK Gene Expression does not Differ Between Uncomplicated and Complicated Recovery Patient Groups

Xiao and colleagues[8] also stratified their trauma patient cohort into uncomplicated (recovery in < 5 days) and complicated (recovery after 14 days, no recovery by Day 28 or death) to further identify genotypic differences. We reanalyzed this dataset for BTK expression using this stratification. When comparing uncomplicated and complicated patients, there were no significant differences at any of the timepoints measured ($P > 0.05$; Supplemental Digital Content Figure 3, http://links.lww.com/SLA/D600).

Treatment with BTKi Improves HS-Induced Circulatory Failure in a Short-Term Follow-Up Acute HS Model

To investigate the effects of the BTK inhibitors (BTKi) acalabrutinib and fenebrutinib on circulatory failure, MAP was measured from the completion of surgery to the termination of the experiment. Baseline MAP values were similar amongst all six groups. When compared to sham-operated rats, HS-rats treated with vehicle exhibited a more pronounced decrease in MAP over time post-resuscitation (Fig. 1A). The MAP of HS-rats treated with either BTKi was significantly higher than that of vehicle treated HS-rats at the end of the resuscitation period ($P < 0.05$; Fig. 1B). No significant differences were observed between HS-rats treated with either BTKi ($P > 0.05$; Fig. 1A). Administration of either BTKi to sham-operated rats had no significant effect on MAP ($P > 0.05$; Fig. 1A). Whilst there were no statistically significant differences in MAP between vehicle treated and BTKi treated sham-operated rats, the BTKi treated sham rats presented with a slightly lower average pressure throughout the experiment. We do not believe this is due to BTKi administration (further information in the Supplement Digital Content, http://links.lww.com/SLA/D600).

Treatment with BTKi Attenuates HS-Induced Organ Damage in a Short-Term Follow-Up Acute HS Model

Here we explored whether pharmacological intervention with BTKi attenuates the MODS associated with HS in rats. When compared to sham-operated rats, rats subjected to HS and treated with vehicle displayed increases in serum urea ($P < 0.05$; Fig. 2A) and creatinine ($P < 0.05$; Fig. 2B); indicating the development of renal dysfunction. When compared to sham-

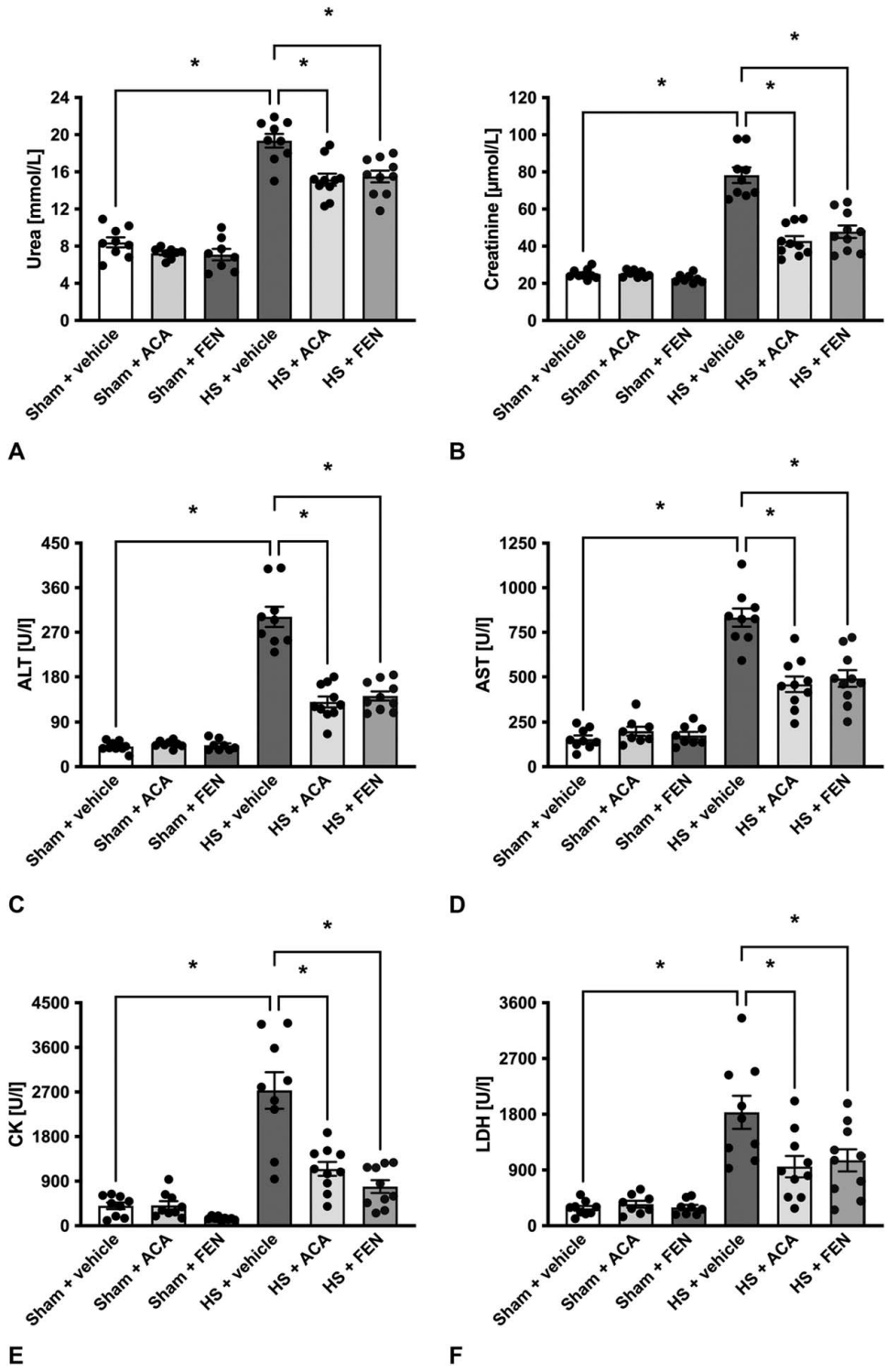

FIGURE 2. Treatment with BTKi attenuates HS-induced organ damage in a short-term follow-up acute HS model. Rats were subjected to hemorrhagic shock (HS) and 4 h after resuscitation, levels of serum (A) urea, (B) creatinine, (C) alanine aminotransferase (ALT), (D) aspartate aminotransferase (AST), (E) creatine kinase (CK) and (F) lactate dehydrogenase (LDH) were determined in vehicle and BTKi treated (acalabrutinib, ACA;fenebrutinib, FEN) rats. Sham-operated rats were used as control. Data are expressed as mean ± SEM of 8–10 animals per group. Statistical analysis was performed using one-way ANOVA followed by a Bonferroni's post-hoc test. $^{*}P < 0.05$ denoted statistical significance.

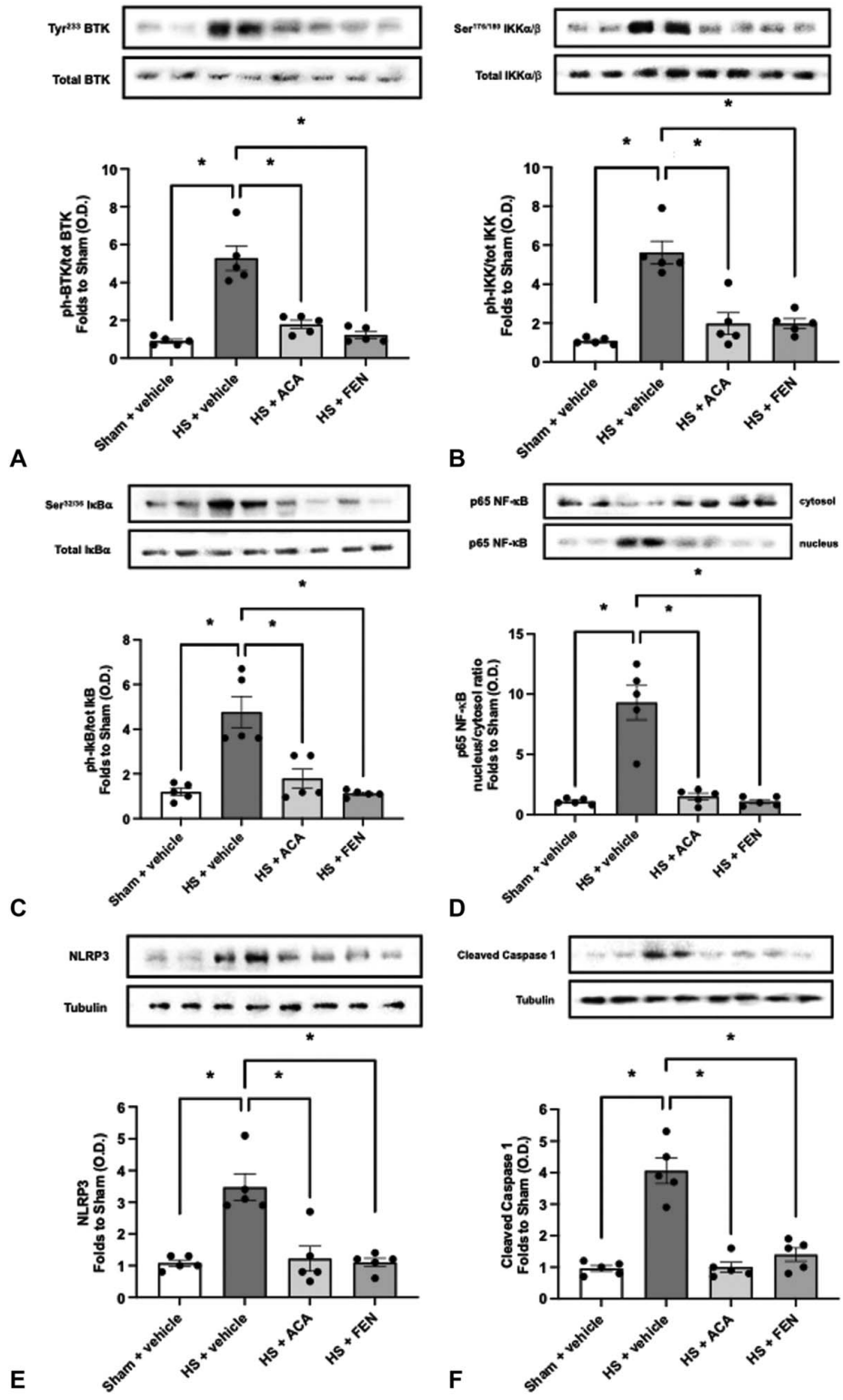

FIGURE 3. Treatment with BTKi attenuates BTK, NF-κB and NLRP3 activation in a short-term follow-up acute HS model. (A) The phosphorylation of BTK at Tyr^{223}, (B) the phosphorylation of IKKa/β at $Ser^{176/180}$, (C) the phosphorylation of IkBα at $Ser^{32/36}$, (D) the nuclear translocation of p65, (E) the activation of NLRP3 and (F) the cleaved (activated) form of caspase 1 of vehicle and BTKi treated (acalabru-tinib, ACA; fenebrutinib, FEN) rats were determined by western blotting in the kidney. Protein expression was measured as relative optical density (O.D.) and normalized to the sham band. Data are expressed as mean ± SEM of five animals per group. Statistical analysis was performed using one-way ANOVA followed by a Bon-ferroni's post-hoc test. $^{*}P < 0.05$ denoted statistical significance.

operated rats, vehicle treated HS-rats exhibited significant increases in ALT ($P < 0.05$; Fig. 2C) and AST ($P < 0.05$; Fig. 2D) indicating the development of hepatic injury, while the increases in CK ($P < 0.05$; Fig. 2E) and amylase ($P < 0.05$; not shown) denote neuromuscular and pancreatic injury, respectively. The significant increase in LDH ($P < 0.05$; Fig. 2F) in vehicle treated HS-rats confirms tissue injury. Treatment of HS-rats with either BTKi significantly attenuated the renal dysfunction, hepatic injury, neuro-muscular injury and general tissue damage caused by HS as shown by the reduction in serum

parameter values (all $P < 0.05$; Figs. 2A–F). Treatment with either BTKi had no significant effect on pancreatic injury ($P > 0.05$; not shown). No significant differences were observed between HS-rats treated with either BTKi ($P > 0.05$; Fig. 2). Administration of either BTKi to sham-operated rats had no significant effect on any of the parameters measured ($P > 0.05$; Fig. 2).

Treatment with BTKi Abolishes Renal BTK Activation in a Short-Term Follow-Up Acute HS Model

Using western blot analysis, we examined whether HS leads to the activation of BTK in the kidney; given that treatment with either BTKi significantly attenuated HS-associated renal dysfunction. The activation of BTK and subsequent BTK-associated signaling pathways consists of the phosphorylation of BTK at Tyr^{223} as the initial stage of the BTK-signaling cascade. When compared to sham-operated rats, HS-rats treated with vehicle displayed significant increases in the phosphorylation of BTK at Tyr^{223}, indicating that BTK is activated in injured kidneys ($P < 0.05$; Fig. 3A). Treatment with BTKi in HS-rats significantly abolished these increases ($P < 0.05$; Fig. 3A). No significant differences were observed between HS-rats treated with either BTKi ($P > 0.05$; Fig. 3A). These data demonstrate that both BTKi abolish the activation of BTK caused by HS.

Treatment with BTKi Abolishes Renal NF-κB Activation in a Short-Term Follow-Up Acute HS Model

The effect of BTK inhibition on the activation of the signaling events leading to the activation of NF-κB, were investigated in the kidney. When compared to sham-operated rats, HS-rats treated with vehicle had significant increases in the phosphorylation of IKKα/β at $Ser^{176/180}$ ($P < 0.05$; Fig. 3B), phosphorylation of IκBα at $Ser^{32/36}$ ($P < 0.05$; Fig. 3C) and the translocation of p65 to the nucleus ($P < 0.05$; Fig. 3D). Treatment of HS-rats with either BTKi significantly abolished these increases ($P < 0.05$; Figs. 3B-D). No significant differences were observed between HS-rats treated with either BTKi ($P > 0.05$; Figs. 3B-D). These data illustrate that both BTKi abolish the activation of NF-κB caused by HS.

Treatment with BTKi Abolishes Renal NLRP3 and Caspase 1 Activation in a Short-Term Follow-Up Acute HS Model

Having discovered that BTKi significantly reduced the activation of NF-κB in the kidney of rats subjected to HS, we next analyzed the potential involvement of the NLRP3 inflammasome complex. When compared to sham-operated rats, HS-rats treated with vehicle exhibited a significantly increased expression of the NLRP3 inflammasome ($P < 0.05$; Fig. 3E) and of the cleaved (activated) form of caspase 1 ($P < 0.05$; Fig. 3F). Treatment of HS-rats with either BTKi significantly inhibited these increases ($P < 0.05$; Figs. 3E,F). No significant differences were observed in the degree of expression of the NLRP3 inflammasome and cleaved caspase 1 between HS-rats treated with either BTKi ($P > 0.05$; Figs. 3E,F). These data demonstrate that both BTKi abolish the activation of the NLRP3 inflammasome and caspase 1 and the subsequent formation of IL–1 β.

BTK Activation Correlates with Renal Dysfunction, NF-κB and NLRP3 Activation in a Short-Term Follow-Up Acute HS Model

Correlation analysis was performed to determine whether the degree of activation of BTK correlates with changes in renal function, NF-κB and NLRP3 activation. Significant positive correlations were found between BTK activation and all parameters investigated (except urine creatinine; Supplemental Digital Content Figure 4, http://links.lww.com/SLA/D600).

Treatment with Acalabrutinib Improves HS-Induced Circulatory Failure in a Long-Term Follow-up Acute HS Model

When comparing acalabrutinib and fenebrutinib, both inhibitors were equally efficacious in the short-term follow-up model but acalabrutinib has the advantage of being FDA approved; hence was investigated in a long-term follow-up acute HS model. Having demonstrated treatment with acalabrutinib improved blood pressure in a short-term follow-up model, we wished to determine whether acalabrutinib would still be effective in a model in which the resuscitation period is prolonged to 24hours. When compared to sham-operated rats, HS-rats treated with vehicle had significantly lower MAP values recorded 24hours post-resuscitation ($P < 0.05$; Fig. 4A); highlighting that either cardiac dysfunction or excessive hypotension[23] was still present. In contrast, MAP values of HS-rats treated with acalabrutinib upon resuscitation were significantly higher even at 24 hours post-resuscitation [when compared with those of vehicle treated rats ($P < 0.05$; Fig. 4A]. Administration of acalabrutinib to sham-operated rats had no significant effect on MAP ($P > 0.05$; Fig. 4A). There were no significant differences in HR between any of the groups ($P > 0.05$; Fig. 4B).

Treatment with Acalabrutinib Attenuates HS-Induced Organ Damage in a Long-term Follow-up Acute HS Model

Having shown that treatment with acalabrutinib ameliorated the MODS associated with HS in a short-term follow-up model, we examined whether this effect was sustained when the resuscitation period was extended to 24hours. As with the short-term follow-up model, when compared to sham-operated rats, rats subjected to HS with long-term follow-up and treated with vehicle displayed significant increases in serum urea ($P < 0.05$; Fig. 5A) and creatinine ($P < 0.05$; Fig. 5B); indicating the development of renal dysfunction. When compared to sham-operated rats, vehicle treated HS-rats exhibited significant increases in ALT ($P < 0.05$; Fig. 5C) and AST ($P < 0.05$; Fig. 5D) indicating the development of hepatic injury, whilst the significant increase in LDH ($P < 0.05$; Fig. 5E) confirmed tissue injury. Treatment of HS-rats with acalabrutinib significantly attenuated the hepatic and general tissue injury caused by HS as shown by the decrease in serum parameter values ($P < 0.05$; Figs. 5C–E). Treatment with acalabrutinib had no significant effect on renal dysfunction ($P > 0.05$; Figs. 5A,B). Administration of acalabrutinib to sham-operated rats had no significant effect on any of the parameters measured ($P > 0.05$; Figs. 5A–E).

Treatment with Acalabrutinib Reduces Myeloperoxidase Activity in a Long-Term Follow-Up Acute HS Model

We next determined myeloperoxidase (MPO) activity in the lung and liver as an indicator of neutrophil infiltration. When

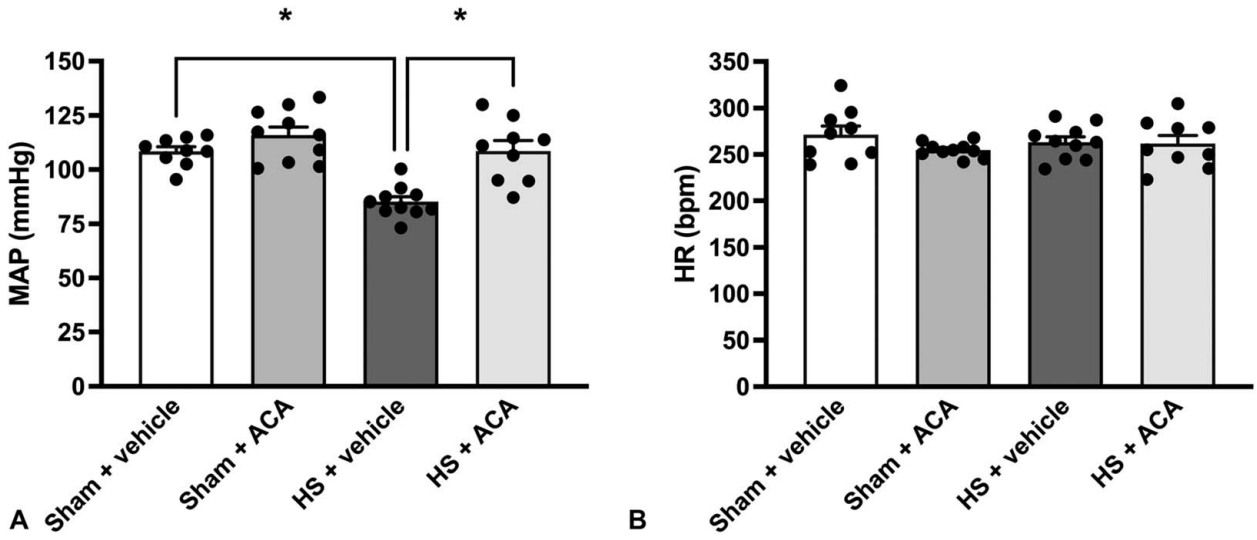

FIGURE 4. Treatment with acalabrutinib improves HS-induced circulatory failure in a long-term follow-up acute HS model. (A) Mean arterial pressure (MAP) and (B) heart rate (HR) were measured 24 h post resuscitation for vehicle and acalabrutinib (ACA) treated rats. Sham-operated rats were used as control. Data are expressed as mean ± SEM of 9–10 animals per group. Statistical analysis was performed using one-way ANOVA followed by a Bonferroni's post-hoc test. $^{*}P < 0.05$ denoted statistical significance.

compared to sham-operated rats, HS-rats treated with vehicle showed a significant increase in MPO activity in the lung ($P < 0.05$; Fig. 5F) and liver ($P < 0.05$; Fig. 5G). Treatment with acalabrutinib in HS-rats significantly attenuated these rises in MPO activity ($P < 0.05$; Figs. 5F,G), suggesting reduced neutrophil recruitment and inflammation. Administration of acalabrutinib to sham-operated rats had no significant effect on pulmonary and hepatic MPO activity ($P > 0.05$; Figs. 5F,G).

DISCUSSION

This study reports that inhibition of BTK activity attenuates organ injury/dysfunction and circulatory failure in acute short-term follow-up (Figs. 1 and 2) and long-term follow-up (Figs. 4 and 5) rat models of HS. Having shown that BTK gene expression is significantly elevated in leukocytes of trauma patients (Supplemental Digital Content Figure 2, http://links.lww.com/SLA/D600), we used a reverse translational approach to investigate whether pharmacological intervention with acalabrutinib or fenebrutinib ameliorates the MODS associated with HS in a well-established rat model. Either irreversible (acalabrutinib) or reversible (fenebrutinib) inhibition of BTK activity significantly attenuated the fall in blood pressure (Fig. 1 short-term follow-up and 4 long-term follow-up) and, hence, the delayed vascular decompensation caused by HS.[23] Moreover, BTKi significantly attenuated the renal dysfunction, hepatic injury and neuromuscular injury caused by HS (Fig. 2 short-term follow-up and 5 long-term follow-up). Similarly, BTKi also reduce disease severity in animal models of lupus nephritis,[24,25] hepatic ischemia-reperfusion,[26] acute lung injury[27–29] and sepsis.[9]

What, then, are the mechanisms by which BTKi attenuate HS-associated organ injury/dysfunction? HS resulted in a significant increase in BTK activity in the kidney (Fig. 3), which correlated with the rise in serum creatinine and urea (Supplemental Digital Content Figure 4, http://links.lww.com/SLA/D600). Indeed, inhibition of BTK activity with acalabrutinib or fenebrutinib in the kidney of HS-rats attenuated the renal dysfunction, suggesting that activation of BTK plays a pivotal role in the pathophysiology. A positive correlation between BTK expression and creatinine also occurs in patients with IgA nephropathy[30] and diabetic nephropathy.[31]

There is good evidence that BTK activation precedes the activation of NF-κB through TLR signaling[32] and trauma results in elevated NF-κB translocation to the nucleus.[19–22] Inhibition of BTK activity with acalabrutinib or fenebrutinib reduced NF-κB activation in the kidney of HS-rats (Fig. 3). We also found a significant positive correlation between the activation of BTK and the phosphorylation of IKKa/β at $Ser^{176/180}$, phosphorylation of IkBα at $Ser^{32/36}$ and translocation of p65 (Supplemental Digital Content Figure 4, http://links.lww.com/SLA/D600). This may suggest that inhibiting the activation of NF-κB contributes to the observed beneficial effects of BTKi in HS. Activation of NF-κB drives the formation of several pro- and anti-inflammatory mediators which include cytokines, chemokines and enzymes.[33] As part of a positive feedback loop, these mediators can activate NF-κB and its upstream signaling components, further amplifying and perpetuating the inflammatory responses mediated by NF-κB which can lead to increased endothelial permeability, tissue hypoperfusion/hypoxia, tissue injury and ultimately MODS.[11]

There is also good evidence that BTK activation influences the assembly and activation of the NLRP3 inflammasome in rodents and humans.[34–36] NLRP3 inflammasome activation drives the production of IL-1 β which plays a crucial role in the systemic inflammation and/or organ dysfunction in trauma.[22] Inhibition of BTK activity with acalabrutinib or fenebrutinib reduced both the assembly and subsequent activation of the NLRP3 inflammasome in the kidney (Fig. 3). We also discovered a significant positive correlation between BTK activation and the activation of NLRP3 and caspase 1 (Supplemental Digital Content Figure 4, http://links.lww.com/SLA/D600). This may suggest that inhibiting the activation of the NLRP3 inflammasome contributes to the observed protective effects of BTKi in HS by lowering the pro-inflammatory effects of IL-1β and resulting tissue inflammation.[37]

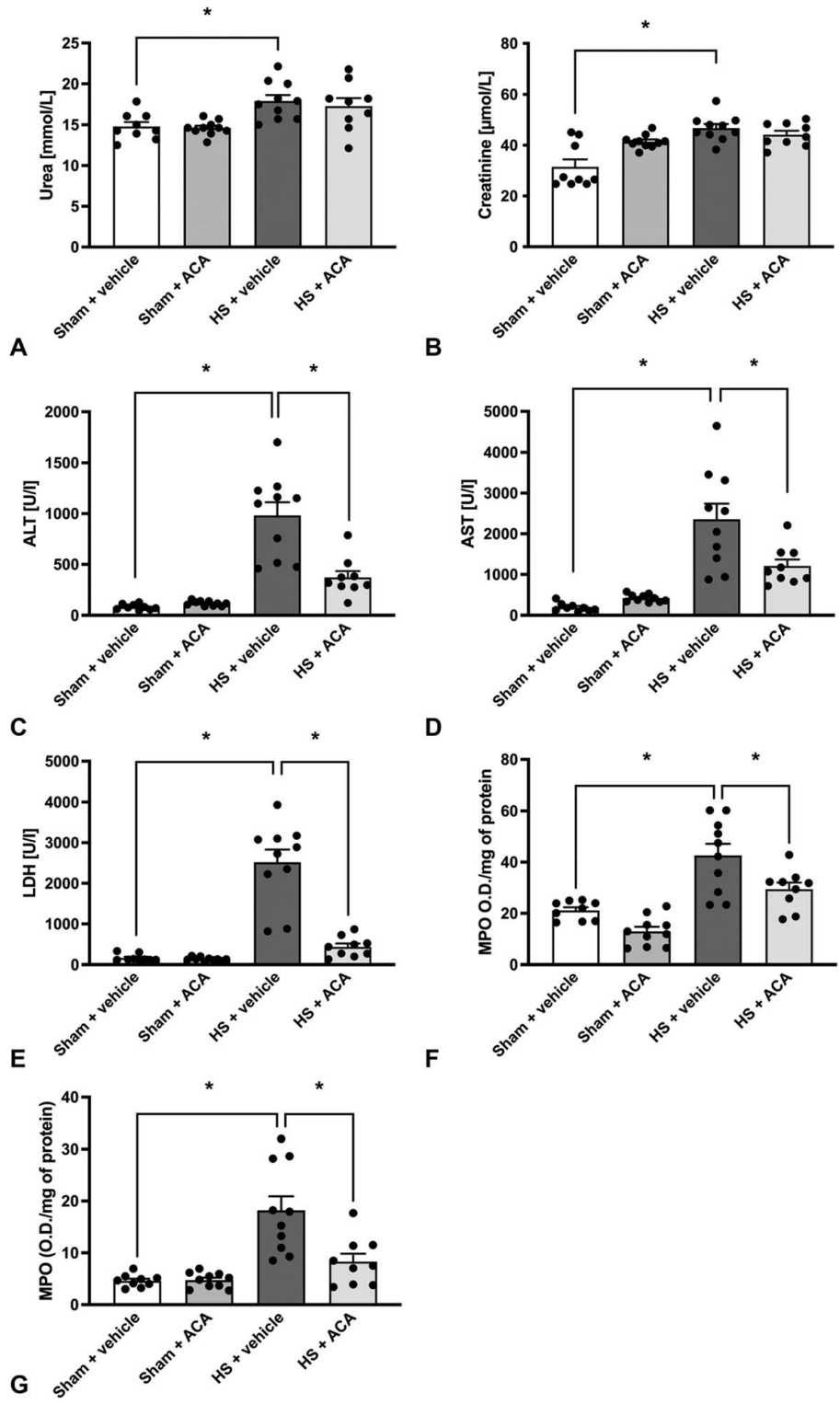

FIGURE 5. Treatment with acalabrutinib attenuates HS-induced organ damage and myeloperoxidase activity in a long-term follow-up acute HS model. Rats were subjected to hemorrhagic shock (HS) and 24 h after resuscitation, levels of serum (A) urea, (B) creatinine, (C) alanine aminotransferase (ALT), (D) aspartate aminotransferase (AST) and (E) lactate dehydrogenase (LDH) and mye-loperoxidase (MPO) activity in the (F) lung and (G) liver were determined for vehicle and acalabrutinib (ACA) treated rats. Sham-operated rats were used as control. Data are expressed as mean ± SEM of 9–10 animals per group. Statistical analysis was performed using oneway ANOVA followed by a Bonferroni's post-hoc test. $^{*}P < 0.05$ denoted statistical significance.

The sterile inflammation caused by HS drives leukocyte recruitment to the tissues and is secondary to the activation of NF-κB and NLRP3 and their transcriptional regulation of pro-inflammatory cytokines.[38–40] Moreover, the expression of adhesion molecules present on leukocytes and endothelial cells is regulated by NF-κB and permits leukocyte extravasation from the circulation to the site of injury.[41] As neutrophils play a key role in HS-associated pulmonary and hepatic inflammation, we evaluated the degree of neutrophil recruitment (measured as MPO activity) in the lung and liver.[42,43] HS resulted in a

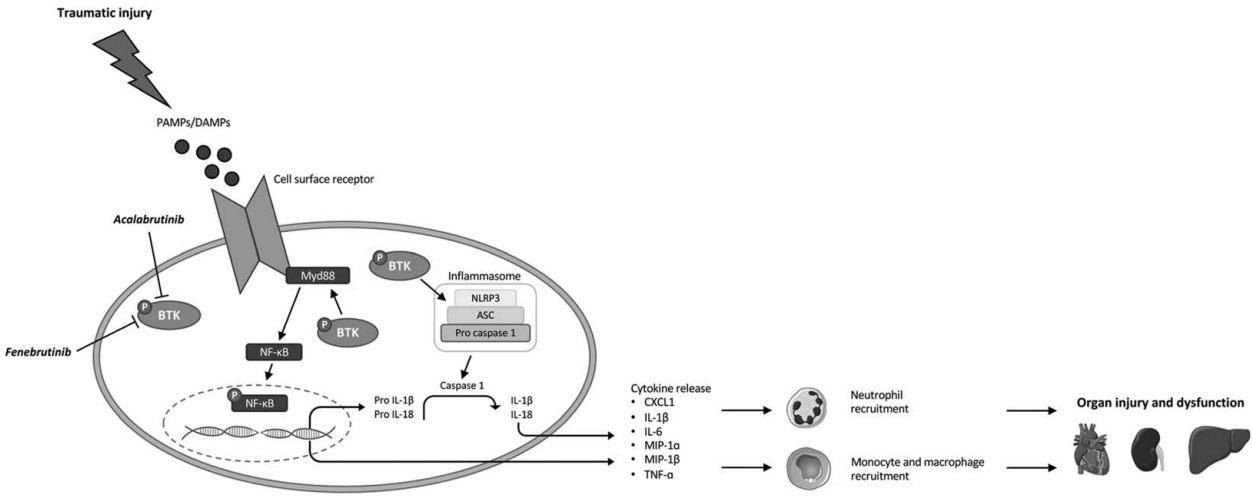

FIGURE 6. Graphical abstract highlighting the role of Bruton's tyrosine kinase (BTK) in the pathophysiology of traumatic injury. Pathogen-associated molecular patterns (PAMPs) and damage-associated molecular patterns (DAMPs) are released following trauma which activate signaling pathways leading to NF-kB activation and pro-inflammatory cytokine production. BTK also activates the NLRP3 inflammasome which results in the cleavage of pro IL–1 β to IL–1 β and further pro-inflammatory cytokine production. Leukocyte recruitment is stimulated by chemotactic cytokines. Excessive systemic inflammation from the combination of cytokine release and innate immune cell recruitment contributes to the onset of multiple organ dysfunction syndrome (MODS). Treatment with BTK inhibitors such as acalabrutinib and fenebrutinib can attenuate trauma-induced inflammation and thus MODS to improve clinical outcomes.

significant increase in pulmonary and hepatic MPO activity which was attenuated by BTKi in HS-rats (Fig. 5, see also Supplement for an extended discussion, http://links.lww.com/SLA/D600). A graphical abstract summarizing the protective effects of BTKi following HS-induced MODS is shown in Fig. 6. Please refer to the Supplement, http://links.lww.com/SLA/ D600 for a discussion of the limitations of this study.

Our results and conclusions are supported by findings in patient cohorts with either COVID-19 or sepsis where BTK has been proposed to play a role in disease pathogenesis; both diseases featuring the hallmarks of excessive systemic inflammation similar to those seen in trauma-associated MODS.[15,44] The beneficial effects of acalabrutinib in COVID-19 patients, as measured by the determination of biomark-ers of inflammation, oxygenation and clinical status, imply that BTK activation plays a role in the pathology.[15] Whilst Parnell and colleagues did not investigate pharmacological intervention with BTKi in patients with sepsis, reanalysis of microarray data (GEO Dataset Number GDS4971) revealed an increased expression (in whole blood) of BTK in septic non-survivors compared to septic survivors; highlighting the potential for BTK to be a predictor of mortality.[10]

CONCLUSIONS

In conclusion, we report here for the first time that treatment with either the irreversible BTKi acalabrutinib or the reversible BTKi fenebrutinib reduces the organ injury/dysfunction and circulatory failure caused by severe hemorrhage in the rat; highlighting a role of BTK in disease pathogenesis. Moreover, experimental trauma-hemorrhage results in a significant upregulation of BTK in the kidney. Administration of either BTKi subsequently attenuates the degree of BTK activation as well as the activation of NF-κB and the NLRP3 inflammasome (measured in the kidney), both of which are key drivers of local and systemic inflammation. Notably, no significant differences were found between the two structurally and mechanistically different inhibitors, suggesting that the observed beneficial effects in experimental trauma-hemorrhage are most likely due to a drug class related effect. Thus, we propose that BTKi may be repurposed for the use in trauma patients to lower the organ injury and inflammation caused by severe hemorrhage and resuscitation.

REFERENCES

1. World Health Organization. *Injuries and Violence: The Facts 2014*. 2014. 120. www.who.int/healthinfo/global_burden_disease/projections/en/.
2. Curry N, Hopewell S, Dorée C, et al. The acute management of trauma hemorrhage: a systematic review of randomized controlled trials. *Crit Care*. 2011;15:1–10.
3. Dewar D, Moore FA, Moore EE, et al. Postinjury multiple organ failure. *Injury*. 2009;40:912–918.
4. Lord JM, Midwinter MJ, Chen YF, et al. The systemic immune response to trauma: an overview of pathophysiology and treatment. *Lancet*. 2014;384:1455–1465.
5. Vetrie D, Vořechovský I, Sideras P, et al. The gene involved in X-linked agammaglobulinaemia is a member of the src family of protein-tyrosine kinases. *Nature*. 1993;361:226–233.
6. Mohamed AJ, Yu L, Bäckesjö CM, et al. Bruton's tyrosine kinase (Btk): function, regulation, and transformation with special emphasis on the PH domain. *Immunol Rev*. 2009;228:58–73.
7. Weber AN, Bittner Z, Liu X, et al. Bruton's tyrosine kinase: an emerging key player in innate immunity. *Front Immunol*. 2017;8:1454.
8. Xiao W, Mindrinos MN, Seok J, et al. A genomic storm in critically injured humans. *J Exp Med*. 2011;208:2581–2590.
9. O'Riordan CE, Purvis GSD, Collotta D, et al. Bruton's tyrosine kinase inhibition attenuates the cardiac dysfunction caused by cecal ligation and puncture in mice. *Front Immunol*. 2019;10:2129.
10. O'Riordan CE, Purvis GSD, Collotta D, et al. X-linked immunodeficient mice with no functional Bruton's tyrosine kinase are protected from sepsis-induced multiple organ failure. *Front Immunol*. 2020;11:581758.
11. Liu SF, Malik AB. NF-κB activation as a pathological mechanism of septic shock and inflammation. *Am J Physiol Lung Cell Mol Physiol*. 2006; 290:L622–L645.

12. Coldewey SM, Rogazzo M, Collino M, et al. Inhibition of IkB kinase reduces the multiple organ dysfunction caused by sepsis in the mouse. *Dis Model Mech.* 2013;6:1031.
13. Sordi R, Chiazza F, Johnson FL, et al. Inhibition of IkB kinase attenuates the organ injury and dysfunction associated with hemorrhagic shock. *Mol Med.* 2015;21:563–575.
14. Nicolson PLR, Welsh JD, Chauhan A, et al. A rationale for blocking thromboin-flammation in COVID-19 with Btk inhibitors. *Platelets.* 2020;31:685–690.
15. Roschewski M, Lionakis MS, Sharman JP, et al. Inhibition of Bruton tyrosine kinase in patients with severe COVID-19. *Sci Immunol.* 2020;5: eabd0110.
16. Soresina A, Moratto D, Marco Chiarini, et al. Two X-linked agammaglobu-linemia patients develop pneumonia as COVID-19 manifestation but recover. *Pediatr Allergy Immunol.* 2020;31:565–569.
17. Burger JA. Bruton tyrosine kinase inhibitors: present and future. *Cancer J.* 2019;25:386–393.
18. Liu X, Zhang J, Han W, et al. Inhibition of BTK protects lungs from trauma-hemorrhagic shock-induced injury in rats. *Mol Med Rep.* 2017;16:192–200.
19. Sordi R, Chiazza F, Collotta D, et al. Resolvin D1 Attenuates the Organ Injury Associated With Experimental Hemorrhagic Shock. *Ann Surg.* 2021;273:1012–1021.
20. Sordi R, Nandra KK, Chiazza F, et al. Artesunate protects against the organ injury and dysfunction induced by severe hemorrhage and resuscitation. *Ann Surg.* 2017;265:408–417.
21. Yamada N, Martin LB, Zechendorf E, et al. Novel synthetic, host-defense peptide protects against organ injury/dysfunction in a rat model of severe hemorrhagic shock. *Ann Surg.* 2018;268:348–356.
22. Martin L, Patel NM, et al. The inhibition of macrophage migration inhibitory factor by ISO-1 attenuates trauma-induced multi organ dysfunction in rats. *medRxiv.* Published online April 29, 2021. DOI: 10.1101/2021.04.28.21255719.
23. Thiemermann C, Szabó C, Mitchell JA, Vane JR. Vascular hyporeactivity to vasoconstrictor agents and hemodynamic decompensation in hemorrhagic shock is mediated by nitric oxide. *Proc Natl Acad Sci USA.* 1993;90:267–271.
24. Chalmers SA, Doerner J, Bosanac T, et al. Therapeutic blockade of immune complex-mediated glomerulonephritis by highly selective inhibition of Bru-ton's tyrosine kinase. *Sci Rep.* 2016;6:26164.
25. Chalmers SA, Glynn E, Garcia SJ, et al. BTK inhibition ameliorates kidney disease in spontaneous lupus nephritis. *Clin Immunol.* 2018;197:205–218.
26. Palumbo T, Nakamura K, Lassman C, et al. Bruton tyrosine kinase inhibition attenuates liver damage in a mouse warm ischemia and reperfusion model. *Transplantation.* 2017;101:322–331.
27. Krupa A, Fol M, Rahman M, et al. Silencing bruton's tyrosine kinase in alveolar neutrophils protects mice from LPS/immune complex-induced acute lung injury. *Am J Physiol Lung Cell Mol Physiol.* 2014;307: L435–L448.
28. Zhou P, Ma B, Xu S, et al. Knockdown of Burton's tyrosine kinase confers potent protection against sepsis-induced acute lung injury. *Cell Biochem Biophys.* 2014;70:1265–1275.
29. Florence JM, Krupa A, Booshehri LM, et al. Inhibiting bruton's tyrosine kinase rescues mice from lethal influenza-induced acute lung injury. *Am J Physiol Lung Cell Mol Physiol.* 2018;315:L52–L58.
30. Wei J, Wang Y, Qi X, et al. Enhanced Bruton's tyrosine kinase activity in the kidney of patients with IgA nephropathy. *Int Urol Nephrol.* 2021;53:1399–1415.
31. Zhao J, Chen J, Li YY, et al. Bruton's tyrosine kinase regulates macrophage-induced inflammation in the diabetic kidney via NLRP3 inflammasome activation. *Int J Mol Med.* 2021;48:1–12.
32. Jefferies CA, Doyle S, Brunner C, et al. Bruton's tyrosine kinase is a Toll/ interleukin-1 receptor domain-binding protein that participates in nuclear factor κB activation by toll-like receptor 4. *J Biol Chem.* 2003;278:26258–26264.
33. Senftleben U, Karin M. The IKK/NF-Kappa B pathway. *Crit Care Med.* 2002;30:S18–S26.
34. Ito M, Shichita T, Okada M, et al. Bruton's tyrosine kinase is essential for NLRP3 inflammasome activation and contributes to ischaemic brain injury. *Nat Commun.* 2015;6:1–11.
35. Liu X, Pichulik T, Wolz OO, et al. Human NACHT, LRR, and PYD domain-containing protein 3 (NLRP3) inflammasome activity is regulated by and potentially targetable through Brutontyrosine kinase. *JAllergyClin Immunol.* 2017;140:1054–1067.
36. Bittner ZA, Liu X, Shankar S, et al. BTK operates aphospho-tyrosine switch to regulate NLRP3 inflammasome activity. *bioRxiv.* Published online June 25, 2020. DOI: 10.1101/864702.
37. Dinarello CA. Biologic basis for interleukin-1 in disease. *Blood.* 1996;87: 2095–2147.
38. Chen CC, Manning AM. Transcriptional regulation of endothelial cell adhesion molecules: a dominant role for NF-κB. *Agents Actions Suppl.* 1995;47:135–141
39. Collins T, Read MA, Neish AS, et al. Transcriptional regulation of endothelial cell adhesion molecules: NF-(B and cytokine-inducible enhancers. *FASEB J.* 1995;9:899–909.
40. Campbell SJ, Anthony DC, Oakley F, et al. Hepatic nuclear factor kB regulates neutrophil recruitment to the injured brain. *Journal of Neuropathology & Experimental Neurology.* 2008;67:223–230.
41. Hayden MS, Ghosh S. NF-κB in immunobiology. *Cell Research 2011 21:2.* 2011;21:223–244.
42. Botha AJ, Moore FA, Moore EE, et al. Postinjury neutrophil priming and activation: an early vulnerable window. *Surgery.* 1995;118:358–365.
43. Partrick D, Moore F, Moore E, et al. Neutrophil priming and activation in the pathogenesis of postinjury multiple organ failure. *New Horiz.* 1996;4:194–210.
44. Parnell GP, Tang BM, Nalos M, et al. Identifying key regulatory genes in the whole blood of septic patients to monitor underlying immune dysfunctions. *Shock.* 2013;40:166–174.

Article IV

Annals of Surgery Publish Ahead of Print
DOI:10.1097/SLA.0000000000005571

OPEN

Inhibition of the JAK/STAT pathway with baricitinib reduces the multiple organ dysfunction caused by hemorrhagic shock in rats

Nikita M Patel[1*], MSci, Debora Collotta[2], PhD, Eleonora Aimaretti[3], MSc, Gustavo Ferreira Alves[2], MSc, Sarah Kröller[4, 5], MSc, Sina M Coldewey[4, 5], MD PhD, Massimo Collino[2], PhD, Christoph Thiemermann[1], MD PhD

[1] William Harvey Research Institute, Barts and The London School of Medicine and Dentistry, Queen Mary University of London, London, United Kingdom

[2] Department of Neurosciences "Rita Levi Montalcini", University of Turin, Turin, Italy

[3] Department of Clinical and Biological Sciences, University of Turin, Turin, Italy

[4] Department of Anesthesiology and Intensive Care Medicine, Jena University Hospital, Jena, Germany

[5] Septomics Research Center, Jena University Hospital, Jena, Germany

***Addresses for correspondence and requests for reprints:**

Nikita Mayur Patel, MSci

William Harvey Research Institute,

Barts and The London School of Medicine and Dentistry,

Queen Mary University of London,

London, United Kingdom

n.m.patel@qmul.ac.uk

Phone: +44 (0) 7852106575

Running title: Baricitinib attenuates hemorrhage-induced MODS

Type of study: Original study

Sources of support: NMP was funded by the William Harvey Research Foundation.

AUTHOR CONTRIBUTIONS

Conception and design: NMP and CT;

Acquisition of data: NMP;

Analysis and interpretation of data: NMP, DC, EA, GFA, SK, SMC, MC, CT

Drafting the manuscript for important intellectual content: NMP and CT

All authors reviewed and approved the manuscript.

STRUCTURED ABSTRACT

Objective: The aim of this study was to investigate (a) the effects of the Janus kinase (JAK)/signal transducer and activator of transcription (STAT) pathway inhibitor (baricitinib) on the MODS in a rat model of hemorrhagic shock (HS) and (b) whether treatment with baricitinib attenuates the activation of JAK/STAT, NF-κB and NLRP3 caused by HS.

Background: Post-traumatic MODS, which is in part due to excessive systemic inflammation, is associated with high morbidity and mortality. The JAK/STAT pathway is a regulator of numerous growth factor and cytokine receptors and, hence, is considered a potential master regulator of many inflammatory signaling processes. However, its role in trauma-hemorrhage is unknown.

Methods: An acute HS rat model was performed to determine the effect of baricitinib on MODS. The activation of JAK/STAT, NF-κB and NLRP3 pathways were analyzed by western blotting in the kidney and liver.

Results: We demonstrate here for the first time that treatment with baricitinib (during resuscitation following severe hemorrhage) attenuates the organ injury and dysfunction and the activation of JAK/STAT, NF-κB and NLRP3 pathways caused by HS in the rat.

Conclusions: Our results point to a role of the JAK/STAT pathway in the pathophysiology of the organ injury and dysfunction caused by trauma/hemorrhage and indicate that JAK inhibitors, such as baricitinib, may be repurposed for the treatment of the MODS after trauma and/or hemorrhage.

KEYWORDS: baricitinib; hemorrhagic shock; ischemia-reperfusion; Janus kinase; multiorgan dysfunction syndrome; trauma

INTRODUCTION

Trauma is one of the major causes of mortality in those aged under 44 and the number of patients dying from trauma surpasses those from tuberculosis, malaria and HIV/AIDS combined[1]. Annually, there are approximately 6 million trauma-associated mortalities worldwide. Trauma-associated hemorrhage accounts for almost 40% of all trauma deaths[2–5] and is a significant driver of multiple organ dysfunction syndrome (MODS)[6–11]. There is good evidence that a) uncontrolled systemic inflammation secondary to the release of damage-associated molecular patterns (DAMPs) from substantial tissue damage and b) ischemia-reperfusion injury contribute to the onset of MODS[12]. However, there are no specific pharmacological interventions clinically used to prevent the onset of HS-induced MODS.

Circulating pro-inflammatory mediators bind to cell-surface receptors and subsequently signal through activation of intracellular protein tyrosine kinases, including the Janus kinase (JAK) family. The JAK family is composed of JAK1, JAK2, JAK3 and tyrosine kinase 2 (TYK2) and these isoforms interact with the signal transducer and activator of transcription (STAT) class of proteins[13]. JAK inhibitors affect the JAK-STAT protein interaction and disrupt the propagation of signals through the JAK/STAT pathway, thus modulating inflammatory signaling processes.

We have recently shown that JAK/STAT inhibition reduced both the diet-related metabolic derangements and the associated organ injury/dysfunction in a murine model of high-fat diet-induced type 2 diabetes[14]. Specifically, treatment with baricitinib, a JAK1/JAK2 inhibitor, resulted in improvements of diet-induced myosteatosis, mesangial expansion and associated

proteinuria in addition to reducing blood cytokine levels, renal dysfunction and skeletal muscle damage.

Driven by the COVID-19 pandemic, strategies focusing on drug repurposing which dampen the cytokine storm and pulmonary injury associated with severe acute respiratory syndrome coronavirus 2 (SARS-CoV-2) have been examined. Recent investigations have shown that baricitinib, which is thought to possess anti-viral properties through its affinity for adaptor-associated kinase-1 and the subsequent reduction in SARS-CoV-2 endocytosis, improves clinical status in patients with COVID-19[15–29]. Thus, baricitinib appears to lower systemic inflammation and several ongoing clinical trials are investigating the potential impact of this repurposing approach on outcome in COVID-19 patients (ClinicalTrials.gov Identifier: NCT04320277, NCT04321993, NCT04346147, NCT04381936, NCT04390464, NCT04399798, NCT04640168, NCT04693026, NCT04832880, NCT04890626, NCT04891133, NCT04970719, NCT05056558, NCT05082714, NCT05074420, NCT04393051).

Baricitinib is used in patients for the treatment of moderate-to-severe active rheumatoid arthritis and atopic eczema/dermatitis, with the latter use approved by the NICE in 2021[30]. Given the evident beneficial effects of baricitinib administration in type 2 diabetes and COVID-19, we wished to explore the potential of repurposing baricitinib in trauma-hemorrhage. Currently, there is limited information about the role of JAK/STAT pathway in trauma[31–33].

METHODS

JAK2 and STAT3 gene expression in human whole blood

Original data were obtained under Gene Expression Omnibus (GEO) accession GSE36809, published by Xiao and colleagues[34]. RNA was extracted from whole blood leukocytes of severe blunt trauma patients (n = 167) over the course of 28 days and healthy controls (n = 37) and hybridized onto an HU133 Plus 2.0 GeneChip (Affymetrix) according to the manufacturer's recommendations. The dataset was reanalyzed for JAK2 and STAT3 gene expression. A further reanalysis was performed dividing the trauma patients into uncomplicated (n = 55) and complicated (n = 41) groups.

Use of Experimental Animals - Ethics Statement

All animal procedures were approved by the Animal Welfare Ethics Review Board of Queen Mary University of London and by the Home Office (License number PC5F29685).

Experimental Design

Male Wistar rats (Charles River Laboratories Ltd., Kent, UK) weighing 260-310 g were kept under standard laboratory conditions and received a chow diet and water *ad libitum*. Baricitinib (Insight Biotechnology, UK) was diluted in 5 % DMSO + 95 % Ringer's Lactate (vehicle) and rats were treated (i.p.) upon resuscitation. A delayed application of baricitinib was performed to simulate delayed clinical interventions. Further information about baricitinib can be found in the supplemental, Supplemental Digital Content 1, http://links.lww.com/SLA/E19.

Hemorrhagic Shock Model

The acute hemorrhagic shock model was performed as previously described in this journal[35–38]. Briefly, forty rats were anesthetized with sodium thiopentone (120 mg/kg i.p. initially and 10 mg/kg i.v. for maintenance as needed) and randomized into four groups: Sham + vehicle (n = 10); Sham + baricitinib (1 mg/kg; n = 9), HS + vehicle (n = 11); HS + baricitinib (1 mg/kg; n = 10). Blood was withdrawn to achieve a fall in mean arterial pressure (MAP) to 35 ± 5 mmHg, which was maintained for 90 min. At 90 min after initiation of hemorrhage (or when 25% of the shed blood had to be reinjected to sustain MAP), resuscitation was performed and either baricitinib (1 mg/kg) or vehicle was administered. At 4 h post-resuscitation, blood was collected for the measurement of biomarkers of organ injury/dysfunction (MRC Harwell Institute, Oxfordshire, UK). Sham-operated rats were used as control and underwent identical surgical procedures, but without hemorrhage or resuscitation. Detailed description of the model can be found in the supplemental (Supplementary Figure 1, Supplemental Digital Content 1, http://links.lww.com/SLA/E19).

Western Blot Analysis

Semi-quantitative immunoblot analysis was carried out in liver and kidney tissue samples as previously described[35,39]. Detailed description of the method can be found in the supplemental, Supplemental Digital Content 1, http://links.lww.com/SLA/E19.

CD68 immunohistochemical staining

Renal sections (2 μm) were deparaffinized and hydrated as previously described[40] and stained for CD68. Detailed description of the method can be found in the supplemental, Supplemental Digital Content 1, http://links.lww.com/SLA/E19.

Periodic acid Schiff staining

Periodic acid Schiff (PAS) staining of renal sections (2 µm) was performed using a PAS staining kit (Carl Roth, Karlsruhe, Germany). Histomorphological changes were evaluated at 20x magnification using a scoring system as previously described[40]. Images were taken using a KEYENCE BZ-X800 microscope and BZ-X800 viewer after performing white balance and auto exposure.

Statistical Analysis

All data in text and figures are expressed as mean ± SEM of *n* observations, where *n* represents the number of animals/experiments/subjects studied. Measurements obtained from the patient groups and vehicle and baricitinib treated animal groups were analyzed by one-way/two-way ANOVA followed by Bonferroni's *post-hoc* test or Kruskal-Wallis test followed by Dunn's *post-hoc* test on GraphPad Prism 8.0 (GraphPad Software, Inc., La Jolla, CA, USA). The distribution of the data was verified by Shapiro-Wilk normality test, and the homogeneity of variances by Bartlett test. When necessary, values were transformed into logarithmic values to achieve normality and homogeneity of variances. $P<0.05$ was considered statistically significant.

RESULTS

JAK2 and STAT3 gene expression is elevated in trauma patients

Xiao and colleagues[34] compared genome-wide gene expression in leukocytes from trauma patients against matched healthy controls. We reanalyzed this dataset for JAK2 and STAT3 expression, as STAT3 is the most commonly stimulated downstream STAT following JAK2 activation. When compared to healthy controls, JAK2 expression was significantly elevated in patients with trauma at all time points ($p<0.05$; Figure 1A). An initial peak was noted at

Day 1 followed by a gradual decrease, however, JAK2 expression still remained elevated at Day 28 after trauma. Similarly, STAT3 expression was significantly increased at all time points ($p<0.05$; Figure 1B) and an initial peak was noted at 12 h followed by a gradual decrease. However, STAT3 expression also still remained elevated at Day 28 after trauma. When comparing trauma patients stratified into uncomplicated (recovery in <5 days) and complicated (recovery after 14 days, no recovery by Day 28 or death) groups, JAK2 expression was significantly higher on Days 4 and 7 ($p<0.05$; Figure 1C) and STAT3 expression was significantly raised at 12 h ($p<0.05$; Figure 1D) in complicated patients when compared to uncomplicated trauma patients. These data indicate that the JAK2/STAT3 pathway may play a role in the pathophysiology of trauma. Please note the y-axis intervals for Figures 1C and 1D are 0.3 and 0.4 respectively which show the intergroup differences are small (but still statistically significant).

Baricitinib attenuates HS-induced organ injury/dysfunction in HS

Here we explored whether pharmacological intervention with the JAK1/JAK2 inhibitor baricitinib administered upon resuscitation attenuates the MODS associated with HS in rats. When compared to sham-operated rats, rats subjected to HS displayed significant increases in serum urea ($p<0.05$; Figure 2A) and creatinine ($p<0.05$; Figure 2B); indicating the development of renal dysfunction. When compared to sham-operated rats, vehicle treated HS-rats exhibited significant increases in ALT ($p<0.05$; Figure 2C) and AST ($p<0.05$; Figure 2D) indicating the development of hepatic injury, while the increases in amylase ($p<0.05$; Figure 2E) and CK ($p<0.05$; Figure 2F) denote pancreatic and neuromuscular injury, respectively. The significant increase in LDH ($p<0.05$; Figure 2F) in vehicle treated HS-rats confirmed tissue injury. Treatment of HS-rats with baricitinib significantly attenuated the renal dysfunction, hepatic injury, pancreatic injury, neuromuscular injury and general tissue

damage caused by HS as shown by the reduction in serum parameter values (all $p<0.05$; Figures 2A-G). Administration of baricitinib to sham-operated rats had no significant effect on any of the parameters measured ($p>0.05$; Figure 2).

Baricitinib abolishes hepatic and renal JAK/STAT activation in HS

Using western blot analysis, we examined whether HS leads to the activation of the JAK2/STAT3 pathway in the liver and kidney, given that treatment with baricitinib significantly attenuated HS-associated hepatic injury and renal dysfunction. When compared to sham-operated rats, vehicle treated HS-rats displayed significant increases in the phosphorylation of hepatic and renal Jak2 at $Tyr^{1007\text{-}1008}$ ($p<0.05$; Figures 3A-B) and Stat3 at Tyr^{705} ($p<0.05$; Figures 3C-D), indicating that the JAK2/STAT3 pathway is activated in the injured liver and kidneys. Treatment of HS-rats with baricitinib significantly abolished these increases in JAK2/STAT3 phosphorylation ($p<0.05$; Figures 3A-D).

Baricitinib abolishes hepatic and renal NF-κB activation in HS

The effect of JAK/STAT inhibition on the activation of NF-κB were investigated in liver and kidney. When compared to sham-operated rats, vehicle treated HS-rats had significant increases in the hepatic and renal phosphorylation of IκBα at $Ser^{32/36}$ ($p<0.05$; Figures 3E-F) and the translocation of p65 to the nucleus ($p<0.05$; Figures 3G-H). Treatment of HS-rats with baricitinib significantly abolished this activation of NF-κB ($p<0.05$; Figures 3E-H).

Baricitinib abolishes hepatic and renal NLRP3 and caspase 1 activation in HS

Having discovered that baricitinib significantly reduced NF-κB activation in the liver and kidney of HS-rats, we next analyzed the potential involvement of the NLRP3 inflammasome complex. When compared to sham-operated rats, vehicle treated HS-rats exhibited

significantly increased hepatic and renal expression of the NLRP3 inflammasome ($p<0.05$; Figures 3I-J) and cleaved (activated) form of caspase 1 ($p<0.05$; Figures 3K-L). Treatment of HS-rats with baricitinib significantly inhibited these increases ($p<0.05$; Figures 3I-L).

JAK2 activation correlates with hepatic injury, renal dysfunction, STAT3, NF-κB and NLRP3 activation in an acute HS model

Correlation analysis was performed to determine whether the degree of activation of JAK correlates with changes in liver condition, renal function, STAT3, NF-κB and NLRP3 activation. Significant positive correlations were found between JAK2 activation and (with the exception of AST) all parameters investigated (Supplementary Figure 2, Supplemental Digital Content 1, http://links.lww.com/SLA/E19).

Baricitinib reduces renal macrophage invasion and tissue injury in HS

Having shown that baricitinib significantly attenuated the HS-induced renal dysfunction, we investigated renal macrophage infiltration and tissue injury determined by CD68 and PAS staining, respectively. When compared to sham-operated rats, vehicle treated HS-rats exhibited a significantly increased expression of CD68 in the kidney ($p<0.05$; Figure 4A). Treatment with baricitinib in HS-rats significantly reduced CD68 expression, indicating an attenuation of renal macrophage invasion ($p<0.05$; Figure 4A). When compared to sham-operated rats, vehicle treated HS-rats displayed a significantly raised renal PAS score ($p<0.05$; Figure 4C). Treatment with baricitinib in HS-rats reduced this rise in PAS score (albeit this change was not statistically significant), suggesting a tissue protective effect of baricitinib in the kidney (Figure 4C).

Effect of baricitinib on HS-induced circulatory failure in HS

To investigate the effects of baricitinib on circulatory failure, MAP was measured from the completion of surgery to the termination of the experiment. Baseline MAP values were similar amongst all four groups. Rats subjected to HS demonstrated a decline in MAP which was ameliorated by resuscitation, but MAP remained lower than that of sham-operated rats during resuscitation (at the equivalent time points, Figure 5). The MAP of baricitinib treated HS-rats was similar to those of vehicle treated HS-rats at the end of the resuscitation period (Figure 5). Administration of baricitinib to sham-operated rats had no significant effect on MAP ($p>0.05$; Figure 5).

DISCUSSION

This study reports that inhibition of JAK/STAT activity attenuates the organ injury/dysfunction associated with HS (acute rat model; Figure 2). Having shown that JAK2 and STAT3 gene expression is significantly elevated in leukocytes of trauma patients (Figures 1A-B) and, most notably, that the expression of JAK2 and STAT3 is higher in trauma patients with a complicated recovery (Figures 1C-D), we used a reverse translational approach to investigate whether pharmacological intervention with the JAK1/JAK2 inhibitor baricitinib ameliorates the MODS associated with HS in a well-established rat model[35–38].

Baricitinib inhibits JAK1 and JAK2 to an equal degree and is currently used in patients with inflammatory diseases, including rheumatoid arthritis and atopic dermatitis[41].We report here for the first time that baricitinib significantly attenuated the renal dysfunction, hepatic injury, pancreatic injury and neuromuscular injury caused by HS (Figure 2). Similarly, JAK inhibition lowers disease severity in animal models of ischemia-reperfusion injury[42–47], sepsis[48–51], acute kidney injury[52] and endotoxemia[53].

What, then, are the mechanisms by which baricitinib attenuates HS-associated organ injury/dysfunction? HS resulted in a significant increase in JAK2/STAT3 activity in the liver and kidneys (Figure 3) which correlated with the rises in ALT, creatinine and urea (Supplementary Figure 2, Supplemental Digital Content 1, http://links.lww.com/SLA/E19). Indeed, inhibition of JAK2/STAT3 activity with baricitinib in the liver and kidneys of HS-rats decreased the hepatic injury and renal dysfunction, suggesting that activation of the JAK2/STAT3 pathway plays a pivotal role in the pathophysiology of the MODS associated with HS. Despite not finding a significant correlation between JAK activation and AST in our study, genome-wide association study-prioritized genes and gene co-expression pattern analysis revealed JAK/STAT signaling was linked to AST-specific gene sets which supports the role of JAK/STAT in liver function[54].

A synergistic interaction between STAT and NF-κB occur on many levels: these include physical interactions of the two molecules, cooperative binding at particular gene promoter subsets to induce target gene expression and cytokine feedback loops, whereby cytokines induced by STAT and NF-κB (e.g. IL-6) can further prolong the activation of both molecules[55]. Trauma leads to increased nuclear translocation of NF-κB[35–38,56]. Inhibition of JAK2/STAT3 activity with baricitinib decreased NF-κB activation in both the liver and kidneys (Figure 3). We also found a significant positive correlation between the activation of JAK2 and the phosphorylation of IκBα at $Ser^{32/36}$ and translocation of p65 (Supplementary Figure 2, Supplemental Digital Content 1, http://links.lww.com/SLA/E19). This may suggest that blocking the activation of NF-κB contributes to the observed effects of baricitinib in HS. Activation of NF-κB drives the production of multiple pro- and anti-inflammatory mediators including enzymes, cytokines and chemokines[57]. As part of a positive feedback loop, these

mediators can activate NF-κB and its upstream signaling components, further amplifying and sustaining the inflammatory responses mediated by NF-κB which can lead to greater permeability of the endothelium, hypoperfused/hypoxic tissues, tissue injury and eventually MODS[58].

The JAK/STAT pathway has also been shown to be linked to the NLRP3 inflammasome, with pharmacological inhibition of JAK reducing the expression and activation of NLRP3 inflammasome components[59,60]. NLRP3 inflammasome activation drives the formation of IL-1β which plays a key role in the systemic inflammation and/or organ dysfunction associated with trauma[35,56]. Inhibition of JAK2/STAT3 activity with baricitinib decreased the assembly and successive activation of the NLRP3 inflammasome in the liver and kidneys (Figure 3). We also discovered a significant positive correlation between JAK2 activation and the activation of NLRP3 and caspase 1 (Supplementary Figure 2, Supplemental Digital Content 1, http://links.lww.com/SLA/E19). A recent phenotypic high-content, high-throughput screen identified targeting JAK to inhibit NLRP3 inflammasome activation[61]. This may suggest that blocking the activation of the NLRP3 inflammasome contributes to the observed protective effects of baricitinib in HS by reducing the pro-inflammatory effects of IL-1β and ensuing tissue inflammation.

The sterile inflammation caused by HS drives the recruitment of leukocytes to the tissues and is secondary to NF-κB and NLRP3 activation and their associated transcriptional regulation of pro-inflammatory cytokines[62–64]. Furthermore, leukocytes and endothelial cells express adhesion molecules, and this is regulated by NF-κB to facilitate leukocyte extravasation from the circulation to the site of damage[65]. It has been shown that experimental injury induces a transcriptomic shift in leukocytes 4 h post trauma and HS and several pathways related to

innate immunity were upregulated; including those involved in myeloid leukocyte activation and differentiation[66]. We measured CD68 expression and PAS score in the kidney as markers of macrophage infiltration and overall tissue injury, respectively[67]. HS resulted in a significant rise in relative CD68 expression and PAS score in the kidney which was attenuated by baricitinib treatment in HS-rats (Figure 4, see also Supplement for an extended discussion, Supplemental Digital Content 1, http://links.lww.com/SLA/E19). A graphical abstract summarizing the protective effects of baricitinib following HS-induced multiple organ dysfunction is shown in Figure 6.

Our results and conclusions are supported by findings in COVID-19 patient cohorts where the JAK/STAT pathway has been proposed to play a role in disease pathogenesis. The beneficial effects of baricitinib in COVID-19 patients, as measured by the improved levels of oxygenation, decreased need for mechanical ventilation (invasive and non-invasive), reduced ICU admission and mortality indicate that JAK/STAT activation contributes to the disease pathology[68]. Parallels can be drawn between COVID-19 and trauma-associated MODS, with both displaying features of an excessive systemic inflammatory state.

LIMITATIONS OF THE STUDY

Although baricitinib demonstrated some striking, beneficial effects in the rat model of HS, there are limitations which should be taken into consideration. An acute model of HS with a single time point was used in this study, which results in systemic inflammation and MODS within a few hours following resuscitation. At 4 h post resuscitation, there is organ injury and dysfunction and significant activation of JAK/STAT, NF-κB and NLRP3. Despite the effectiveness of baricitinib in this acute setting at the 4 h time point, we cannot conclude that the same protective effects will be observed in animal models with a longer follow-up period,

since there are delayed consequences/outcomes of trauma and severe hemorrhage on organ and immune function. Moreover, survival studies are needed to confirm that the observed early reduction in MODS does, indeed, translate to improved outcome and ultimately a decrease in mortality; all of which would strengthen the efficacy data of baricitinib in this study and provide more robust evidence in favor of designing a clinical trial. Organ injury and dysfunction were used as surrogate markers for mortality in our study (as the determination of mortality is not allowed by our ethics and Home Office license). Thus, caution should be taken when interpreting our pre-clinical results and extrapolating them to the clinical scenario. In this study, gender differences were not investigated, as only male rats were used to prevent any sex-dependent confounding effects (variations in female reproductive hormones and X chromosome) and to represent the population usually most affected by trauma (young males). Of note, the majority of trauma patients in our recent TOP-ART clinical trial were male and aged under 30, so the use of male rats is clinically appropriate[69]. Nevertheless, we acknowledge a considerable number of trauma patients are female and the efficacy of baricitinib in female rats should be assessed. Further studies in larger animals (e.g. pigs) and/or higher species may be useful to increase understanding of both the mechanism of action (e.g. blood gas analysis and microcirculatory effects) and verify efficacy of baricitinib in HS. We show that treatment with baricitinib upon resuscitation had no significant effect on arterial blood pressure, suggesting that the beneficial influence of baricitinib in HS may be independent of effects on blood pressure and, hence, microvascular perfusion of the tissues/organs. This could potentially limit the effectiveness of baricitinib treatment in HS, as alternative therapies may be required to counteract the vascular decompensation associated with HS. Nonetheless, clinical studies with large cohorts of trauma patients are required to robustly examine the relationship between JAK activity and clinical outcomes in humans.

CONCLUSIONS

In conclusion, we report here for the first time that baricitinib reduces the organ injury/dysfunction caused by severe hemorrhage in the rat, highlighting a role of the JAK2/STAT3 pathway in disease pathogenesis. Additionally, experimental trauma-hemorrhage results in a significant activation of the JAK2/STAT3 pathway in the liver and kidneys. Administration of baricitinib during resuscitation after major hemorrhage abolished the activation of JAK2/STAT3 as well as the activation of NF-κB and the NLRP3 inflammasome (liver and kidney); both of which are major drivers of local and systemic inflammation. Therefore, we propose that JAK inhibitors, such as baricitinib, may be repurposed to reduce the organ injury and inflammation caused by severe hemorrhage and resuscitation in patients with trauma.

REFERENCES

1. World Health Organization. *Injuries and Violence: The Facts 2014.*; 2014. Accessed May 6, 2021. www.who.int/healthinfo/global_burden_disease/projections/en/

2. Curry N, Hopewell S, Dorée C, Hyde C, Brohi K, Stanworth S. The acute management of trauma hemorrhage: A systematic review of randomized controlled trials. *Critical Care*. 2011;15(2):1-10. doi:10.1186/cc10096

3. Abbafati C, Abbas KM, Abbasi-Kangevari M, et al. Global burden of 369 diseases and injuries in 204 countries and territories, 1990–2019: a systematic analysis for the Global Burden of Disease Study 2019. *The Lancet*. 2020;396(10258):1204-1222. doi:10.1016/S0140-6736(20)30925-9/ATTACHMENT/96EE692B-E8A2-4D2B-AB04-5A9B1490A107/MMC2E.PDF

4. Roth GA, Abate D, Abate KH, et al. Global, regional, and national age-sex-specific mortality for 282 causes of death in 195 countries and territories, 1980–2017: a systematic analysis for the Global Burden of Disease Study 2017. *The Lancet*. 2018;392(10159):1736-1788. doi:10.1016/S0140-6736(18)32203-7/ATTACHMENT/0AAA0B77-F3E8-452C-A5C6-4DEBEAEAE82D/MMC2.PDF

5. Naghavi M, Abajobir AA, Abbafati C, et al. Global, regional, and national age-sex specifc mortality for 264 causes of death, 1980-2016: A systematic analysis for the Global Burden of Disease Study 2016. *The Lancet*. 2017;390(10100):1151-1210. doi:10.1016/S0140-6736(17)32152-9/ATTACHMENT/C3945D9D-7391-4E78-AEB4-8EBF47C0C63B/MMC2.PDF

6. Dewar D, Moore FA, Moore EE, Balogh Z. Postinjury multiple organ failure. *Injury*. 2009;40(9):912-918. doi:10.1016/j.injury.2009.05.024

7. Denk S, Weckbach S, Eisele P, et al. Role of Hemorrhagic Shock in Experimental Polytrauma. *Shock*. 2018;49(2):154-163. doi:10.1097/SHK.0000000000000925

8. Halbgebauer R, Braun CK, Denk S, et al. Hemorrhagic shock drives glycocalyx, barrier and organ dysfunction early after polytrauma. *Journal of Critical Care*. 2018;44:229-237. doi:10.1016/J.JCRC.2017.11.025

9. Kleinveld DJB, Simons DDG, Dekimpe C, et al. Plasma and rhADAMTS13 reduce trauma-induced organ failure by restoring the ADAMTS13-VWF axis. *Blood Advances*. 2021;5(17):3478. doi:10.1182/BLOODADVANCES.2021004404

10. Cabrera CP, Manson J, Shepherd JM, et al. Signatures of inflammation and impending multiple organ dysfunction in the hyperacute phase of trauma: A prospective cohort study. *PLoS Medicine*. 2017;14(7):e1002352. doi:10.1371/journal.pmed.1002352

11. Shepherd JM, Cole E, Brohi K. CONTEMPORARY PATTERNS of MULTIPLE ORGAN DYSFUNCTION in TRAUMA. *Shock*. 2017;47(4):429-435. doi:10.1097/SHK.0000000000000779

12. Lord JM, Midwinter MJ, Chen YF, et al. The systemic immune response to trauma: An overview of pathophysiology and treatment. *The Lancet*. 2014;384(9952):1455-1465. doi:10.1016/S0140-6736(14)60687-5

13. Leonard WJ, O'Shea JJ. Jaks and STATs: Biological implications. *Annual Review of Immunology*. 1998;16:293-322. doi:10.1146/annurev.immunol.16.1.293

14. Collotta D, Hull W, Mastrocola R, et al. Baricitinib counteracts metaflammation, thus protecting against diet-induced metabolic abnormalities in mice. *Molecular Metabolism*. 2020;39:101009. doi:10.1016/j.molmet.2020.101009

15. Richardson P, Griffin I, Tucker C, et al. Baricitinib as potential treatment for 2019-nCoV acute respiratory disease. *The Lancet*. 2020;395(10223):e30-e31. doi:10.1016/S0140-6736(20)30304-4

16. Bronte V, Ugel S, Tinazzi E, et al. Baricitinib restrains the immune dysregulation in patients with severe COVID-19. *Journal of Clinical Investigation*. 2020;130(12):6409-6416. doi:10.1172/JCI141772

17. Cantini F, Niccoli L, Matarrese D, Nicastri E, Stobbione P, Goletti D. Baricitinib therapy in COVID-19: A pilot study on safety and clinical impact. *Journal of Infection*. 2020;81(2):318-356. doi:10.1016/j.jinf.2020.04.017

18. Cantini F, Niccoli L, Nannini C, et al. Beneficial impact of Baricitinib in COVID-19 moderate pneumonia; multicentre study. *Journal of Infection*. 2020;81(4):647-679. doi:10.1016/j.jinf.2020.06.052

19. Rodriguez-Garcia JL, Sanchez-Nievas G, Arevalo-Serrano J, Garcia-Gomez C, Jimenez-Vizuete JM, Martinez-Alfaro E. Baricitinib improves respiratory function in patients treated with corticosteroids for SARS-CoV-2 pneumonia: An observational cohort study. *Rheumatology (United Kingdom)*. 2021;60(1):399-407. doi:10.1093/rheumatology/keaa587

20. Titanji BK, Farley MM, Mehta A, et al. Use of Baricitinib in Patients With Moderate to Severe Coronavirus Disease 2019. *Clinical Infectious Diseases*. 2021;72(7):1247-1250. doi:10.1093/cid/ciaa879

21. Kalil AC, Patterson TF, Mehta AK, et al. Baricitinib plus Remdesivir for Hospitalized Adults with Covid-19. *New England Journal of Medicine*. 2021;384(9):795-807. doi:10.1056/NEJMoa2031994

22. Kartman RN CE, Krishnan V, Liao R, et al. Efficacy and safety of baricitinib for the treatment of hospitalised adults with COVID-19 (COV-BARRIER): a randomised, double-blind, parallel-group, placebo-controlled phase 3 trial. *The Lancet Respiratory*. Published online 2021. doi:10.1016/S2213-2600(21)00331-3

23. Hasan MJ, Rabbani R, Anam AM, Huq SMR. Additional baricitinib loading dose improves clinical outcome in COVID-19. *Open Medicine (Poland)*. 2021;16(1):041-046. doi:10.1515/med-2021-0010

24. Rosas J, Liaño FP, Cantó ML, et al. Experience With the Use of Baricitinib and Tocilizumab Monotherapy or Combined, in Patients With Interstitial Pneumonia Secondary to Coronavirus COVID19: A Real-World Study. *Reumatología Clínica*. Published online November 28, 2020. doi:10.1016/J.REUMA.2020.10.009

25. Pérez-Alba E, Nuzzolo-Shihadeh L, Aguirre-García GM, et al. Baricitinib plus dexamethasone compared to dexamethasone for the treatment of severe COVID-19 pneumonia: A retrospective analysis. *Journal of Microbiology, Immunology and Infection*. Published online July 3, 2021. doi:10.1016/J.JMII.2021.05.009

26. Marconi VC, Ramanan A v, Bono S de, et al. Efficacy and safety of baricitinib for the treatment of hospitalised adults with COVID-19 (COV-BARRIER): a randomised, double-blind, parallel-group, placebo-controlled phase 3 trial. *The Lancet Respiratory Medicine*. 2021;0(0). doi:10.1016/S2213-2600(21)00331-3

27. Stebbing J, Nievas GS, Falcone M, et al. JAK inhibition reduces SARS-CoV-2 liver infectivity and modulates inflammatory responses to reduce morbidity and mortality. *Science Advances*. 2021;7(1):eabe4724. doi:10.1126/sciadv.abe4724

28. Hasan MdJ, Rabbani R, Anam AM, et al. Impact of high dose of baricitinib in severe COVID-19 pneumonia: a prospective cohort study in Bangladesh. *BMC Infectious Diseases*. 2021;21(1). doi:10.1186/S12879-021-06119-2

29. Tziolos N, Karofylakis E, Grigoropoulos I, et al. Real-life effectiveness and safety of baricitinib as adjunctive to standard-of-care treatment in hospitalized patients with severe COVID-19. *Open Forum Infectious Diseases*. doi:10.1093/OFID/OFAB588

30. Overview | Baricitinib for treating moderate to severe atopic dermatitis | Guidance | NICE.

31. Zhao J bing, Zhang Y, Li G zhao, Su X fen, Hang C hua. Activation of JAK2/STAT pathway in cerebral cortex after experimental traumatic brain injury of rats. *Neuroscience Letters*. 2011;498(2):147-152. doi:10.1016/j.neulet.2011.05.001

32. Raible DJ, Frey LC, del Angel YC, et al. JAK/STAT pathway regulation of GABAA receptor expression after differing severities of experimental TBI. *Experimental Neurology*. 2015;271:445-456. doi:10.1016/j.expneurol.2015.07.001

33. Zhang LJ, Ni SZ, Zhou XL, Zhao Y. Hemorrhagic Shock Sensitized the Diaphragm to Ventilator-Induced Dysfunction through the Activation of IL-6/JAK/STAT Signaling-Mediated Autophagy in Rats. *Mediators of Inflammation*. 2019;2019. doi:10.1155/2019/3738409

34. Xiao W, Mindrinos MN, Seok J, et al. A genomic storm in critically injured humans. *The Journal of Experimental Medicine*. 2011;208(13):2581. doi:10.1084/JEM.20111354

35. Patel NM, Oliveira FRMB, Ramos HP, et al. Inhibition of Bruton's Tyrosine Kinase Activity Attenuates Hemorrhagic Shock-Induced Multiple Organ Dysfunction in Rats. *Annals of Surgery*. 2021. doi:10.1097/SLA.0000000000005357

36. Sordi R, Chiazza F, Collotta D, et al. Resolvin D1 Attenuates the Organ Injury Associated With Experimental Hemorrhagic Shock. *Annals of Surgery*. 2021;273(5):1012-1021. doi:10.1097/sla.0000000000003407

37. Sordi R, Nandra KK, Chiazza F, et al. Artesunate protects against the organ injury and dysfunction induced by severe hemorrhage and resuscitation. *Annals of Surgery*. Published online 2017. doi:10.1097/SLA.0000000000001664

38. Yamada N, Martin LB, Zechendorf E, et al. Novel Synthetic, Host-defense Peptide Protects Against Organ Injury/Dysfunction in a Rat Model of Severe Hemorrhagic Shock. *Annals of Surgery*. Published online 2018. doi:10.1097/SLA.0000000000002186

39. Patel NM, Yamada N, Oliveira FRMB, et al. Inhibition of Macrophage Migration Inhibitory Factor Activity Attenuates Haemorrhagic Shock-Induced Multiple Organ Dysfunction in Rats. *Frontiers in Immunology*. 2022;0:1492. doi:10.3389/FIMMU.2022.886421

40. Dennhardt S, Pirschel W, Wissuwa B, et al. Modeling hemolytic-uremic syndrome: In-depth characterization of distinct murine models reflecting different features of human disease. *Frontiers in Immunology*. 2018;9(JUN):1459. doi:10.3389/FIMMU.2018.01459/BIBTEX

41. CHMP. ANNEX I SUMMARY OF PRODUCT CHARACTERISTICS.

42. Yang N, Luo M, Li R, et al. Blockage of JAK/STAT signalling attenuates renal ischaemia-reperfusion injury in rat. *Nephrology Dialysis Transplantation*. 2008;23(1):91-100. doi:10.1093/ndt/gfm509

43. Zhao X, Zhang E, Ren X, et al. Edaravone alleviates cell apoptosis and mitochondrial injury in ischemia-reperfusion-induced kidney injury via the JAK/STAT pathway. *Biological Research*. 2020;53(1):28. doi:10.1186/s40659-020-00297-0

44. Mascareno E, El-Shafei M, Maulik N, et al. JAK/STAT signaling is associated with cardiac dysfunction during ischemia and reperfusion. *Circulation*. 2001;104(3):325-329. doi:10.1161/01.CIR.104.3.325

45. Wen SH, Li Y, Li C, et al. Ischemic postconditioning during reperfusion attenuates intestinal injury and mucosal cell apoptosis by inhibiting JAK/STAT signaling activation. *Shock*. 2012;38(4):411-419. doi:10.1097/SHK.0b013e3182662266

46. Freitas MCS, Uchida Y, Zhao D, Ke B, Busuttil RW, Kupiec-Weglinski JW. Blockade of Janus kinase-2 signaling ameliorates mouse liver damage due to ischemia and reperfusion. *Liver Transplantation*. 2010;16(5):600-610. doi:10.1002/lt.22036

47. Si Y, Bao H, Han L, et al. Dexmedetomidine protects against renal ischemia and reperfusion injury by inhibiting the JAK/STAT signaling activation. *Journal of Translational Medicine*. 2013;11(1):1-12. doi:10.1186/1479-5876-11-141

48. Hui L, Yao Y, Wang S, et al. Inhibition of Janus kinase 2 and signal transduction and activator of transcription 3 protect against cecal ligation and puncture-induced multiple organ damage and mortality. *Journal of Trauma - Injury, Infection and Critical Care*. 2009;66(3):859-865. doi:10.1097/TA.0b013e318164d05f

49. Peña G, Cai B, Deitch EA, Ulloa L. JAK2 inhibition prevents innate immune responses and rescues animals from sepsis. *Journal of Molecular Medicine*. 2010;88(8):851-859. doi:10.1007/s00109-010-0628-z

50. Tsirigotis P, Papanikolaou N, Elefanti A, et al. Treatment of experimental Candida sepsis with a Janus Kinase inhibitor controls inflammation and prolongs survival. *Antimicrobial Agents and Chemotherapy*. 2015;59(12):7367-7373. doi:10.1128/AAC.01533-15

51. Jarneborn A, Mohammad M, Engdahl C, et al. Tofacitinib treatment aggravates Staphylococcus aureus septic arthritis, but attenuates sepsis and enterotoxin induced shock in mice. *Scientific Reports*. 2020;10(1):1-9. doi:10.1038/s41598-020-67928-0

52. Yun Y, Chen J, Wang X, et al. Tofacitinib Ameliorates Lipopolysaccharide-Induced Acute Kidney Injury by Blocking the JAK-STAT1/STAT3 Signaling Pathway. *BioMed Research International*. 2021;2021. doi:10.1155/2021/8877056

53. Ruetten H, Thiemermann C. Effects of tyrphostins and genistein on the circulatory failure and organ dysfunction caused by endotoxin in the rat: A possible role for protein tyrosine kinase. *British Journal of Pharmacology*. 1997;122(1):59-70. doi:10.1038/sj.bjp.0701345

54. Chen VL, Du X, Chen Y, et al. Genome-wide association study of serum liver enzymes implicates diverse metabolic and liver pathology. *Nature Communications 2021 12:1*. 2021;12(1):1-13. doi:10.1038/s41467-020-20870-1

55. Fan Y, Mao R, Yang J. NF-κB and STAT3 signaling pathways collaboratively link inflammation to cancer. *Protein & Cell*. 2013;4(3):176. doi:10.1007/S13238-013-2084-3

56. Martin L, Patel NM, 2# M, et al. The inhibition of Macrophage Migration Inhibitory Factor by ISO-1 attenuates trauma-induced multi organ dysfunction in rats. *medRxiv*. Published online April 29, 2021:2021.04.28.21255719. doi:10.1101/2021.04.28.21255719

57. Senftleben U, Karin M. The IKK/NF-kappa B pathway. *Crit Care Med*. 2002;30:S18-S26. Accessed May 11, 2021. https://pubmed.ncbi.nlm.nih.gov/11782557/

58. Liu SF, Malik AB. NF-κB activation as a pathological mechanism of septic shock and inflammation. *American Journal of Physiology - Lung Cellular and Molecular Physiology*. 2006;290(4). doi:10.1152/ajplung.00477.2005

59. Zhu H, Jian Z, Zhong Y, et al. Janus Kinase Inhibition Ameliorates Ischemic Stroke Injury and Neuroinflammation Through Reducing NLRP3 Inflammasome Activation via JAK2/STAT3 Pathway Inhibition. *Frontiers in Immunology*. 2021;0:2984. doi:10.3389/FIMMU.2021.714943

60. Furuya MY, Asano T, Sumichika Y, et al. Tofacitinib inhibits granulocyte–macrophage colony-stimulating factor-induced NLRP3 inflammasome activation in human neutrophils. *Arthritis Research & Therapy 2018 20:1*. 2018;20(1):1-9. doi:10.1186/S13075-018-1685-X

61. Nizami S, Millar V, Arunasalam K, et al. A phenotypic high-content, high-throughput screen identifies inhibitors of NLRP3 inflammasome activation. *Scientific Reports 2021 11:1*. 2021;11(1):1-12. doi:10.1038/s41598-021-94850-w

62. Chen CC, Manning AM. Transcriptional regulation of endothelial cell adhesion molecules: A dominant role for NF-κB. *Agents and Actions Supplements*. 1995;47:135-141. doi:10.1007/978-3-0348-7343-7_12

63. Collins T, Read MA, Neish AS, Whitley MZ, Thanos D, Maniatis T. Transcriptional regulation of endothelial cell adhesion molecules: NF-κB and cytokine-inducible enhancers. *The FASEB Journal*. 1995;9(10):899-909.

64. Campbell SJ, Anthony DC, Oakley F, et al. Hepatic Nuclear Factor κB Regulates Neutrophil Recruitment to the Injured Brain. *Journal of Neuropathology & Experimental Neurology*. 2008;67(3):223-230. doi:10.1097/NEN.0B013E3181654957

65. Hayden MS, Ghosh S. NF-κB in immunobiology. *Cell Research 2011 21:2*. 2011;21(2):223-244. doi:10.1038/cr.2011.13

66. Debler L, Palmer A, Braumüller S, et al. Hemorrhagic Shock Induces a Rapid Transcriptomic Shift of the Immune Balance in Leukocytes after Experimental Multiple Injury. *Mediators of Inflammation*. 2021;2021. doi:10.1155/2021/6654318

67. Chistiakov DA, Killingsworth MC, Myasoedova VA, Orekhov AN, Bobryshev Y v. CD68/macrosialin: not just a histochemical marker. *Laboratory Investigation 2017 97:1*. 2016;97(1):4-13. doi:10.1038/labinvest.2016.116

68. Lin Z, Niu J, Xu Y, Qin L, Ding J, Zhou L. Clinical Efficacy and Adverse Events of Baricitinib Treatment for Coronavirus Disease-2019 (COVID-19): A Systematic Review and Meta-Analysis. *SSRN Electronic Journal*. Published online 2021. doi:10.2139/SSRN.3929406

69. ISRCTN - ISRCTN15731357: The TOP-ART Study: Trauma Organ Protection - Artesunate. Accessed November 15, 2021. https://www.isrctn.com/ISRCTN15731357

Figure 1: JAK2 and STAT3 gene expression is elevated in trauma patients. Original data was obtained from the Gene Expression Omnibus under dataset accession number GSE36809 which was published by Xiao and colleagues [34]. RNA was extracted from whole blood leukocytes over a 28-day time course from trauma patients (n = 167) and matched healthy controls (n = 37). Data were reanalyzed for (**A**) JAK2 and (**B**) STAT3 gene expression in trauma patients and (**C**, **D**) uncomplicated vs. complicated trauma patient groups. Data are expressed as mean ± SEM. Statistical analysis was performed using one-way or two-way ANOVA followed by a Bonferroni's *post-hoc* test. *p<0.05 denoted statistical significance.

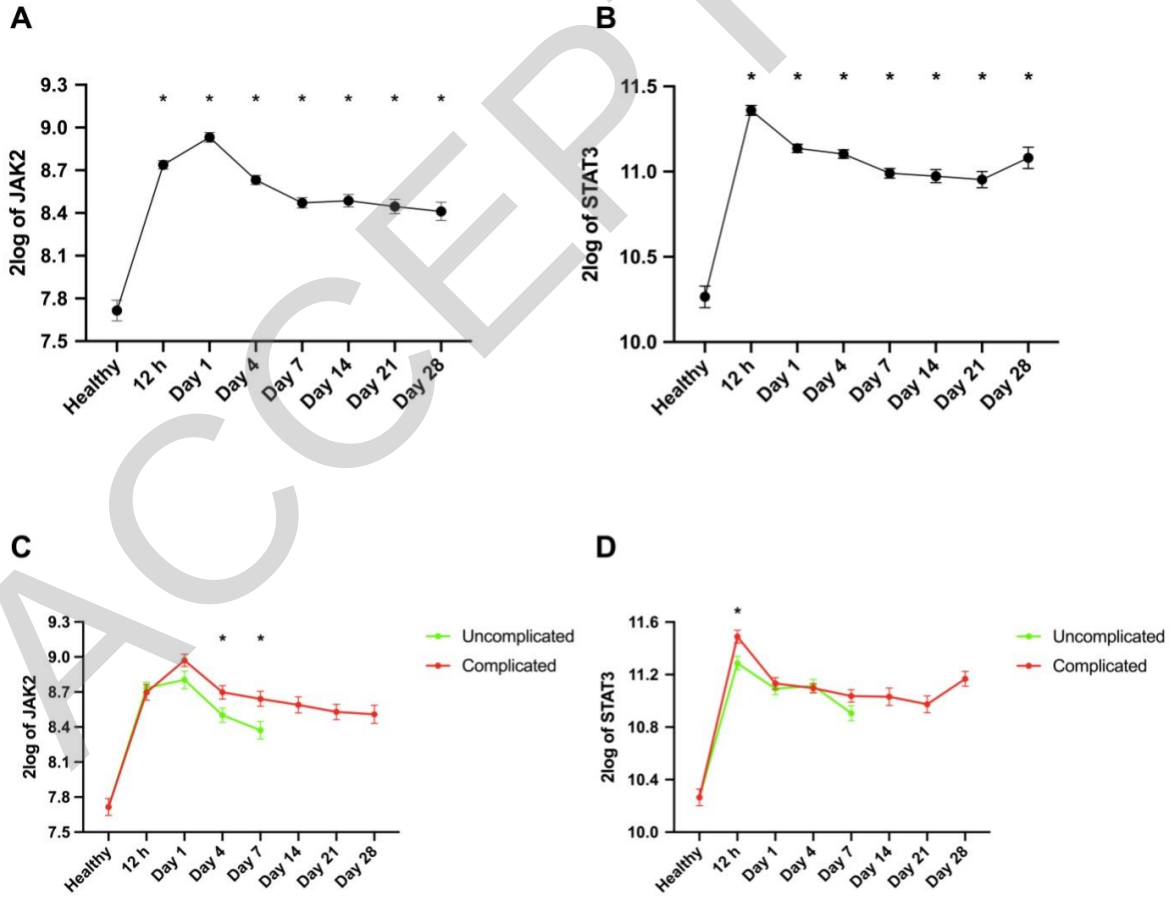

Figure 2: Baricitinib attenuates HS-induced organ injury/dysfunction in HS. Rats were subjected to hemorrhagic shock (HS) and 4 h after resuscitation, levels of serum (**A**) urea, (**B**) creatinine, (**C**) alanine aminotransferase (ALT), (**D**) aspartate aminotransferase (AST), (**E**) amylase, (**F**) creatine kinase (CK) and (**G**) lactate dehydrogenase (LDH) were determined in vehicle and BAR (baricitinib) treated rats. Sham-operated rats were used as control. Data are expressed as mean ± SEM of 9-11 animals per group. Statistical analysis was performed using one-way ANOVA followed by a Bonferroni's *post-hoc* test. *p<0.05 denoted statistical significance.

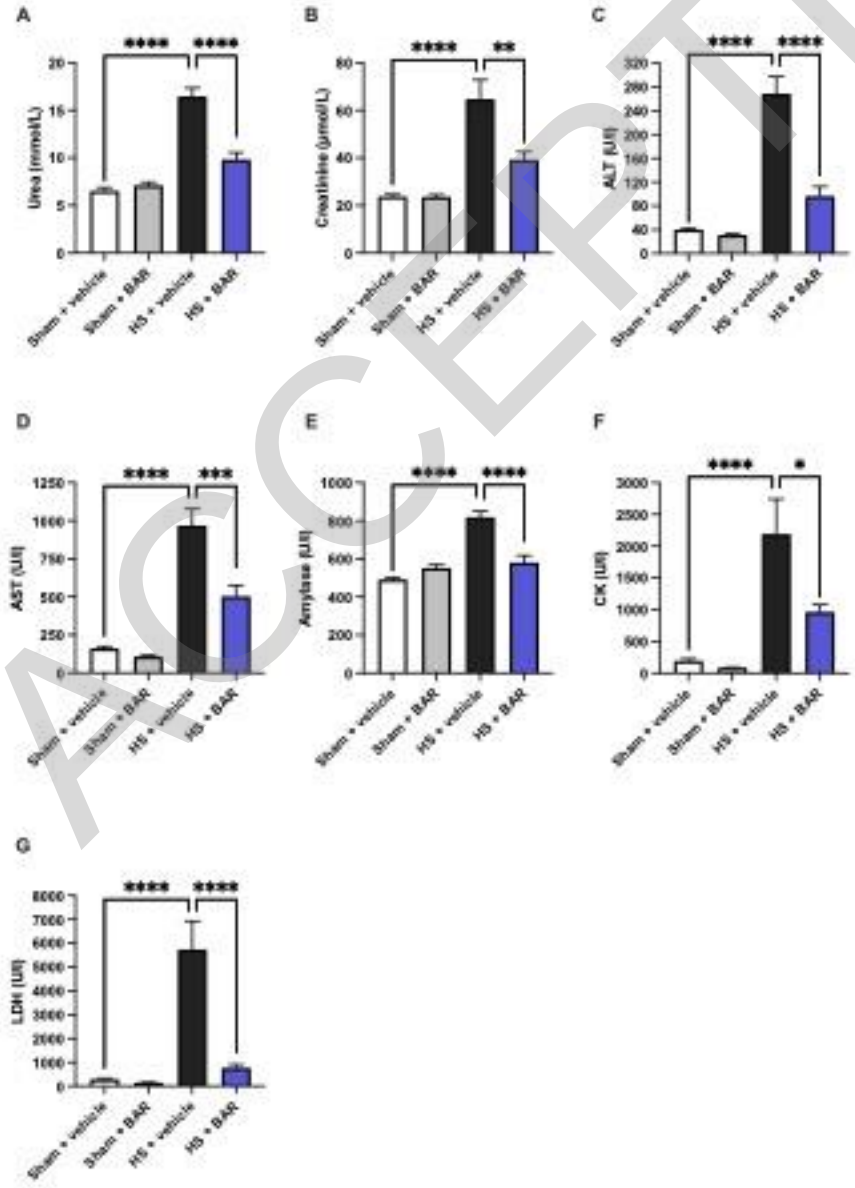

Figure 3: Baricitinib abolishes JAK/STAT, NF-κB and NLRP3 activation in HS. (**A-B**) The phosphorylation of Jak2 at $Tyr^{1007-1008}$, (**C-D**) the phosphorylation of Stat3 at Tyr^{705}, (**E-F**) the phosphorylation of IκBα at $Ser^{32/36}$, (**G-H**) the nuclear translocation of p65, (**I-J**) the activation of NLRP3 and (**K-L**) the cleaved (activated) form of caspase 1 of vehicle and BAR (baricitinib) treated rats were determined by western blotting in the liver and kidney. Protein expression was measured as relative optical density (O.D.) and normalized to the sham band. Data are expressed as mean ± SEM of 4-5 animals per group. Statistical analysis was performed using one-way ANOVA followed by a Bonferroni's *post-hoc* test. *$p<0.05$ denoted statistical significance.

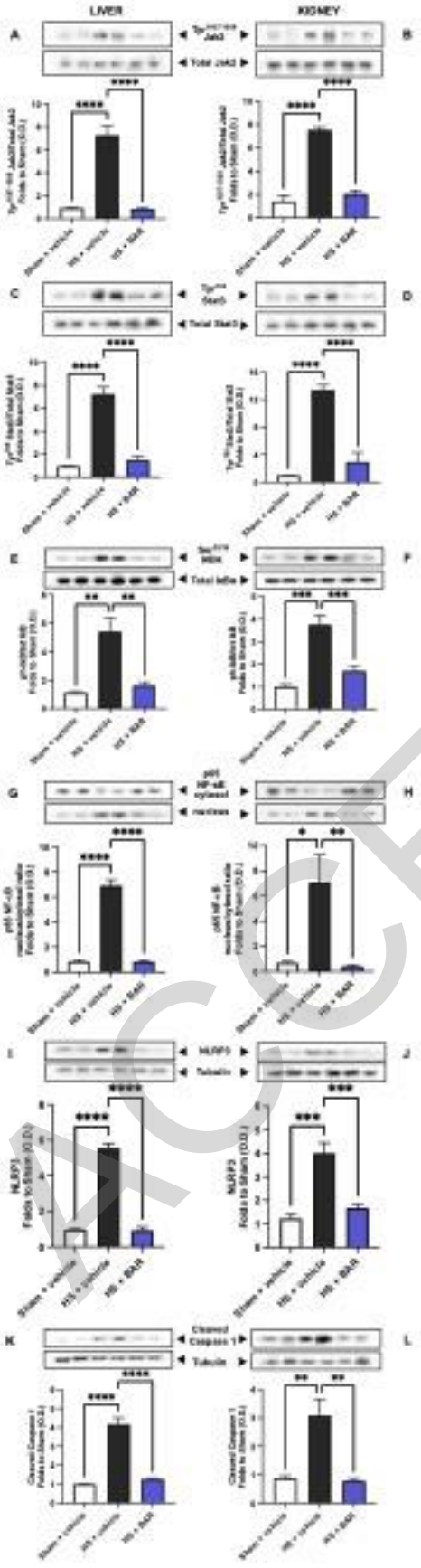
LIVER
KIDNEY
A
B
Total Jak2
C
D
Total Stat3
E
F
Total IκBα
G
H
p65 NF-κB cytosol
nucleus
I
J
NLRP3
Tubulin
K
L
Cleaved Caspase-1
Tubulin
Sham + vehicle
I/R + vehicle
I/R + BAR

Figure 4: Baricitinib reduces renal macrophage invasion and tissue injury in HS. Rats were subjected to hemorrhagic shock (HS) and 4 h after resuscitation, (**A**) relative CD68 expression and (**C**) Periodic acid Schiff (PAS) scores (Score 0: no damage, 1: <25% damaged, 2: 25-50% damaged and 3: >50% damaged) were quantified in renal tissue of vehicle and BAR (baricitinib) treated rats. Representative images of (**B**) CD68 staining (40x magnification) and (**D**) PAS staining (20x magnification) are shown. Black arrows highlight (**B**) sites of positive CD68 staining and (**D**) tubule dilatation (arrow A), detached cell material (arrow B), flattened epithelial cells (arrow C) and beginning stages of tubular brush border loss in proximal tubules (arrow D). Data are expressed as mean ± SEM of eight animals per group. Statistical analysis was performed using (**A**) one-way ANOVA followed by a Bonferroni's *post-hoc* test and (**C**) Kruskal-Wallis test followed by a Dunn's *post-hoc* test. *p<0.05 denoted statistical significance.

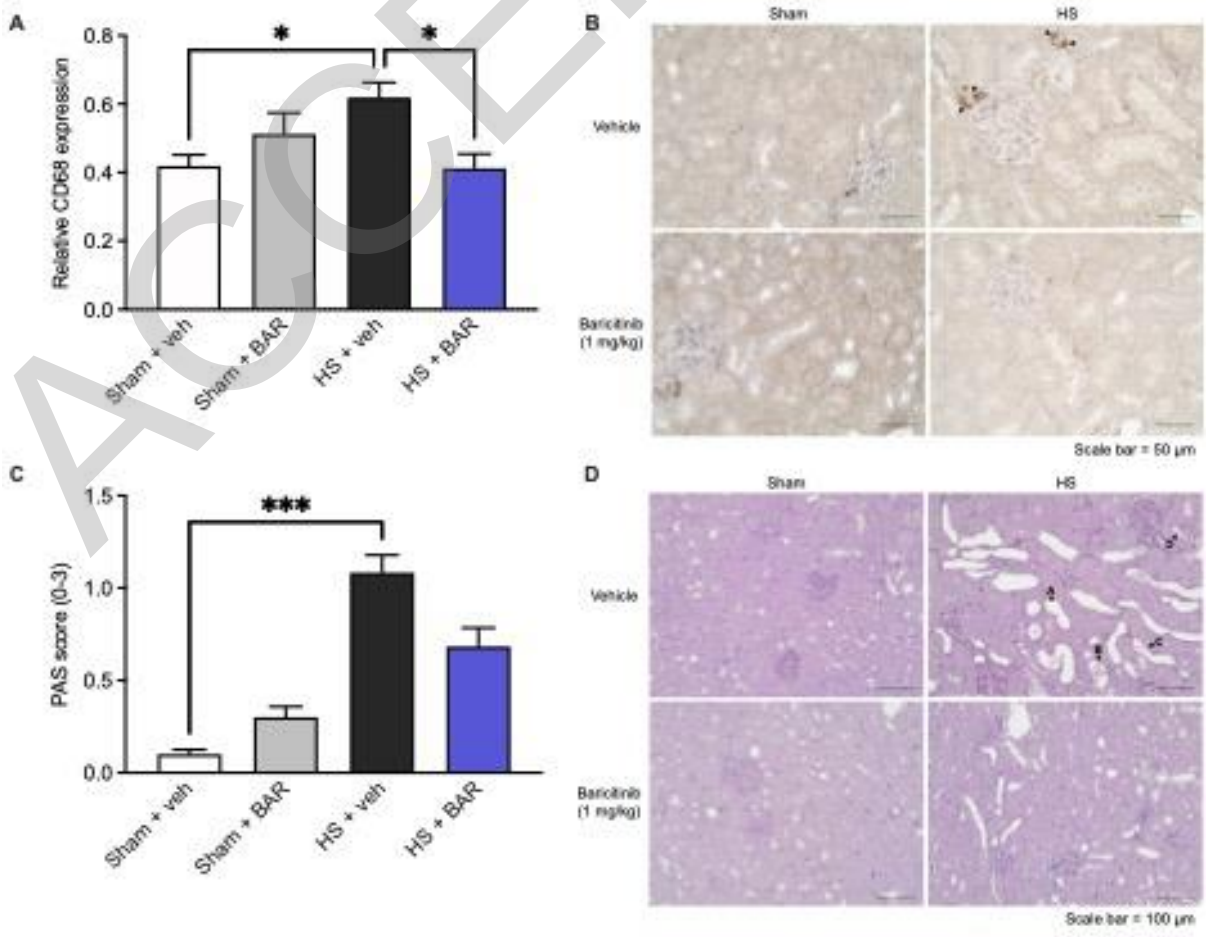

Figure 5: Effect of baricitinib on HS-induced circulatory failure in HS. Mean arterial pressure (MAP) was measured from the completion of surgery to the termination of the experiment for vehicle and BAR (baricitinib) treated rats. Data are expressed as mean ± SEM of 9-11 animals per group. Statistical analysis was performed using two-way ANOVA followed by a Bonferroni's *post-hoc* test. *p<0.05 Sham + vehicle vs. HS + vehicle.

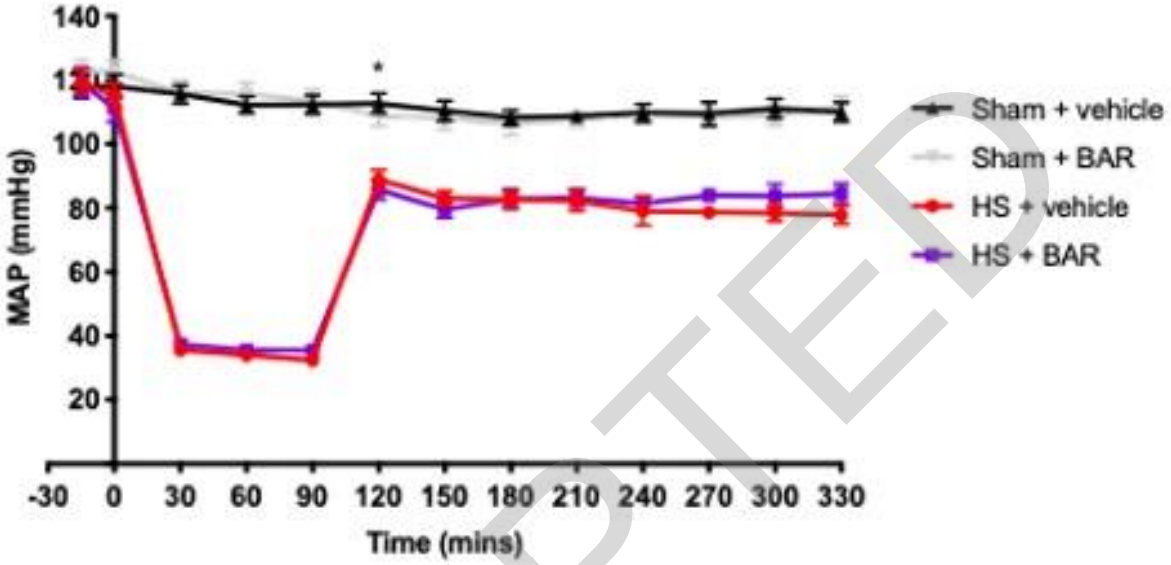

Figure 6: Graphical abstract highlighting the role of Janus kinase (JAK)/signal transducer and activator of transcription (STAT) in the pathophysiology of traumatic injury. Cytokines are released following trauma which trigger signaling pathways leading to JAK/STAT activation and target gene transcription. The activation of the NLRP3 inflammasome results in the cleavage of pro IL-1β to IL-1β and further pro-inflammatory cytokine production. Leukocyte recruitment is also stimulated by cytokine release. Excessive systemic inflammation from the combination of cytokine release and innate immune cell recruitment contributes to the onset of multiple organ dysfunction syndrome (MODS). Treatment with JAK inhibitors such as baricitinib can attenuate trauma-induced inflammation and thus MODS to improve clinical outcomes and patient prognosis.

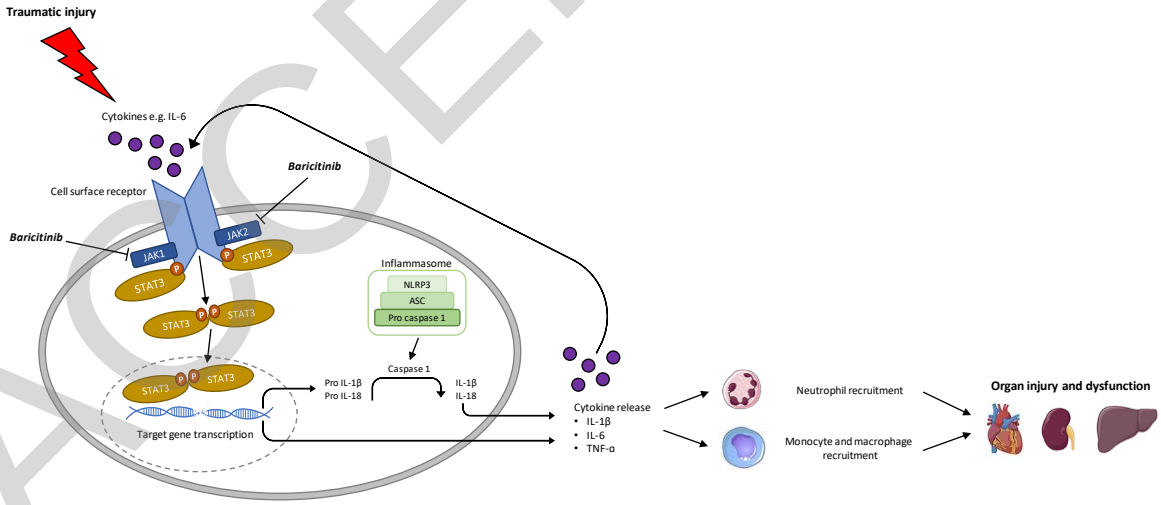

Article V

frontiers | Frontiers in Immunology

ORIGINAL RESEARCH
published: 06 April 2022
doi: 10.3389/fimmu.2022.886421

Inhibition of Macrophage Migration Inhibitory Factor Activity Attenuates Haemorrhagic Shock-Induced Multiple Organ Dysfunction in Rats

Nikita M. Patel[1], Noriaki Yamada[1,2], Filipe R. M. B. Oliveira[3], Lara Stiehler[1,4], Elisabeth Zechendorf[4], Daniel Hinkelmann[4], Sandra Kraemer[4], Christian Stoppe[5], Massimo Collino[6], Debora Collotta[6], Gustavo Ferreira Alves[6], Hanna Pillmann Ramos[3], Regina Sordi[3], Ingo Marzi[7], Borna Relja[7,8], Gernot Marx[4], Lukas Martin[1,4*†] and Christoph Thiemermann[1†]*

[1] William Harvey Research Institute, Barts and The London School of Medicine and Dentistry, Queen Mary University of London, London, United Kingdom, [2] Gifu University Graduate School of Medicine, Department of Emergency and Disaster Medicine Gifu University Hospital Advanced Critical Care Center, Gifu, Japan, [3] Department of Pharmacology, Universidade Federal de Santa Catarina, Florianópolis, Brazil, [4] Department of Intensive Care and Intermediate Care, University Hospital RWTH Aachen, Aachen, Germany, [5] Department of Anesthesiology & Intensive Care Medicine, University Hospital Würzburg, Würzburg, Germany, [6] Department of Neurosciences "Rita Levi Montalcini", University of Turin, Turin, Italy, [7] Department of Trauma, Hand and Reconstructive Surgery, University Hospital Frankfurt, Goethe University, Frankfurt, Germany, [8] Experimental Radiology, Department of Radiology and Nuclear Medicine, Otto-von-Guericke University, Magdeburg, Germany

OPEN ACCESS

Edited by:
Tom E. Mollnes, University of Oslo, Norway

Reviewed by:
Roman Pfeifer, University Hospital Zürich, Switzerland
Philipp Mommsen, Hannover Medical School, Germany

***Correspondence:**
Lukas Martin
lmartin@ukaachen.de
Nikita M. Patel
n.m.patel@qmul.ac.uk

†These authors have contributed equally to this work and share senior authorship

Specialty section:
This article was submitted to Inflammation, a section of the journal Frontiers in Immunology

Received: *28 February 2022*
Accepted: *14 March 2022*
Published: *06 April 2022*

Citation:
Patel NM, Yamada N, Oliveira FRMB, Stiehler L, Zechendorf E, Hinkelmann D, Kraemer S, Stoppe C, Collino M, Collotta D, Alves GF, Ramos HP, Sordi R, Marzi I, Relja B, Marx G, Martin L and Thiemermann C (2022) Inhibition of Macrophage Migration Inhibitory Factor Activity Attenuates Haemorrhagic Shock-Induced Multiple Organ Dysfunction in Rats. Front. Immunol. 13:886421. doi: 10.3389/fimmu.2022.886421

Objective: The aim of this study was to investigate (a) macrophage migration inhibitory factor (MIF) levels in polytrauma patients and rats after haemorrhagic shock (HS), (b) the potential of the MIF inhibitor ISO-1 to reduce multiple organ dysfunction syndrome (MODS) in acute (short-term and long-term follow-up) HS rat models and (c) whether treatment with ISO-1 attenuates NF-κB and NLRP3 activation in HS.

Background: The MODS caused by an excessive systemic inflammatory response following trauma is associated with a high morbidity and mortality. MIF is a pleiotropic cytokine which can modulate the inflammatory response, however, its role in trauma is unknown.

Methods: The MIF levels in plasma of polytrauma patients and serum of rats with HS were measured by ELISA. Acute HS rat models were performed to determine the influence of ISO-1 on MODS. The activation of NF-κB and NLRP3 pathways were analysed by western blot in the kidney and liver.

Results: We demonstrated that (a) MIF levels are increased in polytrauma patients on arrival to the emergency room and in rats after HS, (b) HS caused organ injury and/or dysfunction and hypotension (post-resuscitation) in rats, while (c) treatment of HS-rats with ISO-1 attenuated the organ injury and dysfunction in acute HS models and (d) reduced the activation of NF-κB and NLRP3 pathways in the kidney and liver.

Conclusion: Our results point to a role of MIF in the pathophysiology of trauma-induced organ injury and dysfunction and indicate that MIF inhibitors may be used as a potential therapeutic approach for MODS after trauma and/or haemorrhage.

Keywords: haemorrhagic shock, ischaemia-reperfusion, ISO-1, macrophage migration inhibitory factor, multiple organ dysfunction syndrome, trauma

INTRODUCTION

Trauma is one of the leading causes of death and disability in young people aged under 44 and exceeds the number of deaths caused by HIV, tuberculosis and malaria combined (1). Globally, injuries are responsible for over 9% of all mortalities and annually there are approximately 6 million trauma-related deaths (1, 2). Trauma-associated haemorrhage and haemorrhagic shock (HS) account for nearly 40% of all trauma deaths and is a key driver of multiple organ dysfunction (MODS) (3–7).

Whilst the number of early post-injury deaths have decreased in recent years secondary to improved care in the pre-hospital setting, there has been an accompanying increase in deaths attributed to MODS during the late post-injury phase (4, 8, 9). The mechanisms contributing to MODS include (a) an excessive systemic inflammatory response secondary to the release of damage-associated molecular patterns (DAMPs) from extensive tissue damage and (b) ischaemia-reperfusion (I/R) injury (8, 10).

DAMPs activate the immune system, leading to the release of cytokines which can cause organ injury and dysfunction (11). Moreover, raised cytokine levels are linked to worse prognosis in critically ill patients (12–14). One such cytokine is macrophage migration inhibitory factor (MIF) which is pro-inflammatory and possesses chemokine-like properties by promoting the expression or production of several pro-inflammatory mediators including IL-1β, IL-2, IL-6, IL-8, IL-12, IFN-γ, nitric oxide, TNF-α, cyclooxygenase 2 and matrix metalloproteinases (15–23). Consequently, further leukocytes are directed to the site of injury and/or infection (24–26). MIF also has a role in counter-regulating the immunosuppressive and anti-inflammatory effects of glucocorticoids (27, 28).

It has previously been shown that MIF concentration in the plasma/serum of trauma patients was higher than that of healthy controls (29, 30) and serum MIF levels in blunt trauma patients with MODS were significantly greater than patients without MODS (31, 32). Currently, there are no specific pharmacological treatments which prevent the onset of MODS associated with HS. Therefore, the aim of this study was to investigate the effects of blocking MIF activity with the inhibitor ISO-1 [(S,R)-3-(4-hydroxyphenyl)-4,5-dihydro-5-isoxazole acetic acid methyl ester] on the HS-induced MODS in rats.

METHODS

MIF Gene Expression in Human Whole Blood

Original data was obtained under Gene Expression Omnibus (GEO) accession GSE36809, published by Xiao and colleagues (33). RNA was extracted from whole blood leukocytes of severe blunt trauma patients (n = 167) over the course of 28 days and healthy controls (n = 37) and hybridised onto an HU133 Plus 2.0 GeneChip (Affymetrix) according to the manufacturer's recommendations. The dataset was reanalysed for MIF gene expression.

Ethical Statement

Blood samples of 208 patients were collected after written informed consent was obtained from either the patient or a nominated legally authorised representative. Samples were collected between 2010-2014 from University Hospital Frankfurt of Goethe-University and approved by an institutional ethics committee (Number 312/10) in accordance with the declaration of Helsinki and following STROBE-guidelines (34).

For the short-term follow-up acute HS model, all animal procedures were approved by the Animal Welfare Ethics Review Board of Queen Mary University of London and by the Home Office (Licence number PC5F29685). For the long-term follow-up acute HS model, all animal procedures were approved by the Universidade Federal de Santa Catarina Institutional Committee for Animal Use in Research (Licence number 7396250219) in accordance with the Brazilian Government Guidelines for Animal Use in Research. All *in vivo* experiments are reported in accordance to ARRIVE guidelines.

Patient Study Population and Sample Collection

Blood samples from patients (18-80 years) with blunt or penetrating trauma and ISS ≥ 16 were obtained on Day 0 (arrival to the emergency room); Day 2; Day 5 and Day 7. Exclusion criteria were patient death in the emergency room or within 24 h of hospital admission, known pre-existing immunological disorders, treatment with immunosuppressive or anti-coagulant medication, burns, concomitant acute myocardial infarction and thromboembolic events. Blood samples were collected in pre-chilled ethylenediaminetetraacetic acid tubes (BD vacutainer, Becton Dickinson Diagnostics, Aalst, Belgium) and kept on ice. Blood was centrifuged at 2,000 g for 15 min at 4°C to separate serum and stored at −80°C for further analysis.

Experimental Design

Male Wistar rats (for short-term follow-up acute model: Charles River Laboratories Ltd., UK; for long-term follow-up acute model: Universidade Federal de Santa Catarina, Brazil) weighing 250-350 g were kept under standard laboratory

conditions and received a chow diet and water *ad libitum*. ISO-1 (25 mg/kg; Tocris, UK) was diluted in 5% DMSO + 95% Ringer's Lactate (vehicle) and rats were treated (i.v. in short-term follow-up and i.p. in long-term follow-up) upon resuscitation.

Acute Haemorrhagic Shock Model (Short-Term Follow-Up)

The pressure-controlled short-term follow-up acute HS model was performed as previously described (35–38). Briefly, forty rats were anaesthetised with sodium thiopentone (120 mg/kg i.p. initially and 10 mg/kg i.v. for maintenance as needed and randomised into four groups (n = 10 per group): Sham + vehicle; Sham + ISO-1 (25 mg/kg), HS + vehicle; HS + ISO-1 (25 mg/kg) using the GraphPad online random number generator. The investigator was blinded to the intervention (vehicle or ISO-1) and treatment group allocation was revealed following data analysis. Analgesia was not administered as the rats remain anaesthetised for the duration of the experiment (non-recovery procedure) and as such do not expect the animals to feel pain. Adequacy of anaesthesia was ascertained throughout the experiment by testing the pedal reflex. No animals died during the course of the study, thus all data have been included. Blood was withdrawn to achieve a fall in mean arterial pressure (MAP) to 35 ± 5 mmHg, which was maintained for 90 min. At 90 min after initiation of haemorrhage (or when 25% of the shed blood had to be reinjected to sustain MAP at 35 ± 5 mmHg), resuscitation was performed with the shed blood over a period of 5 min. At 4 h post-resuscitation, blood was collected for the measurement of biomarkers of organ injury/dysfunction (MRC Harwell Institute, Oxfordshire, UK) and organs for *ex vivo* analysis. Sham-operated rats were used as control and underwent identical surgical procedures, but without haemorrhage or resuscitation. Detailed description of the short-term follow-up model can be found in the supplemental (**Supplemental Figure 1A**).

Acute Haemorrhagic Shock Model (Long-Term Follow-Up)

The pressure-controlled long-term follow-up acute HS model was performed as previously described (36). Briefly, thirty rats were administered analgesia with tramadol (10 mg/kg i.p.) 15 min prior to anaesthesia induction with ketamine and xylazine (100 mg/kg and 10 mg/kg i.m. respectively) and randomised into three groups: Sham + vehicle (n = 6); HS + vehicle (n = 12); HS + ISO-1 (25 mg/kg; n = 12) using the GraphPad online random number generator. The investigator was blinded to the intervention (vehicle or ISO-1) and treatment group allocation was revealed following data analysis. Adequacy of anaesthesia throughout the experiment was ascertained by testing the pedal reflex. No animals died during the course of the study, thus all data have been included. Blood was withdrawn to achieve a fall in MAP to 40 ± 2 mmHg, which was maintained for 90 min. At 90 min after initiation of haemorrhage (or when 25% of the shed blood had to be reinjected to sustain MAP at 40 ± 2 mmHg), resuscitation was performed with the shed blood over a period of 5 min plus 1.5 mL/kg Ringer's lactate. At 24 h post-resuscitation, blood was collected for the measurement of organ injury/dysfunction parameters (Hospital Universitário Professor Polydoro Ernani de São Thiago, Brazil) and organs for *ex vivo* analysis. Sham-operated rats were used as control and underwent identical surgical procedures, but without haemorrhage or resuscitation. Detailed description of the long-term follow-up model can be found in the supplemental (**Supplemental Figure 1B**).

MIF ELISA

Human MIF plasma levels (R&D SYSTEMS Human MIF DuoSet) and rat MIF serum levels from the acute HS (short-term follow-up) model (Cusabio Biotech, Wuhan, China) were detected by commercially available ELISAs according to the manufacturer protocol. Detection occurred at 450 nm and 540 nm using iMark® microplate absorbance reader (BioRad). Further details can be found in the **Supplemental Table 1**.

Western Blot Analysis

Semi-quantitative immunoblot analysis was carried out in kidney and liver samples as previously described (36). Detailed description of the method can be found in the supplemental.

CD68 Immunohistochemical Staining

Lung tissue sections were deparaffinised and hydrated and stained for CD68. Detailed description of the method can be found in the supplemental.

Quantification of Myeloperoxidase Activity

Determination of myeloperoxidase activity in lung and liver tissue samples was performed as previously described (36). Detailed description of the method can be found in the supplemental.

Statistical Analysis

All figures are expressed as median with range of *n* observations, where *n* represents the number of animals/experiments/subjects studied. Measurements obtained from the vehicle and ISO-1 treated animal groups were analysed by one-way ANOVA followed by a Bonferroni's *post-hoc* test on GraphPad Prism 8.0 (GraphPad Software, Inc., La Jolla, CA, USA). The distribution of the data was verified by Shapiro-Wilk normality test, and the homogeneity of variances by Bartlett test. When necessary, values were transformed into logarithmic values to achieve normality and homogeneity of variances. To investigate the relationship between the variables, Pearson correlation *r* was performed. $P<0.05$ was considered statistically significant.

RESULTS

MIF Gene Expression Is Elevated in Trauma Patients

Xiao and colleagues (33) compared genome-wide expression in leukocytes from trauma patients against matched healthy controls. We reanalysed this dataset for MIF expression. When compared to healthy controls, MIF expression was significantly

elevated at all time points except Day 1 ($p<0.05$; **Supplemental Figure 2**). An initial increase was noted at 12 h followed by a later peak at Day 7. MIF expression remained elevated at Day 28, the latest timepoint measured.

MIF Gene Expression Does Not Differ Between Uncomplicated and Complicated Recovery Patient Groups

Xiao and colleagues (33) also stratified their trauma patient cohort into uncomplicated (recovery in <5 days) and complicated (recovery after 14 days, no recovery by Day 28 or death) to further identify genotypic differences. We reanalysed this dataset for MIF expression using this stratification. When comparing uncomplicated and complicated patients, there were no significant differences at any of the timepoints measured ($p>0.05$; **Supplemental Figure 3**).

Plasma MIF Levels Are Elevated in Polytrauma Patients and Associated With Longer Stay in ICU and Hospital

To investigate the role of MIF in trauma, 208 patients were included in the study. Detailed patient characteristics can be found in **Table 1**. Polytrauma patients showed significantly increased MIF levels on Day 0 (on arrival to the emergency room, 12398 ± 1262 pg/mL) compared to Day 2 (2866.9 ± 377.8 pg/mL), Day 5 (2335.7 ± 203.4 pg/mL) and Day 7 (2114.6 ± 165.3 pg/mL) (all $p<0.001$; **Figure 1A**). Furthermore, we found a weak positive correlation between MIF levels on Day 0 and both hospital ($r = 0.22$, $n = 199$, $p<0.01$; **Figure 1C**) and ICU ($r = 0.26$, $n = 198$, $p<0.01$; **Figure 1D**) stays. MIF levels on Day 0 were not correlated with baseline characteristics such as age ($r = -0.05$, $n = 200$, $p = 0.49$) and sex ($r = -0.07$, $n = 200$, $p = 0.3$) and only weakly correlated with ISS score ($r = 0.15$, $n = 177$, $p<0.05$) (**Figure 1B**).

MIF Levels Are Elevated in Serum of Rats After Induction of Acute HS (Short-Term Follow-Up)

Having found elevated plasma MIF levels in patients with trauma-haemorrhage, we investigated whether haemorrhage alone (in the absence of physical trauma) is sufficient to drive increases in MIF. To address this question, we used a model of severe haemorrhage followed by resuscitation in the rat. When compared to sham-operated rats, haemorrhage followed by resuscitation resulted in a significant increase in MIF levels ($p<0.001$; **Figure 2A**). Although ISO-1 has been reported to inhibit the effects, rather than the formation, of MIF *in vivo*, we report here that treatment of HS rats with ISO-1 resulted in a significantly lower MIF level when compared to HS rats treated with vehicle ($p<0.05$; **Figure 2A**). Administration of ISO-1 to sham-operated rats had no effect on MIF levels ($p>0.05$; **Figure 2A**).

TABLE 1 | Trauma patient clinical characteristics.

	Trauma (n = 208)
Age (year) (IQR)	47.0 (31-60)
Male sex (%)	156 (75.0)
SOFA (points) (IQR)	5.00 (1.0-7.0)
APACHE II (points) (IQR)	16.0 (6.0-22.0)
ISS score (points) (IQR)	23.0 (17.0-32.0)
LOS ICU (days) (IQR)	8.0 (4.0-15.0)
LOS In-hospital (days) (IQR)	19.0 (13.0-29.0)
MIF D0 [pg/ml] (IQR)	6839 (3713-14205)
MIF D2 [pg/ml] (IQR)	1598.0 (1080.0-2555.5)
MIF D5 [pg/ml] (IQR)	1137.0 (650.0-1960.0)
MIF D7 [pg/ml] (IQR)	1331.9 (814.2-2158.5)

Data are presented as n (%) or median (IQR). D0/2/5/7: Day 0/2/5/7; ICU, intensive care unit; IQR, interquartile ranges (Q1-Q3); LOS, length of stay.

Treatment With ISO-1 Improves HS-Induced Circulatory Failure in Acute HS (Short-Term Follow-Up)

To investigate the effects of ISO-1 on circulatory failure, MAP was measured from the completion of surgery to the termination of the experiment. Baseline MAP values were similar amongst all four groups. Rats subjected to HS demonstrated a decline in MAP which was ameliorated by resuscitation, but still remained lower than that of sham-operated rats during resuscitation (at the equivalent time points, **Figure 2B**). When compared to sham-operated rats, HS-rats treated with vehicle exhibited a more pronounced decrease in MAP over time post-resuscitation. In contrast, MAP of HS-rats treated with ISO-1 was significantly higher than HS-rats treated with vehicle 4 h post-resuscitation ($p<0.001$; **Figure 2B**).

Treatment With ISO-1 Attenuates HS-Induced Organ Damage in Acute HS (Short-Term Follow-Up)

Having demonstrated that treatment with ISO-1 improves HS-induced circulatory failure, we next explored whether ISO-1 attenuates MODS associated with HS in rats. When compared to sham-operated rats, rats subjected to HS and treated with vehicle displayed increases in serum urea ($p<0.001$; **Figure 3A**) and creatinine ($p<0.001$; **Figure 3B**) and a decrease in creatinine clearance ($p<0.001$; **Figure 3C**) indicating the development of renal dysfunction. When compared to sham-operated rats, vehicle treated HS-rats exhibited significant increases in both ALT ($p<0.001$; **Figure 3D**) and AST ($p<0.001$; **Figure 3E**) indicating the development of hepatic injury, while the increases in amylase ($p<0.001$; **Figure 3F**) and CK ($p<0.001$; **Figure 3G**) denote pancreatic and neuromuscular injury, respectively. The significant increase in LDH ($p<0.001$; **Figure 3H**) in HS-rats treated with vehicle confirmed tissue injury whilst the increase in lactate ($p<0.001$; **Figure 3I**) indicated decreased transport of oxygen to the tissues developing from the state of hypoperfusion. Treatment of HS-rats with ISO-1 significantly attenuated the renal dysfunction, hepatic injury, pancreatic injury, neuromuscular injury and general tissue damage caused by HS (all $p<0.05$; **Figures 3A–I**). As HS causes macrophage infiltration into the lungs, we measured $CD68^+$ positive cells as a marker for macrophage invasion. When compared to sham-operated rats (21.75 ± 2.29 per field), HS-rats treated with vehicle displayed a significant increase in macrophage count (47.33 ± 8.75 per field, $p<0.05$). Treatment with ISO-1 in HS-rats did not result in a significant decrease in macrophage count (35.90 ± 4.30 per field; **Supplemental Figure 4**).

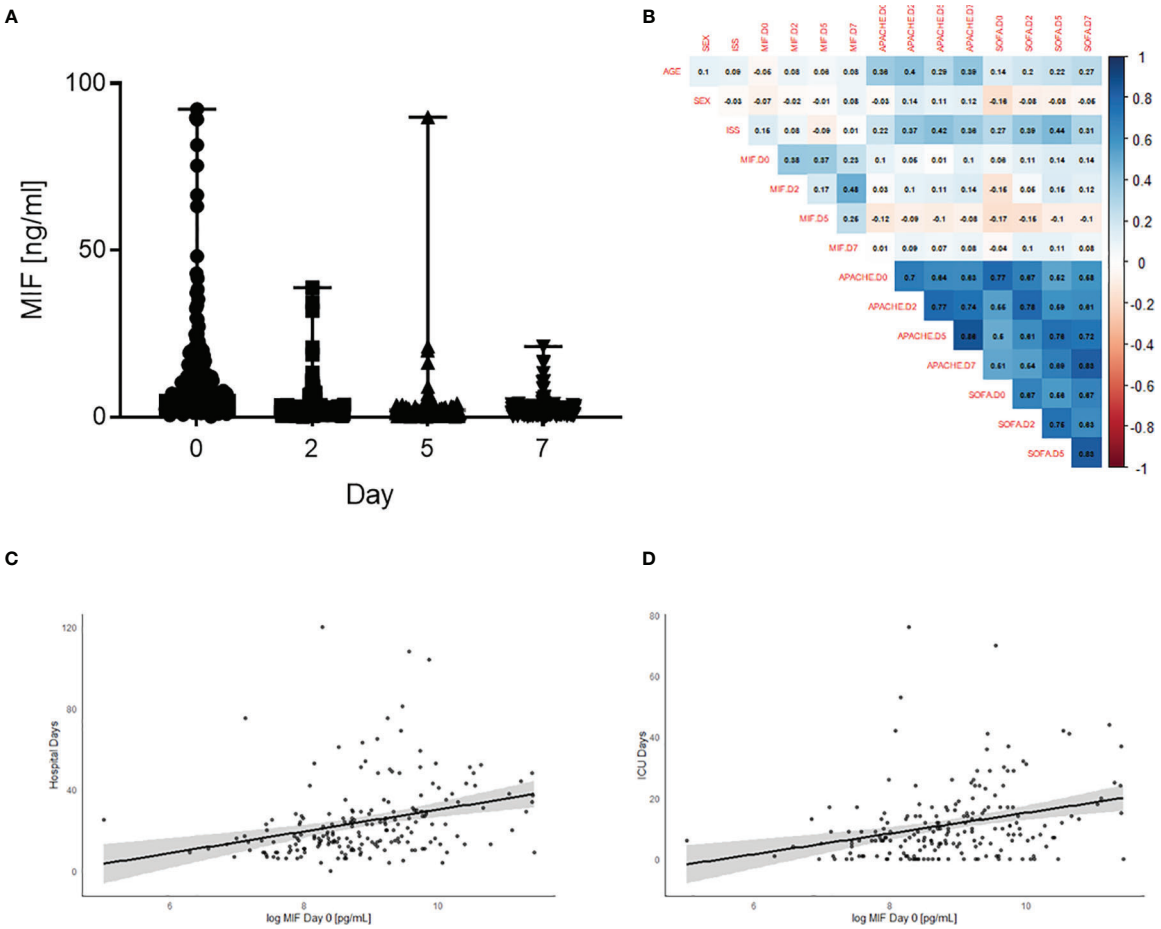

FIGURE 1 | Plasma MIF levels are elevated in polytrauma patients and associated with longer stay in ICU and hospital. **(A)** Plasma MIF levels in trauma patients (n = 208) at different time points: Day 0 (Emergency room), Day 2, Day 5 and Day 7. Data are expressed as median with range. **(B)** Heatmap for correlations between MIF levels and baseline characteristics sex, age, SOFA, ISS and APACHE score. Scatter plot for Day 0 MIF levels against **(C)** hospital stay and **(D)** intensive care unit (ICU) stay.

Serum MIF Levels Are Strongly Associated With Clinical Chemistry and MAP in Acute HS (Short-Term Follow-Up)

Having shown rats subjected to HS had elevated serum MIF levels, we wished to elucidate whether this observed increase correlates with clinical chemistry parameters (measured in serum collected 4 h post-resuscitation) and MAP (measured at 4 h post-resuscitation before sample collection). There was a positive correlation between MIF and all clinical chemistry parameters ($p<0.05$; **Supplemental Figure 5** shown in blue, r values range from 0.64 – 0.77), with the strongest correlations between AST (r = 0.77) and LDH (r = 0.72). There was a negative correlation between MIF and MAP ($p<0.05$; **Supplemental Figure 5** shown in red, r = -0.66).

Treatment With ISO-1 Attenuates Hepatic and Renal NF-κB Activation in Acute HS (Short-Term Follow-Up)

The effect of MIF inhibition on the activation of the signalling events leading to the activation of NF-κB, was investigated in the kidney and liver. When compared to sham-operated rats, HS-rats treated with vehicle had significant increases in the phosphorylation of IKKα/β at $Ser^{176/180}$ ($p<0.001$; **Figure 4A** and $p<0.001$; **Figure 4B**) and translocation of p65 to the nucleus ($p<0.001$; **Figure 4C** and $p<0.05$; **Figure 4D**). Treatment with ISO-1 significantly attenuated the increases in hepatic and renal phosphorylation of IKKα/β at $Ser^{176/180}$ ($p<0.001$; **Figure 4A** and $p<0.001$; **Figure 4B**) and the nuclear translocation of p65 ($p<0.001$; **Figure 4C** and $p<0.05$; **Figure 4D**).

Treatment With ISO-1 Attenuates Hepatic and Renal NLRP3 Inflammasome Activation in Acute HS (Short-Term Follow-Up)

Having discovered treatment with ISO-1 significantly reduced the activation of NF-κB in the kidney and liver of rats subjected to HS, we next analysed the potential involvement of the NLRP3 inflammasome. When compared to sham-operated rats, HS-rats treated with vehicle exhibited a significantly increased expression

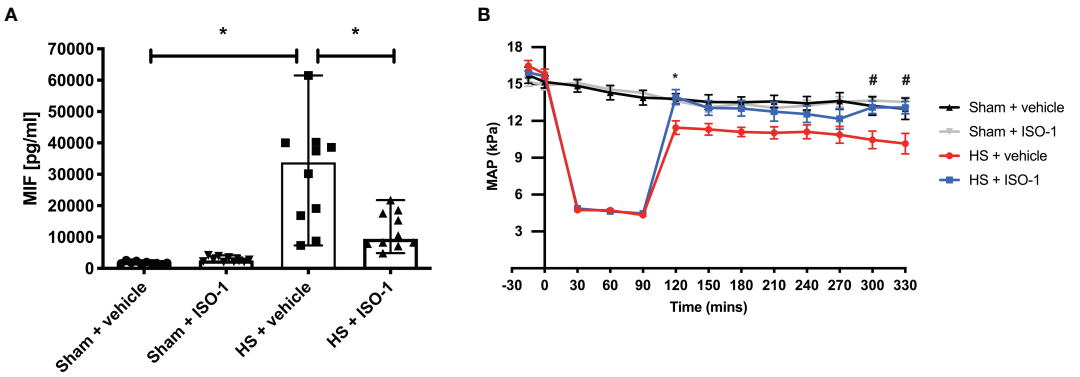

FIGURE 2 | Serum MIF levels are elevated in HS-rats and ISO-1 improves HS-induced circulatory failure in a short-term follow-up acute HS model. **(A)** Serum MIF levels were detected by ELISA in vehicle or ISO-1 treated rats. Data are expressed as median with range of ten animals per group. **(B)** Mean arterial pressure (MAP) was measured from the completion of surgery to the termination of the experiment for all groups. Statistical analysis was performed using one-way ANOVA followed by a Bonferroni's *post-hoc* test. *p < 0.05 Sham + vehicle vs. HS + vehicle; #p < 0.05 HS + vehicle vs. HS + ISO-1.

of the NLRP3 inflammasome (p<0.001; **Figure 4E** and p<0.001; **Figure 4F**) and cleavage of pro-caspase 1 to caspase 1 (p=0.008; **Figure 4G** and p<0.001; **Figure 4H**). Treatment with ISO-1 significantly inhibited the hepatic and renal expression of NLRP3 (p<0.001; **Figure 4E** and p<0.001; **Figure 4F**) and cleavage of pro-caspase 1 to caspase 1 (p=0.015; **Figure 4G** and p<0.001; **Figure 4H**).

Treatment With ISO-1 Improves HS-Induced Circulatory Failure in Acute HS (Long-Term Follow-Up)

Having demonstrated treatment with ISO-1 improved blood pressure in a short-term follow-up model, we wished to determine whether ISO-1 would still be effective in a model in which the resuscitation period is prolonged to 24 h. When compared to sham-operated rats, HS-rats treated with vehicle had significantly lower MAP values at 24 h post-resuscitation (p<0.001; **Figure 5A**); highlighting that either cardiovascular dysfunction or excessive hypotension was still present. In contrast, MAP of HS-rats treated with ISO-1 was significantly higher at 24 h than vehicle treated rats (p<0.05; **Figure 5A**). There were no significant differences in HR between any of the three groups investigated (p>0.05; **Figure 5B**).

Treatment With ISO-1 Attenuates HS-Induced Organ Damage and Myeloperoxidase Activity in Acute HS (Long-Term Follow-Up)

Having shown that treatment with ISO-1 ameliorated the MODS associated with HS in a short-term follow-up model, we examined whether this effect was sustained when the resuscitation period was extended to 24 h. As with the short-term follow-up model, when compared to sham-operated rats, rats subjected to HS with long-term follow-up and treated with vehicle displayed significant increases in serum urea (p<0.05; **Figure 6A**) and creatinine (p<0.001; **Figure 6B**) indicating the development of renal dysfunction. When compared to sham-operated rats, vehicle treated HS-rats exhibited significant increases in ALT (p<0.001; **Figure 6C**), AST (p<0.001; **Figure 6D**), lipase (p<0.05; **Figure 6E**) and LDH (p<0.05; **Figure 6F**). Treatment of HS-rats with ISO-1 significantly attenuated the renal dysfunction, hepatic injury and tissue damage caused by HS (all p<0.05; **Figures 6A–D, F**). Having demonstrated that treatment with ISO-1 reduced the cell infiltration in the lung in a short-term follow-up acute HS model, we measured myeloperoxidase (MPO) activity in the lung and liver as an indicator of neutrophil infiltration. When compared to sham-operated rats, HS-rats treated with vehicle showed a significant increase in MPO activity in the lung (p<0.001; **Figure 6G**) and liver (p<0.05; **Figure 6H**). Treatment with ISO-1 in HS-rats significantly attenuated these rises in MPO activity (p<0.001; **Figure 6G** and p<0.05; **Figure 6H**).

DISCUSSION

This study reports that inhibition of MIF activity attenuates organ injury/dysfunction and circulatory failure in acute short-term follow-up (**Figures 2**, **3**) and long-term follow-up (**Figures 5**, **6**) rat models of HS. Having shown that MIF gene expression is significantly elevated in leukocytes of trauma patients (**Supplemental Figure 2**) and plasma MIF levels are raised in polytrauma patients (**Figure 1**), we used a reverse translational approach to investigate whether pharmacological intervention with ISO-1 ameliorates the MODS associated with HS in a well-established rat model. Inhibition of MIF activity significantly attenuated the fall in blood pressure (**Figure 2** short-term follow-up and **Figure 5** long-term follow-up) and, hence, the delayed vascular decompensation caused by HS (39). Moreover, ISO-1 significantly attenuated the renal dysfunction, hepatic injury and neuromuscular injury caused by HS (**Figure 3** short-term follow-up and **Figure 6** long-term follow-up); highlighting the drug efficacy at both timepoints. Similarly, ISO-1 also reduces disease severity in animal models of sepsis

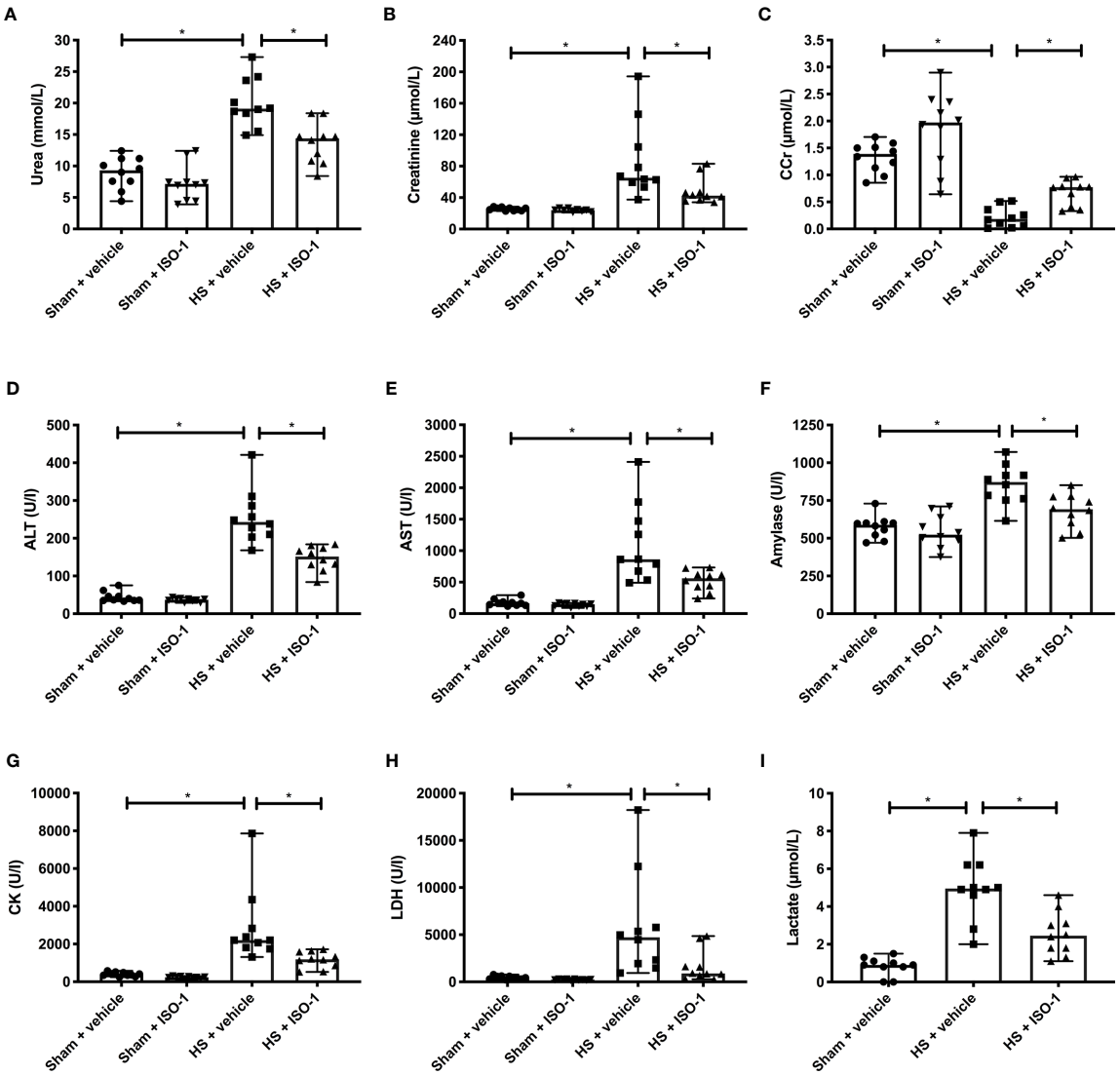

FIGURE 3 | Treatment with ISO-1 attenuates HS-induced organ damage in a short-term follow-up acute HS model. Rats were subjected to haemorrhagic shock (HS) and 4 h after resuscitation, levels of serum **(A)** urea, **(B)** creatinine, **(C)** creatinine clearance (CCr), **(D)** alanine aminotransferase (ALT), **(E)** aspartate aminotransferase (AST), **(F)** amylase, **(G)** creatine kinase (CK), **(H)** lactate dehydrogenase (LDH) and **(I)** lactate were determined. Sham-operated rats were used as control. Data are expressed as median with range of ten animals per group. Statistical analysis was performed using one-way ANOVA followed by a Bonferroni's *post-hoc* test. *$p < 0.05$ denoted statistical significance.

(40), acute pancreatitis (41–46), pneumonia (47), asthma (48), COPD (49), cystitis (50) and colitis (51).

We have illustrated that severe haemorrhage followed by resuscitation in the rat caused a significant increase in serum MIF levels, the magnitude of which was similar to the one seen in trauma patients. This finding implies that haemorrhage (rather than physical trauma) is the main driver for the observed increase in MIF in rats and possibly also in humans. Whilst the elevated plasma MIF levels in our cohort of polytrauma patients do not necessarily indicate an increase in synthesis, the increased gene expression measured by Xiao and colleagues (33) does suggest an associated rise in MIF production.

Post-traumatic complications can result in prolonged stays in ICU and in hospital. In the acute setting, there is a lack of diagnostic or risk stratification tools which allow the identification of the potential clinical outcome of trauma patients. We determined a significant positive correlation between elevated MIF levels in polytrauma patients and the overall length of ICU and hospital stays. These findings indicate that high plasma MIF levels at time of hospital admission are strongly predictive for a longer stay in ICU and hospital. Indeed, the human plasma MIF levels and gene expression data provide evidence supporting the role of MIF in trauma, as both gene expression and plasma levels increase following trauma. Most

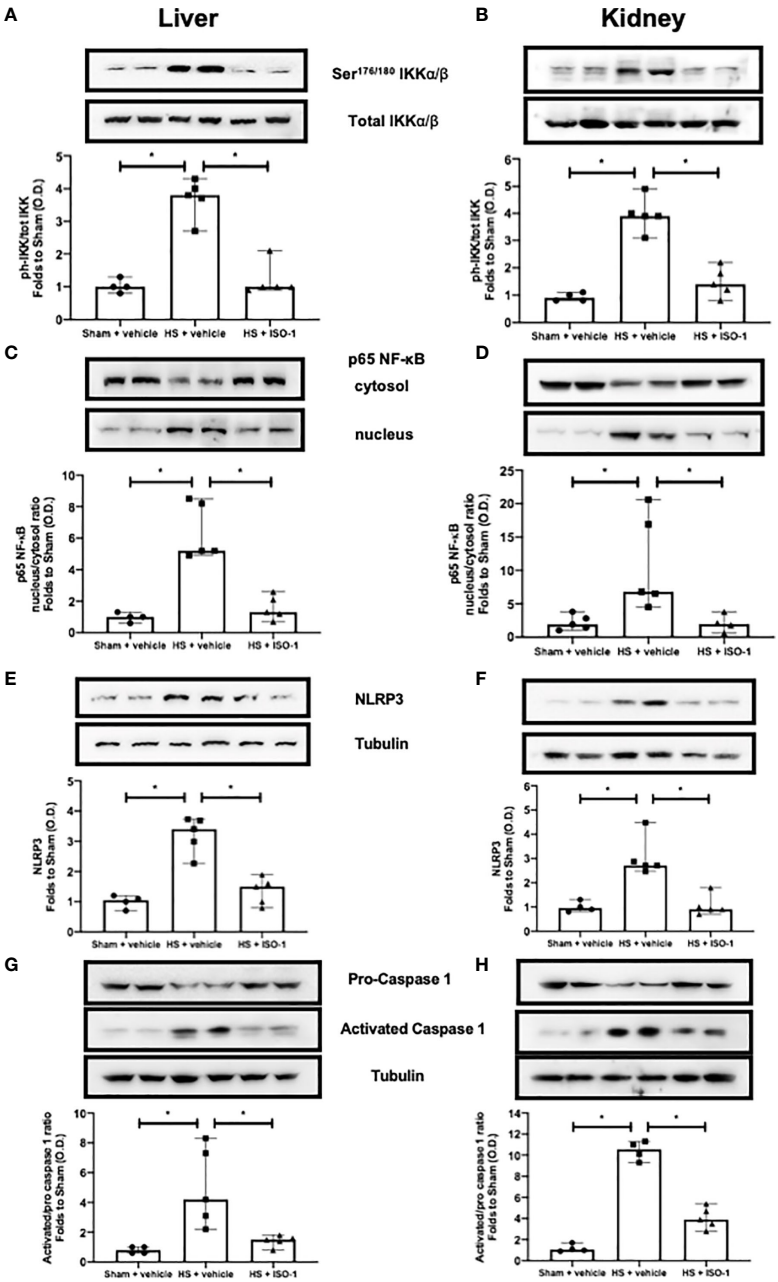

FIGURE 4 | Treatment with ISO-1 attenuates NF-κB and NLRP3 activation in a short-term follow-up acute HS model. **(A, B)** The phosphorylation of IKKα/β at $Ser^{176/180}$, **(C, D)** nuclear translocation of p65, **(E, F)** activation of NLRP3 and **(G, H)** cleavage of pro-caspase 1 of vehicle and ISO-1 treated rats were determined by western blot in the liver and kidney. Protein expression was measured as relative optical density (O.D.) and normalised to the sham band. Data are expressed as median with range of 4-5 animals per group. Statistical analysis was performed using one-way ANOVA followed by a Bonferroni's *post-hoc* test. *$p < 0.05$ denoted statistical significance.

notably, MIF was a better predictor of hospital stay than either ISS or SOFA scores. For every further increase of MIF on admission by 5000 pg/mL, the stay of patients in hospital is prolonged by ~1.2 days. Similarly, Cho and colleagues showed that trauma patients with elevated MIF levels had longer ICU stays than patients with lower or normal MIF levels (52).

Nevertheless, we found a weak positive but significant correlation between MIF levels on admission and ISS which supports the findings of Chuang and colleagues' study illustrating higher MIF levels were associated with worse clinical severity scores (APACHE II, RTS and TRISS) (30). Although clinical severity scores cannot be measured in rats,

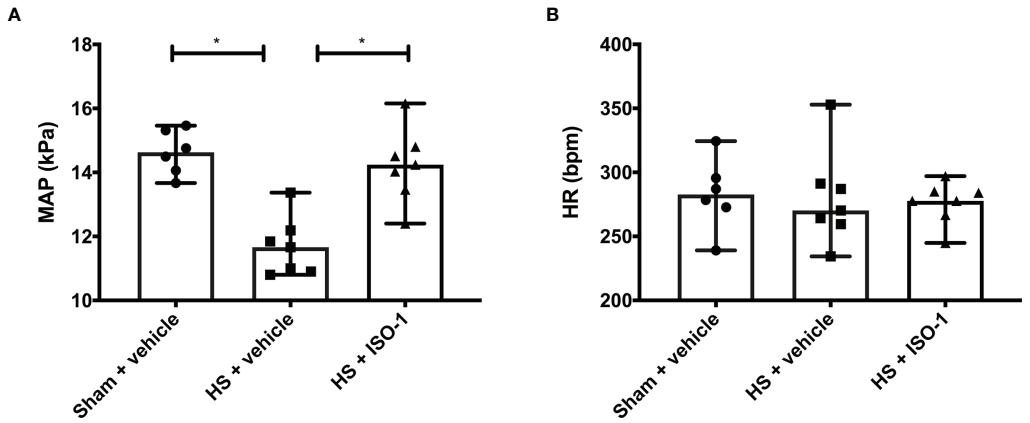

FIGURE 5 | Treatment with ISO-1 improves HS-induced cardiac dysfunction in a long-term follow-up acute HS model. **(A)** Mean arterial pressure (MAP) and **(B)** heart rate (HR) were measured 24 h post resuscitation for vehicle and ISO-1 treated rats. Data are expressed as median with range. Sham + vehicle (n = 6), HS + vehicle (n = 7) and HS + ISO-1 (n = 7). Statistical analysis was performed using one-way ANOVA followed by a Bonferroni's *post-hoc* test. *p < 0.05 denoted statistical significance.

we found significant positive correlations between serum MIF levels and clinical chemistry parameters and a significant negative correlation between MIF and MAP both of which can be considered as indicators organ function (**Supplementary Figure 5**).

What, then, are the mechanisms by which ISO-1 attenuates HS-associated organ injury/dysfunction? It is recognised that key signalling pathways, such as those leading to NF-κB activation, initiate the production of pro-inflammatory mediators such as cytokines, chemokines and enzymes (53). As part of a positive feedback mechanism, these inflammatory mediators can induce activation of NF-κB and its upstream signalling machinery, further amplifying and propagating the NF-κB-mediated inflammatory responses. This can result in a more permeable endothelium, hypoxic/hypoperfused tissues, tissue injury and ultimately MODS (54). Trauma has been shown to increase the translocation of NF-κB to the nucleus (35–38). Inhibition of MIF activity with ISO-1 reduced NF-κB activation in the kidney and liver of HS-rats (**Figure 4**). This may suggest that inhibiting NF-κB activation contributes to the observed protective effects of ISO-1 in HS. It should be noted that MIF has been shown to upregulate TLR4 expression, leading to increased translocation of NF-κB into the nucleus (55) and interact with thioredoxin-interacting protein to induce NF-κB activity (56).

Activation of the NLRP3 inflammasome stimulates IL-1β production which plays a crucial role in trauma-associated systemic inflammation and organ dysfunction/injury (36). Inhibition of MIF activity with ISO-1 reduced both the assembly and subsequent activation of the NLRP3 inflammasome in the kidney and liver of HS-rats (**Figure 4**). This may suggest that inhibiting NLRP3 inflammasome activation contributes to the observed beneficial effects of ISO-1 in HS by decreasing the pro-inflammatory effects related to increased IL-1β production and ensuing tissue inflammation (57). Of note, MIF has been proposed to play a role in the activation of the NLRP3 inflammasome (58, 59).

The sterile inflammation caused by HS is associated with increased recruitment of leukocytes to the tissues and is secondary to NF-κB and NLRP3 activation and their transcriptional regulation of pro-inflammatory cytokines (60–62). Furthermore, the leukocyte and endothelial cell surface expression of adhesion molecules is regulated by NF-κB and promotes leukocyte extravasation from the circulation to the injury site (63). We found a significant increase in $CD68^+$ cells in the lung (**Supplementary Figure 4**) and in pulmonary and hepatic MPO activity (**Figure 6**), markers of macrophage and neutrophil recruitment respectively, after induction of HS in rats. Treatment of HS-rats with ISO-1 did not significantly reduce the number of pulmonary $CD68^+$ cells and thus, macrophage infiltration into the lung. In contrast, administration of ISO-1 to HS-rats attenuated the rise in MPO activity related to increased neutrophil recruitment. Taken together, these results could imply that ISO-1 attenuates neutrophil, but not macrophage recruitment in HS. Indeed, an anti-MIF antibody was shown to attenuate the LPS-induced migration and accumulation of neutrophils in the lung (64). These observations can be explained by the chemokine-like properties of MIF, which facilitate the activation and recruitment of leukocytes during immune surveillance and inflammation (65, 66). Initially, MIF was eponymously described by its ability to inhibit random macrophage migration *in vitro* (67, 68). However, it is now known that MIF can mediate the recruitment of mononuclear cells in a number of disease states (69–72). A possible explanation as to why ISO-1 did not significantly reduce pulmonary macrophage invasion is that the presence of other inflammatory mediators, such as IL-1β, IL-6 and TNF-α, could have stimulated the migration of macrophages, but we would need to measure these mediators to confirm this theory.

LIMITATIONS

Although ISO-1 displayed some striking, beneficial effects in the acute HS models, there are study limitations which should be taken into consideration. In total, 208 patients were included in

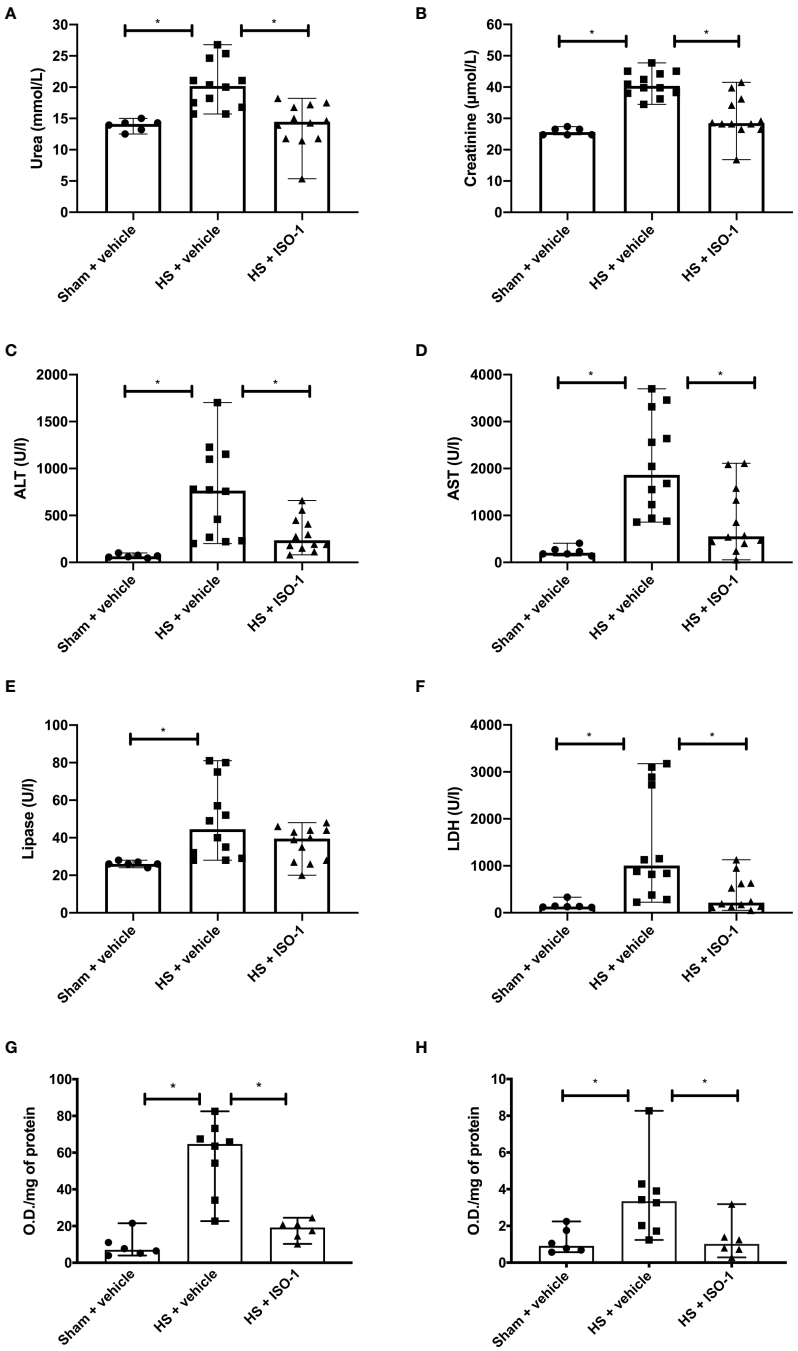

FIGURE 6 | Treatment with ISO-1 attenuates HS-induced organ damage and myeloperoxidase activity in a long-term follow-up acute HS model. Rats were subjected to haemorrhagic shock (HS) and 24 h after resuscitation, levels of serum **(A)** urea, **(B)** creatinine, **(C)** alanine aminotransferase, (ALT), **(D)** aspartate aminotransferase (AST), **(E)** lipase and **(F)** LDH were determined were determined in vehicle and ISO-1 treated rats. Sham-operated rats were used as control. Sham + vehicle (n = 6), HS + vehicle (n = 12) and HS + ISO-1 (n = 12). Myeloperoxidase activity in **(G)** lung and **(H)** liver were determined for vehicle and ISO-1 treated rats. Sham + vehicle (n = 6), HS + vehicle (n = 8) and HS + ISO-1 (n = 6). Data are expressed as median with range. Statistical analysis was performed using one-way ANOVA followed by a Bonferroni's *post-hoc* test. *p<0.05 denoted statistical significance.

the study, however, in some instances there were insufficient plasma volumes available for some of the measured timepoints. Therefore, some correlation analyses were performed with a reduced number of samples/patients. Following trauma, there is an increased inflammatory response, and we were able to measure elevated plasma MIF levels in polytrauma patients. However, we cannot exclude the possibility that the increased plasma levels are not exclusively associated with polytrauma. The

animal models used in our study do not encompass all aspects of trauma/HS and further long-term survival experiments are needed to verify that the observed early reduction in MODS does, indeed, translate to improved outcome and ultimately reduced mortality. Hence, caution must be exercised when interpreting the pre-clinical results and extrapolating to the clinical scenario. Additionally, future studies in larger animals/higher species may be useful to confirm efficacy and to further examine the mechanism(s) of action (e.g. microcirculatory effects and blood gas analysis) of ISO-1 in HS. It should be noted that only healthy young male rats were used and, hence, age and gender differences and the presence of co-morbidities were not investigated (but may well impact outcome). Moreover, clinical studies with larger cohorts of trauma patients are required to robustly examine the relationship between MIF activity, inhibition and clinical outcomes in humans. Whilst we did not measure the long-term stability of MIF in the patient samples collected between 2010-2014, we were able to demonstrate significant and time-related elevations in MIF in the blood of patients with trauma and haemorrhage. Indeed, the peak levels of MIF observed in patients on admission to the hospital (measured in samples that were several years old) were similar to the peak levels measured in rats with severe haemorrhage (that we measured within weeks of completing the experiments). Nevertheless, we cannot, however, entirely rule out that the levels of MIF in patients with trauma-haemorrhage would have been even higher if the MIF determinations would have been carried out earlier after the trauma occurred.

CONCLUSIONS

In conclusion, we demonstrate here for the first time that MIF levels are elevated in polytrauma patients on arrival to the emergency room and higher MIF levels are associated with longer stays in ICU and hospital overall. The finding that HS alone (in the absence of physical trauma) in rats resulted in a rise in MIF levels similar to that seen in polytrauma patients supports the view that haemorrhage is the main driver for the elevations in MIF. Furthermore, treatment with ISO-1 reduces the organ injury/dysfunction and circulatory failure caused by severe haemorrhage in the rat, highlighting a role of MIF in disease pathogenesis. Administration of ISO-1 attenuates the degree of NF-κB and NLRP3 inflammasome activation (measured in the kidney and liver), both of which are key drivers of local and systemic inflammation. Thus, we propose that MIF inhibitors may be used in trauma patients to lower the organ injury and inflammation caused by severe haemorrhage and resuscitation.

DATA AVAILABILITY STATEMENT

Publicly available datasets were analysed in this study. This data can be found here: https://www.ncbi.nlm.nih.gov/geo/query/acc.cgi?acc=gse36809.

ETHICS STATEMENT

The studies involving human participants were reviewed and approved by University Hospital Frankfurt of Goethe-University - Institutional Ethics Committee (Number 312/10). The patients/participants provided their written informed consent to participate in this study. The animal study was reviewed and approved by Animal Welfare Ethics Review Board of Queen Mary University of London and by the Home Office (Licence number PC5F29685) and Universidade Federal de Santa Catarina Institutional Committee for Animal Use in Research (Licence number 7396250219).

AUTHOR CONTRIBUTIONS

Conception and design: NMP, LM, and CT. Animal experiments: NY, NMP, FRMBO, HPR, and RS. Human sample analysis: LM, EZ, GM, IM, BR, DH, LS, and CS. Animal sample analyses: NY, NMP, LM, CT, LS, EZ, FRMBO, HPR, SK, DC, MC, GFA, and RS. Clinical study and patient data analyses: LM, EZ, CT, IM, BR, DH, LS, NMP, and CS. Statistical analyses: NY, NMP, DH, LM, and CT. Drafting the manuscript for important intellectual content: LS, LM, EZ, NMP, and CT. All authors reviewed and approved the manuscript.

FUNDING

NMP was funded by the William Harvey Research Foundation. HPR and FRMBO were funded by National Council for Scientific and Technological Development (CNPq) fellowship. This study was supported by the German Research Foundation to LM (DFG, MA 7082/3-1), to CS (DFG, STO 1099/8-1) and by an intramural grant to EZ (START 131/19), National Council for Scientific and Technological Development to RS (CNPq, Brazil, Grant 409018/2018-0).

ACKNOWLEDGMENTS

We would like to thank Dr. Ronald Tompkins and Dr. Wenzhong Xiao for their support in the human MIF gene expression data analysis.

SUPPLEMENTARY MATERIAL

The Supplementary Material for this article can be found online at: https://www.frontiersin.org/articles/10.3389/fimmu.2022.886421/full#supplementary-material

REFERENCES

1. World Health Organization. *Injuries and Violence: The Facts 2014* (2014). Available at: www.who.int/healthinfo/global_burden_disease/projections/en/.
2. Haagsma JA, Graetz N, Bolliger I, Naghavi M, Higashi H, Mullany EC, et al. The Global Burden of Injury: Incidence, Mortality, Disability-Adjusted Life Years and Time Trends From the Global Burden of Disease Study 2013. *Injury Prev* (2016) 22(1):3–18. doi: 10.1136/injuryprev-2015-041616
3. Curry N, Hopewell S, Dorée C, Hyde C, Brohi K, Stanworth S. The Acute Management of Trauma Hemorrhage: A Systematic Review of Randomized Controlled Trials. *Crit Care* (2011) 15(2):1–10. doi: 10.1186/cc10096
4. Dewar D, Moore FA, Moore EE, Balogh Z. Postinjury Multiple Organ Failure. *Injury* (2009) 40:912–8. doi: 10.1016/j.injury.2009.05.024
5. Geeraedts LMG, Kaasjager HAH, van Vugt AB, Frölke JPM. Exsanguination in Trauma: A Review of Diagnostics and Treatment Options. *Injury* (2009) 40 (1):11–20. doi: 10.1016/j.injury.2008.10.007
6. Dutton RP, Stansbury LG, Leone S, Kramer E, Hess JR, Scalea TM. Trauma Mortality in Mature Trauma Systems: Are We Doing Better? An Analysis of Trauma Mortality Patterns, 1997-2008. *J Trauma - Injury Infect Crit Care* (2010) 69(3):620–6. doi: 10.1097/TA.0b013e3181bbfe2a
7. Teixeira PGR, Inaba K, Hadjizacharia P, Brown C, Salim A, Rhee P, et al. Preventable or Potentially Preventable Mortality at a Mature Trauma Center. *J Trauma* (2007) 63(6):1338–47. doi: 10.1097/TA.0b013e31815078ae
8. Lord JM, Midwinter MJ, Chen YF, Belli A, Brohi K, Kovacs EJ, et al. The Systemic Immune Response to Trauma: An Overview of Pathophysiology and Treatment. *Lancet* (2014) 384:1455–65. Lancet Publishing Group. doi: 10.1016/S0140-6736(14)60687-5
9. Sauaia A, Moore EE, Johnson JL, Chin TL, Banerjee A, Sperry JL, et al. Temporal Trends of Postinjury Multiple-Organ Failure: Still Resource Intensive, Morbid, and Lethal. *J Trauma Acute Care Surg* (2014) 76(3):582. doi: 10.1097/TA.0000000000000147
10. Relja B, Mörs K, Marzi I. Danger Signals in Trauma. *Eur J Trauma Emergency Surg* (2018) 44(3):301. doi: 10.1007/s00068-018-0962-3
11. Chen GY, Nuñez G. Sterile Inflammation: Sensing and Reacting to Damage. *Nat Rev Immunol* (2010) 10:826–37. NIH Public Access. doi: 10.1038/nri2873
12. Halbgebauer R, Braun CK, Denk S, Mayer B, Cinelli P, Radermacher P, et al. Hemorrhagic Shock Drives Glycocalyx, Barrier and Organ Dysfunction Early After Polytrauma. *J Crit Care* (2018) 44:229–37. doi: 10.1016/j.jcrc.2017.11.025
13. Manson J, Thiemermann C, Brohi K. Trauma Alarmins as Activators of Damage-Induced Inflammation. *Br J Surg* (2012) 99:12–20. doi: 10.1002/bjs.7717
14. Jackman RP, Utter GH, Muench MO, Heitman JW, Munz MM, Jackman RW, et al. Distinct Roles of Trauma and Transfusion in Induction of Immune Modulation After Injury. *Transfusion* (2012) 52(12):2533–50. doi: 10.1111/j.1537-2995.2012.03618.x
15. Calandra T, Bernhagen J, Metz CN, Spiegel LA, Bacher M, Donnelly T, et al. MIF as a Glucocorticoid-Induced Modulator of Cytokine Production. *Nature* (1995) 377(6544):68–71. doi: 10.1038/377068a0
16. Bacher M, Metz CN, Calandra T, Mayer K, Chesney J, Lohoff M, et al. An Essential Regulatory Role for Macrophage Migration Inhibitory Factor in T-Cell Activation. *Proc Natl Acad Sci USA* (1996) 93(15):7849. doi: 10.1073/pnas.93.15.7849
17. Donnelly SC, Bucala R. Macrophage Migration Inhibitory Factor: A Regulator of Glucocorticoid Activity With a Critical Role in Inflammatory Disease. *Mol Med Today* (1997) 3:502–7. doi: 10.1016/S1357-4310(97)01133-7
18. Bozza M, Satoskar AR, Lin G, Lu B, Humbles AA, Gerard C, et al. Targeted Disruption of Migration Inhibitory Factor Gene Reveals its Critical Role in Sepsis. *J Exp Med* (1999) 189(2):341–6. doi: 10.1084/jem.189.2.341
19. Mitchell RA, Liao H, Chesney J, Fingerle-Rowson G, Baugh J, David J, et al. Macrophage Migration Inhibitory Factor (MIF) Sustains Macrophage Proinflammatory Function by Inhibiting P53: Regulatory Role in the Innate Immune Response. *Proc Natl Acad Sci* (2002) 99:345–50. doi: 10.1073/pnas.012511599
20. Calandra T, Roger T. Macrophage Migration Inhibitory Factor: A Regulator of Innate Immunity. *Nat Rev Immunol* (2003) 30:S27–35. doi: 10.1002/0471203076.emm0331
21. Rodríguez-Sosa M, Rosas LE, David JR, Bojalil R, Satoskar AR, Terrazas LI. Macrophage Migration Inhibitory Factor Plays a Critical Role in Mediating Protection Against the Helminth Parasite Taenia Crassiceps. *Infection Immun* (2003) 71(3):1247. doi: 10.1128/IAI.71.3.1247-1254.2003
22. Onodera S, Kaneda K, Mizue Y, Koyama Y, Fujinaga M, Nishihira J. Macrophage Migration Inhibitory Factor Up-Regulates Expression of Matrix Metalloproteinases in Synovial Fibroblasts of Rheumatoid Arthritis. *J Biol Chem* (2000) 275(1):444–50. doi: 10.1074/jbc.275.1.444
23. Onodera S, Nishihira J, Iwabuchi K, Koyama Y, Yoshida K, Tanaka S, et al. Macrophage Migration Inhibitory Factor Up-Regulates Matrix Metalloproteinase-9 and -13 in Rat Osteoblasts: Relevance To Intracellular Signaling Pathways. *J Biol Chem* (2002) 277(10):7865–74. doi: 10.1074/jbc.M106020200
24. Calandra T, Bernhagen J, Mitchell RA, Bucala R. The Macrophage is an Important and Previously Unrecognized Source of Macrophage Migration Inhibitory Factor. *J Exp Med* (1994) 179(6):1895–902. doi: 10.1084/jem.179.6.1895
25. Calandra T, Echtenacher B, le Roy D, Pugin J, Metz CN, Hültner L, et al. Protection From Septic Shock by Neutralization of Macrophage Migration Inhibitory Factor. *Nat Med* (2000) 6(2):164–70. doi: 10.1038/72262
26. Benigni F, Atsumi T, Calandra T, Metz C, Echtenacher B, Peng T, et al. The Proinflammatory Mediator Macrophage Migration Inhibitory Factor Induces Glucose Catabolism in Muscle. *J Clin Invest* (2000) 106(10):1291. doi: 10.1172/JCI9900
27. Baugh JA, Bucala R. Macrophage Migration Inhibitory Factor. *Crit Care Med* (2002) 30(1 Suppl):S27–35. doi: 10.1097/00003246-200201001-00004
28. Calandra T, Bucala R. Macrophage Migration Inhibitory Factor: A Counter-Regulator of Glucocorticoid Action and Critical Mediator of Septic Shock. *J Inflammation* (1995) 47(1–2):39–51.
29. Joshi PC, Poole GV, Sachdev V, Zhou X, Jones Q. Trauma Patients With Positive Cultures Have Higher Levels of Circulating Macrophage Migration Inhibitory Factor (MIF). *Res Commun Mol Pathol Pharmacol* (2000) 107(1–2):13–20.
30. Chuang C-C, Hung C-J, Tsai M-C, Yeh T-M, Chuang Y-C. High Concentrations of Circulating Macrophage Migration Inhibitory Factor in Patients With Severe Blunt Trauma: Is Serum Macrophage Migration Inhibitory Factor Concentration a Valuable Prognostic Factor? *Crit Care Med* (2004) 32(3):734–9. doi: 10.1097/01.CCM.0000117170.13320.F4
31. Hayakawa M, Katabami K, Wada T, Minami Y, Sugano M, Shimojima H, et al. Imbalance Between Macrophage Migration Inhibitory Factor and Cortisol Induces Multiple Organ Dysfunction in Patients With Blunt Trauma. *Inflammation* (2010) 34(3):193–7. doi:10.1007/s10753-010-9223-2
32. Shih HC, Huang MS, Lee CH. Polymorphonuclear Cell Priming Associated With NF-kB Activation in Patients With Severe Injury is Partially Dependent on Macrophage Migration Inhibitory Factor. *J Am Coll Surgeons* (2010) 211 (6):791–7. doi: 10.1016/j.jamcollsurg.2010.07.028
33. Xiao W, Mindrinos MN, Seok J, Cuschieri J, Cuenca AG, Gao H, et al. A Genomic Storm in Critically Injured Humans. *J Exp Med* (2011) 208(13):2581. doi: 10.1084/jem.20111354
34. von Elm E, Altman DG, Egger M, Pocock SJ, Gøtzsche PC, Vandenbroucke JP. The Strengthening the Reporting of Observational Studies in Epidemiology (STROBE) Statement: Guidelines for Reporting Observational Studies. *Lancet (London England)* (2007) 370(9596):1453–7. doi: 10.1016/S0140-6736(07)61602-X
35. Sordi R, Chiazza F, Collotta D, Migliaretti G, Colas RA, Vulliamy P, et al. Resolvin D1 Attenuates the Organ Injury Associated With Experimental Hemorrhagic Shock. *Ann Surg* (2021) 273(5):1012–21. doi: 10.1097/SLA.0000000000003407
36. Patel NM, Oliveira FRMB, Ramos HP, Aimaretti E, Alves GF, Coldewey SM, et al. Inhibition of Bruton's Tyrosine Kinase Activity Attenuates Hemorrhagic Shock-Induced Multiple Organ Dysfunction in Rats. *Ann Surg* (2021). doi: 10.1097/SLA.0000000000005357
37. Sordi R, Nandra KK, Chiazza F, Johnson FL, Cabrera CP, Torrance HD, et al. Artesunate Protects Against the Organ Injury and Dysfunction Induced by Severe Hemorrhage and Resuscitation. *Ann Surg* (2017) 265:408–17. doi: 10.1097/SLA.0000000000001664
38. Yamada N, Martin LB, Zechendorf E, Purvis GSD, Chiazza F, Varrone B, et al. Novel Synthetic, Host-Defense Peptide Protects Against Organ Injury/Dysfunction in a Rat Model of Severe Hemorrhagic Shock. *Ann Surg* (2018) 268:348–56. doi: 10.1097/SLA.0000000000002186
39. Thiemermann C, Szabo C, Mitchell JA, Vane JR. Vascular Hyporeactivity to Vasoconstrictor Agents and Hemodynamic Decompensation in Hemorrhagic Shock is Mediated by Nitric Oxide. *Proc Natl Acad Sci USA* (1993) 90(1):267–71. doi: 10.1073/pnas.90.1.267

40. Al-Abed Y, Dabideen D, Aljabari B, Valster A, Messmer D, Ochani M, et al. ISO-1 Binding to the Tautomerase Active Site of MIF Inhibits its Pro-Inflammatory Activity and Increases Survival in Severe Sepsis. *J Biol Chem* (2005) 280:36541–4. doi: 10.1074/jbc.C500243200
41. Wang B, Zhao K, Hu W, Ding Y, Wang W. Protective Mechanism of MIF Inhibitor ISO-1 on Intrahepatic Bile Duct Cells in Rats With Severe Acute Pancreatitis. *Digestive Dis Sci* (2021) 66(10):3415–26. doi: 10.1007/s10620-020-06674-9
42. Li M, Yu J, Zhao L, Mei F-C, Zhou Y, Hong Y-P, et al. Inhibition of Macrophage Migration Inhibitory Factor Attenuates Inflammation and Fetal Kidney Injury in a Rat Model of Acute Pancreatitis in Pregnancy. *Int Immunopharmacol* (2019) 68:106–14. doi: 10.1016/j.intimp.2018.12.068
43. Zhou Y, Zhao L, Mei F, Hong Y, Xia H, Zuo T, et al. Macrophage Migration Inhibitory Factor Antagonist (S,R)3-(4-hydroxyphenyl)-4,5-dihydro-5-isoxazole Acetic Acid Methyl Ester Attenuates Inflammation and Lung Injury in Rats With Acute Pancreatitis in Pregnancy. *Mol Med Rep* (2018) 17(5):6576–84. doi: 10.3892/mmr.2018.8672
44. Liu Y, Liu Y, Wang Q, Song Y, Chen S, Cheng B, et al. MIF Inhibitor ISO-1 Alleviates Severe Acute Pancreatitis-Associated Acute Kidney Injury by Suppressing the NLRP3 Inflammasome Signaling Pathway. *Int Immunopharmacol* (2021) 96:107555. doi: 10.1016/j.intimp.2021.107555
45. Guo ZD, Zhao L, Wang P, Deng WH, Shi Q, Zuo T, et al. Fetal Liver Injury Ameliorated by Migration Inhibitory Factor Inhibition in a Rat Model of Acute Pancreatitis in Pregnancy. *J Obstetrics Gynaecol Res* (2018) 44(3):374–83. doi: 10.1111/jog.13538
46. Zhu C, Liu Y, Song Y, Wang Q, Liu Y, Yang S, et al. Deletion of Macrophage Migration Inhibitory Factor Ameliorates Inflammation in Mice Model Severe Acute Pancreatitis. *Biomedicine Pharmacotherapy = Biomedecine pharmacotherapie* (2020) 125:109919. doi: 10.1016/j.biopha.2020.109919
47. Hou XQ, Gao YW, Yang ST, Wang CY, Ma ZY, Xia XZ. Role of Macrophage Migration Inhibitory Factor in Influenza H5N1 Virus Pneumonia. *Acta Virologica* (2009) 53(4):225–31. doi: 10.4149/av_2009_04_225
48. Chen PF, Luo YL, Wang W, Wang JX, Lai WY, Hu SM, et al. ISO-1, a Macrophage Migration Inhibitory Factor Antagonist, Inhibits Airway Remodeling in a Murine Model of Chronic Asthma. *Mol Med* (2010) 16(9–10):400–8. doi: 10.2119/molmed.2009.00128
49. Russell KE, Chung KF, Clarke CJ, Durham AL, Mallia P, Footitt J, et al. The MIF Antagonist ISO-1 Attenuates Corticosteroid-Insensitive Inflammation and Airways Hyperresponsiveness in an Ozone-Induced Model of COPD. *PloS One* (2016) 11(1):e0146102. doi: 10.1371/journal.pone.0146102
50. Vera PL, Iczkowski KA, Howard DJ, Jiang L, Meyer-Siegler KL. Antagonism of Macrophage Migration Inhibitory Factor Decreases Cyclophosphamide Cystitis in Mice. *Neurourology Urodynamics* (2010) 29(8):1451–7. doi: 10.1002/nau.20878
51. Shah YM, Ito S, Morimura K, Chen C, Yim SH, Haase VH, et al. Hypoxia-Inducible Factor Augments Experimental Colitis Through a MIF-Dependent Inflammatory Signaling Cascade. *Gastroenterology* (2008) 134(7):2036. doi: 10.1053/j.gastro.2008.03.009
52. Cho YD, Choi SH, Kim JY, Park SJ, Yoon YH, Cho HJ, et al. Macrophage Migration Inhibitory Factor Levels Correlate With an Infection in Trauma Patients. *Ulusal travma ve acil cerrahi dergisi = Turkish J Trauma Emergency surgery: TJTES* (2017) 201723(3):193–8. doi: 10.5505/tjtes.2016.04780
53. Senftleben U, Karin M. The IKK/NF-Kappa B Pathway. *Crit Care Med* (2002) 30:S18–26. doi: 10.1097/00003246-200201001-00003
54. Liu SF, Malik AB. NF-κb Activation as a Pathological Mechanism of Septic Shock and InflammationAmerican Journal of Physiology - Lung Cellular and Molecular Physiology. *Am J Physiol Lung Cell Mol Physiol* (2006) 290:L622–45. doi: 10.1152/ajplung.00477.2005.
55. Roger T, David J, Glauser MP, Calandra T. MIF Regulates Innate Immune Responses Through Modulation of Toll-Like Receptor 4. *Nature* (2001) 414 (6866):920–4. doi: 10.1038/414920a
56. Kim MJ, Kim WS, Kim DO, Byun JE, Huy H, Lee SY, et al. Macrophage Migration Inhibitory Factor Interacts With Thioredoxin-Interacting Protein and Induces NF-κb Activity. *Cell signalling* (2017) 34:110–20. doi: 10.1016/j.cellsig.2017.03.007
57. Dinarello CA. Biologic Basis for Interleukin-1 in Disease. *Blood* (1996) 87:2095–147. American Society of Hematology. doi: 10.1182/blood.V87.6.2095.bloodjournal8762095
58. Lang T, Lee JPW, Elgass K, Pinar AA, Tate MD, Aitken EH, et al. Macrophage Migration Inhibitory Factor is Required for NLRP3 Inflammasome Activation. *Nat Commun* (2018) 9(1):1–15. doi: 10.1038/s41467-018-04581-2
59. Shin MS, Kang Y, Wahl ER, Park HJ, Lazova R, Leng L, et al. Macrophage Migration Inhibitory Factor Regulates U1 Small Nuclear RNP Immune Complex-Mediated Activation of the NLRP3 Inflammasome. *Arthritis Rheumatol (Hoboken NJ)* (2019) 71(1):109–20. doi: 10.1002/art.40672
60. Chen CC, Manning AM. Transcriptional Regulation of Endothelial Cell Adhesion Molecules: A Dominant Role for NF-κb. *Agents Actions Suppl* (1995) 47:135–41. doi: 10.1007/978-3-0348-7343-7_12
61. Collins T, Read MA, Neish AS, Whitley MZ, Thanos D, Maniatis T. Transcriptional Regulation of Endothelial Cell Adhesion Molecules: NF-κb and Cytokine-Inducible Enhancers. *FASEB J* (1995) 9(10):899–909. doi: 10.1096/fasebj.9.10.7542214
62. Campbell SJ, Anthony DC, Oakley F, Carlsen H, Elsharkawy AM, Blomhoff R, et al. Hepatic Nuclear Factor κb Regulates Neutrophil Recruitment to the Injured Brain. *J Neuropathology Exp Neurol* (2008) 67(3):223–30. doi: 10.1097/NEN.0b013e3181654957
63. Hayden MS, Ghosh S. NF-κb in Immunobiology. *Cell Res* (2011) 21(2):223–44. doi: 10.1038/cr.2011.13
64. Makita H, Nishimura M, Miyamoto K, Nakano T, Tanino Y, Hirokawa J, et al. Effect of Anti-Macrophage Migration Inhibitory Factor Antibody on Lipopolysaccharide-Induced Pulmonary Neutrophil Accumulation. *Am J Respir Crit Care Med* (1998) 158(2):573–9. doi: 10.1164/ajrccm.158.2.9707086
65. Bernhagen J, Krohn R, Lue H, Gregory JL, Zernecke A, Koenen RR, et al. MIF is a Noncognate Ligand of CXC Chemokine Receptors in Inflammatory and Atherogenic Cell Recruitment. *Nat Med* (2007) 13(5):587–96. doi: 10.1038/nm1567
66. Gregory JL, Leech MT, David JR, Yang YH, Dacumos A, Hickey MJ. Reduced Leukocyte–Endothelial Cell Interactions in the Inflamed Microcirculation of Macrophage Migration Inhibitory Factor–Deficient Mice. *Arthritis Rheumatism* (2004) 50(9):3023–34. doi: 10.1002/art.20470
67. David JR. Delayed Hypersensitivity *In Vitro*: Its Mediation by Cell-Free Substances Formed by Lymphoid Cell-Antigen Interaction. *Proc Natl Acad Sci* (1966) 56(1):72–7. doi: 10.1073/pnas.56.1.72
68. Bloom BR, Bennett B. Mechanism of a Reaction in Vitro Associated With Delayed-Type Hypersensitivity. *Science* (1966) 153(3731):80–2. doi: 10.1126/science.153.3731.80
69. Leech M, Metz C, Santos L, Peng T, Holdsworti-I SR, Bucala R, et al. Involvement of Macrophage Migration Inhibitory Factor in the Evolution of Rat Adjuvant Arthritis. *Arthritis Rheumatism* (1998) 41(5):910–7. doi: 10.1002/1529-0131(199805)41:5<910::AID-ART19>3.0.CO;2-E
70. Burger-Kentischer A, Göbel H, Kleemann R, Zernecke A, Bucala R, Leng L, et al. Reduction of the Aortic Inflammatory Response in Spontaneous Atherosclerosis by Blockade of Macrophage Migration Inhibitory Factor (MIF). *Atherosclerosis* (2006) 184(1):28–38. doi: 10.1016/j.atherosclerosis.2005.03.028
71. Schober A, Bernhagen J, Thiele M, Zeiffer U, Knarren S, Roller M, et al. Stabilization of Atherosclerotic Plaques by Blockade of Macrophage Migration Inhibitory Factor After Vascular Injury in Apolipoprotein E-Deficient Mice. *Circulation* (2004) 109(3):380–5. doi: 10.1161/01.CIR.0000109201.72441.09
72. Gregory JL, Morand EF, McKeown SJ, Ralph JA, Hall P, Yang YH, et al. Macrophage Migration Inhibitory Factor Induces Macrophage Recruitment *via* CC Chemokine Ligand 2. *J Immunol* (2006) 177(11):8072–9. doi: 10.4049/jimmunol.177.11.8072

Conflict of Interest: The authors declare that the research was conducted in the absence of any commercial or financial relationships that could be construed as a potential conflict of interest.

Article VI

frontiers | Frontiers in Immunology

TYPE Original Research
PUBLISHED 02 September 2022
DOI 10.3389/fimmu.2022.992614

OPEN ACCESS

EDITED BY
Laura Dugo,
Campus Bio-Medico University, Italy

REVIEWED BY
Rosanna Di Paola,
University of Messina, Italy
Valerio Chiurchiù,
National Research Council, CNR, Italy

*CORRESPONDENCE
Massimo Collino
massimo.collino@unito.it

†These authors have contributed equally to this work

SPECIALTY SECTION
This article was submitted to Inflammation, a section of the journal Frontiers in Immunology

RECEIVED 12 July 2022
ACCEPTED 08 August 2022
PUBLISHED 02 September 2022

CITATION
Alves GF, Stoppa I, Aimaretti E, Monge C, Mastrocola R, Porchietto E, Einaudi G, Collotta D, Bertocchi I, Boggio E, Gigliotti CL, Clemente N, Aragno M, Fernandes D, Cifani C, Thiemermann C, Dianzani C, Dianzani U and Collino M (2022) ICOS-Fc as innovative immunomodulatory approach to counteract inflammation and organ injury in sepsis.
Front. Immunol. 13:992614.
doi: 10.3389/fimmu.2022.992614

ICOS-Fc as innovative immunomodulatory approach to counteract inflammation and organ injury in sepsis

Gustavo Ferreira Alves[1], Ian Stoppa[2], Eleonora Aimaretti[3], Chiara Monge[4], Raffaella Mastrocola[3], Elisa Porchietto[5], Giacomo Einaudi[5], Debora Collotta[1], Ilaria Bertocchi[1], Elena Boggio[2], Casimiro Luca Gigliotti[2], Nausicaa Clemente[2], Manuela Aragno[3], Daniel Fernandes[6], Carlo Cifani[5], Christoph Thiemermann[7], Chiara Dianzani[4], Umberto Dianzani[2†] and Massimo Collino[1*†]

[1]Department of Neurosciences (Rita Levi Montalcini), University of Turin, Turin, Italy, [2]Department of Health Sciences, Università del Piemonte Orientale, Novara, Italy, [3]Department of Clinical and Biological Sciences, University of Turin, Turin, Italy, [4]Department of Drug Science and Technology, University of Turin, Turin, Italy, [5]Pharmacology Unit, School of Pharmacy, University of Camerino, Camerino, Italy, [6]Department of Pharmacology, Federal University of Santa Catarina, Florianópolis, Brazil, [7]William Harvey Research Institute, Bart's and The London School of Medicine and Dentistry, Queen Mary University of London, London, United Kingdom

Inducible T cell co-stimulator (ICOS), an immune checkpoint protein expressed on activated T cells and its unique ligand, ICOSL, which is expressed on antigen-presenting cells and non-hematopoietic cells, have been extensively investigated in the immune response. Recent findings showed that a soluble recombinant form of ICOS (ICOS-Fc) can act as an innovative immunomodulatory drug as both antagonist of ICOS and agonist of ICOSL, modulating cytokine release and cell migration to inflamed tissues. Although the ICOS-ICOSL pathway has been poorly investigated in the septic context, a few studies have reported that septic patients have reduced ICOS expression in whole blood and increased serum levels of osteopontin (OPN), that is another ligand of ICOSL. Thus, we investigated the pathological role of the ICOS-ICOSL axis in the context of sepsis and the potential protective effects of its immunomodulation by administering ICOS-Fc in a murine model of sepsis. Polymicrobial sepsis was induced by cecal ligation and puncture (CLP) in five-month-old male wild-type (WT) C57BL/6, $ICOS^{-/-}$, $ICOSL^{-/-}$ and $OPN^{-/-}$ mice. One hour after the surgical procedure, either CLP or Sham (control) mice were randomly assigned to receive once ICOS-Fc, ^{F119S}ICOS-Fc, a mutated form uncapable to bind ICOSL, or vehicle intravenously. Organs and plasma were collected 24 h after surgery for analyses. When compared to Sham mice, WT mice that underwent CLP developed within 24 h a higher clinical severity score, a reduced body temperature, an increase in plasma cytokines (TNF-α, IL-1β, IL-6, IFN-γ and IL-10), liver injury (AST and ALT) and kidney (creatinine and urea) dysfunction. Administration of ICOS-Fc to WT CLP mice reduced all of these abnormalities caused by sepsis. Similar beneficial effects were not seen in CLP-mice

10.3389/fimmu.2022.992614

treated with ^{F119S}ICOS-Fc. Treatment of CLP-mice with ICOS-Fc also attenuated the sepsis-induced local activation of FAK, P38 MAPK and NLRP3 inflammasome. ICOS-Fc seemed to act at both sides of the ICOS-ICOSL interaction, as the protective effect was lost in septic knockout mice for the ICOS or ICOSL genes, whereas it was maintained in OPN knockout mice. Collectively, our data show the beneficial effects of pharmacological modulation of the ICOS-ICOSL pathway in counteracting the sepsis-induced inflammation and organ dysfunction.

KEYWORDS

sepsis, inflammation, ICOS (inducible co-stimulatory molecule), cecal ligation and puncture, osteopontin (OPN)

Introduction

Sepsis is a life-threatening medical emergency characterized by a complex interplay of pro- and anti-inflammatory host responses, resulting in multiple organ dysfunction that can ultimately lead to death (1). Currently, deaths from sepsis correspond to nearly 20% of all deaths worldwide, and there is still no specific treatment available (2). The inducible T cell co-stimulator (ICOS, also known as CD278) belongs to the CD28 family of co-stimulatory immunoreceptors. It is a type I transmembrane glycoprotein whose expression is rapidly upregulated upon T cells activation (3). ICOS binds to its unique ligand (ICOSL, also known as CD275 or B7h), a member of the B7 family highly expressed on antigen-presenting cells (APCs) and non-hematopoietic cells under inflammatory stimuli (4–5). Thus far, the role of ICOS-ICOSL interaction has been poorly investigated in sepsis, although recent findings report that ICOS expression is reduced in whole blood of septic patients (6), and that reduced ICOS levels are strongly associated with organ dysfunction (7). To date, it is very well documented that the ICOS-ICOSL axis may display bidirectional effects. On the one hand, ICOS triggering modulates cytokine production in activated T cells and contributes to T regulatory (Treg) cells differentiation and survival (8–9). Given the fact that both animals and septic patients have an increased percentage of circulating Treg cells (10–12), it is suggestive that ICOS triggering may play a role in the septic immunosuppressive status. On the other hand, ICOSL triggering by ICOS may exert anti-inflammatory effects *via* responses, such as modulating the maturation and migration of macrophage and dendritic cells and the endothelial cell adhesiveness (13).

Recently, another ligand for ICOSL has been identified, osteopontin (OPN), an inflammatory mediator that binds to ICOSL in an alternative binding domain to that used by ICOS. Intriguingly, ICOS and OPN exert different and often opposite effects upon ICOSL triggering since OPN stimulates, whereas ICOS inhibits, migration of several cell types and tumor angiogenesis (14–16). Conventionally, a soluble recombinant form of ICOS (ICOS-Fc) has been designed by fusing a cloned extracellular portion of human or mouse ICOS with an Fc IgG1 portion and this molecule has been shown to trigger ICOSL thus promoting down-stream responses (17).

In vitro, ICOS-Fc inhibits adhesiveness of endothelial cells toward polymorphonuclear cells and tumor cells and migration of endothelial cells and tumor cells (15). These ICOS-Fc effects can also be recorded in dendritic cells (DC), along with modulated cytokine release and antigen cross-presentation in class I major histocompatibility complex molecules (13), while in osteoclasts, ICOS-Fc inhibits differentiation and function (18). *In vivo*, ICOS-Fc inhibits tumor growth and metastasis, development of osteoporosis, liver damage induced by acute inflammation following treatment with CCl4, and it favors skin wound healing (18–21). Nevertheless, little is known about the molecular mechanism(s) involved in ICOSL-mediated inflammatory response. The p38 MAPK, a well-known mediator that drives inflammation through upregulation of several pro-inflammatory cytokines such as TNF-α and IL-6 (22), and the NOD-like receptor protein 3 (NLRP3) inflammasome, able to induce the release of IL-1β and IL-18 and promote cell death by pyroptosis (23), are two of the most well characterized signaling pathways involved in the activation of the cytokine storm that contributes to organ dysfunction during sepsis. Furthermore, their pharmacological or genetic inhibition has been shown to reduce sepsis-related mortality (22–24). Finally, a non-receptor protein kinase namely Focal adhesion kinase (FAK) has been recently reported to signal inflammation downstream of the Toll-like receptor 4 upon lipopolysaccharide (LPS) challenge in macrophages and lung tissues (25). Therefore, here we investigated, for the first time, the pathological role of ICOS-ICOSL axis in the context of sepsis, its impact on selective inflammatory pathways and the potential protective effects of its

immunomodulation by administering ICOS-Fc in an experimental model of sepsis.

Material and methods

Animals and ethical statement

Inbred wild-type (WT, C57BL/6) mice, ICOSL knockout mice (ICOSL$^{-/-}$, B6.129P2-*Icosl*^{tm1Mak}/J), ICOS knockout mice (ICOS$^{-/-}$, B6.129P2-*Icos*^{tm1Mak}/J) and OPN knockout mice (OPN$^{-/-}$, B6.129S6(Cg)-*Spp1*^{tm1Blh}/J) were purchased from Envigo laboratories, (IT) and The Jackson Laboratory (Bar Harbor, ME, USA). Mice were housed under standard laboratory conditions, such as room temperature (25 ± 2°C) and light-controlled with free access to water and rodent chow for four weeks prior starting the experimental procedures. All animal protocols reported in this study followed the ARRIVE guidelines (26) and the recommendations for preclinical studies of sepsis provided by the MQTiPSS (27) The procedures were approved by the University's Institutional Ethics Committee as well as the National Authorities (Protocol number: 855/2021).

Cecal ligation and puncture (CLP)-induced sepsis model

Polymicrobial sepsis was carried out by CLP surgery in male, five-month-old mice. Mice were initially placed in an anesthetisia chamber (3% isoflurane -IsoFlo, Abbott Laboratories – delivered in oxygen 0.4 L/min), then kept under anaesthesia throughout surgery with 2% isoflurane delivered in oxygen 0.4 L/min *via* a nosecone. The body temperature was maintained at 37 °C through a homoeothermic blanket and constantly monitored by a rectal thermometer. Briefly, a mid-line laparotomy (~1.0 cm) was performed in the abdomen, exposing the cecum. The cecum was then totally ligated just below the ileocecal valve and a G-21 needle was used to puncture the ligated cecum in a single through-and-through manner. A small amount (droplet, ~3mm) of fecal content was released from the cecum which was carefully relocated into the peritoneum. Sham mice underwent the same surgical procedure, but without CLP. All animals received Carprofen (5 mg/kg, s.c.) as an analgesic agent and resuscitation fluid (0.9% NaCl, 50 mL/kg, s.c.) at 37°C. Mice were constantly monitored post-surgical and then placed back into fresh clean cages.

At 24 h, body temperature and a clinical score to assess symptoms consistent with murine sepsis were recorded blindly. The following 6 criteria were used for the clinical score: lethargy, piloerection, tremors, periorbital exudates, respiratory distress and diarrhea. An observed clinical score >3 was considered as severe sepsis, while a score between 3 and 1 was considered as moderate sepsis (28).

Study design

Seventy-two mice were randomized into eight groups (9 mice per group): Sham + Vehicle, CLP + Vehicle, CLP + ICOS-Fc, CLP + ^{F119S}ICOS-Fc, CLP ICOSL$^{-/-}$ + Vehicle, CLP ICOS$^{-/-}$ + Vehicle, CLP ICOS$^{-/-}$ + ICOS-Fc and OPN$^{-/-}$ + Vehicle. Treatment was given once one hour after surgery, where mice received either ICOS-Fc (100 µg each), ^{F119S}ICOS-Fc (100 µg each) or Vehicle (PBS, pH 7.4, 100 µl each) by intravenous injection (Figure 1).

Blood collection and organ harvesting

Twenty-four h after surgery all mice were anesthetized with isoflurane (3%) delivered in oxygen (0.4 L/min) and euthanized by cardiac exsanguination. Whole blood was withdrawn from each mouse in vials (EDTA 17.1 µM/mL) and plasma content was obtained after centrifugation (13,000 *g*, 10 min at R.T.). Organ samples (liver and kidney) were harvested and placed in cryotubes which were snap frozen in liquid nitrogen for storage at freezer -80°C. The samples were then analyzed in a blinded fashion (Figure 1).

Biomarkers of organ injury and systemic inflammation

Plasma samples were used to measure systemic levels of aspartate aminotransferase (AST) (#7036) and alanine aminotransferase (ALT) (#7018) (as markers of hepatocellular injury), creatinine (#7075) and urea (#7144) (as markers of renal dysfunction) using colorimetric clinical assay kits (FAR Diagnostics, Verona, Italy) according to the manufacturer's instructions. Systemic cytokine levels were determined in plasma using the Luminex suspension bead-based multiplexed Bio-Plex Pro™ Mouse Cytokine Th17 Panel A 6-Plex (#M6000007NY) assay (Bio-Rad, Kabelsketal, Germany). The cytokines (IL-1β, IL-6, TNF-α, IFN-γ, IL-17 and IL-10) were measured following the manufacturer's instructions.

Myeloperoxidase (MPO) activity analysis

MPO activity analysis was carried out in liver and kidney samples as previously described (29). Tissue samples (~100 mg) were homogenized (1:5 w-v) in 20 mM PBS (pH 7.4) and then centrifuged at 4°C (13,000 g, 10 min). Pellets were resuspended in

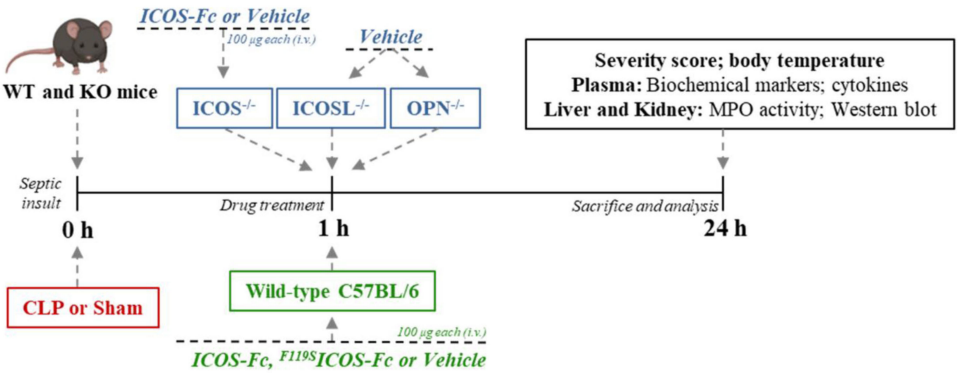

FIGURE 1
Timeline of the experimental design to investigate the role of ICOS-Fc in sepsis. Wild-type mice and/or ICOSL, ICOS and OPN knockout mice were randomly selected to undergo either Sham or CLP surgery. One hour later, mice received once either Vehicle (PBS, 100 µL), ICOS-Fc (100 µg) or ^{F119S}ICOS-Fc (100 µg) intravenously. At 24 h all parameters were analyzed.

500 µL of hexadecyltrimethylammonium bromide buffer (0.5% HTAB in 50 mM PBS, pH 6.0). A second centrifugation at 4°C (13,000 g, 10 min was performed and the supernatants (30 µL) were assessed for MPO activity by measuring spectrophotometrically (650 nm) the H_2O_2-dependent oxidation of 3,3′,5,5′-tetramethylbenzidine (TMB). Bicinchoninic acid (BCA) protein assay (Pierce Biotechnology Inc., Rockford, IL, USA) was used to quantify the protein content in the final supernatant. MPO activity was expressed as optical density (O.D.) at 650 nm per mg of protein.

Western blot analysis

Semi-quantitative immunoblot technique was carried out in hepatic and renal tissue samples as previously described (30). Total proteins were extracted from 50 mg of each tissue and the total content was quantified using BCA protein method following the manufacturer's instructions. Briefly, total proteins (50 µg/well) were separated by 8 and 10% sodium dodecyl sulphate-polyacrylamide gel electrophoresis (SDS-PAGE) and transferred to a polyvinylidene difluoride (PVDF) membrane, which was then blocked with 5% non-fat dry milk prepared in TBS-T buffer for 1 h at RT, followed by incubation with primary antibodies at the dilution 1:1000., rabbit anti-Thr^{180}/anti-Tyr^{182} p38 (Cell Signaling #9211); rabbit anti-total p38 (Cell Signaling #9212); mouse anti-NRLP3 (Adipogen- AG-20B-0014-C100); rabbit anti-Caspase-1 (Cell Signaling #24232); rabbit anti-Tyr^{397} FAK (Cell Signaling #3283); rabbit anti-total FAK (Cell Signaling #3285). The membranes were then incubated with a secondary antibody conjugated with horseradish peroxidase (HRP) at the dilution 1:10000 for 1 h at RT (anti-mouse or anti-rabbit, Cell Signaling #7076 and #7074, respectively). Afterwards, the membranes were stripped and incubated with rabbit anti-β-actin (Cell Signaling #4970). Immune complexes were visualized by chemiluminescence and the densitometric analysis was performed using Bio-Rad Image Lab Software 6.0.1. Results were normalized to sham bands.

Statistical analysis and data presentation

Sample size was determined on the basis of prior power calculations using G-Power 3.1^{TM} software (31). Data are expressed as dot plots (for each mouse) and as mean ± S.E.M of 9 mice per group. Shapiro-Wilk and Bartlett tests were used to verify data distribution and the homogeneity of variances, respectively. The statistical analysis was performed by one-way ANOVA, followed by Bonferroni's *post-hoc* test. Data not normally distributed, a non-parametric statistical analysis was applied through Kruskal-Wallis followed by Dunn's *post hoc*-test as indicated in the figure legends. Statistical significance was set at $P < 0.05$. Statistical analysis was performed using GraphPad Prism® software version 7.05 (San Diego, California, USA).

Materials

Unless otherwise stated, all reagents were purchased from the Sigma-Aldrich Company Ltd. (St. Louis, Missouri, USA).

Results

ICOS-Fc-mediated immunomodulation attenuates clinical status and organ injury/dysfunction triggered by sepsis

Sepsis was induced by CLP in WT mice treated with vehicle, ICOS-Fc or ^{F119S}ICOS-Fc (unable to bind ICOSL) and clinical scores and body temperature were recorded after 24 h. Moreover, sepsis was induced in mice deficient for ICOS, ICOSL, or OPN to assess the role the endogenous molecules of the ICOS/ICOSL/OPN system. Finally, a group of ICOS-deficient mice received ICOS-Fc treatment to evaluate the effect of the drug in the absence of the endogenous ICOS.

Results showed that, as expected, CLP-induced sepsis in WT mice led to a higher clinical severity score (Figure 2A) when compared to Sham WT mice, which was also associated with lower body temperature (Figure 2B). Intriguingly, treatment with ICOS-Fc improved both clinical score and hyphotermia in WT septic mice, whereas treatment with ^{F119S}ICOS-Fc had no effect (Figures 2A, B). Analysis of CLP knockout mice showed that ICOS$^{-/-}$ and ICOSL$^{-/-}$ mice showed similar clinical scores and decreased body temperatures as WT mice, whereas OPN$^{-/-}$ mice developed milder sepsis, with lower clinical scores and higher body temperature than WT mice. In ICOS$^{-/-}$ mice, treatment with ICOS-Fc induced similar positive effects as in WT mice (Figures 2A, B).

To investigate organ injury or dysfunction, plasma levels of ALT, AST, creatinine and urea were evaluated in these mice. Figure 3 shows that results mirrored those shown in Fig.2: CLP-induced sepsis caused striking increase of ALT, AST, creatinine and urea levels in WT type mice, and these levels were decreased by treatment with ICOS-Fc, but not ^{F119S}ICOS-Fc. Levels of these markers were increased also in CLP ICOS$^{-/-}$ and ICOSL$^{-/-}$ mice and urea levels were even higher in ICOS$^{-/-}$ than in WT mice. In CLP ICOS$^{-/-}$ mice, treatment with ICOS-Fc significantly decreased all these markers. In CLP OPN$^{-/-}$ mice, levels of these markers were significantly lower than in CLP WT mice.

ICOS-Fc administration modulates experimental sepsis-induced cytokine storm

The 6 cytokines were measured systemically in plasma samples by using a multiplex array. Figure 4 shows that, in WT mice, CLP-induced sepsis led to a cytokine storm with significant increase of levels of IL-1β, IL-6, IL-10, TNF-α, IFN-γ and a slight not significant increase of IL-17 compared to Sham mice. Administration of ICOS-Fc to WT CLP mice induced a significant decrease of IL-1β and TNF-α, whereas ^{F119S}ICOS-Fc had no effect. Levels of IL-1β, IL-6, IL-10, TNF-α, and IFN-γ were also increased in CLP ICOS$^{-/-}$ and ICOSL$^{-/-}$ mice at levels similar to those observed in CLP WT mice. Moreover, CLP ICOSL$^{-/-}$ mice showed higher levels of IL-17 than Sham mice, and CLP ICOS$^{-/-}$ mice displayed higher levels of TNF-α and, especially, IL-10 than CLP WT mice. The CLP ICOS$^{-/-}$ mice treated with ICOS-Fc significantly decreased levels of IL-1β, IL-6 and IL-10 compared to the untreated counterparts. In CLP OPN$^{-/-}$ mice, the increase of these cytokines was in general

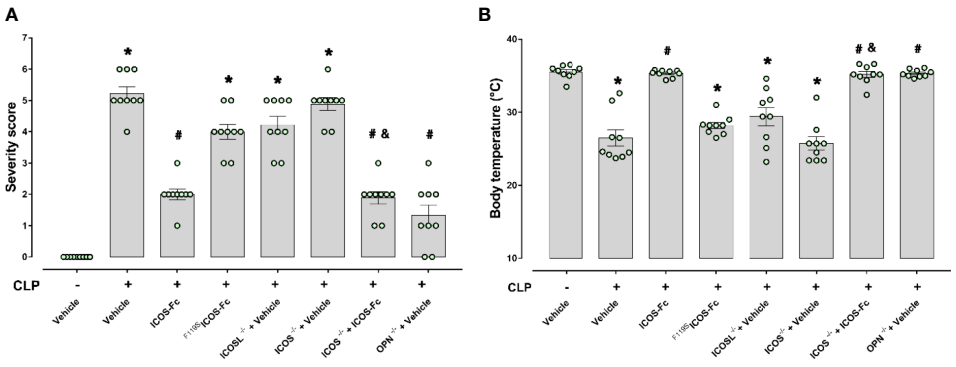

FIGURE 2
Role of the ICOS-ICOSL axis in the clinical status of experimental sepsis. Wild-type mice and/or ICOSL, ICOS and OPN knockout mice were randomly selected to undergo either Sham or CLP surgery. One hour later, mice received once either Vehicle (PBS, 100 µL), ICOS-Fc (100 µg) or ^{F119S}ICOS-Fc (100 µg) intravenously. At 24 h, severity score **(A)** and body temperature **(B)** were recorded. Data are expressed as dot plots (for each animal) and as mean ± S.E.M of 9 mice per group. Severity score was analyzed by a non-parametric test (Kruskal-Wallis) followed by Dunn's *post hoc*-test, whereas a parametric test (one-way ANOVA) followed by Bonferroni's *post hoc*-test was used for body temperature. *p<0.05 *vs* Sham + Vehicle; $^{\#}$p<0.05 *vs* CLP + Vehicle; $^{\&}$p<0.05 *vs* ICOS$^{-/-}$ + Vehicle.

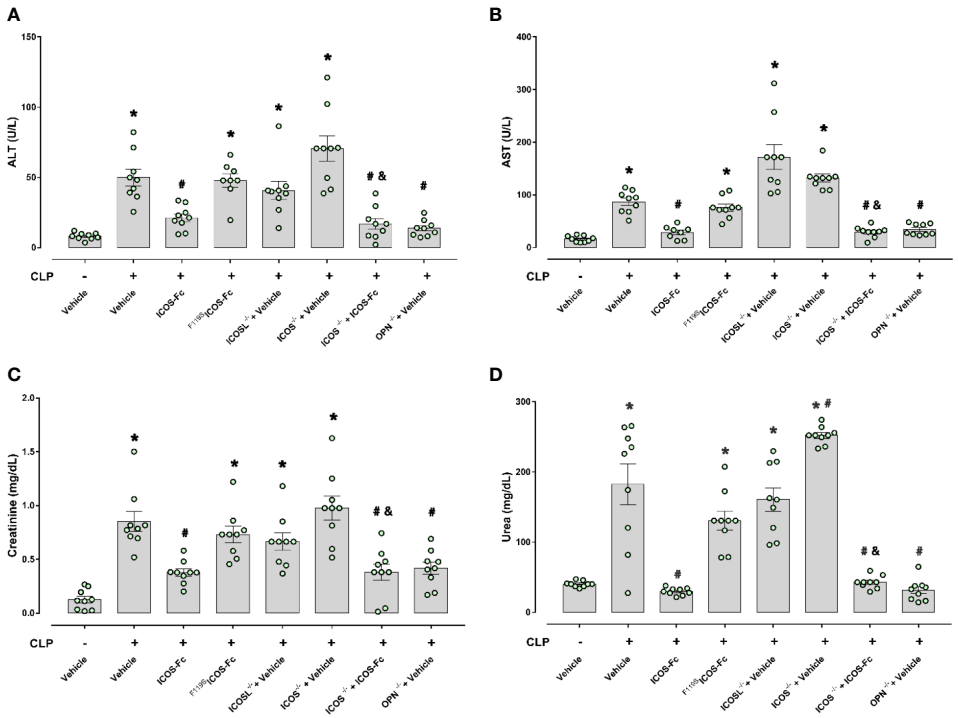

FIGURE 3
Effect of ICOS-ICOSL axis immunomodulation on sepsis-induced organ damage biomarkers. Wild-type mice and/or ICOSL, ICOS and OPN knockout mice were randomly selected to undergo either Sham or CLP surgery. One hour later, mice received once either Vehicle (PBS, 100 µL), ICOS-Fc (100 µg) or ^{F119S}ICOS-Fc (100 µg) intravenously. At 24 h, blood samples were withdrawn from each mouse and plasma levels of alanine transaminase (ALT) **(A)**, aspartate transaminase (AST) **(B)**, creatinine **(C)** and urea **(D)** were determined. Data are expressed as dot plots (for each animal) and as mean ± S.E.M of 9 mice per group. Statistical analysis was performed by one-way ANOVA followed by Bonferroni's *post hoc* test. *p<0.05 *vs* Sham + Vehicle; $^{\#}$p<0.05 *vs* CLP + Vehicle; $^{\&}$p<0.05 *vs* ICOS$^{-/-}$ + Vehicle.

moderate, with levels of IL-6, IL-10, TNF-α and IFN-γ higher than in Sham mice, and levels of IL-1β and IL-6 lower than in CLP WT mice.

ICOS-Fc treatment reduces sepsis-induced increase in MPO activity in the kidney

MPO activity was assessed in the liver and kidney, as an indirect biomarker of leukocyte tissue infiltration (Figure 5). When compared to Sham mice, CLP WT mice had increased MPO activity in both liver and kidney samples, and MPO activity was significanly decreased by ICOS-Fc (but not ^{F119S}ICOS-Fc treatment) in the kidney, but not in the liver. In the liver, MPO activity was similarly increased also in CLP ICOS$^{-/-}$, ICOSL$^{-/-}$, and OPN$^{-/-}$ mice, and it was not modified by ICOS-Fc treatment in CLP ICOS$^{-/-}$ mice. In the kidney, MPO activity was increased in CLP ICOS$^{-/-}$ and ICOSL$^{-/-}$ mice, and treatment with ICOS-Fc decreased MPO activity in CLP ICOS$^{-/-}$ mice. By contrast, CLP OPN$^{-/-}$ mice showed lower MPO levels in the kidney than CLP WT mice.

ICOS-Fc treatment reduces local FAK/p38 signalling and NLRP3 inflammasome activation in septic mice

In order to better elucidate the molecular mechanism underlying the beneficial effects evoked by ICOS-Fc administration, we focused on WT mice investigating the changes in some signaling cascades, previously documented to be affected by the ICOS-ICOSL axis and, at the same time, known to exert key role in sepsis pathogenesis. Western blot analysis showed that CLP mice showed significant increase of the phosphorylation of FAK at Tyr^{397} and p38 MAPK at Thr^{180}/Tyr^{182} in both hepatic (Figures 6A, C) and renal (Figures 6B, D) tissues, when compared to Sham mice. Interestingly, mice treatment with ICOS-Fc significantly attenuated the degree of phosphorylation of FAK/p38 axis in both tissues, thus suggesting reduced activation of these signaling pathways (Figures 6A–D).

We then assessed the activation of the inflammasome, by evaluating the expression of NLRP3 and cleaved caspase-1 in both liver and kidney samples (Figures 6E–H). Results showed that, in both tissues, CLP-induced sepsis significantly increased both

10.3389/fimmu.2022.992614

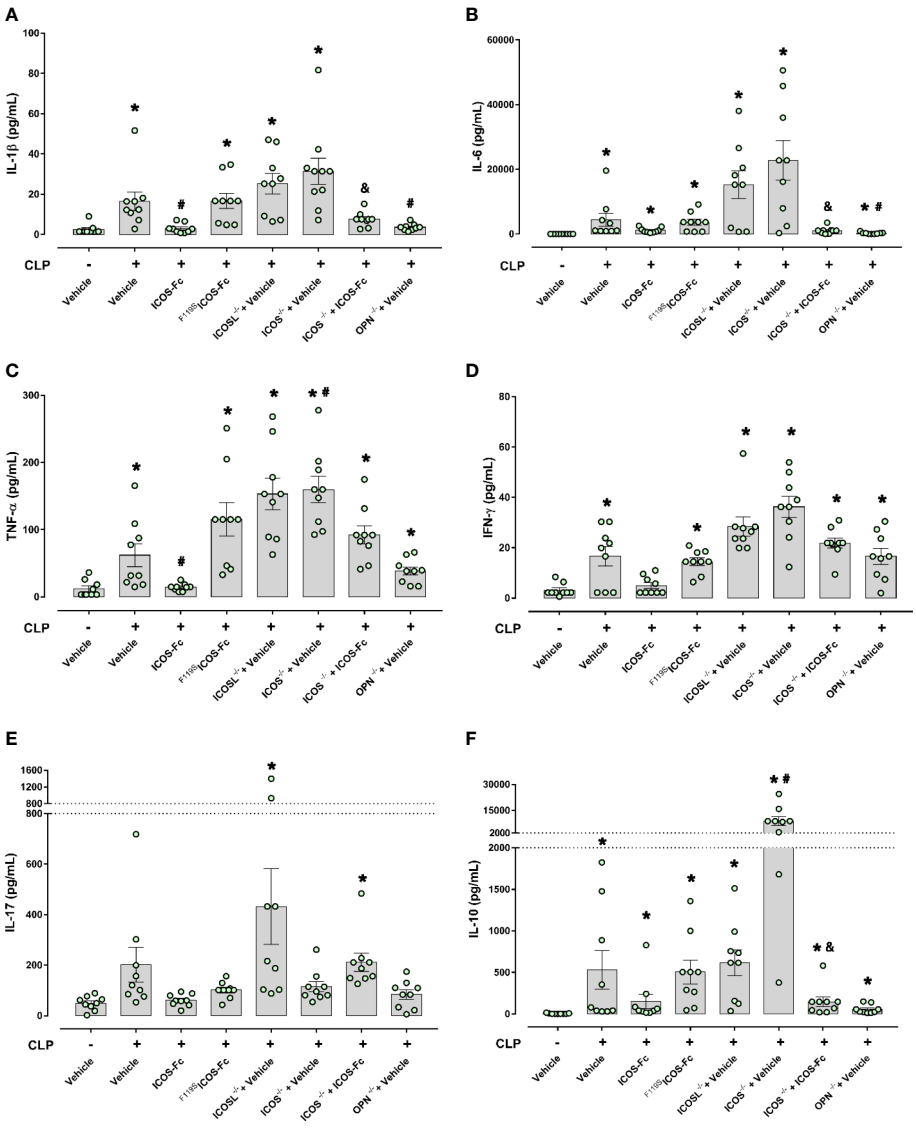

FIGURE 4
Effect of ICOS-ICOSL axis immunomodulation on systemic cytokines during experimental sepsis. Wild-type mice and/or ICOSL, ICOS and OPN knockout mice were randomly selected to undergo either Sham or CLP surgery. One hour later, mice received once either Vehicle (PBS, 100 µL), ICOS-Fc (100 µg) or ^{F119S}ICOS-Fc (100 µg) intravenously. At 24 h, blood samples were withdrawn from each mouse and plasma levels of IL-1β **(A)**, IL-6 **(B)**, TNF-α **(C)**, IFN-γ **(D)**, IL-17 **(E)** and IL-10 **(F)** were determined. Data are expressed as dot plots (for each animal) and as mean ± S.E.M of 9 mice per group. Statistical analysis was performed by one-way ANOVA followed by Bonferroni's *post hoc* test. *p<0.05 *vs* Sham + Vehicle; $^{\#}$p<0.05 *vs* CLP + Vehicle; $^{\&}$p<0.05 *vs* ICOS$^{-/-}$ + Vehicle.

molecules, and the increase was inhibited by mice treatment with ICOS-Fc (Figures 6E–H).

Discussion

Currently, most research on sepsis is focused on blocking the initial hyperinflammation, which in turn has resulted in promising outcomes. However, recent reports showed that both pro- and anti-inflammatory responses occur immediately and simultaneously after the onset of sepsis and most patients who survive this initial hyperinflammatory phase develop an immunosuppressive phase that can progress to late deaths (1, 32 and 33). Among the main causes of death in this immunosuppressive phase, the failure to control a primary infection and/or secondary hospital-acquired infections stands out (34). In the present study we report for the first time

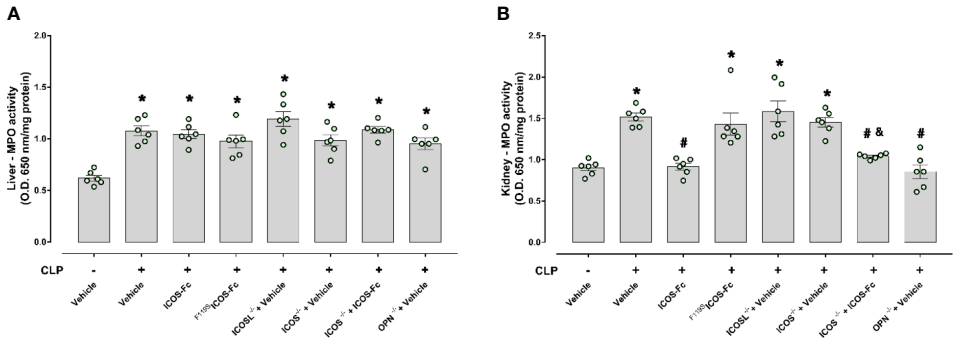

FIGURE 5
Effect of ICOS-ICOSL axis immunomodulation on sepsis-induced neutrophil (MPO activity) infiltration. Wild-type mice and/or ICOSL, ICOS and OPN knockout mice were randomly selected to undergo either Sham or CLP surgery. One hour later, mice received once either Vehicle (PBS, 100 µL), ICOS-Fc (100 µg) or ^{F119S}ICOS-Fc (100 µg) intravenously. At 24 h, liver and kidney samples were harvested. Through an *in vitro* assay, myeloperoxidase (MPO) activity was measured in liver **(A)** and kidney **(B)**. Data are expressed as dot plots (for each animal) and as mean ± S.E.M of 6 mice per group. Statistical analysis was performed by one-way ANOVA followed by Bonferroni's *post hoc* test. *p<0.05 *vs* Sham + Vehicle; $^{\#}$p<0.05 *vs* CLP + Vehicle; $^{\&}$p<0.05 *vs* ICOS$^{-/-}$ + Vehicle.

that ICOS-ICOSL axis may play a role in regulation of uncontrolled inflammation and organ injury induced by sepsis and that treatment of septic mice with ICOS-Fc may represent a novel immunomodulatory pharmacological approach that can simultaneously counteract both sepsis-induced hyperinflammation and immunosuppression.

These findings were obtained by evoking polymicrobial sepsis in either WT mice and knockout mice for ICOS, ICOSL and OPN genes. As expected, severe sepsis (score ≥3) was observed in vehicle-treated septic mice, suggesting potential late deaths, since the clinical scoring system is used as a surrogate marker of mortality. This detrimental effect was also associated with low body temperature (~27°C), as similarly, hypothermia is another surrogate marker of mortality, as a 5°C decrease over time or <30°C has also been shown to predict death in CLP-induced septic mice (35). Moreover, septic mice showed liver and kidney damage, displayed by increase of plasma AST/ALT and creatinine/urea levels, respectively, which is in line with the notion that sepsis can cause multiple organ failure including hepatocellular injury and renal dysfunction.

Intriguingly, treatment with ICOS-Fc substantially ameliorated the clinical picture by significantly decreasing all these parameters of sepsis. The effect was specific since no protection was detected following administration of ^{F119S}ICOS-Fc (a mutated form of ICOS-Fc carrying a phenylalanine-to-serine substitution at position 119).

Theoretically, the protective activity of ICOS-Fc might be ascribed to a twofold mechanism, i.e. on the one hand to the inhibition of the endogenous ICOS activity and, on the other hand, to triggering of the endogenous ICOSL. However, the effectiveness of ICOS-Fc not only in WT mice but also in ICOS$^{-/-}$ mice, lacking the endogenous ICOS, strongly suggest that the main protective effect on sepsis is due to triggering of ICOSL, which is in line with previous works showing that ICOSL triggering by ICOS-Fc elicits several anti-inflammatory activities both *in vitro* and *in vivo* (13, 15, 16, 19).

These results are in keeping also with recent findings showing that ICOS-Fc protects against liver damage through a shift of pro-inflammatory monocyte-derived macrophages to an anti-inflammatory phenotype (20). In parallel, the direct renoprotective effect triggered by ICOS-Fc treatment is supported by a recent study showing a key role of ICOSL in preventing early kidney disease, possibly through a selective binding to podocyte αvβ3 integrin, in which ICOSL serves as an αvβ3-selective antagonist that maintains adequate glomerular filtration (36).

The use of knockout mice highlighted that, in sepsis, a key role may be played by OPN as all the above septic parameters were significantly decreased in OPN$^{-/-}$ mice, so that OPN deficiency mirrored the effect of ICOS-Fc in WT mice. This finding is in line with data showing that, in humans, OPN levels are increased in sepsis (37) and OPN might be involved in the sepsis pathogenesis, possibly by supporting IL-6 secretion (38). Moreover, several reports showed that ICOS-Fc inhibits several proinflammatory activities of OPN *in vitro* and *in vivo* (16, 37, 39 and 40). Our findings are in keeping also with recent data showing that macrophage-derived OPN promotes glomerular injury in an experimental model of inflammatory and progressive kidney disease (41). OPN is an heavily phosphorylated extracellular protein, expressed and secreted by several cell types, including macrophages,

10.3389/fimmu.2022.992614

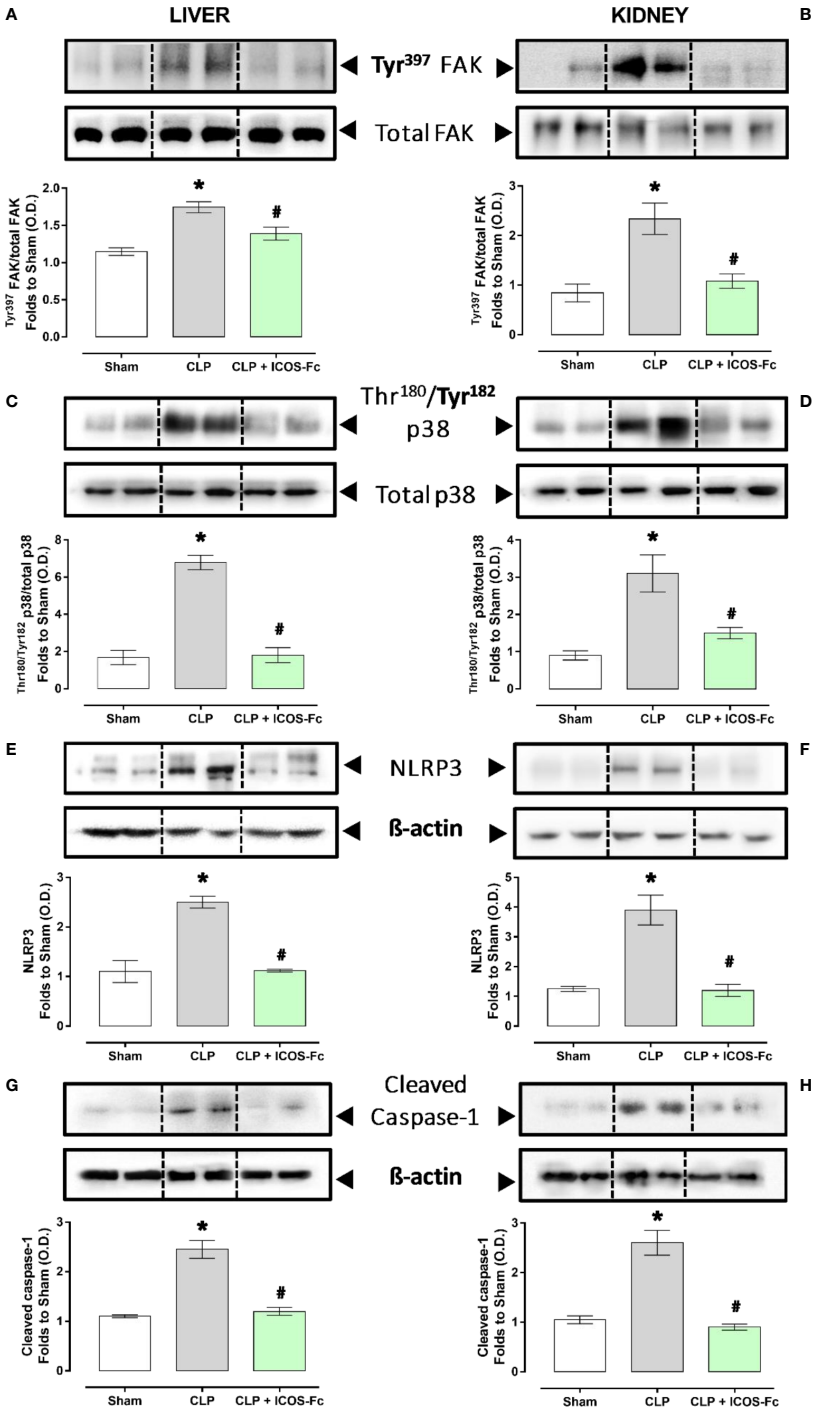

FIGURE 6
Effect of ICOS-ICOSL axis immunomodulation on tissue inflammatory pathways during experimental sepsis. Wild-type mice and/or ICOSL, ICOS and OPN knockout mice were randomly selected to undergo either Sham or CLP surgery. One hour later, mice received once either Vehicle (PBS, 100 µL), ICOS-Fc (100 µg) or ^{F119S}ICOS-Fc (100 µg) intravenously. At 24 h, liver and kidney samples were harvested, and total proteins were extracted from them. Western blotting analysis for phosphorylation of Tyr^{397} on FAK in the liver **(A)** and kidney **(B)** were normalized to total FAK; Phosphorylation of Thr^{180}/Tyr^{182} on p38 in the liver **(C)** and kidney **(D)** were normalized to total p38; NLRP3 expression in the liver **(E)** and kidney **(F)** were corrected against β-actin and normalized using the Sham related bands; Cleaved caspase-1 expression in the liver **(G)** and kidney **(H)** were corrected against β-actin and normalized using the Sham related bands. Densitometric analysis of the bands are expressed as relative optical density (O.D.). Data are expressed as dot plots (for each animal) and as mean ± S.E.M of 4-5 mice per group. Statistical analysis was performed by one-way ANOVA followed by Bonferroni's *post hoc* test. *p<0.05 *vs* Sham + Vehicle; $^{\#}$p<0.05 *vs* CLP + Vehicle.

endothelial cells, dendritic cells and T-cells. It can act as a cytokine mediating several biological functions, including cell migration, adhesion, activation of inflammatory cells, and modulation of T cell activation supporting differentiation of proinflammatory type 1 (Th1) and type 17 (Th17) Th cells (42).

Analysis of plasmatic cytokines showed that, in all mouse strains, sepsis was accompanied by increase of IL-1β, IL-6, IL-10, TNF-α and IFN-γ. Moreover, increase of TNF-α and, especially, IL-10 was particularly striking in $ICOS^{-/-}$ mice, which may point out that ICOS deficiency causes a dysregulation of activation of M1 and M2 macrophages. However, treatment with ICOS-Fc significantly decreased IL-1β and TNF-α in WT mice and IL-1β, IL-6 and IL-10 in $ICOS^{-/-}$ mice indicating that ICOS-Fc substantially downmodulates the cytokine storm in sepsis. In $OPN^{-/-}$ mice, increase of these cytokines was in general moderate, with a significant decrease of IL-1β and IL-6, in line with the mild sepsis developed by these mice.

Among the main inflammatory pathways activated during sepsis, we report a local (liver and kidney) overactivation of the FAK and p38 MAPK pathways in CLP mice. Previously, we have shown that the FAK pathway mediates inflammation through p38 MAPK and that this inflammatory axis plays a role in exacerbating inflammation (28). Activation of this axis promotes increased expression/secretion of pro-inflammatory cytokines such as TNF-α, IL-6, IL-1β and IL-17, which in turn contribute to the cytokine storm and multiple organ failure (MOF) associated with sepsis (43). Intriguingly, treatment of septic mice with ICOS-Fc significantly attenuated FAK and p38 MAPK phosphorylation, thus reducing their activation during septic insult, with a following impact on the development of the above-mentioned cytokine storm. These findings are in accordance with previous studies focused on tumor cell migration, whose treatment with ICOS-Fc reduces FAK and p38 MAPK activation both *in vitro* and *in vivo* (15, 19). As we and other have recently shown, FAK activation may also affect the overexpression and activation of another peculiar inflammatory pathway, NLRP3 inflammasome complex (28, 44). Thus, we wondered here whether ICOS-Fc could also infer with this cross-talk mechanism linking FAK to NLRP3 activation within the septic context. We report here that experimental sepsis led to an overactivation of the NLRP3 complex and consequent activation of its downstream mediator caspase-1, which were significantly reduced by treatment with ICOS-Fc, thus leading to reduced systemic release of IL-1β. In addition to the impact on the aforementioned inflammatory pathways, ICOS-Fc administration seems to directly affect leukocyte migration in CLP mice, as documented by the changes in MPO activity, a well-known biomarker of neutrophil infiltration, in both liver and kidney homogenates (45). Specifically, we documented that the sepsis-induced increase in MPO activity in renal tissues, was significantly counteracted by ICOS-Fc treatment. This effect, on the other hand, was absent when CLP mice were treated with ^{F119S}ICOS-Fc. Intriguingly, increased MPO activity was recorded in liver homogenates from septic mice, regardless of drug treatment or genetic intervention, when compared to Sham mice. Despite ICOS-Fc has been shown to reduce the migration of polymorphonuclear cells into inflamed tissues (15), these discrepant events observed in liver and kidney tissue may be the result of different levels of ICOSL expression. This finding corroborates a previous study reporting that hepatocytes did not express ICOSL, when compare to other organs, such as the kidney (46). Thus, suggesting that the hepatic protection induced by ICOS-Fc in septic mice is mainly due to a local and systemic resolution of inflammation rather than a reduction in leukocyte infiltration. A schematic representation summarizing the role of ICOS-ICOSL axis in the pathogenesis of sepsis and the protective effects of ICOS-Fc following sepsis-induced multiple organ failure is shown in Figure 7.

Despite the originality of our findings, we are aware of several limitations of our study, including the lack of extension of these findings to other important functional organs related to MOF during sepsis, such as the lungs and the cardiac tissue, along with the lack of analysis suggestive of the direct effect of ICOS-Fc treatment in preventing immunosuppression. Albeit the *in vivo* protocol described here is in accordance with the main recommendations provided by MQTiPSS consensus guidelines (27), we are not authorized to perform a survival study to assess the long-term effect of ICOS-Fc due to ethical reasons. Thus, further studies are needed to extend the clinical relevance of our findings as well as to gain a better insight into the safety profile of the proposed drug treatment.

Conclusions

In conclusion, we demonstrate here, for the first time, that the ICOS-ICOSL axis plays a crucial role in the development of systemic inflammation and organ damage induced by a clinically relevant sepsis model. These findings were confirmed by an exacerbation of septic injury in mice knockout for the ICOS and ICOSL genes. Interestingly, we also documented its draggability by showing protection when ICOS-Fc, a recombinant protein which act as an antagonist of ICOS and an agonist of ICOSL, was administered during sepsis. The beneficial effects of this innovative pharmacological approach are likely due to a potential cross-talk mechanisms involving the FAK-p38-NLRP3 inflammasome axis. A greater

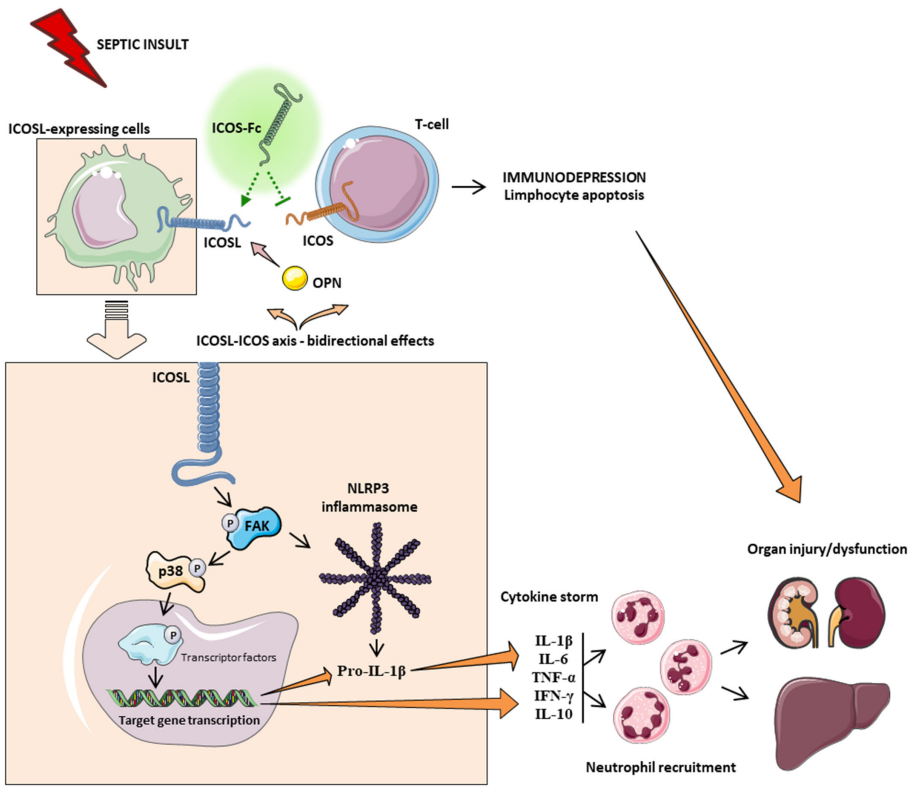

FIGURE 7
Schematic representation on the role of ICOS-ICOSL axis in the pathogenesis of sepsis. Septic insult results in an imbalance in the ICOS-ICOSL axis, leading to bidirectional harmful effects, where, on the one hand, the triggering of ICOS can induce immunosuppression, while, on the other hand, the signaling pathway downstream of the ICOSL protein leads to overactivation of FAK-p38-NLRP3 axis, promoting the transcription of pro-inflammatory genes, as well as the cleavage of pro IL-1β into IL-1β and subsequent production of pro-inflammatory cytokines. Leukocyte recruitment is also stimulated by the release of cytokines. Systemic hyperinflammation (cytokine storm), along with polymorphonuclear cell recruitment, contributes to the onset of multiple organ failure. Treatment with ICOS-Fc can attenuate sepsis-induced hyperinflammation and therefore MOF to improve clinical outcomes.

understanding of the molecular basis of ICOS-Fc-mediated effects is needed to harness its actions as a potentially powerful immunomodulatory tool for counteracting inflammation and organ injury in sepsis.

Data availability statement

The raw data supporting the conclusions of this article will be made available by the authors, without undue reservation.

Ethics statement

The animal study was reviewed and approved by Ethical committee OPBA University of Turin and Italian Ministry of Health, Italy.

Author contributions

GA, CD, UD, and MC conceived and designed the experiments. GA, IS, EA, CM, RM, EP, GE, DC, and NC performed the experiments. GA, EA, CM, RM, IB, EB, CG, NC, MA, DF, CT, CC, CD, UD, and MC analyzed the data. GA, CD, UD, CT, and MC, writing - review and editing. All authors have read and agreed to the published version of the manuscript.

Funding

The Università degli Studi di Torino has supported and funded this work (Ricerca Locale 2020 and 2021) and by the Associazione Italiana Ricerca sul Cancro (IG20714), Milan Italy.

Acknowledgments

Parts of the Figure 7 were drawn by using pictures from Servier Medical Art. Servier Medical Art by Servier is licensed

Conflict of interest

The authors declare that the research was conducted in the absence of any commercial or financial relationships that could be construed as a potential conflict of interest.

Publisher's note

References

1. Hotchkiss RS, Monneret G, Payen D. Sepsis-induced immunosuppression: From cellular dysfunctions to immunotherapy. *Nat Rev Immunol* (2013) 13:862–74. doi: 10.1038/nri3552

2. Rudd KE, Johnson SC, Agesa KM, Shackelford KA, Tsoi D, Kievlan DR, et al. Global, regional, and national sepsis incidence and mortality, 1990 – 2017 : analysis for the global burden of disease study. *Lancet* (2020) 395:200–11. doi: 10.1016/S0140-6736(19)32989-7

3. Hutloff A, Dittrich AM, Beier KC, Eljaschewitsch B, Kraft R, Anagnostopoulos I, et al. ICOS is an inducible T-cell co-stimulator structurally and functionally related to CD28. *Nature* (1999) 100:263–6. doi: 10.1038/16717

4. Yoshinaga SK, Whoriskey JS, Khare SD, Sarmiento U, Guo J, Horan T, et al. T-Cell co-stimulation through B7RP-1 and ICOS. *Nature* (1999) 1:827–32. doi: 10.1038/45582

5. Swallow MM, Wallin JJ, Sha WC. B7h, a novel costimulatory homolog of B7.1 and B7.2, is induced by TNFa. *Immunity* (1999) 11:423–32. doi: 10.1016/s1074-7613(00)80117-x

6. Möhnle P, Hirschberger S, Hinske LC, Briegel J, Hübner M, Weis S, et al. MicroRNAs 143 and 150 in whole blood enable detection of T-cell immunoparalysis in sepsis. *Mol Med* (2018) 24:1–14. doi: 10.1186/s10020-018-0056-z

7. Menéndez R, Méndez R, Almansa R, Ortega A, Alonso R, Suescun M, et al. Simultaneous depression of immunological synapse and endothelial injury is associated with organ dysfunction in community-acquired pneumonia. *J Clin Med* (2019) 8:1–10. doi: 10.3390/jcm8091404

8. Burmeister Y, Lischke T, Dahler AC, Mages HW, Lam K-P, Coyle AJ , et al. ICOS controls the pool size of effector-memory and regulatory T cells. *J Immunol* (2008) 180:774–82. doi: 10.4049/jimmunol.180.2.774

9. Chen Q, Mo L, Cai X, Wei L, Xie Z, Li H, et al. ICOS signal facilitates Foxp3 transcription to favor suppressive function of regulatory T cells. *Int J Med Sci* (2018) 15:666–73. doi: 10.7150/ijms.23940

10. Luan Y, Yin C, Qin Q, Dong N, Zhu X, Sheng Z. Effect of regulatory T cells on promoting apoptosis of T lymphocyte and its regulatory mechanism in sepsis. *J Interf Cytokine Res* (2015) 35:969–80. doi: 10.1089/jir.2014.0235

11. Saito K, Wagatsuma T, Toyama H, Ejima Y, Hoshi K, Shibusawa M, et al. Sepsis is characterized by the increases in percentages of circulating CD4 + CD25 + regulatory T cells and plasma levels of soluble CD25. *J Exp Med* (2008) 216:61–8. doi: 10.1620/tjem.216.61

12. Leng F, Liu J, Liu Z, Yin J, Qu H-P. Increased proportion of CD4 d CD25 d Foxp3 d regulatory T cells during early-stage sepsis in ICU patients. *J Microbiol Immunol Infect* (2013) 46:338–44. doi: 10.1016/j.jmii.2012.06.012

13. Occhipinti S, Dianzani C, Chiocchetti A, Boggio E, Clemente N, Gigliotti CL, et al. Triggering of B7h by the ICOS modulates maturation and migration of monocyte-derived dendritic cells. *J Immunol* (2013) 190:1125–34. doi: 10.4049/jimmunol.1201816

14. Lund SA, Giachelli CM. The role of osteopontin in inflammatory processes. *J Cell Commun Signal* (2009) 3:311–22. doi: 10.1007/s12079-009-0068-0

15. Dianzani C, Minelli R, Mesturini R, Chiocchetti A, Barrera G, Boscolo S, et al. B7h triggering inhibits umbilical vascular endothelial cell adhesiveness to tumor cell lines and polymorphonuclear cells. *J Immunol* (2010) 185:3970–9. doi: 10.4049/jimmunol.0903269

16. Raineri D, Dianzani C, Cappellano G, Maione F, Baldanzi G, Iacobucc I, et al. Osteopontin binds ICOSL promoting tumor metastasis,". *Commun Biol* (2020) 3:1–15. doi: 10.1038/s42003-020-01333-1

17. Di Niro R, Ziller F, Florian F, Crovella S, Stebel M, Bestagno M, et al. Construction of miniantibodies for the *in vivo* study of human autoimmune diseases in animal models. *BMC Biotechnol* (2007) 7:1–10. doi: 10.1186/1472-6750-7-46

18. Gigliotti CL, Boggio E, Clemente N, Shivakumar Y, Toth E, Sblattero D, et al. ICOS-ligand triggering impairs osteoclast differentiation and function *In vitro* and *In vivo*. *J Immunol* (2016) 197:3905–16. doi: 10.4049/jimmunol.1600424

19. Dianzani C, Minelli R, Gigliotti CL, Occhipinti S, Giovarelli M, Conti LM, et al. B7h triggering inhibits the migration of tumor cell lines. *J Immunol* (2014) 192:4921–31. doi: 10.4049/jimmunol.1300587

20. Ramavath NN, Gadipudi LL, Provera A, Gigliotti LC, Boggio E, Bozzola C, et al. Inducible T-cell costimulator mediates Lymphocyte/Macrophage interactions during liver repair. *Front Immunol* (2021) 12:786680. doi: 10.3389/fimmu.2021.786680

21. Stoppa I, Gigliotti CL, Clemente N, Pantham D, Dianzani C, Monge C, et al. ICOSL stimulation by ICOS-fc accelerates cutaneous wound healing *In vivo*. *Int J Mol Sci* (2022) 23:1–12. doi: 10.3390/ijms23137363

22. O'Sullivan AW, Wang JH, Redmond HP. NF-κB and P38 MAPK inhibition improve survival in endotoxin shock and in a cecal ligation and puncture model of sepsis in combination with antibiotic therapy. *J Surg Res* (2009) 152:46–53. doi: 10.1016/j.jss.2008.04.030

23. Cornelius DC, Travis OK, TramelI RW, Borges-Rodriguez M, Baik CH, Greer M, et al, et al. NLRP3 inflammasome inhibition attenuates sepsis-induced platelet activation and prevents multi-organ injury in cecal-ligation puncture. *PLoS One* (2020) 15:1–15. doi: 10.1371/journal.pone.0234039

24. Lee S, Nakahira K, Dalli J, Siempos II, Norris PC, Colas RA, et al. NLRP3 inflammasome deficiency protects against microbial sepsis *via* increased lipoxin B4 synthesis. *Am J Respir Crit Care Med* (2017) 196:713–26. doi: 10.1164/rccm.201604-0892OC

25. Chen X, Zhao Y, Wang X, Lin Y, Zhao W, Wu D, et al. FAK mediates LPS-induced in fl ammatory lung injury through interacting TAK1 and activating TAK1-NF κ b pathway. *Cell Death Differ* (2022) 13:1–12. doi: 10.1038/s41419-022-05046-7

26. du Sert NP, Hurst V, Ahluwalia A, Alam S, Avey MT, Baker M, et al. The arrive guidelines 2.0: Updated guidelines for reporting animal research. *PloS Biol* (2020) 18:1–12. doi: 10.1371/journal.pbio.3000410

27. Osuchowski MF, Ayala A, Bahrami S, Bauer M, Boros M, Cavaillon J-M, et al. Minimum quality threshold in pre-clinical sepsis studies (mqtipss): An international expert consensus initiative for improvement of animal modeling in sepsis. *Shock* (2018) 50:377–80. doi: 10.1097/SHK.0000000000001212

28. Alves GF, Aimaretti E, Einaudi G, Mastrocola R, Oliveira JG, Collotta D, et al. Pharmacological inhibition of FAK-Pyk2 pathway protects against organ damage and prolongs the survival of septic mice. *Front Immunol* (2022) 13:837180. doi: 10.3389/fimmu.2022.837180

29. Kovalski V, Prestes AP, Oliveira JG, Alves GF, Colarites D, El Mattos J, et al. Protective role of cGMP in early sepsis. *Eur J Pharmacol* (2017) 807:174–81. doi: 10.1016/j.ejphar.2017.05.012

30. Nandra KK, Collino M, Rogazzo M, Fantozzi R, Patel NSA, Thiemermann C. "Pharmacological preconditioning with erythropoietin attenuates the organ injury and dysfunction induced in a rat model of hemorrhagic shock,". *DMM Dis Model Mech* (2013) 6:701–9. doi: 10.1242/dmm.011353

31. Faul F, Erdfelder E, Lang A-G, Buchner A. G*Power 3: A flexible statistical power analysis program for the social, behavioral, and biomedical sciences. *Behav Res Methods* (2007) 39:175–91. doi: 10.3758/bf03193146

32. Tsirigotis P, Chondropoulos S, Gkirkas K, Meletiadis J, Dimopoulou I. "Balanced control of both hyper and hypo-inflammatory phases as a new treatment paradigm in sepsis,". *J Thorac Dis* (2016) 8:E312–6. doi: 10.21037/jtd.2016.03.47

33. Boomer JS, To K, Chang KC, Takasu O, Osborne DF, Walton AH, et al. Immunosuppression in patients who die of sepsis and multiple organ failure. *J Am Med Assoc* (2011) 306:2594–605. doi: 10.1001/jama.2011.1829

34. Otto GP, Sossdorf M, Claus RA, Rödel J, Menge K, Reinhart K, et al. The late phase of sepsis is characterized by an increased microbiological burden and death rate. *Crit Care* (2011) 15:1–8. doi: 10.1186/cc10332

35. Mai SHC, Sharma N, Kwong AC, Dwivedi DJ, Khan M, Grin PM, et al. Body temperature and mouse scoring systems as surrogate markers of death in cecal ligation and puncture sepsis. *Intensive Care Med Exp* (2018) 6:1–14. doi: 10.1186/s40635-018-0184-3

36. Koh KH, Cao Y, Mangos S, Tardi NJ, Dande RR, Lee HW, et al. Nonimmune cell–derived ICOS ligand functions as a renoprotective αvβ3 integrin–selective antagonist. *J Clin Invest* (2019) 129:1713–26. doi: 10.1172/JCI123386

37. Castello LM, Baldrighi M, Molinari L, Salmi L, Cantaluppi V, Vaschetto R, et al. The role of osteopontin as a diagnostic and prognostic biomarker in sepsis and septic shock. *Cells* (2019) 8:1–12. doi: 10.3390/cells8020174

38. Uchibori T, Matsuda K, Shimodaira T, Sugano M, Uehara T, Honda T. IL-6 trans-signaling is another pathway to upregulate osteopontin. *Cytokine* (2017) 90:88–95. doi: 10.1016/j.cyto.2016.11.006

39. Hirano Y, Aziz M, Yang W-L, Wang Z, Zhou M, Ochani M, et al. Neutralization of osteopontin attenuates neutrophil migration in sepsis-induced acute lung injury. *Crit Care* (2015) 19:1–15. doi: 10.1186/s13054-015-0782-3

40. Fortis S, Khadaroo RG, Haitsma JJ, Zhang H. Osteopontin is associated with inflammation and mortality in a mouse model of polymicrobial sepsis. *Acta Anaesthesiol Scand* (2015) 59:170–5. doi: 10.1111/aas.12422

41. Trostel J, Truong LD, Roncal-Jimenez C, Miyazaki M, Miyazaki-Anzai S, Kuwabara M, et al. Disease different effects of global osteopontin and macrophage osteopontin in glomerular injury. *Am J Physiol - Ren Physiol* (2018) 315:F759–68. doi: 10.1152/ajprenal.00458.2017

42. Boggio E, Dianzani C, Gigliotti CL, Soluri MF, Clemente N, Cappellano G, et al. Thrombin cleavage of osteopontin modulates its activities in human cells *in vitro* and mouse experimental autoimmune encephalomyelitis *in vivo*. *J Immunol Res* (2016) 2016:1–13. doi: 10.1155/2016/9345495

43. Chaudhry H, Zhou J, Zhong Y, Ali MM, Mcguire F, Nagarkatti PS, et al. Role of cytokines as a double-edged sword in sepsis. *In Vivo (Brooklyn)* (2013) 27:669–84.

44. Chung IC, OuYang C-N, Yuan S-N, Li H-P, Chen J-T, Shieh H-R, et al. Pyk2 activates the NLRP3 inflammasome by directly phosphorylating ASC and contributes to inflammasome-dependent peritonitis. *Sci Rep* (2016) 6:1–13. doi: 10.1038/srep36214

45. Yu H, Liu Y, Wang M, Restrepo RJ, Wang D, Kalogeris TJ, et al. Myeloperoxidase instigates proinflammatory responses in a cecal ligation and puncture rat model of sepsis. *Am J Physiol - Hear Circ Physiol* (2020) 319:H705–21. doi: 10.1152/ajpheart.00440.2020

46. Wahl C, Bochtler P, Chen L, Schirmbeck R, Reimann J. B7-H1 on hepatocytes facilitates priming of specific cd8 t cells but limits the specific recall of primed responses. *Gastroenterology* (2008) 135:980–8. doi: 10.1053/j.gastro.2008.05.076